



University  
of Glasgow

Lee, Yeong Yeh (2013) *An in-depth study on the movement and location of the gastro-oesophageal junction.*

PhD thesis

<http://theses.gla.ac.uk/4434/>

Copyright and moral rights for this thesis are retained by the author

A copy can be downloaded for personal non-commercial research or study, without prior permission or charge

This thesis cannot be reproduced or quoted extensively from without first obtaining permission in writing from the Author

The content must not be changed in any way or sold commercially in any format or medium without the formal permission of the Author

When referring to this work, full bibliographic details including the author, title, awarding institution and date of the thesis must be given

# An in-depth study on the movement and location of the gastro-oesophageal junction

Yeong Yeh Lee  
MD, MRCP (UK), DTM&H (Lond), MMed

Submitted in fulfilment of the requirements  
for the Degree of PhD in Gastroenterology

Institute of Cardiovascular & Medical Sciences  
College of Medical, Veterinary and Life Sciences  
University of Glasgow



UNIVERSITY  
*of*  
GLASGOW

March 2013

## Abstract

Understanding the physiology of gastro-oesophageal junction (GOJ) is important as failure of its function is associated with reflux disease, hiatus hernia and cancer. It has been suggested that the increased intra-abdominal pressure produced by central obesity may increase acid reflux during transient lower oesophageal sphincter relaxations (TLOSRS) and also predispose to short segment reflux.

In recent years, we have seen impressive developments in high resolution technologies allowing measurement of luminal pressure, pH and impedance. One obvious deficiency is our lack of technique to monitor the movement and location of the GOJ over a prolonged period of time. Both in-vitro and in-vivo studies indicated that it was possible to monitor the position of the GOJ by means of clipping a magnet to the squamo-columnar junction and which was detected by a novel linear probe consisting of a series of Hall Effect sensors. The accuracy for detection of position of the GOJ with this new technique was superior to 10 mm and was as good as fluoroscopy in the detection of position with a correlation co-efficient of 0.96. Without the risk of radiation associated with fluoroscopy, the new probe could be applied over a much longer period than had been previously possible.

Three factors were identified from in-vitro studies which could limit accuracy of the Hall Effect-based probe. These factors were firstly, poor magnet orientation and distance, secondly, the effect of temperature, and thirdly the presence of other ferromagnetic materials. Newer probe having 3-dimensional capabilities is in development. The temperature effect could be reduced by calibrating the probe within a water bath heated to body temperature prior to insertion. Using alongside a 2.7 mm manometer, the ferromagnetic effect could be reduced.

While oesophageal shortening during TLOSRS is due to longitudinal muscle contraction but relatively little is known about the behaviour of the GOJ during its restitution. The return movement of the GOJ is particularly important as failure of this process will produce a persisting hiatus hernia. Detailed examination on migration of the GOJ during TLOSRS and swallows

had been performed in 12 healthy subjects. Proximal displacement of the GOJ was present transiently during TLOSRS and swallows but the displacement of up to 9 cm (median 4.3 cm) during TLOSRS represented very severe herniation of the GOJ. In addition, there was a rapid initial return of the GOJ following TLOSRS when the CD was relaxed and its correlation with amplitude suggested it is due to elastic recoil of the POL. This marked stretching of the POL during TLOSRS may contribute to its weakening and development of established hiatus hernia.

Epidemiological evidence suggests an association between obesity, reflux disease and hiatus hernia but mechanisms are unclear. Study was performed to assess the structure and function of the GOJ in asymptomatic subjects with and without obesity and the effects of elevating intra-abdominal pressure with waist belt. Sixteen subjects were recruited to achieve two groups defined by normal (eight) or increased (eight) waist circumference, matched for age and gender. Our studies demonstrated that increased WC and waist belt caused marked changes in the functioning of the GOJ and LOS leading to increased gastric acid penetration within the high pressure zone. This appears to occur by retrograde flow within the closed sphincter and by increased short segment reflux during TLOSRS and subsequent impaired clearance. This increased intra-sphincteric acid exposure is occurring in asymptomatic volunteers and may explain the high incidence of inflammation and columnar metaplasia observed at the GOJ in asymptomatic subjects. Our observations may also be relevant to the aetiology of adenocarcinoma of the cardia which shares epidemiological risk factors of the oesophageal adenocarcinoma but has a much weaker association with reflux symptoms.

To conclude, a new technique has been developed allowing accurate and prolonged detection of position and movement of the GOJ without any radiation risk. Using alongside high resolution manometry and pHmetry, the new technique allows detailed examination of the structure and function of the GOJ providing important insights on the pathophysiology of reflux disease in normal subjects with and without central obesity and waist belt.

# Table of Contents

Abstract.....	ii
Table of contents.....	v
List of tables.....	x
List of figures.....	xi
Publications and awards.....	xv
Acknowledgements.....	xviii
Author's declaration.....	xx
List of abbreviations.....	xxi
<b>CHAPTER 1: BACKGROUND OF MY THESIS.....</b>	<b>1</b>
1.1 Introduction.....	2
1.2 Biology of the normal oesophagus.....	4
1.2.1 The common embryonic development.....	4
1.2.2 Anatomy and physiology of the oesophagus.....	5
1.3 Biological importance of the GOJ.....	8
1.3.1 Defining the normal GOJ.....	8
1.3.2 Biological constituents and physiology of the GOJ.....	11
1.3.2.1 Intrinsic lower oesophageal sphincter.....	11
1.3.2.2 Crural diaphragm.....	12
1.3.2.3 Phreno-oesophageal ligament.....	13
1.3.2.4 Angle of His and flap valve.....	14
1.4 GOJ dynamics in swallows and TLOSRS.....	15
1.4.1 Physiology of the GOJ in swallows and TLOSRS.....	15
1.4.2 Introduction to oesophageal manometry.....	16
1.4.3 The normal swallow.....	20
1.4.3.1 Pressure and dynamics of the GOJ in a normal swallow...	21
1.4.3.2 What is phrenic ampulla? .....	22
1.4.3.3 GOJ movement and the phrenic ampulla.....	24
1.4.4 TLOSRS.....	26
1.4.4.1 A paradigm shift in traditional views.....	26
1.4.4.2 Manometric characteristics of a TLOSRS.....	27
1.4.5 Proximal movement of the GOJ during TLOSRS.....	29
1.4.5.1 Radiographic technique.....	30
1.4.5.2 Manometric shortening of the oesophagus.....	34
1.4.5.3 High frequency intra-luminal ultrasound.....	35
1.5 Measuring the SCJ and its relevance to GORD.....	41
1.5.1 Introduction.....	41
1.5.2 Traditional acid reflux disease.....	42
1.5.2.1 Definition and epidemiology of GORD.....	42
1.5.2.2 Defining GORD by oesophageal acid exposure.....	44
1.5.2.3 TLOSRS, the mechanism underlying traditional reflux.....	45
1.5.2.4 Limitations of traditional acid reflux.....	47
1.5.3 Acid pocket and short segment reflux.....	48
1.5.4 Acid pocket in GORD and hiatus hernia.....	51
1.6 The abnormal GOJ: hiatus hernia.....	53
1.6.1 Introduction.....	53
1.6.2 What is hiatus hernia? A brief history and overview.....	54
1.6.3 What causes hiatus hernia? .....	57
1.6.3.1 Mechanical challenge from raised IAP.....	59

1.6.3.2 Acid-induced oesophageal shortening.....	60
1.6.3.3 Changes in connective tissue and crural muscle.....	61
1.6.3.4 Abnormal physiology associated with hiatus hernia.....	62
1.7 Effects of obesity on the GOJ and GORD.....	63
1.7.1 Introduction.....	63
1.7.2 IAP and obesity and their effects on the GOJ.....	64
1.7.3 Obesity and GORD.....	66
1.8 A summary of literature reviews.....	68
1.9 Objectives of research.....	69
<b>CHAPTER 2: MATERIALS AND METHODS.....</b>	<b>71</b>
2.1 Introduction.....	72
2.2 Upper gastrointestinal endoscopy.....	72
2.2.1 Description of equipment.....	72
2.2.2 Preparation for test.....	72
2.2.3 Description of procedure.....	73
2.3 Imaging studies.....	75
2.4 The GOJ locator probe.....	76
2.4.1 Technical details and calibration.....	76
2.4.2 Calibration and cleaning.....	77
2.4.2 Parameters measured with the locator technique.....	77
2.5 A curve-fitting approach to movement of the GOJ during TLOSRS...	79
2.6 High resolution 36-channel manometry system.....	85
2.6.1 Technical details.....	85
2.6.2 Definitions of pressure-time data.....	86
2.7 High resolution 12-channel pHmetry.....	90
2.8 Combining different catheters, their time synchronization and techniques for nasal intubation.....	91
2.8.1 Combining different catheters into one assembly.....	91
2.8.2 Synchronizing between different systems.....	92
2.8.3 Technique for nasal intubation of combined assembly.....	94
2.9 Software and data processing.....	94
2.10 Test meals.....	95
2.11 Waist belt.....	97
2.12 Specialised Gastrointestinal Investigation Unit.....	98
2.13 Data and statistical analysis.....	99
2.14 Ethical committee approval.....	101
<b>CHAPTER 3: DEVELOPING THE GOJ LOCATOR SYSTEM.....</b>	<b>102</b>
3.1 Overview.....	103
3.2 Hall Effect and magnet.....	103
3.2.1 Introduction.....	103
3.2.2 What is Hall Effect? .....	104
3.2.3 Good and bad of Hall Effect sensors.....	106
3.2.4 Basic features of Hall Effect sensors.....	107
3.2.5 Permanent rare earth magnets.....	108
3.2.6 Basic characteristics of magnet and magnetic fields.....	109
3.3 Developing the 2-D GOJ locator probe.....	110
3.3.1 Introduction.....	110
3.3.2 A brief history on conception of the novel probe.....	110
3.3.3 Components of the 2-D locator probe.....	111
3.3.3.1 Allegro® A1395 sensors.....	111
3.3.3.2 Printed circuit boards and microprocessor.....	112
3.3.4 The importance of magnet.....	115

3.3.4.1 Magnet material and dimension.....	115
3.3.4.2 Placement of magnet on the endoclip.....	116
3.3.4.3 Placement of magnet within the GOJ.....	118
3.4 Conclusion.....	119
<b>CHAPTER 4: IN-VITRO AND IN-VIVO STUDIES ON THE GOJ LOCATOR PROBE.....</b>	<b>120</b>
4.1 Background.....	121
4.2 In-vitro studies.....	122
4.2.1 Effects of orientation on the accuracy.....	122
4.2.1.1 Experimental setup and methods.....	122
4.2.1.2 Results: Signal Strength.....	125
4.2.1.3 Results: Position accuracy.....	130
4.2.2 Effects of temperature on the locator probe.....	133
4.2.2.1 Methods.....	133
4.2.2.2 Results.....	133
4.2.3 “Thermal drift” of the manometer probe.....	136
4.2.3.1 Methods.....	137
4.2.3.2 Results.....	137
4.2.4 Electromagnetic interference with other probes.....	139
4.2.4.1 Methods.....	139
4.2.4.2 Results.....	140
4.2.5 Magnet in the MRI environment - a pilot study.....	142
4.2.5.1 Background.....	142
4.2.5.2 Methods - measuring the translational force.....	143
4.2.5.3 Results.....	145
4.3 In-vivo validation studies.....	146
4.3.1 Introduction and aims.....	146
4.3.2 Methods.....	147
4.3.2.1 Study subjects.....	147
4.3.2.2 Study protocols.....	147
4.3.2.3 Data and statistical analysis.....	147
4.3.3 Results.....	149
4.4 Discussion.....	152
4.5 Summary and conclusion.....	156
<b>CHAPTER 5: THE 3-D GOJ LOCATOR PROBE.....</b>	<b>158</b>
5.1 Introduction.....	159
5.2 Hall Effect 3-D GOJ locator probe.....	159
5.2.1 Components of the 3-D probe.....	159
5.2.1.1 Hall Effect sensor - Allegro® A1395.....	159
5.2.1.2 Circuitry and microprocessor.....	160
5.2.1.3 Magnet choice and placement.....	164
5.2.2 A probe with better accuracy.....	164
5.2.3 Problems faced with the new probe.....	166
5.3 New generation 3-D GOJ Locator probe.....	167
5.3.1 Introduction.....	167
5.3.2 An overview to the MEMSIC 3-axis sensor.....	167
5.3.3 An overview to the circuit board design.....	169
5.3.4 Concluding remark.....	170
5.4 Summary and conclusion.....	170
<b>CHAPTER 6: KINETICS OF TRANSIENT HIATUS HERNIA OCCURRING DURING TLOSRS AND SWALLOWING IN NORMAL SUBJECTS.....</b>	<b>172</b>

6.1 Introduction.....	173
6.2 Methodology.....	174
6.2.1 Study subjects.....	174
6.2.2 Magnet placement.....	174
6.2.3 Study protocol.....	175
6.2.4 Defining parameters for TLOSRS and swallows.....	177
6.2.4.1 Manometric parameters for TLOSRS and swallows.....	177
6.2.4.2 GOJ migration parameters for TLOSRS and swallows.....	178
6.2.5 Statistical analysis.....	180
6.3 Results: Behaviour of the GOJ during TLOSRS.....	181
6.3.1 LOS relaxation during TLOSRS.....	181
6.3.2 Behaviour of GOJ migration during TLOSRS.....	182
6.3.3 Subsequent oesophageal contractile event.....	184
6.3.4 Variability between individuals.....	184
6.4 Results: Comparing behaviour of the GOJ between TLOSRS and swallows.....	185
6.4.1 LOS relaxation during swallows.....	185
6.4.2 Behaviour of GOJ migration during swallows.....	185
6.4.3 Comparing GOJ migration between TLOSRS and swallows...	186
6.4.4 Comparing locator probe and HRM.....	188
6.4.5 Clearance of magnet from study subjects.....	190
6.5 Discussion: Transient or potential hiatus hernia or both? .....	191
6.6 Summary and conclusion.....	198
<b>CHAPTER 7: CENTRAL OBESITY AND WAIST BELT CAUSE PARTIAL HIATUS HERNIA AND INTRASPINCTERIC ACID REFLUX IN ASYMPTOMATIC HEALTHY VOLUNTEERS.....</b>	<b>199</b>
7.1 Introduction and aims.....	200
7.2 Methodology.....	202
7.2.1 Study subjects.....	202
7.2.2 Study design or protocol.....	202
7.2.2.1 Study day zero.....	204
7.2.2.2 Study day one.....	204
7.2.2.3 Study day two and three.....	204
7.2.2.4 Study day four.....	206
7.2.3 Recording equipment.....	206
7.2.3.1 Three-dimensional GOJ locator probe.....	206
7.2.3.2 High resolution slim-line 36-channel manometer.....	207
7.2.3.3 High definition 12-channel pH catheter.....	208
7.2.4 Definitions and data analysis.....	208
7.2.4.1 Analysis on manometric characteristics of the GOJ.....	209
7.2.4.2 Analysis on relative locations of anatomical structures within the GOJ.....	209
7.2.4.3 Analysis on migration of the GOJ during TLOSRS.....	210
7.2.4.4 Analysis on acid exposure within the GOJ.....	210
7.2.4.5 Analysis on mechanism of short segment acid reflux.....	211
7.2.5 Statistical analysis.....	211
7.3 Results.....	211
7.3.1 Upper GI symptoms reported during study.....	212
7.3.2 Manometric characteristics of the GOJ.....	212
7.3.2.1 Expiratory GOJ pressure.....	212
7.3.2.2 Inspiratory GOJ pressure.....	214
7.3.3 Location of components within the GOJ.....	215

7.3.3.1 Upper and lower border of the LOS and diaphragm.....	215
7.3.3.2 Squamo-columnar junction.....	218
7.3.4 pH transition point.....	222
7.3.4.1 Acid exposure at pH transition point.....	222
7.3.4.2 The location of pH transition point.....	222
7.3.4.3 Acid exposure below pH transition point.....	223
7.3.5 Acid exposure above pH transition point.....	225
7.3.5.1 Traditional acid reflux.....	225
7.3.5.2 Short segment reflux.....	225
7.3.6 Chest x-ray at 6-8 weeks after study.....	227
7.4 Discussion.....	227
7.5 Summary and conclusion.....	233
<b>CHAPTER 8: CONCLUSIONS AND FUTURE STUDIES.....</b>	<b>235</b>
8.1 Summary and conclusions.....	236
8.2 Limitations and challenges.....	237
8.3 What the future beholds? .....	240
<b>LIST OF REFERENCES.....</b>	<b>244</b>

## List of tables

1.1	TLOSRS in normal subjects and subjects with GORD.....	46
1.2	Hiatus hernia and BMI.....	59
2.1	Calculation of AIC for different orders of polynomial equations.....	82
3.1	Differences between samarium and neodymium rare earth magnet.....	108
4.1	Effects of rotation and proximity on locator probe position error and standard deviation.....	131
4.2	Analyses on orientations with poor signal strength < 10mV and orientations with error < 10mm for experiments of $\leq 10$ mm between the magnet and the probe.....	132
4.3	Ex-vivo experiments to assess translational force on samarium cobalt disc magnet in the 1.5T MRI.....	145
4.4	Ex-vivo experiments to assess translational force on stainless Steel Quickclip2® without any magnet (Keymed Olympus, UK) in the 1.5T MRI.....	146
4.5	Comparison and correlation of data from locator probe and fluoroscopy screenings.....	151
4.6	Analysis of signal strength reliability during total recording time for each volunteer.....	152
6.1	Characteristics of LOS relaxation during TLOSRS and swallows...	181
6.2	Characteristics of GOJ migration during TLOSRS and swallows...	182
6.3	Coefficient of variations (CV) between and within individuals in different characteristics of GOJ migration during TLOSRS.....	185
6.4	ROC curve analysis of GOJ migration and LOS relaxation characteristics in TLOSRS vs. swallows.....	189
7.1	Effect of central obesity and waist belt on expiratory GOJ pressure.....	213
7.2	Effect of obesity and waist belt on inspiratory GOJ pressure.....	215
7.3	Effect of central obesity and waist belt on relative locations of anatomical structures of the GOJ.....	216
7.4	Effect of central obesity and waist belt on proximal migration of the SCJ during TLOSRS.....	221
7.5	Regional differences in acid exposure at the GOJ during fasting and after meal.....	224
7.6	Mechanism of short segment acid reflux.....	227

## List of figures

1.1	Anatomy of the oesophagus.....	6
1.2	A cross-section of the oesophagus.....	7
1.3	A complex anatomy of the normal GOJ.....	9
1.4	SCJ or the Z line seen during upper endoscopy (black arrows).....	10
1.5	The angle of His is extended within the lumen as a large fold/flap valve seen prominently from endoscopy (white arrow).....	14
1.6	A typical colour pressure topography of a swallow in a normal subject using the HRM system (Sierra Scientific Instruments Inc., US).....	17
1.7	Capacitive sensor.....	19
1.8	High definition recording of the GOJ using the new 3-D HRM.....	20
1.9	Intraluminal manometric recording (left) and videofluoroscopic imaging (right) of the GOJ during a standard 10-ml barium swallow.....	23
1.10	High resolution manometric tracing of a normal swallow.....	24
1.11	3D-HRM and fluoroscopy tracings superimposed by movement of the SCJ.....	25
1.12	This illustrates the classic study by Dodds et al using tantalum markers sewn into the wall of oesophagus in feline.....	31
1.13	Mucosal clips movement superimposed on fluoroscopy and manometry tracing.....	33
1.14	LOS shortening during TLOSRS.....	34
1.15	Schematic diagram illustrating the changes in CSA and thickness of muscularis propria at axial location y in both resting ( * ) and contracted state.....	36
1.16	Ultrasound images showing the edges which outline the inner wall of circular muscle and outer wall of longitudinal muscle.....	38
1.17	Using M-mode of HFIUS, Mittal et al. measures the muscle thickness as a marker of LMC during a swallow.....	39
1.18	A schematic diagram showing the temporal correlation between the circular and longitudinal muscle contraction of the oesophagus during (A) swallow and (B) TLOSRS.....	41
1.19	pH tracings recorded using catheter pull-through technique during fasting and postprandial period.....	48
1.20	Colour contour plots from 12-channel high definition pH probe....	50
1.21	With SPECT scan, the acid pocket is seen as accumulation of scintigraphic activity in the proximal stomach.....	52
1.22	Types of hiatus hernia, A - sliding type and B - para-oesophageal type.....	55
1.23	Grading of flap-valve.....	56

1.24	Manometric grading on the separation of lower sphincter components during hiatus hernia.....	58
2.1	Clip fixing device with endoclip (model HX-201UR-135, Olympus, UK) that passes through the working channel of a standard 27F endoscope.....	74
2.2	Photo illustrating a single use endoclip (model HX-201UR-135, Olympus, UK) with a small samarium cobalt magnet attached by heat shrinkable polyvinylidene fluoride (PMG Plastronic, UK) (shown with black arrow).....	75
2.3	An example of x-ray screening of the clip position relative to the inserted probe.....	76
2.4	Illustration of parameters to measure migration of the GOJ with the locator probe.....	78
2.5	Average velocities in each quadrant A-D, calculated by distance migrated in that quadrant divided by the duration of quadrant....	80
2.6	Curve-fitting using 6 <sup>th</sup> order polynomial equation.....	81
2.7	Determination of maximal rate (s) or velocities in different phases of migration of the GOJ during TLOSRS using elementary calculus.....	84
2.8	The smaller 2.7 mm “slimline” manometer (A) and the larger 4.2 mm diameter manometer (B) are shown.....	85
2.9	A colour contour plot extracted from the Manoview® analysis software.....	87
2.10	Illustration of manometry parameters measured with TLOSRS.....	88
2.11	The assembly of 12 channel high definition pH probe.....	90
2.12	A schematic diagram on the relative positioning of different probes in the combined assembly for studies in chapter 6.....	92
2.13	Respiratory sensor that connects to the Medtronic Polygraf® machine.....	93
2.14	An example of high resolution colour plot displayed using the DRContour version 6.0 program.....	96
2.15	A photo showing two sizes (medium and large) of abdominal belts and the sphygmomanometer (pressure cuff).....	97
2.16	The working station in the specialised GI unit.....	99
3.1	Diagram depicting the Hall Effect-based locator probe within the oesophagus and straddling the GOJ.....	104
3.2	Principle of Hall Effect.....	105
3.3	An example of miniature-sized Hall Effect transducer with integrated circuits.....	106
3.4	B-H curves of ferromagnetic material.....	109
3.5	A schematic diagram of the locator system.....	112
3.6	Microprocessor unit.....	114
3.7	An example of display for the position and signal strength output from the Hall Effect probe using the PolygramNET™	

software.....	114
3.8 Disc-shaped magnet.....	116
3.9 Metal clip with magnet.....	117
4.1 Setup of in-vitro experiments.....	123
4.2 Assessment of accuracy with the magnet at different distances and orientation relative to the probe.....	124
4.3 Rotation A and D.....	125
4.4 Relationship between signal strength (mV) against various orientations in rotation A, B, C and D.....	126
4.5 Rotation B.....	127
4.6 Rotation C.....	128
4.7 Relationship between signal strength (mV) against distances at 5, 10 and 15 mm in rotation A, B, C and D.....	129
4.8 Signal strength and position drift at 17°C and 33°C, over 1 hour.....	134
4.9 Signal strength and Position vs. temperature at initial low signal strength (SS) (above) and initial high SS (below).....	135
4.10 Thermal drift of the HRM system.....	136
4.11 Pressure-time graphs from a single experiment for all 36 sensors.....	138
4.12 Experiments on magnetic interference between the metallic sensors of solid-state manometer (Given imaging, USA) and the locator probe as recorded by the Polygraf® machine.....	141
4.13 Photographic depiction on the experiment for measuring translational force of magnet (s) and endoclip.....	143
4.14 Measuring translational force in the MRI environment.....	144
4.15 Graphs showing four studied manoeuvres from four different volunteers.....	150
5.1 A sketch on the design of the 3-D GOJ locator probe.....	160
5.2 A sketch showing the side profile of the proposed probe with sensor “y” on the tab at right angle to sensor “x” on the main strip.....	161
5.3 Manufactured flexible circuit board without any sensors yet populated.....	162
5.4 Flexible circuit board populated with sensors.....	162
5.5 The front interface of the microprocessor unit.....	163
5.6 The back interface of the microprocessor unit.....	164
5.7 Colour contour plot with superimposed GOJ movement recorded with the old 2-D Hall Effect probe during a TLOSР.....	165
5.8 Colour contour plot with superimposed GOJ movement recorded with the new 3-D Hall Effect probe during a TLOSР.....	166
5.9 A graphical diagram of AMR sensor.....	168
5.10 The new circuit board populated with the MEMSIC sensor.....	170
6.1 A schematic diagram of the combined assembly of 36 channel HRM and the GOJ locator probe and its positioning within the	

	oesophagus.....	175
6.2	High resolution colour contour display of combined data from the locator probe and manometer in a 90s frame.....	177
6.3	High resolution contour display of combined data from GOJ locator probe and HRM.....	179
6.4	Two examples of GOJ movement during swallows are shown.....	180
6.5	Correlations between velocities of phases during descent of the GOJ (phases C and D) and amplitude of proximal migration of the GOJ during TLOSRS.....	183
6.6	The movement of the GOJ (thick white line) superimposed on colour contour manometry plot.....	187
6.7	ROC curve showing AUCs for GOJ migration and LOS relaxation parameters.....	188
6.8	Comparing GOJ migration and LOS shortening.....	190
6.9	A summary of physiological processes occurring during the proximal movement and return of the GOJ associated with a TLOSRS.....	192
6.10	A summary of physiological processes occurring during the proximal movement of the GOJ associated with a swallow.....	195
7.1	Flow chart showing the study design.....	203
7.2	A schematic diagram of the combined assembly of 36 channel slim-line high resolution manometer, 3-dimensional GEJ locator probe and 12-channel pH catheter.....	205
7.3	A schematic diagram of the novel 3-dimensional locator probe....	208
7.4	An example of colour contour plot displayed using a custom-made program.....	207
7.5	Partial hiatus herniation and short segment acid reflux after meal.....	220
7.6	Mechanism of short segment reflux.....	226
8.1	A schematic of the envisaged ambulatory locator system.....	241
8.2	Non-luminal external locator technique.....	242

## Publications and Awards

### Journal publications

#### First-author

Development and validation of a probe allowing accurate and continuous monitoring of location of squamo-columnar junction

Yeong Yeh Lee, John P. Seenan, James G.H. Whiting, Elaine V. Robertson, Mohammad H. Derakhshan, Angela A. Wirz, Donald Smith, Chris Hardy, Andrew Kelman, Patricia Connolly, Kenneth E.L. McColl

*Medical Engineering and Physics* 2012; 34(3): 279-89.

Kinetics of transient hiatus hernia during transient lower esophageal sphincter relaxations and swallows in healthy subjects

Yeong Yeh Lee, James G.H. Whiting, Elaine V. Robertson, Mohammad H. Derakhshan, Angela A. Wirz, Donald Smith, Douglas Morrison, Andrew Kelman, Patricia Connolly, Kenneth E.L. McColl

*Neurogastroenterology and Motility* 2012; 24(11): 990-e539.

Measuring movement and location of the gastro-esophageal junction: research and clinical implications

Yeong Yeh Lee, James G.H. Whiting, Elaine V. Robertson, Mohammad H. Derakhshan, Donald Smith, Kenneth E.L. McColl

*Scandinavian Journal Gastroenterology* 2013; 48(4): 401-11.

#### Co-author

High-resolution esophageal manometry: addressing thermal drift of the manoscan system

Elaine V. Robertson, Yeong Yeh Lee, Mohammad H. Derakhshan, Angela A. Wirz, James G.H. Whiting, John P. Seenan, Patricia Connolly, Kenneth E.L. McColl

*Neurogastroenterology and Motility* 2012; 24(1): 61-4, e11.

Mechanism of association between BMI and dysfunction of the gastro-oesophageal barrier in patients with normal endoscopy

Mohammad H. Derakhshan, Elaine V. Robertson, Jonathan Fletcher, Gareth-Rhys Jones, Yeong Yeh Lee, Angela A. Wirz, Kenneth E.L. McColl

*Gut* 2012; 61(3): 337-43.

Towards minimally invasive monitoring for gastroenterology - An external Squamocolumnar Junction Locator

James G.H. Whiting, Nasser Djennati, Yeong Yeh Lee, Elaine V. Robertson, Mohammad H. Derakhshan, Patricia Connolly, Kenneth E.L. McColl

34<sup>th</sup> Annual International IEEE EMBS Conference 2012 (978-1-4577-1787-1/12)

Central obesity in asymptomatic volunteers is associated with increased intra-sphincteric acid reflux and lengthening of cardiac mucosa

Elaine V. Robertson, Mohammad H. Derakhshan, Angela A. Wirz, Yeong Yeh Lee, John Paul Seenan, Stuart A. Ballantyne, Scott Harvey, Andrew W. Kelman, James J. Going, Kenneth E.L. McColl

*Gastroenterology* 2013; accepted for publication 18 June 2013

## Abstracts

The development of squamo-columnar junction locator probe and its performance on bench studies

Yeong Yeh Lee, James G.H. Whiting, Elaine V. Robertson, John P. Seenan, Patricia Connolly, Kenneth E.L. McColl

*Gut* 2011; 60(Suppl 1): A182

[Poster presentation; British Society of Gastroenterology Meeting Annual Meeting 2011, Birmingham]

Squamo-columnar junction locator probe: an in-vivo validation study

Yeong Yeh Lee, James G.H. Whiting, Elaine V. Robertson, John P. Seenan, Mohammad H. Derakhshan, Angela A. Wirz, Patricia Connolly, Kenneth E.L. McColl

*Gut* 2011; 60(Suppl 1):A181-82

[Poster presentation; British Society of Gastroenterology Meeting Annual Meeting 2011, Birmingham, UK]

Squamo-columnar junction locator probe: from bench to in-vivo study

Yeong Yeh Lee, James G.H. Whiting, Elaine V. Robertson, John P. Seenan, Mohammad H. Derakhshan, Angela A. Wirz, Patricia Connolly, Kenneth E.L. McColl

*Gastroenterology* 2011; 140(5): S95-6

[Oral presentation; Digestive Disease Week 2011, Chicago, IL, USA]

Characterization of proximal movement of gastro-esophageal junction during transient lower esophageal sphincter relaxations using a novel Hall Effect probe

Yeong Yeh Lee, James G.H. Whiting, Elaine V. Robertson, Mohammad H. Derakhshan, Angela A. Wirz, Andrew Kelman, Kenneth E.L. McColl

*Gastroenterology* 2012; 142(5): S95

[Oral presentation; Digestive Disease Week 2012, San Diego, CA, USA]

Transient hiatus hernia during transient lower oesophageal sphincter relaxations

Yeong Yeh Lee, James G.H. Whiting, Elaine V. Robertson, Mohammad H. Derakhshan, Angela A. Wirz, Andrew Kelman, Douglas Morrison, Kenneth E.L. McColl

*Gut* 2012; 61(Suppl 2): A39

[Oral presentation; Digestive Diseases Federation 2012, Liverpool, UK]

Kinetics of transient hiatus hernia during transient lower esophageal sphincter relaxations and swallows in healthy volunteers

Yeong Yeh Lee, James G.H. Whiting, Elaine V. Robertson, Mohammad H. Derakhshan, Angela A. Wirz, Douglas Morrison, Patricia Connolly, Kenneth E.L. McColl  
 [Oral presentation; XIIth Little Brain Big Brain Meeting, Leuven]

Development of a novel probe allowing accurate and continuous monitoring of location of squamo-columnar junction

Yeong Yeh Lee, James G.H. Whiting, Elaine V. Robertson, John P. Seenan, Mohammad H. Derakhshan, Angela A. Wirz, Patricia Connolly, Kenneth E.L. McColl

*Journal of Neurogastroenterology & Motility* 2013; 19(Suppl 1): SP20

[Oral presentation; 3<sup>rd</sup> Biennial Congress of the Asian Neurogastroenterology and Motility Association, Penang, Malaysia]

Central obesity and waist belt cause partial hiatus hernia and short segment acid reflux in healthy volunteers

Yeong Yeh Lee, James G.H. Whiting, Elaine V. Robertson, Mohammad H. Derakhshan, Angela A. Wirz, Douglas Morrison, Alexander Weir, Donald Smith, Andrew Kelman, Kenneth E.L. McColl

*Gut* 2013; 62(Suppl 1): A103-4

[Poster of Distinction; British Society of Gastroenterology Annual Meeting 2013, Glasgow, United Kingdom]

## Awards

Graham-Wilson Travelling Scholarship April 2011

Visiting fellow to Upper GI physiology Unit, Royal London Hospital, UK

American Gastroenterological Association Research foundation 2012 - Moti L. and Kamla Rustgi International Travel Award

Travelling award to Digestive Disease Week 2012, San Diego, CA, USA

Travel grant to the 3<sup>rd</sup> Biennial Congress of the Asian Neurogastroenterology and Motility Association 2013, Penang, Malaysia

## Others

2011 American Society Gastrointestinal Endoscopy (ASGE) Video Forum: A background to the development of a novel squamo-columnar junction locator probe

The Glasgow Insight into Science and Technology (GIST) Magazine: Acid Reflux and Magnetism

## Manuscript-in-preparation

Waist belt and central obesity cause partial hiatus hernia and intrasphincteric acid reflux in asymptomatic healthy volunteers

Measuring movement and location in enclosed spaces using 3-axis anisotropic magneto-resistive sensor array

## Acknowledgement

First of all, I would like to express my sincerest thanks and gratitude to my supervisor and mentor, Professor Kenneth E. L. McColl. His enthusiasm and ideas have been a constant source of inspiration to me throughout my entire period of PhD. His support and encouragement allow me to overcome the most difficult periods. His assistance with my studies and publications allows me to produce good quality contribution to science and medicine.

Without study volunteers, my research work could not have been possible. I am very thankful to all volunteers who have taken their valuable time and effort to attend my clinical studies. Many volunteers have even provided me their encouragement and support during my difficult times of which I am extremely grateful.

My special thanks go to all staffs from Gartnavel General Hospital who had helped me tremendously during research and administrative procedures. Among them include Sister Angela Wirz who has provided her experience and enthusiasm in my work. Also staffs from the endoscopy department who have helped me with all endoscopic procedures which at times can be demanding or challenging. The staffs from radiology department have been very helpful during fluoroscopic procedures of which I am also thankful.

My deepest thanks go to my research collaborators who have provided their technical knowledge and support during the developmental phase of the medical device. They include Mr James Whiting, Dr Nasser Djennati and Professor Patricia Connolly from the Biomedical Engineering Department, University of StrathClyde. In particular, Mr James Whiting has involved extensively in the circuitry design and testing of the new 3-dimensional locator probe. Staffs from the Medical Devices Unit, Southern General Hospital especially Dr Donald Smith and Mr Alexander Weir have provided tremendous assistance in all aspects of the probe development. In particular, they have assisted in producing the microprocessor box and software to run the microprocessor. Dr Andrew Kelman who besides developing the computer programs (DrNewData6 and DrContour6), he has been a great source of

knowledge and encouragement of which I am extremely thankful. Dr Douglas Morrison has assisted in developing a curve-fit model of movement of the gastro-oesophageal junction of which I am grateful.

Special thanks go to Dr John Paul Seenan and Mr Chris Hardy who have provided the initial ground works on the 2-dimensional locator probe. I am also grateful to Dr Elaine Robertson and Dr Mohammad Derakhshan who are my research colleagues and friends. Both have contributed ideas and thoughts to my research project besides from their encouragement and support. I have also involved in parts of their research projects, also relevant to mine, resulting in 2 publications of which I am one of co-author. In particular, the paper on thermal drift of the Sierra Scientific's high resolution manometry, of which, I have performed background bench works and data analysis.

My deepest gratitude goes to Mrs Dorothy Ronney and Mrs Janice Arnott who did not just provide administrative support but also constant encouragement and laughter that lighten up my days during stressful periods.

This PhD will not be possible without the scholarship provided to me through the Academic Staffs Higher Education Scheme (ASHES) of Universiti Sains Malaysia for which I am extremely grateful. I would like to take this opportunity to thank my dean, Professor Abdul Aziz Baba and my colleagues from the Department of Medicine who have been very encouraging and helpful.

Last but not least, I would like to thank my wife Siang Ching and my daughter Yu-En who have provided me with support, encouragement and joy during challenging and stressful periods of the project.

## **Author's Declaration**

### **Declaration of Originality**

12 March 2013

This thesis is submitted in fulfillment for the degree of Doctor of Philosophy in gastroenterology. I fully declare that this thesis has been composed by own self, and the work described is my own research.

Yeong Yeh Lee  
**MD MRCP (UK) DTM&H (Lond) MMed**

## List of abbreviations

AMR	anisotropic magnetoresistive
AUC	area under curve
BMI	body mass index
CD	crural diaphragm
CDP	contractile deceleration point
CI	confidence interval
CM	circular muscle (s) of the oesophagus
CSA	cross-sectional area
CT	computed tomography
CV	coefficient of variation
2- or 3-D	2 or 3 dimension
EMG	electromyography
GA	general anaesthesia
GI	gastro-intestinal
GO	gastro-oesophageal
GOJ	gastro-oesophageal junction
GOPG	gastro-oesophageal pressure gradient
GORD	gastro-oesophageal reflux disease
GOR	gastro-oesophageal reflux
<i>H. pylori</i>	<i>Helicobacter pylori</i>
HPZ	high pressure zone
HRM	high resolution manometry
IAP	intra-abdominal pressure
IGP	intra-gastric pressure
IOP	intra-oesophageal pressure
IQR	inter-quartile range
IV	intra-venous
LM	longitudinal muscle of the oesophagus
LMC	longitudinal muscle contraction
LOS	lower oesophageal sphincter
LOSR	lower oesophageal sphincter relaxation
MRI	magnetic resonance imaging
NHS	National Health Service

OR	odds ratio
PACS	Picture Archiving and Communications System
PIP	pressure inversion point
POL	phreno-oesophageal ligament
PPI	proton-pump inhibitor
ROC	receiver operating characteristics
SCJ	squamo-columnar junction
SD	standard deviation
SEM	standard error of mean
TLOSR	transient lower oesophageal sphincter relaxation
UK	United Kingdom
UOS	upper oesophageal sphincter
USA	United States of America
WC	waist circumference
WHR	waist-hip ratio

# CHAPTER 1

## BACKGROUND OF MY THESIS

---

- 1.1 Introduction
- 1.2 Biology of the normal oesophagus
- 1.3 Biological importance of the GOJ
- 1.4 GOJ dynamics during swallows and TLOSRS
- 1.5 Measuring the SCJ and its relevance to GORD
- 1.6 The abnormal GOJ: hiatus hernia
- 1.7 Effects of obesity on the GOJ and GORD
- 1.8 Summary of literature review
- 1.9 Objectives of research

# 1 BACKGROUND OF MY THESIS

## 1.1 INTRODUCTION

Gastro-oesophageal (GO) reflux disease and its complications of Barrett's oesophagus and oesophageal adenocarcinoma have increased markedly in the developed world over the past three decades. This is of particular concern in Scotland as the country has the highest recorded incidence of oesophageal carcinoma in the world.

The reason for the rising incidence of reflux disease and its complications is unknown but the concurrent increase in abdominal obesity may be important. There is a positive association between body mass index (BMI) and both GO reflux (GOR) disease and oesophageal adenocarcinoma but the mechanism of the association is unclear. It has been suggested that the increased intra-abdominal pressure (IAP) associated with a high BMI may increase acid reflux during transient lower oesophageal sphincter relaxations (TLOSRS) and also predispose to hiatus hernia.

TLOSRS are episodes when there is complete relaxation of both the extrinsic component of the lower oesophageal sphincter (LOS) consisting of crura of the diaphragm (CD) and also the intrinsic component comprising the oesophageal smooth musculature. These relaxations last 10 - 50 seconds and are most frequent during the postprandial period. GOR is most common during TLOSRS.

Relatively little is known about the behaviour of migration of the GO junction (GOJ) during TLOSRS. This is due to the fact that the loss of sphincter tone makes the location of the GOJ invisible to oesophageal manometry. Most studies on movement of the GOJ during TLOSRS have applied radio-opaque clips to the squamo-columnar junction (SCJ) and started fluoroscopic screening when a TLOSRS was thought to be commencing. However, the restraints imposed by ionizing radiation exposure markedly limit the information available from this technique. These studies have,

however, indicated marked craniad movement of the GOJ during TLOSRS (median 3 cm).

One of the important risk factors for severe GOR disease (GORD) is the presence of hiatus hernia in which the GOJ is displaced in a craniad direction so that it is above the diaphragmatic hiatus. This abnormality is thought to arise as a result of weakness of the CD and of the phreno-oesophageal ligament (POL) which anchors the GOJ at the diaphragmatic hiatus. The POL consists of elastic fibres and muscle fibres and is thought to be responsible for producing restitution of the GOJ to its correct position within the diaphragmatic hiatus following TLOSRS. The frequency of TLOSRS is similar in patients with vs. without GOR. Besides TLOSRS, other mechanisms may also cause GOR in the presence of hiatus hernia including low LOS pressure, swallow-associated normal LOSR and straining during periods with low LOS pressure.

The primary aim of this research is to study the behaviour of migration of the GOJ during TLOSRS using a novel technique. The migration of the GOJ during TLOSRS and swallows is first characterised in normal healthy volunteers. The behaviour of migration of the GOJ during TLOSRS is then studied in a group of obese and non-obese subjects. It is hypothesised that a dysfunction in the behaviour of migration of the GOJ during TLOSRS in GORD is one of the primary effects of raised IAP and obesity.

A short background to the oesophagus and the complex but an important area of the distal oesophagus before it enters the proximal stomach will be presented. This is the GOJ which forms the gastro-oesophageal barrier to the offensive refluxate from the stomach. With GORD affecting 1 in 5 of the world population, the GOJ is probably the next most important structure besides the heart. Interestingly, the GOJ lies just next to the heart in the chest and right in the centre of the human body. With this important function of the GOJ, an understanding to its anatomy and physiology is crucial. From its humble beginning during the embryo stage, the GOJ develops into an elegant piece of anatomical and physiological marvel. It is maybe this novelty that is also the reason it is brought down to its knees from numerous mechanical offences associated with obesity.

## 1.2 BIOLOGY OF THE NORMAL OESOPHAGUS

### 1.2.1 The common embryonic development

The gastrointestinal tract is formed by two germ layers in the embryo namely the endoderm and mesoderm starting after 3<sup>rd</sup> week of gestation. As the head of embryo develops, the foregut forms from infolding of lateral folds including the rostral part of yolk sac which later consists of oral cavity, pharynx, oesophagus, stomach and proximal small intestine. By 4<sup>th</sup> week, the oesophagus rapidly elongates due to rapid growth of the head region. By 7<sup>th</sup> week, the oesophagus is an easily recognized muscular tube extending from tracheal bud dorsal to the heart and down into septum transversum (which forms the diaphragm) and the stomach recognised as a saccular structure. The mesoderm in the 10 mm embryo forms the circular muscle layer of oesophagus and contributes to the formation of CD and POL. The longitudinal muscle of oesophagus and circular muscle of stomach develop much later and only at 90 mm stage the muscular layers of oesophagus and stomach resemble that of an adult.

The oesophagus during the first and early second trimester is lined by undifferentiated stratified columnar epithelium of approximately three cells deep. It is later replaced by stratified ciliated columnar epithelium at about 90 mm stage except at both ends of the oesophagus which are occupied by small area of tall simple columnar epithelium. Subsequently in early third trimester, the stratified ciliated columnar epithelium in mid-oesophagus is replaced by stratified squamous epithelium which later extends to replace the entire oesophagus by term except for some small residual areas in the upper oesophagus. In the third trimester, there is a small area of undifferentiated columnar epithelium which appears glandular but non-secretory lying between the squamous epithelium and the gastric oxyntic mucosa. This is described as the “cardiac mucosa” by de Hertogh et al. (2003) and Derdoy et al. (2003) and the “transitional zone” by Park et al. (2003) and Zhou et al. (2001).

The fetal “cardiac mucosa” is a misnomer since this epithelium is found in the intra-abdominal segment of the oesophagus and not in the stomach. This is only true if the angle of His is accepted as the landmark of the GOJ.

### 1.2.2 Anatomy and physiology of the oesophagus

The oesophagus starts from the cricoid cartilage, passes through the posterior mediastinum and lies dorsal to the trachea, heart and the aorta. It then extends a few centimeters below the diaphragmatic hiatus before joining with the stomach (DeNardi and Riddell, 1991). The overall length of the oesophagus varies with the length of trunk or sexes but in an average normal adult, it is approximately 23 - 25 cm (**Figure 1.1**). The incisor tooth is a common reference point used for endoscopic and manometric measurement. The oesophagus length in a normal adult is approximately 40 cm from the incisor teeth but it can vary from 30 to 43 cm. The length of oesophagus in children correlates closely with their height. It is closed by the upper oesophageal sphincter (UOS) proximally and lower oesophageal sphincter (LOS) distally.

The primary physiology of the oesophagus is transport of an ingested food bolus into the stomach and this is mediated by a complex neuromuscular process called a swallow/deglutition or primary peristalsis. Swallowing also allows the clearance of refluxed gastric contents. The saliva that is transported from the mouth during swallows helps to neutralise any trace of acid reflux at the distal oesophagus. Primary peristalsis is triggered by the presence of food bolus in the pharynx and the vagal afferent sends neural impulses to the swallowing centre in the mid-brain. The subsequent motor event is initiated via efferent vagal nerve to the muscles in the oesophageal wall. In a secondary peristalsis, an autonomic response is generated following the distension of the distal oesophageal lumen and this is mediated by the local enteric nervous system. It is an important mechanism in clearing of acid volume following acid reflux (Schoeman & Holloway, 1995).

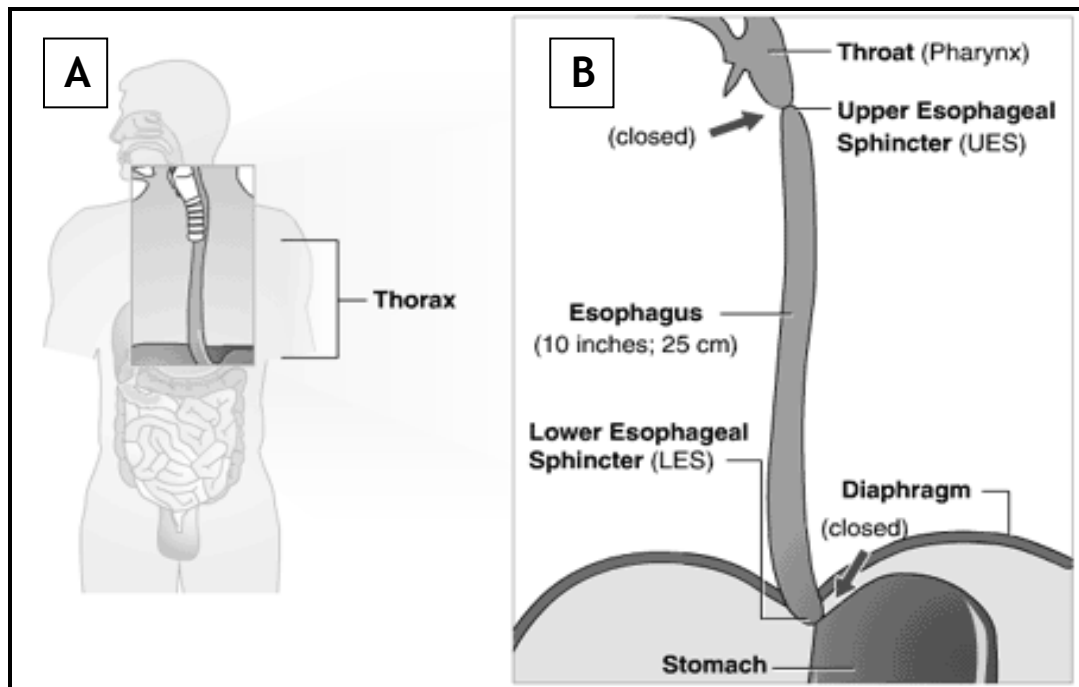


**Figure 1.1:** Anatomy of the oesophagus. A: a view of the thorax, B: the expanded view of the A showing the anatomy of oesophagus.

The oesophagus in cross-section consists of concentric layers of tissue (**Figure 1.2**) including the innermost mucosa, the submucosa, the muscularis propria and the adventitia. In a fasting state, the mucosa which consists of stratified squamous epithelium is thrown into folds which can be fully expanded during endoscopy from air insufflation. The mucosa transits into columnar epithelium of the stomach at the SCJ.

The muscular coat of oesophagus in the muscularis propria consists of an outer longitudinal layer which is thicker and inner circular layer which is thinner. This is in contrast with the rest of the gastrointestinal tract. The longitudinal layer consists of two bands of muscles originating at the cricoid cartilage. These bands of muscles extend dorsally and then become continuous with the outer longitudinal layer of the stomach at the GOJ. The circular muscle layer of the oesophagus continues over the stomach and divides in the region of the cardia to form the middle circular and the inner oblique layers. The inner oblique layer passes over the angle of His and crosses at right angles with the middle circular layer to form a muscular ring (collare Helveti). This ring may play a role in the competence of the GOJ.

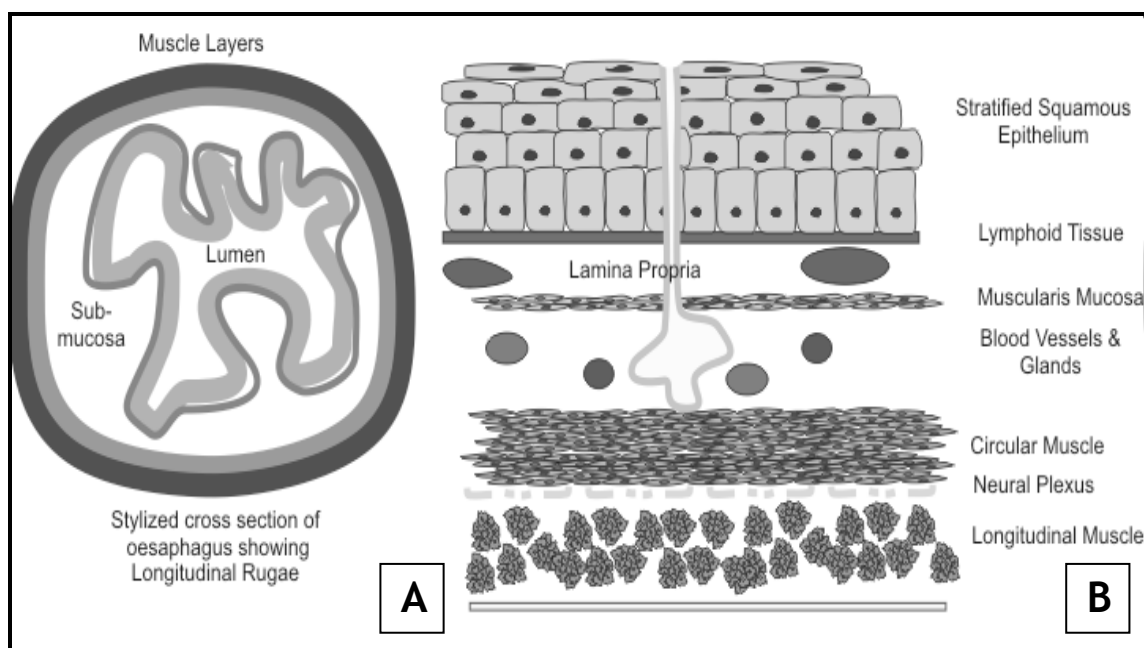


**Figure 1.2:** A cross-section of the oesophagus. A: cross-sectional view, B: layers of the oesophageal wall.

The muscles are fully striated in the proximal 2 - 6% and fully smooth in the distal 50 - 60%. At the transition zone near the arch of the aorta, there is a mixture of both striated and smooth muscles and this zone is seen as a band of low pressure with high resolution manometry (HRM). The speed of peristaltic propagation can vary along the length of the oesophagus which depends largely on the muscle type. The striated muscles in the proximal oesophagus allow a higher velocity of peristaltic propagation than the smooth muscles in the more distal oesophagus.

The contractions of the circular muscles (CM) generate circumferential tension, peristalsis and bolus transport. The longitudinal muscles (LM) shorten the oesophagus locally during peristalsis. Auerbach plexus of the local enteric nervous system which sits between the two muscle layers, forms the nerve supply for the muscles. The human oesophagus can shorten by about 7% overall during a swallow with most of the shortening occurring at the distal oesophagus (approximately 18%).

During swallowing, contractions of the CM are coordinated closely with the LM and the contractions are sequential following a peristaltic wave. The LM contraction (LMC) temporally precedes the CM contraction wave throughout the oesophagus but the peak contraction amplitude occurs concurrently for both the LM and the CM (Mark A Nicosia *et al.*, 2011). The local shortening provided by LMC provides a mechanical advantage to bolus transport by compressing the CM and increasing their density and total muscle tension. This therefore reduces the total required contractile force. Indeed, peristaltic transport is purely mechanical in nature and is allowed by favorable pressure gradients created by well-oiled muscle machinery in the oesophagus.

Deglutitive inhibition is an elegant piece of oesophageal physiology that requires a well-coordinated neuromyogenic mechanism, failure of which underlies motor disorders including achalasia and nutcracker oesophagus (Meyer, Gerhardt, & Castell, 1981; Sifrim & Jafari, 2012). The peristaltic activity of a swallow is inhibited by a second swallow if the interval between swallows is inadequate for the first peristalsis to complete (interval usually <10 s). The inhibition affects both the LM and the CM and the period of inhibition is roughly inversely proportional to the propagation speed of the inhibited peristaltic wave (Guoxiang Shi *et al.*, 2003).

## 1.3 BIOLOGICAL IMPORTANCE OF THE GOJ

### 1.3.1 Defining the normal GOJ

LOS marks the end of distal oesophagus of which the caudal end of the sphincter marks the start of the GOJ. Approximately 2 cm of the oesophagus lies below the diaphragm and it contains the abdominal portion of LOS. Anatomy surrounding this region is remarkably complicated (**Figure 1.3**). The actual defining landmark of the GOJ is still unknown and remains debatable. The GOJ can be defined physiologically using manometry techniques or through anatomical landmarks (endoscopy or surgical specimens) and microscopically.

Manometry is a technique allowing measurement of pressure within the hollow organs and sphincters. Details of this technique are given in section 1.4.2 and section 2.6. Oesophageal manometry can readily identify the high pressure zone (HPZ) which consists of circumferential pressure exerted by the LOS and CD. The lower border of LOS defined manometrically marks the start of the junction. However, the manometrically defined lower border of LOS can be influenced by many factors including manometric techniques used, changes in intragastric pressure (IGP) related to meals or other causes of raised IAP and various diseases involving the GOJ for example GORD and hiatal hernia.

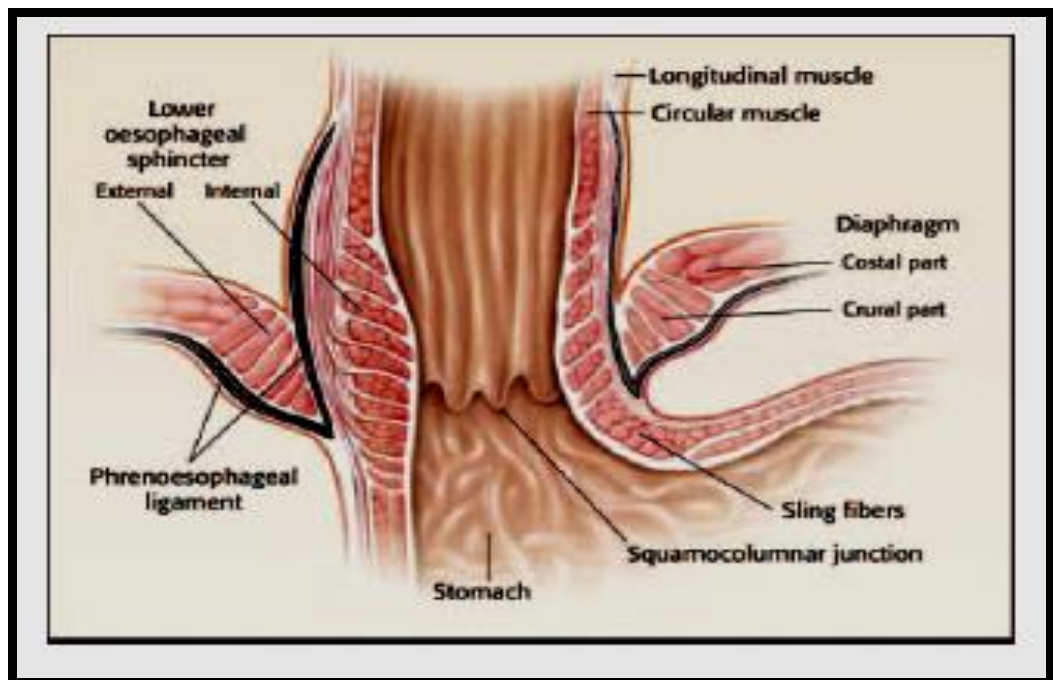


**Figure 1.3:** A complex anatomy of the normal GOJ. Adapted with permission from GI motility online 2006 (doi: 10.1038/gimo14).

Anatomically, the GOJ begins from the upper border of peritoneal reflection from the stomach onto the diaphragm or at the level of angle of His. The use of both landmarks is limited in clinical practice and is probably more useful in resected surgical specimens. Endoscopic landmarks are also used to define the GOJ. The upper margin of diaphragm indentation and

proximal margin of gastric folds are useful landmarks of the GOJ and closely approximate the physiological definition (< 5 mm) (Wallner, 2009). The SCJ or Z line is another landmark easily seen endoscopically except during severe oesophagitis and Barrett's oesophagus (**Figure 1.4**). It marks the transition from the whitish squamous epithelium to the pinkish columnar epithelium. The Z line often lies within the LOS at approximately 1 - 2 cm above distal border of the LOS.

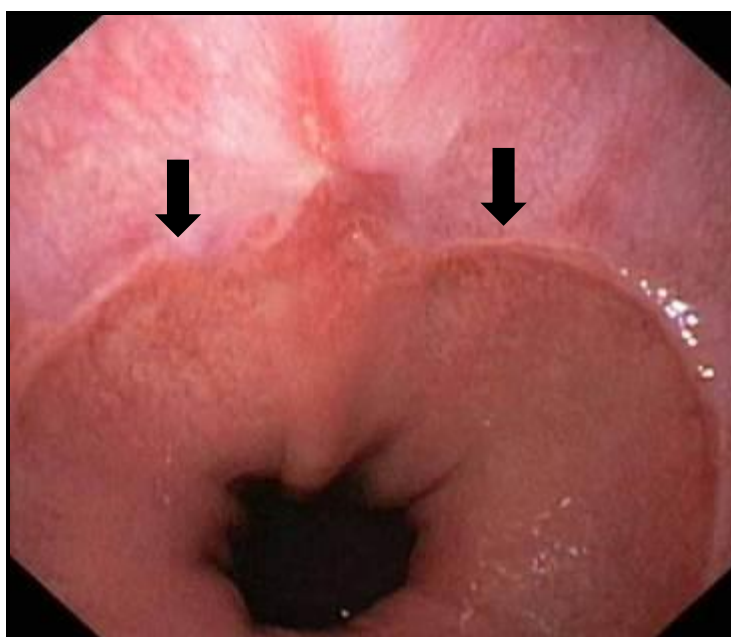


**Figure 1.4:** SCJ or the Z line seen during upper endoscopy (black arrows).

Prior to 1957, the accepted histological definition for the GOJ was the end of squamous epithelium or the SCJ. However Allison and Johnstone in 1953 found a columnar-lined oesophagus distal to the SCJ from resected specimens of sliding hiatus hernia (Allison and Johnstone, 1953). The question is whether the columnar-lined epithelium is normal or abnormal oesophageal tissue? Chandrasoma and co-workers, in their autopsy studies, have elegantly shown that 56% of patients did not have a cardiac mucosa and the overall length of cardiac and oxyntocardiac mucosa was less than 1 cm between the SCJ and gastric oxyntic mucosa (Chandrasoma et al., 2000). The authors reach the conclusion that these epithelia represent metaplastic oesophageal

tissue rather than gastric tissue, and if this is accepted, then the true GOJ is the proximal limit of gastric oxyntic mucosa.

The definitions so far do not always coincide with each other and they can be poorly reproducible between patients. In addition, these external definitions are often poorly concordant with the microscopic appearance. Currently, endoscopic landmarks do not adequately define the GOJ but this may change in future. The availability of new technologies, for example the confocal microscopy can allow a virtual histological evaluation of the mucosa and therefore potentially provides a better evaluation of what is termed the GOJ.

## **1.3.2 Biological constituents and physiology of the GOJ**

### **1.3.2.1 Intrinsic lower oesophageal sphincter**

The intrinsic LOS is an important GO barrier to reflux of gastric contents and serving this function necessitates a HPZ maintained by tonic contraction. With a length of approximately 3 - 4 cm, half of its length lies distal to the SCJ and therefore is intra-abdominal in location (**Figure 1.3**) (R H Holloway, 2000). A normal resting sphincter pressure is approximately 10 - 30 mmHg relative to the IGP. Its peak pressure corresponds closely to the level of the SCJ and can increase in response to increases in IAP similarly to the CD. This is important in order to maintain the integrity of the GOJ during periods of abdominal straining.

The tonic contraction operates through myogenic and neurogenic mechanisms but the major mechanism in humans appears to be neurogenic. This is mediated through the cholinergic nerves with its activity reduced by more than 2/3 with the administration of atropine. Myogenic tone is provided by intracellular calcium which allows a generation of continuous contractile action potentials without fatigue. As such, the activity of intrinsic LOS can be greatly affected by meal, time of the day, circulating peptides/hormones and drugs. It has the lowest pressure after meal and the highest pressure at night time.

### 1.3.2.2 Crural diaphragm

Anatomically, the diaphragm is divided into the costal part which originates from the ribs and the crural part or CD (**Figure 1.3**) which attaches to the vertebral column. Both have separate embryological origin; the CD arises from the dorsal mesentery of oesophagus and the costal diaphragm arises from myoblasts originating from the lateral body wall (Langman, 1975).

The diaphragmatic hiatus consists of the CD which forms a muscular canal in the top half (2.5 cm) of the intra-abdominal segment of the oesophagus. The lower half (2.5 cm) forms a gutter which opens anteriorly. This gutter is closed anteriorly by the POL and left lobe of liver which therefore also forms a canal, the so-called “phrenohepatic canal” (Delmas and Roux, 1938). The upper half of the muscular canal consists of predominantly right crus in most of cadaveric dissection studies (Delattre et al., 1985). When viewed from coronal section, the diaphragmatic canal resembles an hourglass with a narrow middle part.

The CD is supplied by the right and left inferior phrenic arteries. The left inferior phrenic artery courses more medially than the right inferior phrenic artery and is therefore more easily injured during surgery. The posteromedial branches of the phrenic nerves supply the CD. The crural muscles receive bilateral phrenic motor innervation. This means that if one of the phrenic nerves is injured, the crural function is still maintained. The muscles surrounding the diaphragmatic hiatus (CD) consists of slow-twitch oxidative fibres which generate a less fatiguing tonic contraction (Riley and Berger, 1979).

In the 1950's, even though many investigators believed in the anti-reflux action of the CD, this could not be proven because of the lack in appropriate experimental techniques (Ingelfinger, 1958). Two great challenges in studying the diaphragm include its movement during respiration and its anatomical superimposition with intrinsic LOS. Physiological measures of intraluminal pressure at the GOJ alone cannot separate the contributions from both structures unless in the presence of hiatus hernia.

The first evidence for the role of CD being a main component of the LOS pressure was shown in cats where the respiratory-induced oscillations in the cat's LOS pressure was proven to result from the diaphragm electrical activity (Boyle et al., 1985). The definitive study comes from Klein et al in 1993. In that study, the HPZ detected by using manometry in 10 patients had maintained sphincter-like properties despite the resection of intrinsic LOS. This suggests that the HPZ is the CD which acts as a sphincter in the absence of intrinsic LOS. Contraction of the CD during respiration increases the LOS pressure by approximately 5 - 10 mmHg but may reach 50 - 150 mmHg with deep inspiration and straining.

### 1.3.2.3 Phreno-oesophageal ligament

The significance of POL on the function of the GOJ still remains controversial. It receives very little attention from any anatomy textbooks. POL is a ligament or a membrane (Laimer's membrane) that arises circumferentially from the margins of the diaphragmatic hiatus and inserts into the wall of oesophagus at approximately the level of the SCJ.

Macroscopically, the POL has a thickness of 1 - 2 mm, widest (1.5 - 2.0 cm) on either side of the oesophagus and narrowest (1.0 - 1.5 cm) anteriorly and posteriorly. It appears as a continuation from transversalis fascia below the diaphragm, and as the ligament passes medially, it divides into a thicker upper leaflet and thinner lower leaflet with a potential triangular space in between (the paraoesophageal space). The lower leaflet appears attenuated or even absent in older subjects.

Histologically, the POL forms two layers with contribution from the endothoracic fascia (which was not seen macroscopically since it is thinner) as well as the transversalis fascia which is thicker. There is abundance of elastic and collagen fibres in the POL which are arranged in a wavy parallel fashion, with some scattered smooth muscle and fibroblasts. The ligament is richly supplied with blood vessels, lymphatics and nerve fibres.

The upper leaflet of POL inserts deeply into the muscular layer of the oesophagus but the lower leaflet only ends at the adventitia layer. Older

subjects particularly in those above 60 years old tend to lose their collagen fibres and a huge gain in adipose tissue. Such structural changes might result in disorganization of elastic recoil, a decrease in tension resistance and therefore a predisposition to hiatus hernia.

### 1.3.2.4 Angle of His and flap valve

The angle of His is a sharp angle on the greater curvature aspect of the GOJ formed by the oblique entrance of the oesophagus into the stomach (**Figure 1.5**) (L D Hill and R A Kozarek, 1999).

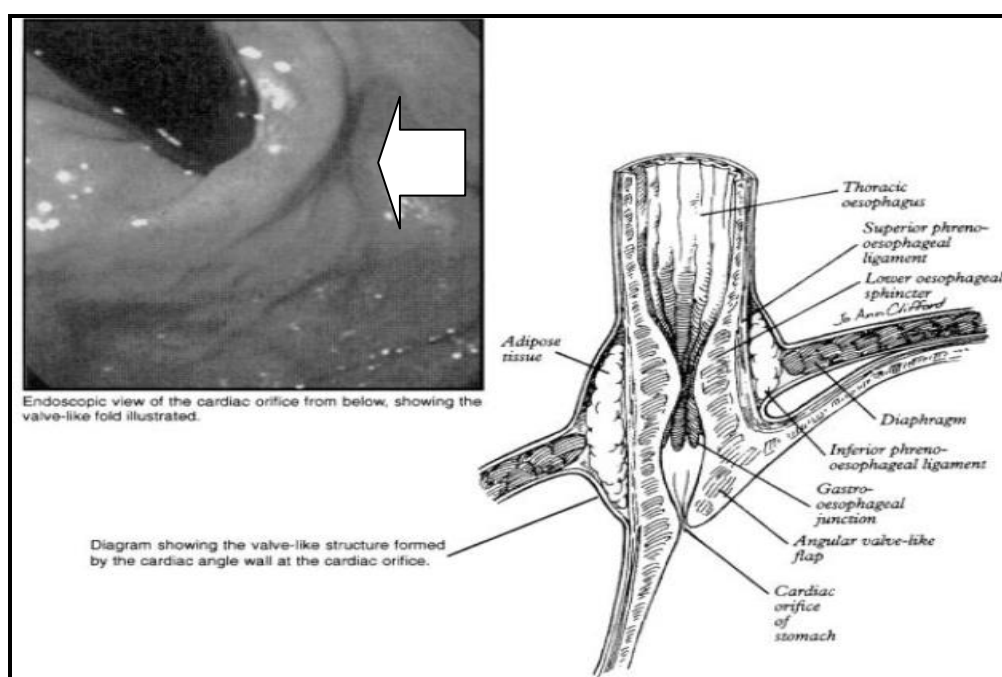


**Figure 1.5:** The angle of His is extended within the lumen as a large fold/flap valve seen prominently from endoscopy (white arrow) (L D Hill and R A Kozarek, 1999).

It has been shown in cadavers that angle of His contributes to the flap valve effect which enhances the GOJ integrity (Thor *et al.*, 1987). The flap valve is lost with GORD and in hiatal hernia which further proves its existence (Xirouchakis *et al.*, 2009).

A novel 3D MRI imaging recently allows for a more detailed quantitative assessment of the anatomy surrounding the GOJ and proximal stomach (Roy et al., 2012). The angle of His became more acute on expiration but it did not change with meals. However changes in the proximal gastric morphology, a result of distension with food, could augment the intra-abdominal segment of the GOJ and therefore increasing the effectiveness of the flap valve.

## **1.4 GOJ DYNAMICS IN SWALLOWS AND TLOSRS**

### **1.4.1 Physiology of the GOJ in swallows and TLOSRS**

The GOJ plays an important role as the GO barrier to the reflux of gastric content. Many studies have been reported on the role of both intrinsic and extrinsic components of the LOS in maintaining the integrity of the GO barrier. The physiology of the LOS can be studied in detail due to the emergence of manometry techniques in recent decades which allow precise measurement of function of the circular smooth muscle. The invention of a sleeve sensor allows a more precise measurement on the function of the LOS since the relative movement of the GOJ as a result of swallowing and respiration can be compensated.

What is less known about the GOJ is its physiology during swallowing and TLOSRS. Swallowing is a complex neuromuscular process with both voluntary and involuntary phases and it involves the mouth, pharynx, UOS, oesophageal body and the GOJ. Its function is to receive the food bolus and to propel it down into the stomach. This can be achieved with a well-coordinated process of peristalsis and the subsequent opening of the GOJ that allows the food bolus to enter the stomach. Less is known about how exactly the GOJ functions during the food passage into the stomach. The positive GOPG will force the gastric contents into the oesophagus as the GOJ opens during swallowing but the GOJ overcomes this by the formation and emptying of the phrenic ampulla. What precisely happens during the formation and emptying of the phrenic ampulla is still very much elusive. This will be discussed in subsequent sections.

Similarly with TLOSRS, less is known about what exactly happens at the GOJ during normal physiology. It is known that TLOSRS is the most important mechanism underlying GORD, and this has been shown in numerous published reports over the years (Peter J Kahrilas, 2003). How a normal physiological process like TLOSRS becomes pathological is unknown. TLOSRS involves firstly a trigger from the distended proximal stomach after a meal. This trigger subsequently causes a series of well-coordinated processes involving the relaxation of the LOS, CD and POL to allow the opening of the GOJ and then passage of gastric contents in an oral direction for example the passage of air during belching. The precise nature of the processes involving the LOS, CD and POL is still under investigation and the following sections will provide a background to its mechanism.

Firstly, a brief introduction to the technique of manometry is given in the next section.

## **1.4.2 Introduction to oesophageal manometry**

Manometry is a technique allowing measurement of pressure within hollow organs and sphincters and it therefore provides an assessment of their neuromuscular activities. Oesophageal manometry measures the peristaltic activity that drives bolus transport from the pharynx into the stomach as well as function of upper and lower oesophageal sphincters.

The first attempt to measure oesophageal function was the use of balloon-tipped catheters in the 19<sup>th</sup> century. Later, pneumo-hydraulic perfusion systems and solid state systems were introduced in the 20<sup>th</sup> century and measurement accuracy has since improved (Ayazi & Crookes, 2010). However, the measurement of sphincters remained difficult due to their movement during swallows and respiration. The introduction of station pull-through technique by Fyke et al. in 1956 could sample the LOS pressure reliably but the method was time consuming and often not well-tolerated by patients (Code *et al.*, 1956). The Dent sleeve sensor was introduced in 1976 and it measures the maximal LOS pressure along its length regardless of sphincter movement (Dent, 1976).

High resolution manometry (HRM) arrived in the late 1990s when Clouse et al. introduced the concept of topographic or contour plots (**Figure 1.6**) and the development of micro-manometric solid state assemblies allowing multiple sensors in one catheter (Clouse and Staiano, 1991). Having done so, with close proximity of sensors to each other, the intraluminal pressure measurement becomes a spatial continuum after interpolation between sensors. The innovative technology has been improved for practical clinical use and has been marketed successfully by a few companies in the US and Europe. This technology has since gained global attention and widespread use among oesophageal researchers.

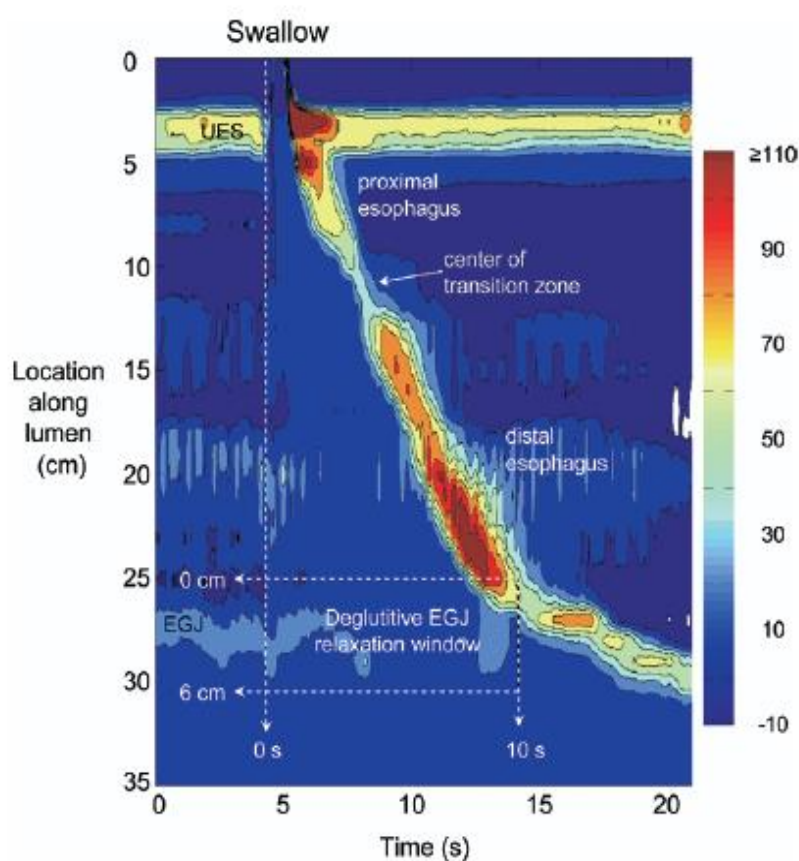


**Figure 1.6:** A typical colour pressure topography of a swallow in a normal subject using the HRM system (Sierra Scientific Instruments Inc., US) (Peter J Kahrilas and Daniel Sifrim, 2008a).

For example, the 36 solid-state, circumferentially sensors spaced at 1-cm interval in a 4.2 mm diameter catheter marketed by Sierra Scientific Instruments Inc., LA, US (Manoscan® brand) is one of the most advanced and

widely used HRM system in the world. This is also the system used in our experiments (chapter 2). With the closely-spaced sensors, all parts of the oesophagus can be monitored simultaneously without the need for pull-through or repositioning (unlike conventional water-perfused system). The sensors measure over a length of 2.5 mm, with each-cm having an array of 12-microtransducers (Tact-array technology) circumferentially placed. The outputs from these microtransducers are then averaged to provide a mean value for that level.

The system incorporates sophisticated algorithms to display the huge amount of manometric data from all sensors as pressure-time topography plots (**Figure 1.6**) and indicated as colour continuums. The technique allows a precise demonstration of relative timing of sphincter relaxation and segmental muscle contraction. Reproducible measurements of sphincter pressure can be made, and is not confounded by the CD or movement of the sphincter. Several studies have shown the advantage of HRM over conventional manometry with sleeve sensor in measuring the lower sphincter relaxations and reflux events (Rohof, Boeckxstaens & Hirsch, 2011; Roman, Zerbib, Belhocine, *et al.*, 2011; Pandolfino, Ghosh, Zhang, *et al.*, 2006).

The colour contour plots produced are easily appraised by busy clinicians and this is greatly aided with computer software. With the availability of this new technique, motility disorders have since been better defined and more recently, the Chicago classification for motility disorders has resulted from this new technology (J E Pandolfino *et al.*, 2009). Other advantages include increased patient comfort without the need for pull-through or repositioning, reduced examination time (26% less time in a study), and fewer recording artifacts (Sadowski and Broenink, 2008). In addition, it is easier to educate patients with colour plots than conventional lines. Clinical management also improves with increase ease in diagnosis, less inappropriate investigations or treatment (Ayazi and Peter F Crookes, 2010).

The disadvantages of the Manoscan® HRM system include the high cost and the technology is liable to thermal effect (John E Pandolfino, Ghosh, *et al.*, 2006). The liability to thermal effect is due to the capacitive-type sensors used in the catheter. Briefly, capacitive sensors are based on capacitive

coupling where two plates are placed on either side of an insulating dielectric material (**Figure 1.7**).

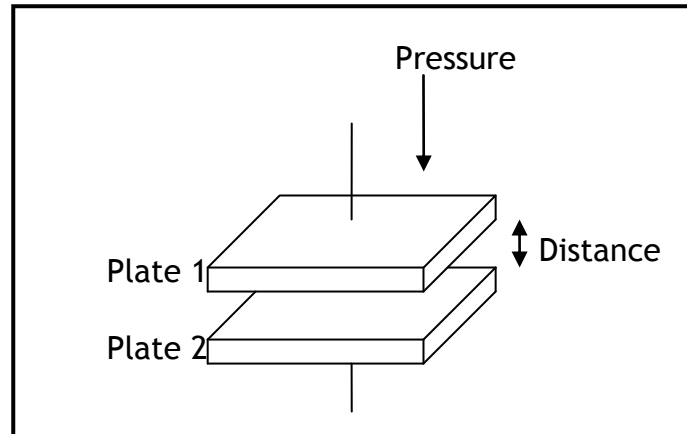


**Figure 1.7** : Capacitive sensor.

The distance between two plates varies with applied pressure, which when measured, corresponds to a value of the applied pressure. Offset error occurs when a constant value is added to the output value, effectively shifting the baseline and all other values. Temperature change is the main contributor to this error, which can be reduced by calibrating at the temperature in which the sensor is to be used. In addition to offset error, there is also a baseline drift as a result of the “creep” and “hysteresis” phenomenon. It is beyond the scope of this manuscript to fully explain these phenomena. Basically, “creep” is deformation of material under stress over time and “hysteresis” is the material not returning to its original shape over time. Fortunately, the thermal effect of sensors is almost linear and correction factors can be applied to re-establish the zero reference. The correction algorithm has been put in place in the Manoscan® HRM system by the manufacturer.

The latest development in the field of HRM technique is high-definition monometry which can provide an almost 3-dimensional view of the GOJ (**Figure 1.8**) (Peter J Kahrilas, Ghosh, *et al.*, 2008). Most importantly, the CD

can be isolated from the GOJ in terms of its axial position, radial asymmetry and magnitude. This new system will have closer spaced sensors, with 4 banks of 4 rings each where the rings are spaced 3 mm apart and the banks 4 mm apart. Each ring has 8 radial sensors and therefore 128 independent pressure recordings (8 sensors x 4 rings x 4 banks) spanning 4.8 cm. More studies are on-going with this new technology.

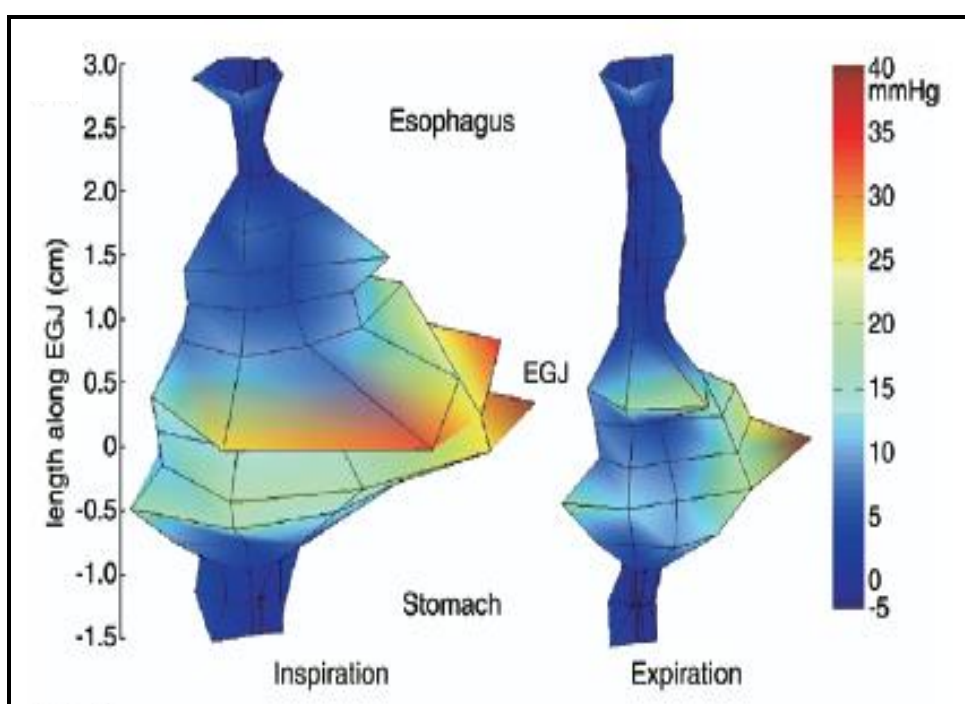


**Figure 1.8:** High definition recording of the GOJ using the new 3-D HRM (Peter J Kahrilas, Ghosh, *et al.*, 2008).

### 1.4.3 The normal swallow

Swallow (or deglutition or primary peristalsis) is a primary physiology of the oesophagus. A brief overview on the physiology of swallowing has been given in section 1.2.2. The current section discusses briefly on the manometric characteristics of a normal swallow. The focus of this section is the behaviour of the GOJ as the peristalsis arrives at the distal oesophagus.

### 1.4.3.1 Pressure and dynamics of the GOJ in a normal swallow

It is not the intention of the current section to provide an in-depth discussion on the physiology and pressure characteristics of a swallow. This has been covered in other published papers (Diamant, 1989; Cook, 1991). Instead, the current section provides an overview to the pressure dynamics of the GOJ in a normal swallow with insights from the new HRM technique.

Both swallows and TLOSRS exhibited similar LOS relaxation characteristics, and it is important to have objective definitions allowing a distinction between the two. Holloway and colleagues were the first to objectively define manometric characteristics of LOS relaxation during TLOSRS and how these characteristics were different from swallows (R H Holloway *et al.*, 1995). In the study, swallow-induced LOS relaxation was determined in dry and wet-swallows using a sleeve sensor. It was found that the onset of LOS relaxation usually started after swallowing with a minority started before. The fall in LOS pressure was initially rapid, followed by a slower reduction as it reached the nadir pressure. The duration of LOS relaxations was almost less than 7 s unless in failed swallows, slowed swallows and multiple rapid swallows. The nadir pressure of the LOS during swallows was almost always above the gastric pressure.

With the availability of HRM and e-sleeve function, the GOJ pressure and morphology can be better defined (John E Pandolfino, Ghosh, *et al.*, 2006). The LOS relaxation parameters measured using HRM (mentioned above) were similar to conventional manometry. The concept of integrated relaxation resistance (IRR) is proposed by the authors to be a more clinically useful measure for GOJ resistance during swallows. The measure of IRR incorporates both duration and e-sleeve relaxation pressures (normal mean 1.3 mmHg/s). In addition, the HRM permits a more precise LOS pressure examination during respiratory excursion due to a better appreciation of movement of the CD (approximately 0.85 cm during inspiration) and a more precise measure of length of the LOS (mean 3.7 cm).

Distal oesophageal shortening is another important measure during swallows. The manometry technique allows measurement of circular muscle

function but not longitudinal muscle function. The behaviour of shortening during peristalsis was studied in 8 subjects with concomitant manometry and fluoroscopic evaluation of applied oesophageal clips (G Shi *et al.*, 2002). During primary peristalsis, the most proximal segment began to shorten about 1 s after onset of LOS relaxation and achieved maximal shortening about 3 s later. The most distal segment achieved more shortening than proximal segment and it occurs concurrently with the arrival of peristalsis and termination of LOS relaxation. With secondary peristalsis, rather than contracting sequentially, both proximal and distal segments began to shorten 2-3 s after onset of LOS relaxation. Again, the distal segment achieves more shortening than proximal segment with secondary peristalsis. This distal shortening is probably a part of LOS relaxation process. The simultaneous pattern of shortening during secondary peristalsis was similar to TLOSRS suggesting a similar control mechanism between the two processes.

#### 1.4.3.2 What is phrenic ampulla?

There is a region in the GOJ distal to the insertion of POL that has always been a mystery in terms of anatomy and function. The multiple names attached to this region including abdominal oesophagus, empty segment and phrenic ampulla emphasized its controversy. This region has a length of approximately 3 - 4 cm below the SCJ.

During shortening of oesophagus in swallows, this region will tent through the diaphragmatic hiatus and is seen as a globular structure on radiographs termed as the “phrenic ampulla” (Friedland, 1978; Clark *et al.*, 1970). A study by Lin *et al* suggests that the phrenic ampulla is a physiologically distinct region from the tubular oesophagus (Lin *et al.*, 1995).

Using concomitant intraluminal manometry and videofluoroscopy technique, the formation and emptying process of the ampulla was studied in detail (**Figure 1.9**). In 18 healthy volunteers, a water-perfused manometer with 8 recording sites at the GOJ was passed nasally and 10-ml barium swallows were then imaged using video-fluoroscopy. The phrenic ampulla formed as the peristaltic wave reached the GOJ (**Figure 1.9**).

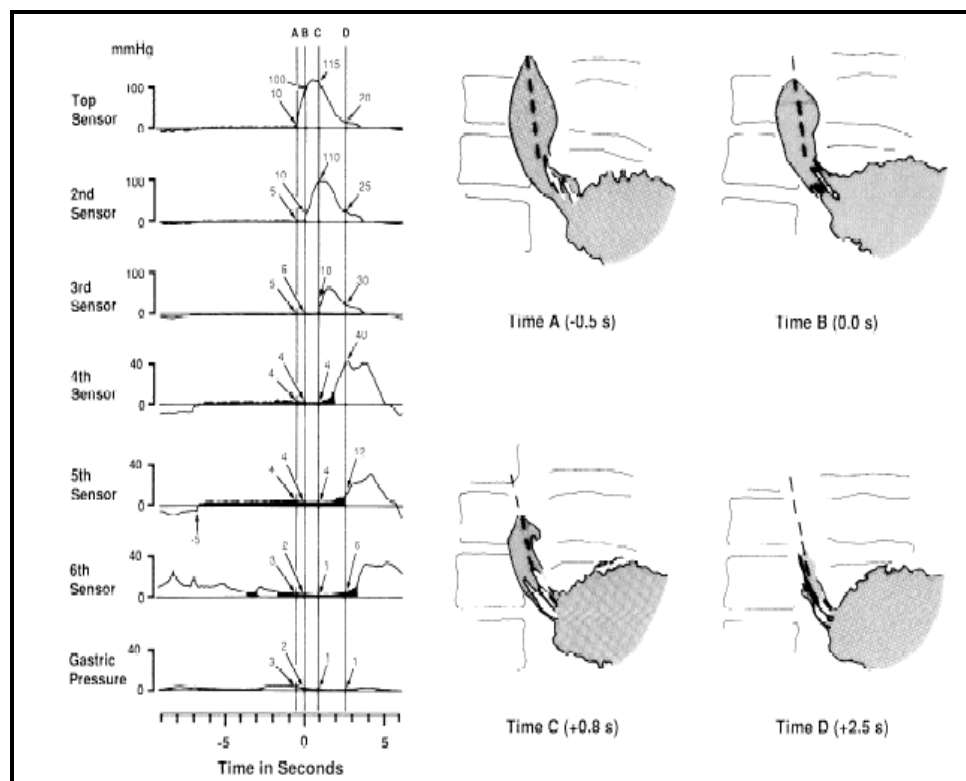


**Figure 1.9:** Intraluminal manometric recording (left) and videofluoroscopic imaging (right) of the GOJ during a standard 10-ml barium swallow. Position of each manometric sensor is marked by a tantalum bar (dashed line). Vertical lines on the manometric recording correspond to times A-D of fluoroscopy. Shaded segments on the manometric recordings indicates times that sensor was recording intrabulus pressure (Lin *et al.*, 1995).

This was indicated by the transition from an acute-angled inverted “v” of the oesophagus to a widened inverted “v” (Figure 1.9 - Time A→B). The formation of the phrenic ampulla could be shown more clearly when abdominal compression and Mueller’s were performed since both maneuver increased the outflow resistance and thereby causing a more prolonged ampulla emptying process. It was also found that the propagation velocity during the ampulla emptying was much slower when compared to a peristalsis wave being 1 cm/s vs. 4 cm/s. The mechanism of emptying of the ampulla was more pressure-driven rather than peristaltic-driven characteristic of the tubular oesophagus. Finally, the contact pressure within an ampulla was much lower when compared to within the oesophagus (40 mmHg vs. 80 mmHg).

These behaviors are similarly seen in a small reducing hiatal hernia. As the hernia enlarges, the process becomes more prolonged and less efficient. The authors further suggest that the failure of POL with age and degeneration leads firstly to the enlargement of phrenic ampulla and eventually a non-reducing hiatal hernia.

### 1.4.3.3 GOJ movement and the phrenic ampulla

With the advent of HRM and a more recent development, 3D-HRM, the physiology of phrenic ampulla formation and emptying could be studied in more detail (Kwiatek *et al.*, 2011). The contractile deceleration point (CDP) is a landmark on the pressure topography where the peristaltic wave slows down and it signals the formation of the phrenic ampulla. This was proven using concomitant recording of the solid state HRM and video-fluoroscopy in 18 healthy subjects (J E Pandolfino *et al.*, 2010) (**Figure 1.10**).

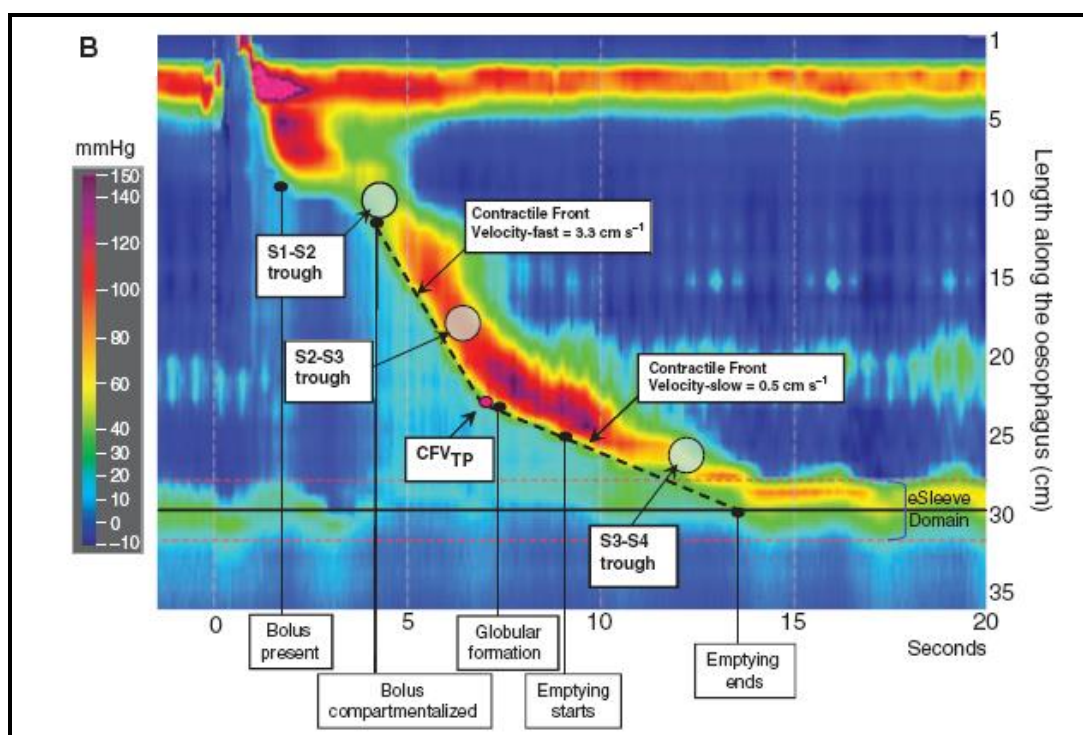


**Figure 1.10:** High resolution manometric tracing of a normal swallow. The red dot indicates the CDP where the faster contractile front velocity (CFV) of peristalsis slows down at the GOJ when the ampulla forms. Descriptions on the formation and emptying of the ampulla are shown in text-boxes (Kwiatek *et al.*, 2011).

In 15 normal subjects, the movement of the clip which was placed at the SCJ was imaged using fluoroscopy during ampulla formation and emptying and this movement was superimposed with the 3D-HRM tracings (Figure 1.11) (Monika A Kwiatek *et al.*, 2012). Proximal migration of the SCJ reached 1.5 cm above the hiatal centre at the onset of ampullary emptying and at the time of the CDP. The SCJ reached its peak amplitude of 1.6 cm at approximately 25% of ampullary emptying time.

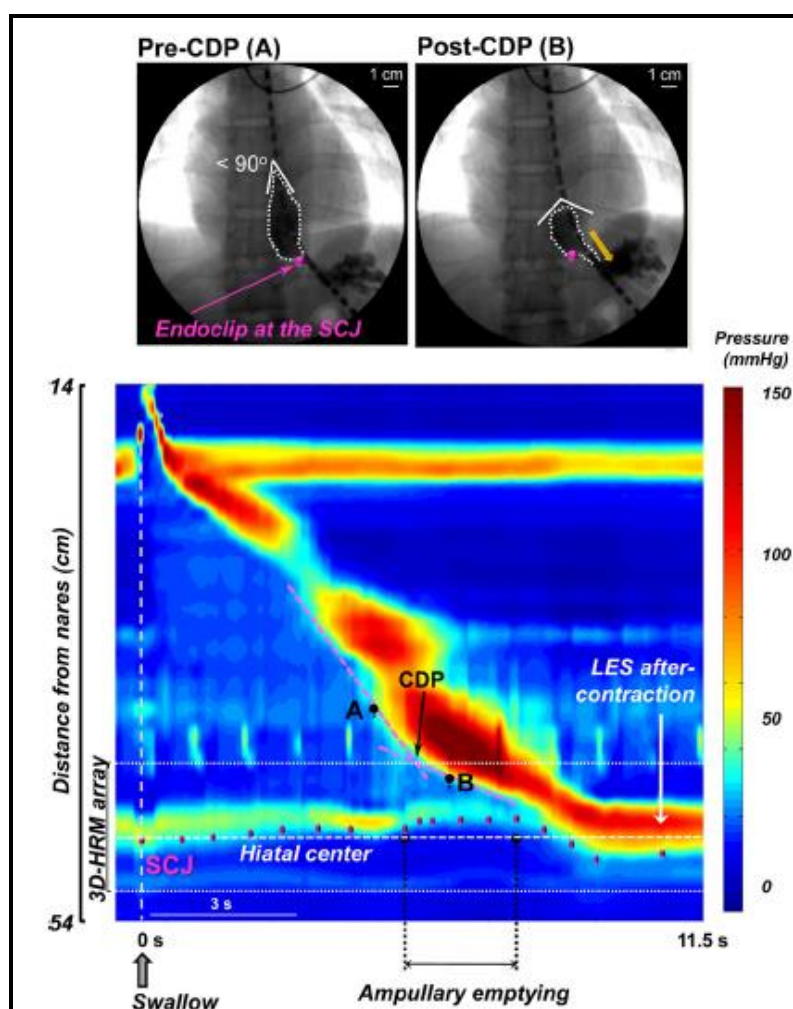


**Figure 1.11:** 3D-HRM and fluoroscopy tracings superimposed by movement of the SCJ. Before CDP at point A, the inverted v of a propagating peristaltic wave can be seen at an acute angle on the fluoroscopy and the acute angle widened substantially post-CDP at point B. The magenta dots indicate the movement of the SCJ during the ampulla formation and emptying phase (Kwiatek *et al.*, 2011).

## 1.4.4 TLOSRS

### 1.4.4.1 A paradigm shift in traditional views

Prior to 1980, it was thought that GOR was a consequence of a weak LOS. However, studies in the 1980s had shown that most reflux events in normal subjects and those with reflux oesophagitis occurred during brief intermittent LOSR rather than because of persistently weak LOS tone.

This led to a paradigm shift in thoughts about mechanisms underlying acid reflux disease, that abnormally frequent reflux was a result of TLOSRS rather than LOS dysfunction. The implications were huge especially when therapeutic strategies were being considered. A greater understanding on the mechanism of poor LOS control in reflux disease was crucially needed.

Since the first observation of non-swallow related LOSR by McNally *et al.* in 1964, there have been numerous studies trying to gain a better understanding of this presumably “physiological” phenomenon (McNally *et al.*, 1964). It was initially thought that TLOSRS were merely a physiological mechanism for venting of gastric air or belch. Only in 1980, Dent and colleagues demonstrated for the first time the association between TLOSRS and gastro-oesophageal reflux disease using a novel sleeve sensor (Dent *et al.*, 1980).

Initially, the terminology for defining TLOSRS was confusing partly because swallow associated LOSR and multiple swallows were included in the original descriptions. While swallows were associated with reflux however these were recognised as events separate from TLOSRS. During the early years of research, recognition of TLOSRS had been mostly arbitrary depending on investigators’ approximations and experiences. This variability had led to differences and difficulties in interpreting the results between studies.

This changed in 1995 when Holloway and colleagues systematically analysed the manometric evidence and produced a set of criteria that objectively define TLOSRS (R H Holloway *et al.*, 1995). While the criteria allowed a more standardized comparison between studies, the manometric

criteria alone, were later deemed to be inadequate. This is pertinent in the light of recognition that CD inhibition and marked shortening of oesophagus are other important features in TLOSRS.

#### 1.4.4.2 Manometric characteristics of a TLOSRS

In the early days, TLOSRS were variably described using variables including the rate and amplitude of LOS pressure reduction, the time interval during which this LOS pressure reduction occurred, duration of LOSR and relationship between swallows and onset of LOSR (Mittal *et al.*, 1995). Due to relatively arbitrary definitions used among different studies therefore, there have been difficulties in comparing findings between studies. This changed in 1995 when Holloway and colleagues objectively set out manometric criteria to define TLOSRS.

The main differential for a TLOSRS event is swallow-induced LOSR. From analysis of swallow-induced LOS relaxation and swallow-independent LOSR associated with reflux, the following criteria were set out by Holloway (R H Holloway *et al.*, 1995):

1. Absence of swallowing for 4 s before to 2 s after the onset of LOS relaxation.
2. Relaxation rate of  $\geq 1$  mmHg/s
3. Time from onset of relaxation to complete relaxation of  $\leq 10$  s
4. Nadir pressure of  $\leq 2$  mmHg
5. Excluding LOS relaxations associated with multiple swallows, LOS pressure falls that fulfill the last 3 criteria but have a duration  $> 10$  s can also be judged to be TLOSRS irrespective of the timing of the onset of the LOS pressure fall to swallowing

Involving 23 normal subjects and 9 patients with GORD, the study by Holloway and colleagues utilized a sleeve sensor to record the LOS pressure

and a pharyngeal side-hole sensor to record swallowing. Sleeve sensor was introduced by Dent and colleagues in 1976 and it records the maximal pressure along a membrane and this reduces movement artifacts of the GOJ which is the main limitation of single side-hole sensor (Dent, 1976). While the sleeve sensor is more accurate in LOS pressure recording, it can marginally underestimate the duration of LOSR when compared to single side-hole sensor. The duration of swallow associated LOSR can be underestimated due to incoming peristaltic wave and the less inhibited CD.

Another limitation is the identification of onset of LOS relaxation which can be difficult when the basal LOS pressure is unstable. This can introduce observer bias and reduce the sensitivity of the criteria. Fluctuations in LOS pressure either spontaneous or due to downward drifts can also occasionally pose diagnostic difficulties. These drifts decay in a linear fashion rather than the exponential rate seen in TLOSRS.

Since spontaneous swallows are so common the possibility exists that some of the TLOSRS can be missed due to close proximity between these two events. While duration of LOSR can differentiate between the two, swallows with failed peristalsis or multiple swallows which often have longer duration of LOS relaxation can be easily mistaken for TLOSRS.

The advent of HRM in the 20<sup>th</sup> century has brought in new developments in the measurement and evaluation of oesophageal physiology. Studies have compared the new HRM techniques with the sleeve sensor in the detection of LOS relaxation associated with reflux (Bredenoord *et al.*, 2005; Rohof, Boeckxstaens & Hirsch, 2011). The rate of detection of TLOSRS is similar between HRM and sleeve techniques. However TLOSRS associated with reflux events are more commonly detected using HRM than sleeve technique (132 events vs. 119 events respectively,  $P = 0.015$ ).

While Holloway's criteria have been around for 15 years, they have never been rigorously tested for accuracy and variability within and between assessors. This has been investigated recently and is pertinent due to their increasing use in pharmacologic trials. In a recent study, Holloway reported that there was a relatively poor agreement between scoring based on expert

opinions and scoring based on published criteria (Holloway *et al.*, 2012). Even scoring based on expert opinions differed more between-assessors (mean Kappa coefficient=0.45) than within-assessors (mean Kappa coefficient = 0.67).

Among reasons for the poor agreement between assessors included the low basal pressure, unstable gastric pressure and unclear swallow signal seen in some of the recordings. Cleaning of data by removing the technically flawed sections of recording only improved the agreement by 5%. Additional criteria were then included to the original criteria to evaluate whether these may improve the agreement. These criteria are as following: (i) inhibition of CD (ii) contractile events after TLOSRS. The agreement did significantly improve with the use of enhanced criteria between assessors but not within assessors. The best agreement at 84% between paired recordings was reached in a consensus analysis performed collectively by three expert observers.

Clearly, a good quality recording and experienced judgment are important determinants for a higher accuracy in diagnosing TLOSRS using manometric criteria. However even with consensus analysis involving two or more expert assessors, the Kappa agreement was only considered as moderate and this suggests that there is still an element of subjectivity in the identification of TLOSRS. The current study utilized a 16-channel perfused manometry with Dent sleeve and not HRM. It is apparent that HRM performs better than the sleeve technique particularly in a reflux situation but whether this translates to a better identification of TLOSRS is still unknown. Additional criteria particularly GOJ axial movement may improve the objectivity in identifying TLOSRS.

#### **1.4.5 Proximal movement of the GOJ during TLOSRS**

Early studies in both animals and humans have shown that oesophageal peristalsis is associated with oesophageal shortening (Dodds *et al.*, 1973; Edmundowicz & Clouse, 1991). The oesophageal musculature consists of longitudinal and circular muscle and this is similar to the small and large bowel of the GI tract. Proximal movement of the distal oesophagus during

peristalsis is due to the contraction of the longitudinal muscle and it works against the gravity or the weight of the rest of GI tract. Therefore it is not surprising that the longitudinal muscle in the oesophagus is much thicker than the rest of the GI tract.

More recently, in TLOSRS, the proximal movement of the distal oesophagus in particular the GOJ is reported to be much more exaggerated than in normal peristalsis. Using a clip attached endoscopically to the SCJ, the movement of the GOJ can be visualized using fluoroscopic technique (Pandolfino *et al.*, 2006). In TLOSRS, the GOJ can move as much as 9 cm proximally and this is in great contrast with a swallow of which the GOJ only moves 1.5 - 2 cm proximally.

The current chapter aimed to review available literature on the measurement of the GOJ movement during TLOSRS using currently available techniques. The advantages and limitations of these techniques are discussed.

#### **1.4.5.1 Radiographic technique**

The classic study by Dodds *et al.* utilized the use of four tantalum markers sewn into the wall of the distal oesophagus in feline and these markers were tracked radiographically during peristalsis (Dodds *et al.*, 1973). It was demonstrated that shortly after the onset of peristalsis, all the markers except the one at the hiatus moved proximally together (**Figure 1.12**).

For the first time, this study confirmed that the GOJ moves proximally during swallows which implies the role of longitudinal muscle contraction (LMC) during the GOJ movement. The mechanical activity of LMC during GOJ movement was subsequently proven in a study by Sugarbaker *et al.* where the investigators applied a series of miniature strain gauges in the axis of muscle fibers in opossums (Sugarbaker *et al.*, 1984).

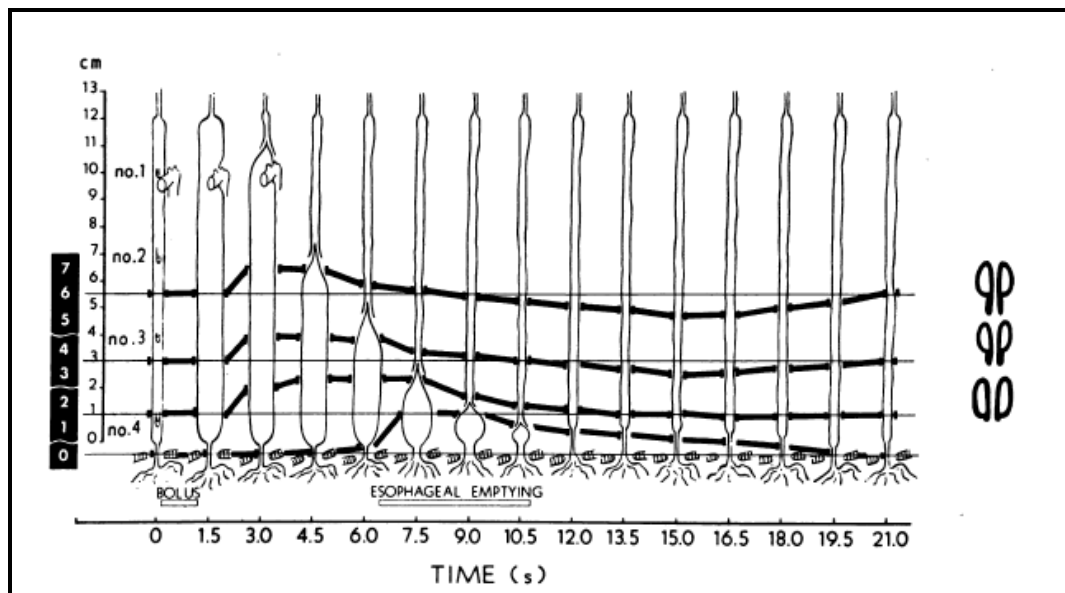


**Figure 1.12:** This illustrates the classic study by Dodds et al. using tantalum markers sewn into the wall of oesophagus in feline (Dodds *et al.*, 1973). In a wet swallow, as the contraction wave propagates in the upper oesophagus, the tantalum markers can be seen to move proximally. With subsequent progress of the wave, the markers start to return to its original position. The whole sequence lasts for approximately 18s. The bolus does not empty into stomach until the peristaltic wave reaches mid-oesophagus and emptying is not complete until the wave reaches the cardia.

The few studies in humans using metal clips attached to the mucosa have demonstrated similar proximal movement of the GOJ during swallows when the clip movements were visualised using fluoroscopic technique. In the study by Poudroux et al., three 11-mm stainless steel clips were clipped to the mucosa and the axial movement of clip was assessed using video-fluoroscopy (Poudroux *et al.*, 1997). It was shown that during peristalsis, contraction for both the circular and longitudinal muscles occurred at the propagating segment with the longitudinal muscle leading the circular muscle.

It was argued that the method of mucosal clipping was not directly indicative of longitudinal muscle contraction. It was first suggested by Palmer when he noticed “mysterious spontaneous migrations” of clips during fluoroscopy (Palmer, 1953). The axial movement of clip is potentially

influenced by other factors including contraction of the muscularis mucosa or even relative movement between the mucosa and the submucosa due to shear distortion of mucosa. However studies by Pouderoux concur with studies by Dodds and Sugarbaker above that utilized different techniques other than mucosal clips. All of these studies demonstrate a similar pattern and degree of LMC. This suggests that mucosal clipping is a valid indicator of longitudinal muscle contraction and that this is largely determined by contraction of the muscularis propria.

Placement of metal clips requires an endoscopic approach which not all study subjects can tolerate. Furthermore placement of clips can be technically challenging due to peristalsis and respiratory movement. Previous studies utilized a number of clips being placed in the oesophagus so that the relative motion between the 3 - 5 cm spaced clips were measured and compared. It has been shown that such an approach can significantly underestimate shortening of localized longitudinal muscle (M A Nicosia *et al.*, 2001).

With the growing interest on TLOSRS and their association with GORD, investigators have attempted to study oesophageal shortening during the period of spontaneous LOS relaxation. By placing two mucosal clips with one clip at the SCJ and the other clip 10 cm proximally, Pandolfino and colleagues identify TLOSRS using concurrent high resolution solid state manometry and studied the relative clip movements using videotaped fluoroscopy (Pandolfino *et al.*, 2006) (**Figure 1.13**). The investigators managed to record 93 TLOSRS in a two-hour study after a high fat meal but only 62 of these TLOSRS with good fluoroscopic visualizations could be analyzed. It was shown that oesophageal shortening during TLOSRS was most prominent at the distal placed clip and the proximal clip only showed minimal proximal movement. The excursion of the clip placed at SCJ was a median of 3 cm with a range between 0 and 9 cm. This amount of GOJ excursion during TLOSRS is clearly much larger than what is expected for normal swallows.

The study by Pandolfino *et al.* clearly demonstrated the proximal movement of GOJ during TLOSRS but the fluoroscopic technique employed in

the study had a number of limitations. Firstly, fluoroscopy is associated with exposure to radiation and this can limit the total amount of time that the patient can be exposed. It has been shown that cumulative radiation exposure increases the risk of cancer with time. Secondly, since TLOSRS are identified using manometric approach there is a potential for false positives as well as false negatives. As many as 30% of TLOSRS can be missed when identified using manometric criteria and imaging the false negatives further increases the dose of radiation exposure. Furthermore, the difficulty in identifying the actual onset of TLOSRS and the delay in starting the imaging process meant that the early part of GOJ movement is most likely missed.

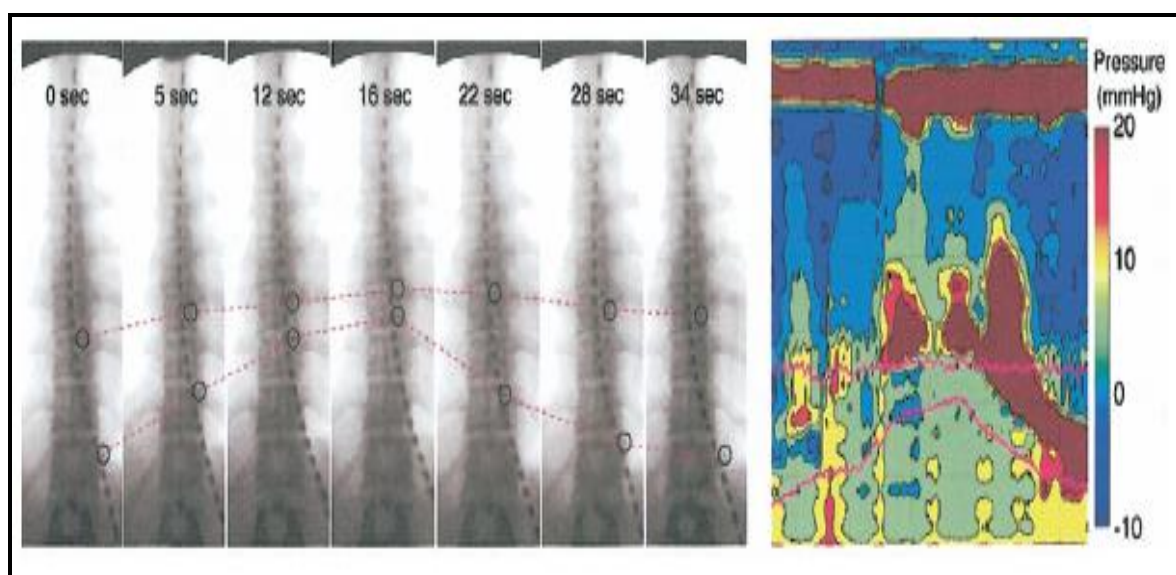


**Figure 1.13:** Mucosal clips movement superimposed on fluoroscopy and manometry tracing. In the study by Pandolfino et al., the movement of mucosal clip during a TLOSRS is imaged using fluoroscopic technique (Pandolfino *et al.*, 2006). Two clips were applied with one clip at SCJ and another placed 10cm proximally. It can be seen in this figure on the left that during a TLOSRS the clip at SCJ moves proximally more prominently than the more proximally placed clip. When this excursion is superimposed onto the manometry tracing on the right, it is evident that the excursion mirrors the high pressure bands due to movement of the LOS proximally.

With the above limitations, it is clear that radiographic technique is not ideal and that other technique is needed to study TLOSRS over a prolonged

period of time. This is pertinent especially when TLOSRS are relatively infrequent events and are influenced by posture and meals.

### 1.4.5.2 Manometric shortening of the oesophagus

While manometry is useful to measure the physiology of circular muscle and LOS, it is less useful with longitudinal muscle. During TLOSRS, it can be observed that the LOS moves proximally and this is manifested as axial movement of pressure bands (Figure 1.14).

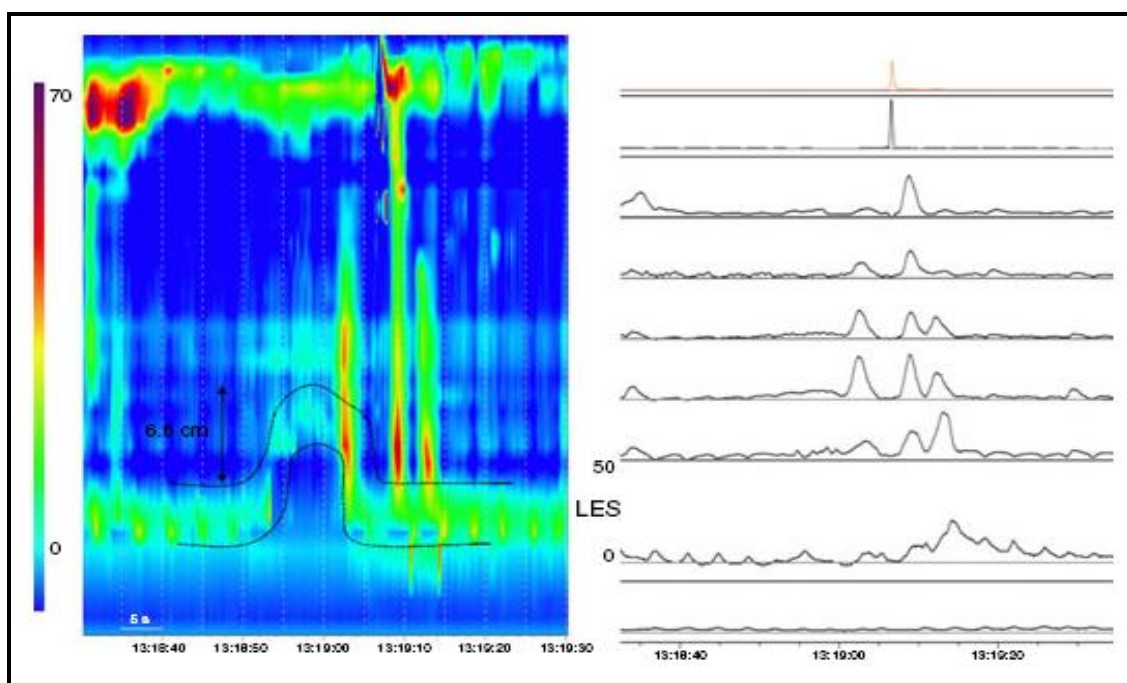


**Figure 1.14:** LOS shortening during TLOSRS. During TLOSRS, oesophageal shortening can be seen as axial movement of pressure bands of LOS. The amplitude of this shortening can be measured by determining the movement of upper border of LOS, in the example above it moves 6.6 cm proximally (Rohof *et al.*, 2011). Legend: LES; lower oesophageal sphincter

From the study by Pandolfino *et al.*, the fluoroscopic movement of a clip was seen to mirror the axial movement of LOS but no direct comparison between the two techniques was mentioned. The magnitude of this shortening was studied in more detail by Rohof *et al.* and it was found that

the upper border of LOS moves proximally by 3.0 cm in TLOSRS compared to 1.2 cm in wet swallows (Rohof *et al.*, 2011). Oesophageal shortening was greater during TLOSRS associated with reflux than those without reflux (3.1 cm vs. 2.5 cm,  $P < 0.05$ ). The recognition of TLOSRS in HRM was facilitated by oesophageal shortening compared to sleeve manometry.

Since this technique has not been validated with other techniques we do not know how accurate it is in measuring longitudinal shortening. What is apparent is this method seems to complement the manometric pressure criteria in aiding the identification of TLOSRS. More recently, “LOS lift” has been investigated as a marker for longitudinal shortening (Mittal *et al.*, 2012). In this study, 8 subjects were studied using a custom-made HRM allowing 24-h recording. It was shown that swallow-associated LOS relaxation is associated with a small LOS lift. This lift cannot be appreciated during complete TLOSRS due to a fully relaxed LOS in contrast to incomplete TLOSRS. The lift seen during incomplete TLOSRS is greater than those associated with swallows.

#### **1.4.5.3 High frequency intra-luminal ultrasound**

Since oesophageal shortening during TLOSRS is due to contraction of longitudinal muscle, a technique which can measure its contraction properties or its muscle cross section may allow estimation of GOJ movement. One technique to measure longitudinal muscle stress directly is the use of strain gauges implanted within the muscle wall (Sugarbaker *et al.*, 1984b). It has been proven to be useful using an animal model, but placing strain gauges in humans is not possible. In humans, radiographic technique to measure clip motion as described above has been the only method to assess LMC until more recently when the high frequency intra-luminal ultrasound (HFIUS) technique is introduced.

Due to radiation exposure, the use of radiographic technique for prolonged period is limited for research purpose. This is not a problem for intra-luminal ultrasound. This technique does not require placement of any metal clips and therefore avoid any upper endoscopy. HFIUS records LMC based on the principle that as the oesophagus shortens, a corresponding

increase in cross-section area (CSA) or thickness of the muscular propria is seen (Mittal *et al.*, 2005; Nicosia, Brasseur, Liu, *et al.*, 2001).

To illustrate the principle (Figure 1.15), imagine a thin mass of muscularis propria at certain axial location (y) in the oesophagus during the resting state (\*) and the same mass at a later time during the propagation of contraction wave (#). Because muscle is a matrix of liquid and deformable solid (proteins, cellular materials, collagen etc.) which are incompressible, therefore the density and volume of muscularis propria at y during resting and contracted state remains the same. The volume of muscularis propria at y = thickness (L) x cross-section area (A) and since the volume at resting (\*) is the same as in the contracted (#) state then,  $L^*A^* = L^{\#}A^{\#}$ . Thus,

$$\frac{L^{\#}}{L^*} = \frac{1}{A^{\#}/A^*}$$

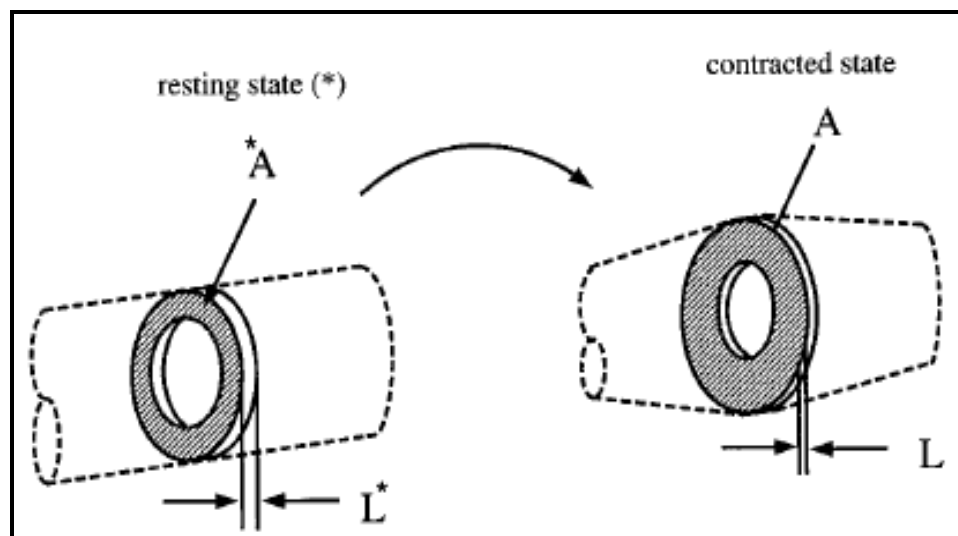


**Figure 1.15:** Schematic diagram illustrating the changes in CSA and thickness of muscularis propria at axial location y in both resting (\*) and contracted state (Nicosia *et al.*, 2001).

If there is a local increase in muscle CSA ( $A^{\#}/A^* > 1$ ) there is a corresponding decrease in local longitudinal shortening ( $L^{\#}/L^* < 1$ ) at the same location, y. Images from HFIUS can measure  $A^{\#}/A^*$  which unambiguously infer

longitudinal muscle shortening. A potential error however is that the muscle surface could have moved 1 - 2cm relative to the ultrasound transducer and therefore may have under or over-estimates the  $A^{\#}/A^*$  but quantitatively this error is shown to be small (Nicosia *et al.*, 2001).

The quantification of longitudinal shortening based on CSA during swallows has been studied by Nicosia *et al* in 4 healthy subjects using a concurrent 20MHz ultrasound transducer in B-mode and water-perfused manometry placed in the mid-oesophagus (**Figure 1.16**). Briefly, B-mode (brightness mode) utilizes a linear array of transducers that simultaneously scans a plane through the body and can be viewed as two-dimensional image. It cannot be stressed enough that the transducer must be of sufficient resolution and depth in order to image the deeply located muscles. Quality of images can also be degraded by high frequency noise or “speckles” due to signals from sources smaller than the resolution of transducer. This could be overcome with the use of a filter. The image processing and interpretation of hundreds of images were time-intensive and very much depended on the experience of the investigator in sonography. Custom software was designed to automatically detect the muscle-edge with good accuracy but identification of interconnective tissue between circular and longitudinal muscle remained difficult.

Despite the above practical limitations, the study could quantify a greater local longitudinal shortening when compared to mucosal clip studies spaced 3 - 5 cm (0.34 cm compared to 0.6 cm and 0.8 cm in studies by Kahrilas *et al* and Poudroux *et al* respectively). This implied that mucosal clips measure a more global shortening or an average of a segment of longitudinal shortening and therefore underestimate the maximum local shortening measured with HFIUS. A limitation is however that the measurement of muscle thickness cannot be used alone as a sole indicator of LMC. In the absence of LMC, the muscle layer thickness can change depending on proportion of lumen radius in an inverse relationship. This happened during “distension phase” when the oesophagus is filled and lumen expands but both longitudinal and circular muscles are in rested state.

Another finding in the study was that LMC enveloped the peristaltic contraction of circular muscle and the peak contractions for both muscles were aligned temporally. This spatial and temporal coordination between longitudinal and circular muscle contraction is of mechanical advantage since it increases the contractile force and reduces average muscle tension (Sugarbaker *et al.*, 1984a).

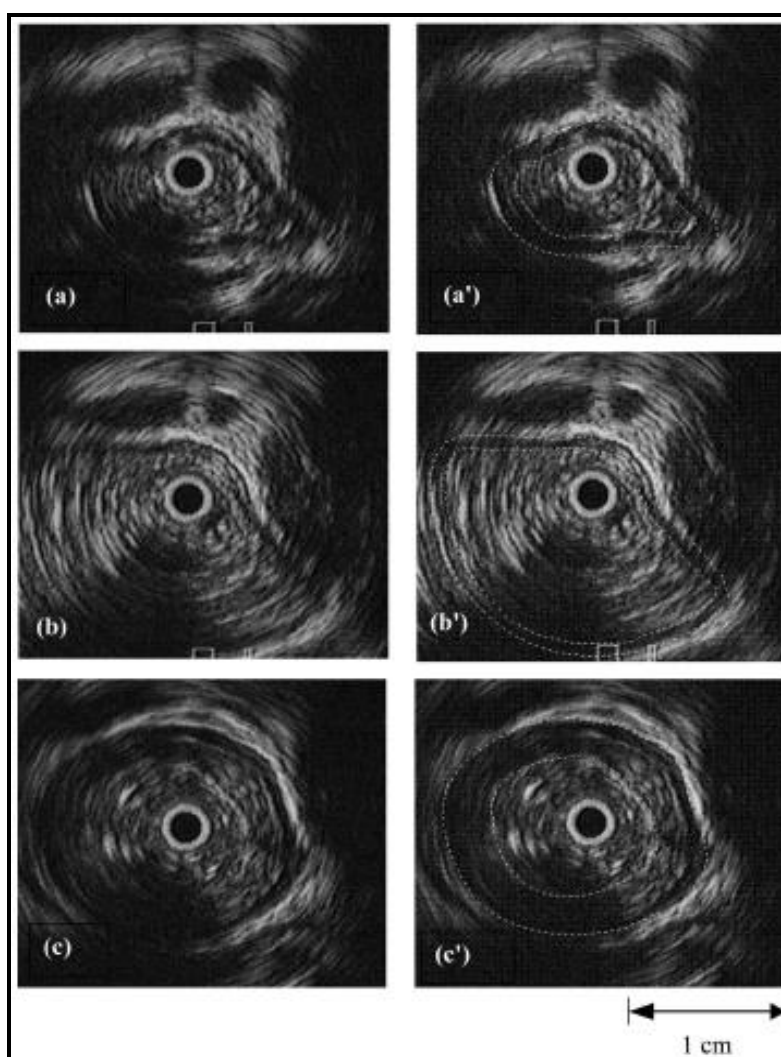


**Figure 1.16:** Ultrasound images showing the edges which outline the inner wall of circular muscle and outer wall of longitudinal muscle. These are taken at 3 different time periods of a swallow (a) resting (b) distension of oesophagus by the bolus and (c) contracted state (Nicosia *et al.*, 2001).

While Nicosia *et al.* uses the HFIUS technique to evaluate LMC in swallows, Mittal *et al.* uses this technique to evaluate LMC in swallows and TLOSRS. Whether LMC occurs before or after LOS relaxation is not exactly known. Pandolfino *et al.* proposes that following LOS relaxation, LMC then opens up the LOS and subsequently GOR. However Mittal shows that an axial pull on

the LOS causes a neurologically mediated relaxation of LOS suggesting that LMC may actually induce LOS relaxation (Dogan *et al.*, 2007).

In the study of LMC in TLOSrs, Mittal *et al.* passed a combined assembly of 8-channel sleeve sensor, 4.5 mm catheter and 3.5-Fr 30-MHz ultrasound transducer in 17 subjects. Instead of using muscle CSA measured using B-mode, muscle thickness measured using M-mode was used as a marker of LMC (Figure 1.17).

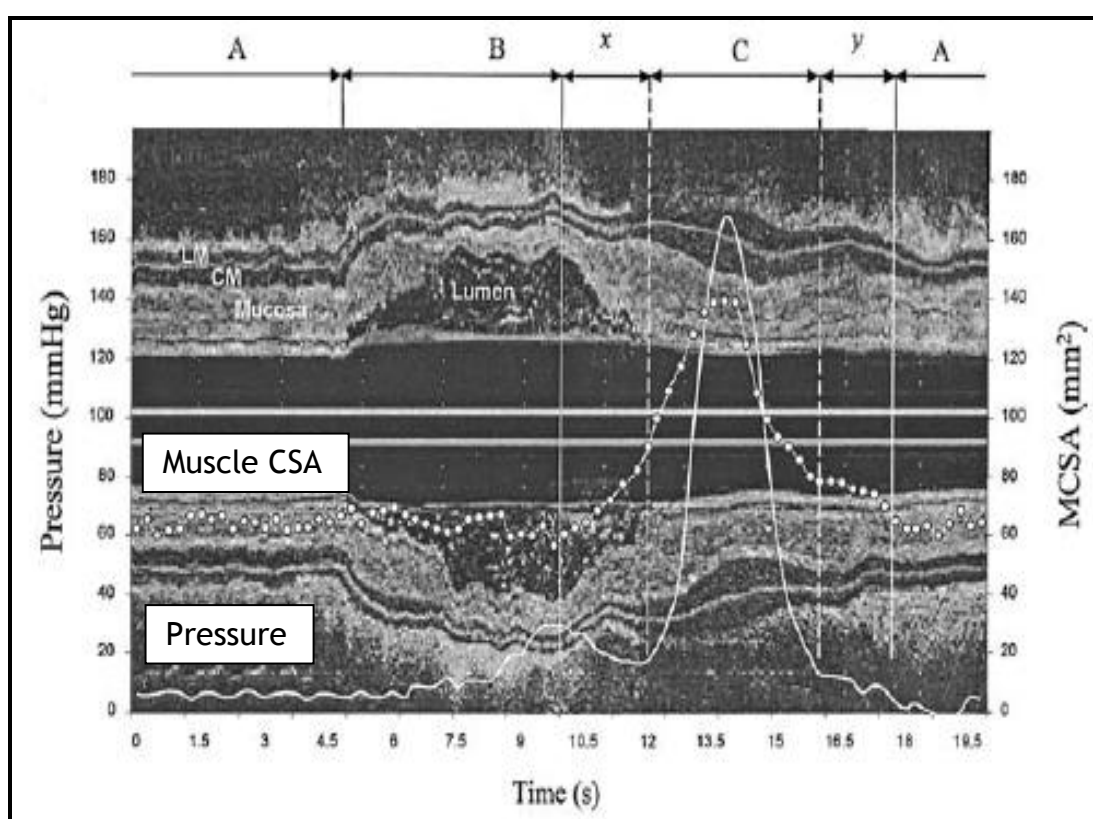


**Figure 1.17:** Using M-mode of HFIUS, Mittal *et al.* measures the muscle thickness as a marker of LMC during a swallow (Mittal *et al.*, 2005). The tracings of intra-oesophageal pressure and muscle CSA (MCSA) are superimposed on the M-mode in this figure (boxes). Legend: A, baseline oesophagus; B, bolus-induced distension and thinning of mucosa and muscle layers; C, oesophageal contraction; the time difference between onset of CSA and pressure is likely due to delay in recording circular muscle contraction by manometry and y, time lag between return of pressure and MCSA to baseline.

Briefly, with M-mode (motion mode), pulses are emitted in rapid succession and over time, this is analogous to taking a video of the ultrasound. Studies have shown a good correlation between muscle CSA and muscle thickness as indicators of LMC. Muscle thickness was chosen because the measurement of muscle CSA is more time consuming and is affected by luminal changes.

With swallows, the increase in muscle thickness started 0.5 - 0.8 s prior to onset of peristaltic wave. The peak pressure and peak muscle thickness were seen to occur at approximately the same time (**Figure 1.18A**). With TLOSRS, it was shown that the distal oesophageal LMC began  $1.7 \pm 1$  s prior to onset of LOS relaxation and lasted for  $23.7 \pm 3$  s (**Figure 1.18B**). There was initially a slow rise but LMC later accelerated while the LOS relaxed and the CD inhibited. The LMC continued throughout the period of TLOSRS and returned to baseline following after-contractions. The maximal muscle thickness during TLOSRS was  $2.7 \pm 0.6$  mm from a baseline of  $1.3 \pm 0.3$  mm and this was greater than the maximal muscle thickness during swallows of  $2.4 \pm 0.5$  mm ( $P < 0.05$ ).

The results appear to support that LMC induces relaxation of LOS through axial pulling of LOS since LMC was shown to start prior to the onset of TLOSRS. It was argued that in Pandolfino's study, the onset of LMC cannot be determined precisely since the fluoroscopy was started only after they have identified the onset of TLOSRS on manometry.

As a conclusion, intraluminal ultrasound technique is an attractive method to visualize the function of longitudinal muscle during peristalsis and TLOSRS. Without radiation exposure and probe-based, it is technically easier. What limits the technique is the image processing and analysis which is time-consuming and depends on the experience of investigator. With the improvement in ultrasound technology and refinement in the design of automated analytical software, HFIUS may turn out to be a very useful tool.

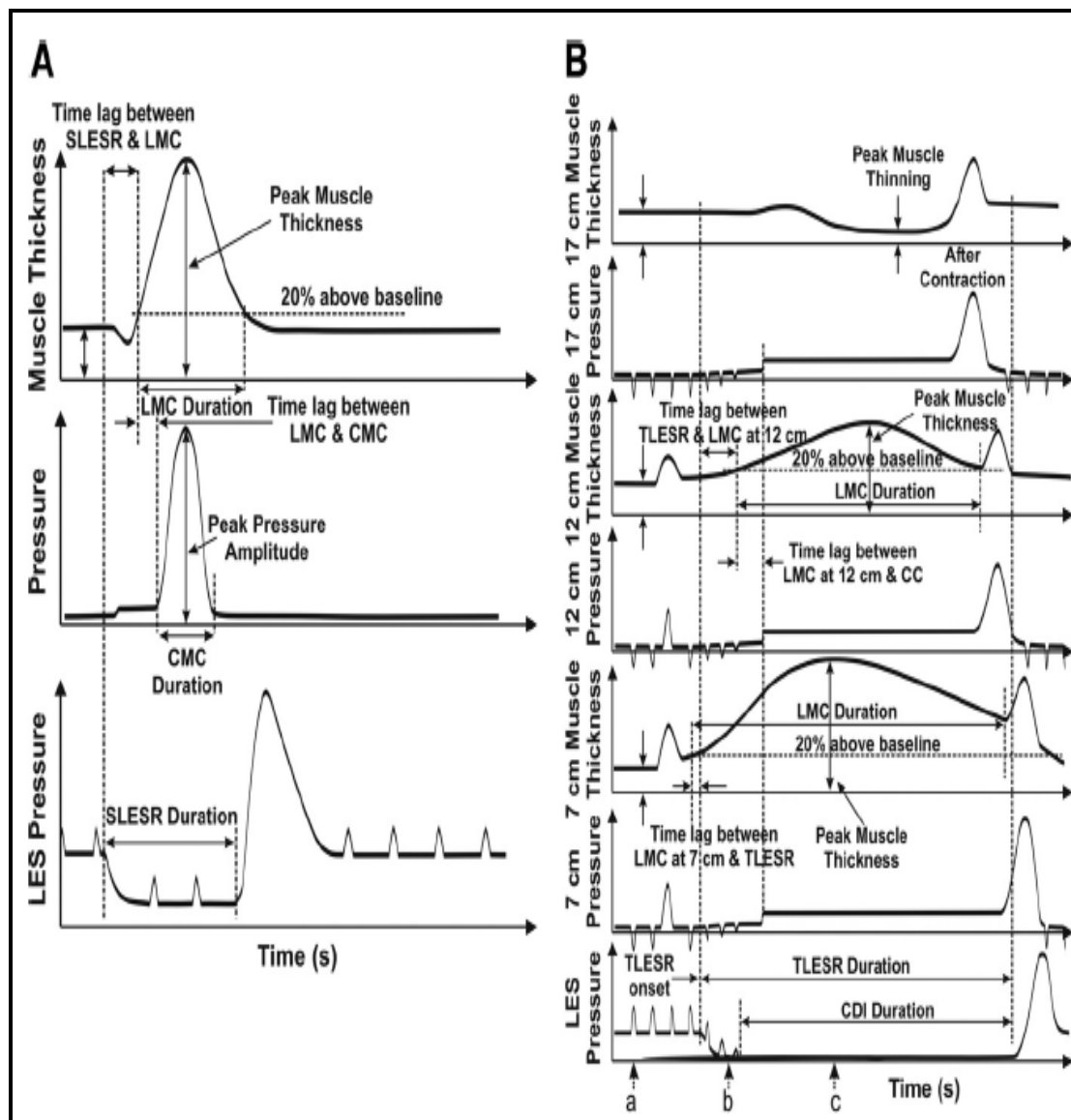


**Figure 1.18:** A schematic diagram showing the temporal correlation between the circular and longitudinal muscle contraction of the oesophagus during (A) swallow and (B) TLOS (Arash Babaei *et al.*, 2008). Legend: LMC, longitudinal muscle contraction; CMC, circular muscle contraction; CDI, crural diaphragm inhibition; CC, common cavity pressure

## 1.5 MEASURING THE SCJ AND ITS RELEVANCE TO GORD

### 1.5.1 Introduction

Traditionally, the measurement of acid reflux is performed with a pH sensor placed 5 cm above the LOS in order to avoid the inadvertent recording of

gastric acid during shortening of the oesophagus in swallows and TLOSRS. It has been recently reported that acid in the most proximal cardia region of the stomach escapes the buffering effects of food and remains highly acidic during the postprandial period. This un-buffered pocket of acid is observed to traverse the SCJ and can extend 1 - 2 cm into the distal oesophagus. This suggested the existence of short segment reflux and may account for the high prevalence of intestinal metaplasia and cancer at the GOJ which is occurring in many asymptomatic subjects without evidence of conventional reflux disease.

The availability of multi-channel high resolution pHmetry allows one to measure acid exposure across the GOJ but the location of the SCJ is unknown. Bravo capsule may allow one to capture acid exposure at a fixed point within the distal esophagus but it is less useful for studying reflux near the SCJ as it may interfere with the function of sphincter. Apart from fluoroscopic imaging technique, there is no other method allowing a continuous and precise measurement of position of the SCJ.

The following sections will firstly introduce traditional acid reflux and its limitations. It is followed by discussion on short segment reflux and why in such situations, a reliable technique is needed to measure the SCJ in association with pH changes.

## **1.5.2 Traditional acid reflux disease**

### **1.5.2.1 Definition and epidemiology of GORD**

The term “reflux” originates from “refluxus”, a Medieval Latin word meaning “to flow back”. GOR, as the term suggests, is flow of gastric contents (gastric juice, air or bile) into the lower oesophagus and is a normal and common physiologic phenomenon intermittently experienced by most people particularly after a meal. It becomes a disease when amount and frequency of reflux (commonly acid) exceeded its normal limits and causing symptoms and poor health due to its associated complications. Typical oesophageal symptoms associated with GORD include heartburn, regurgitation and

dysphagia but a diagnosis of GORD based on symptoms is only appropriate in 70% of cases. There are also extra-oesophageal symptoms including cough, non-cardiac chest pain and wheezing. Complications associated with GORD include mucosal damage or oesophagitis, stricture, Barrett's oesophagus and oesophageal adenocarcinoma. These complications are usually detected during upper endoscopy and or imaging studies.

While the disease has been present for a long time, only in the last two decades has it received clinical attention. Besides from reaching epidemic proportion in terms of prevalence within the Western population, the disease is associated with poor quality of life and increasing medical costs. Using a validated self-reported questionnaire, among 2200 Olmsted County residents aged 25 - 74, the prevalence for GORD symptoms (heartburn and/or acid regurgitation) experienced at least weekly was 19.8% (95% CI: 17.7 - 21.9) (Locke *et al.*, 1997). In a more recent study involving 116, 536 respondents from the 2007 National Health and Wellness Survey (NHWS), 23% reported GORD symptoms with 39% reported as having disrupting GORD (defined as GORD symptoms for at least 2 days/week in addition to either night-time symptoms or use of prescribed/over-the-counter medication at least twice a week during the past month) (Toghanian *et al.*, 2010). Respondents with disrupting GORD utilized more healthcare resources, poorer health-related quality of life and greater impairments in health-related work productivity and absenteeism. Within the primary practice, the incidence of GORD was 4.5 new diagnoses per 1000 person-years in 1996 (95% CI: 4.4 - 4.7) based on systematic review of 17 articles using the General Practice Research Database (H El-Serag *et al.*, 2009).

Even though GORD is reported to be rare in Asia, this has changed significantly over the past few years. Data from the Korean National Health Insurance had shown that the prevalence for "doctor-diagnosed GORD" increased from 4.6% to 7.3% between 2005 and 2008 especially in the younger age groups (30-39 years old)(Kyoung-Min Kim *et al.*, 2012). From population based studies, the prevalence of symptomatic GORD in Eastern Asia was 2.5-4.8% before 2005 but this increased to 5.2% - 8.5% between 2005 and 2010. The prevalence for endoscopic reflux oesophagitis was also increased in Eastern Asia from 3.4% - 5.0% before 2000, to 4.3% - 15.7% after 2005 (Hye-

Kyung Jung, 2011). Some of the possible risk factors responsible for this increasing prevalence of GORD seen in Asia include a reduction in *H. pylori* infection, obesity and increasing dietary fat intake (Ting K Cheung *et al.*, 2008).

### 1.5.2.2 Defining GORD by oesophageal acid exposure

Aside from symptoms, GORD can be defined by measurement of acid exposure at the oesophagus over 24-48 hours by using a catheter-based pH monitoring system (Spencer, 1969). A pH catheter uses either glass or antimony sensor with a reference electrode. Due to shortening of oesophagus during swallows and TLOSRS, the pH probe is traditionally placed at 5 cm above the LOS to avoid false-positive measurement of gastric acid. An accepted definition for GOR is a sudden drop in the intra-oesophageal pH to below 4.0, with nadir pH reached within 30 s from the start of the drop. The reasons being that the pepsin, the gastric proteolytic enzyme is inactivated above this pH (Piper and Fenton, 1965) and that heartburn is commonly reported below pH of 4.0 (Tuttle, Rufin & Bettarello, 1961).

DeMeester score is commonly used to provide an objective interpretation of pHmetry. Briefly, the score is a composite of pH < 4 for total, upright and recumbent, number of reflux episodes in 24 hours, number of reflux episodes > 5 minutes and the longest episode (L F Johnson and T R Demeester, 1974). For an outpatient 24-h ambulatory pH test, a composite score and the percent total time pH < 4 provided the most efficient interpretation of the test with a sensitivity of 96%, a specificity of 100% (Jamieson *et al.*, 1992). Nowadays, the DeMeester score is automatically calculated by commercially available softwares.

One of the limitations of the DeMeester score is that symptoms have not been taken into account in the scoring. It is known that up to 15% of patients with GORD symptoms may have a normal endoscopy and pH monitoring (Eriksen *et al.*, 1991). In such cases, symptom index (SI) may be useful to separate patients with acid-sensitive oesophagus from functional heartburn. The SI can be calculated by dividing the number of symptoms preceded by a reflux episode within a 5-minute window by the total number of symptoms

(Johnston *et al.*, 1992). It can be expressed as a percentage and interpreted as positive if  $\geq 50\%$ . Recently, a shorter time window of 2-minute after onset of reflux is proposed (H G Lam *et al.*, 1994). An important weakness of SI is the possibility that multiple reflux episodes but few symptoms may occur by chance.

Due to above limitations, a more complex statistical approach proposed by Weusten *et al.* is the symptom association probability (SAP) (B L Weusten *et al.*, 1994). Commercially available software calculates the SAP in percentage that evaluates whether the pattern of reflux and symptoms may occur by chance or not. A SAP of greater than 95% is considered positive.

### **1.5.2.3 TLOSRS, the mechanism underlying traditional reflux**

Since the 1970s, it was recognised that not all reflux episodes were associated with failure of the LOS. Later studies have shown that there is increased likelihood for reflux during TLOSRS and frequency of TLOSRS is increased in patients with GORD but this remains controversial (**Table 1.1**).

Out of 11 reported studies on TLOSRS using similar definitions and experimental settings, 4 studies have shown an increase in rates of TLOSRS with GORD but remaining 7 studies did not show a difference. In a study by Trudgill and Riley, it was found that the rates of TLOSRS were not increased in patients with GORD (N J Trudgill and Riley, 2001).

Reasons for these differences are not entirely clear. Possible reasons include methodology difference between studies, posture and presence of hiatus hernia. It is known that a supine posture can suppress TLOSRS. Furthermore, hiatus hernia can lower the trigger of TLOSRS especially in supine position and in patients with GORD. More recently, obesity is reported to have increased rates of TLOSRS and increase rates of acid exposure during TLOSRS (Justin Che-Yuen Wu *et al.*, 2007).

Table 1.1 TLOSRS in normal subjects and subjects with GORD

Authors	Rate of TLOSRS		% TLOSRS with acid reflux	
	Normal	GORD	Normal	GORD
Dodds et al.	241/10/12 h	344/10/12 h	34	66
Holloway et al.	1/60 min	5/60 min	50	68
Penagini et al.	2.6/60 min	6.6/60 min	52	65
Mittal and McCallum	24.8/180 min	25.4/180 min	37	65
Kahrilas and Gupta	1.2/ 60 min	0.7/ 60 min	15	20
Schoeman et al.	4.3/ 60 min	5.4/ 60 min	34	63.5
Penagini et al.	3.5/ 60 min	6.4/ 60 min	32	62
Lidums et al.	5.7/ 60 min	15/ 180 min	36	41.5
Sifrim	7.5/ 60 min	7.5/ 60 min	34	68
Trudgill	3/ 60 min	2.5 / 60 min	37	65

These studies confirmed that TLOSRS are a physiological phenomenon and common in postprandial period in both normal subjects and in subjects with GORD. Most studies (9/11) have reported a higher incidence of acid reflux during TLOSRS in patients with GORD. Common cavity phenomenon is a manometric marker for reflux during TLOSRS but impedance (described in next section) study found that refluxates during common cavity are commonly a mixture of gas and non-acidic liquid in the postprandial period (D Sifrim *et al.*, 1999). This means that there must be other reasons for more acidic refluxate in patients with GORD. One possible reason is the presence of acid pocket which will be discussed in the following section (1.5.3). Another reason is some patients with GORD have an increased basal acid secretion (Collen *et al.*, 1994). The high basal acid, the delay in gastric emptying and impaired secondary peristalsis in patients with GORD therefore increase the risk for acid refluxate.

### 1.5.2.4 Limitations of traditional acid reflux

So far, it has been discussed that symptoms can miss up to 30% of GORD. While this may improve by incorporating pH measurement, there is a significant proportion of reflux which is still missed. It has been increasingly recognised that mildly acidic and non-acid reflux are getting more common largely due to routine uses of proton-pump inhibitors by primary care practitioners. These episodes cannot be detected by conventional pH monitoring. A new technique can overcome this problem - the multichannel intraluminal impedance (MII).

First described by Silny et al., impedance is a technique that measures resistance to alternating current across two electrodes based on the bolus content of oesophageal lumen (Silny, 1991). High impedance is recorded with air due to its poor conductance (therefore high resistance - above 5000 ohm) and low impedance is recorded with liquid due its good conductance (therefore low resistance - below 1000 ohm). Having multiple impedance electrodes on a catheter can therefore determine the chemical properties of contents, the direction of content flow and height of refluxate. Combining the impedance electrodes with 1 - 2 pH sensors can allow a more comprehensive characterization of reflux episodes.

The traditionally positioned pH sensor at 5 cm above the LOS can miss pathology close to the GOJ. It has been recently recognised that proximal cardia of the stomach escapes the buffering effects of food and remains highly acidic during the postprandial period (Fletcher *et al.*, 2001). This unbuffered acid pocket may traverse the SCJ and extend 1 - 2 cm into the distal oesophagus. There is a possibility for existence of short segment reflux with acid reaching the most distal intrasphincteric segment of the oesophagus but not traversing the whole of sphincter. This meant that a conventionally placed pH electrode will miss the short segment reflux. Both acid pocket and short segment reflux are described in more detail in the next section 1.5.3.

### 1.5.3 Acid pocket and short segment reflux

The GO reflux commonly occurs after meals but this is surprising since there is marked reduction in acidity of gastric contents after eating due to buffering by ingested food. When performing dual gastric and oesophageal pH measurement, it has been observed that the pH of the oesophageal electrode was more acidic. Later experimental studies performed in healthy volunteers and patients with GORD using 24-hour dual gastric and oesophageal pH recordings confirmed the above observation. Using catheter pull-through technique, the postprandial recording had shown a region of high acidity and this corresponded to the location of the pH step-up point observed under fasting condition (Figure 1.19).

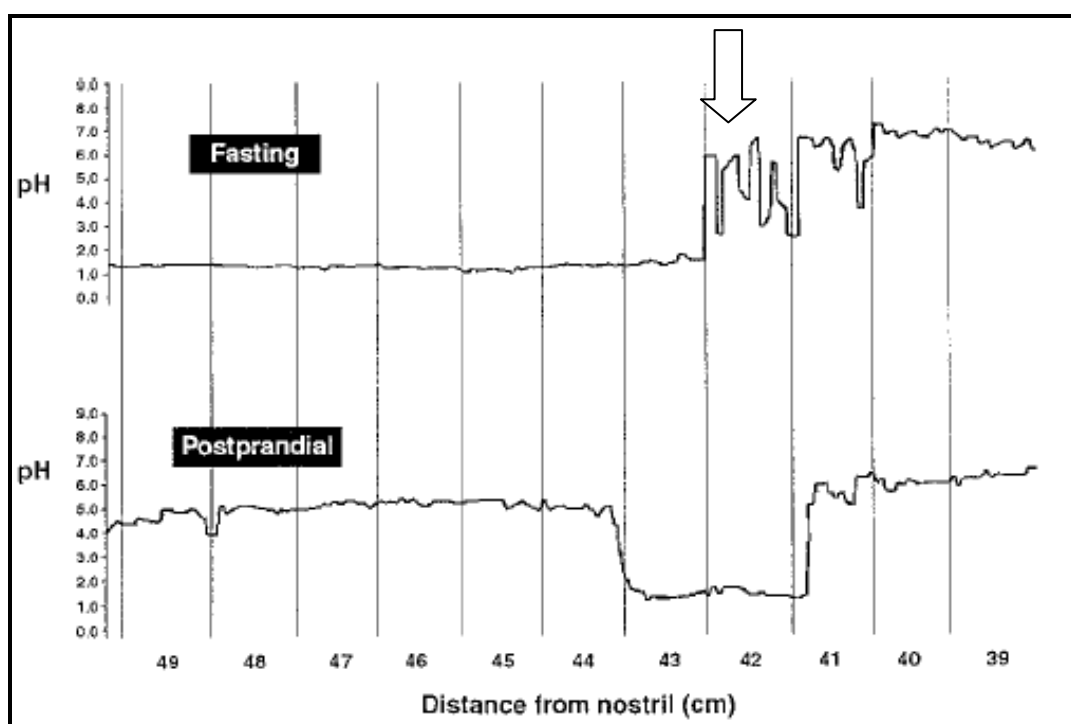


**Figure 1.19:** pH tracings recorded using catheter pull-through technique during fasting and postprandial period (John E Pandolfino *et al.*, 2007). The white arrow indicates the pH step-up point during fasting period but the same region is acidic during postprandial period.

This region of high acidity or “acid pocket” escapes the buffering effect of food with a median distance of 2 cm. It indicates that the pH step-up at the GOJ migrated 2 cm proximally after meal. The reason for this proximal migration is unclear (Fletcher *et al.*, 2001). These authors postulated that the reason could be twofold. One reason is that the GOJ is being displaced upward and therefore both the pH step-up and the SCJ migrated together. The other possible reason is that the distended proximal stomach is pulling the lower GOJ apart allowing migration of the pH step-up relative to the SCJ, a mechanism first proposed by Oberg *et al.* in 1997 (Oberg *et al.*, 1997). To elucidate which is the mechanism, the authors subsequently placed a clip at the SCJ and radiographs taken to monitor its movement relative to the pH step-up point. After meals, the SCJ did not change in 9 out of 10 normal volunteers but the pH step-up migrated proximally by 1.6 cm. This finding supported the second postulated mechanism which was the opening of the distal GOJ, at least in the non-obese subjects.

One controversy which arises is whether the acid, a pocket or volume of fluid or just a layer of acid coating the GOJ? Pandolfino *et al.* found that the HPZ was intact during the phenomena and this suggests a closed lumen which will not allow fluid transition (John E Pandolfino *et al.*, 2007). Therefore, it is argued that rather than a volume or pocket of acid, it is better termed as “acid film”. However, in condition of low LOS pressure (for example during GORD), acid pocket is more appropriate since the acid fluid can escape through the LOS. Using a novel 12-channel high definition pH catheter, acid pocket was studied in 15 health volunteers to investigate whether it behaves like “acid film” without any potential for causing reflux disease or otherwise (Clarke *et al.*, 2009). It was observed that half of the reflux episodes during postprandial period had their origin from the acid pocket contained within the region of gastric cardia (**Figure 1.20**). This was similarly observed in studies using the Bravo capsule placed at the cardia (John E Pandolfino *et al.*, 2005). Such observation in normal volunteers provided the evidence that acid pocket contains volume of acid with potential for causing reflux.

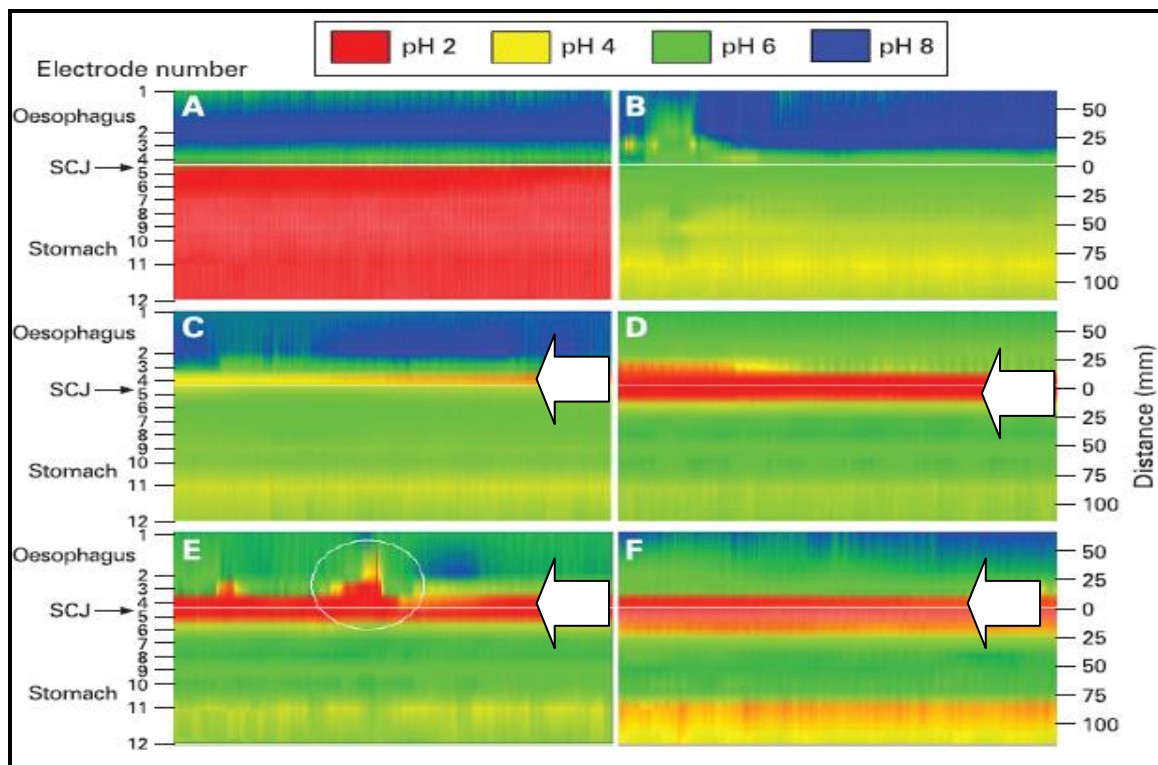


**Figure 1.20:** Colour contour plots from 12-channel high definition pH probe (Clarke *et al.*, 2009). The example shown is changes of acidity near the GOJ from fasting (A) into postprandial period (B - 3 min, C- 17 min, D - 43.5 min, E - 47.5 min and F - 73.5 min). The thin white line is the SCJ. The large white arrow indicates the acid pocket first emerging during time B. An episode of acid reflux (circle) arising from the acid pocket is also shown during time E.

Another controversy is how does the proximal stomach region escape the buffering effect of food? During a fasting period, it has been observed that the proximal stomach lacks acidity compared to the more distal region (Clarke *et al.*, 2009) (Figure 1.20 - time A). This is because the region is covered by non-acid secreting cardia mucosa (due to lack of parietal cells) and also the pressure from the LOS occludes the highly acidic gastric juice secreted immediately distal to it. Following a meal, the periphery of the gastric lumen will be the most acidic due to its proximity to secreting mucosa, and the centre will be least acidic due to buffering effect of food. Distension of stomach following a meal reduces the gastric folds density per surface area but the proximal cardia region escapes the distension due to activity of the CD and intrinsic LOS. This allows the preservation of high mucosal surface in the proximal stomach allowing formation of acid pocket (McColl *et al.*, 2010).

The first observation of existence of short segment reflux arises from the study on acid pocket as described above when the pH electrode was withdrawn from the stomach into the oesophagus at 1 cm increments every one minute (Jonathan Fletcher *et al.*, 2001). Little has been known about its duration and frequency and this led to a subsequent study comparing pH from an electrode endoscopically placed at the most distal oesophagus (5 mm from SCJ) with that of a conventionally placed electrode (6 cm above SCJ) (J Fletcher *et al.*, 2004). A total of 14 subjects with chronic dyspepsia but normal upper endoscopy were enrolled but data were available for 11 subjects. The median percentage of time pH < 4 was 11.7% at the distal electrode and 1.8% at the proximal electrode. The DeMeester score was 45 at the distal electrode and 8 at the proximal electrode. Similar to conventional reflux, short segment reflux was more frequent after meals. However, in contrast to conventional reflux which was more common in the supine position, short segment reflux was similar in supine and upright posture. While TLOSRS are the most common mechanism underlying conventional reflux, short segment reflux may instead be related to the presence of acid pocket, both commonly occurs after meal.

#### **1.5.4 Acid pocket in GORD and hiatus hernia**

With the above section providing evidence for the potential of acid pocket in causing intermittent reflux in particular short segment reflux among healthy volunteers, it would be prudent to study the role of acid pocket in pathology in particular GORD and in the presence of hiatus hernia. A detail description on hiatus hernia will be given in the following section. This section only deals with the role of acid pocket in hiatus hernia.

In a study, the acid pocket was compared between 14 subjects with GORD and 12 healthy subjects (Clarke *et al.*, 2008). Three important differences were noted between the two groups. Firstly, subjects with GORD had a higher incidence of acid pocket than in normal subjects (23/32 studies vs. 11/24 studies). Secondly, the acid pockets in subjects with GORD were larger and extended more distally than in normal subjects (3 cm vs. 2 cm). The third difference was the acid pockets extended closer to the proximal margin of

the gastric folds in subjects with reflux disease (0 cm vs. 1.1 cm). The causes for the larger pocket and its more proximal extension might have been due to abnormal pathology of the GOJ (hiatus hernia).

The above observations have been supported by a study performed in a group of 22 subjects with GORD (10 with hiatus hernia > 3 cm) where the acid pocket was visualised using single photon computed tomography (SPECT) (Beaumont *et al.*, 2010). The  $^{99m}\text{Tc}$ -pertechnetate injected intravenously, is secreted by parietal cells and using SPECT scan, the accumulation of scintigraphic activity can be demonstrated (Kuiken *et al.*, 2002). The validation study using this technique had shown that the acid pocket at the proximal stomach contains volume of acid, further proving that it is not acid film (**Figure 1.21**).

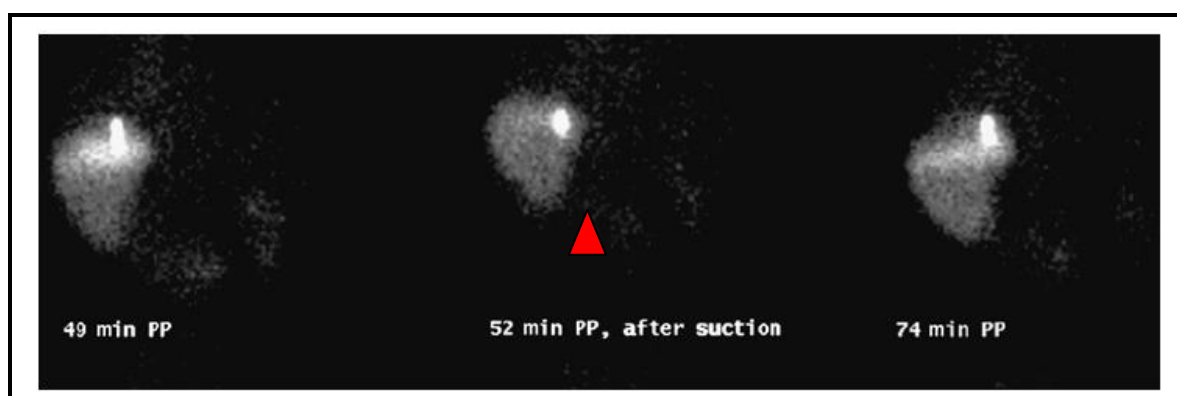


**Figure 1.21:** With SPECT scan, the acid pocket is seen as accumulation of scintigraphic activity in the proximal stomach. With aspiration (red arrow), the scintigraphic activity reduces and then slowly recovers (Kuiken *et al.*, 2002).

In the above study using SPECT scan, there were a few important observations. Firstly, it was shown that the acid pocket was larger and more likely to extend into the hiatal sac above the diaphragm in patients with hiatus hernia. Secondly, acid reflux during a TLOSr occurred more often in patients with hiatus hernia especially large ones. Thirdly, the risk for having acidic reflux was higher with the position of the acid pocket nearer or more

proximal to the diaphragm, and this position was influenced by the presence of hiatus hernia. To summarise, the authors suggested that oesophageal shortening (hiatus hernia) especially when it was above the diaphragm increased the risk for acid reflux. The enlarged proximal acid pocket in hiatus hernia meant a larger acid reservoir was available to reflux whenever the LOS spontaneously relaxed or failed in pathological situation.

With the above observations in mind, the following section provides an overview to hiatus hernia, an important anatomical abnormality to the GOJ resulting in a higher risk for GORD.

## **1.6 THE ABNORMAL GOJ: HIATUS HERNIA**

### **1.6.1 Introduction**

The pathogenesis of hiatus hernia formation has remained elusive for years. For a long time, it is assumed that the proximal stomach has the tendency to migrate to the chest since the IAP significantly exceeds the intra-thoracic pressure. While not all hiatus hernia is associated with GORD, many patients with GORD have hiatus hernia. The risk for reflux is higher in those patients having a larger hiatus hernia (M P Jones *et al.*, 2001). The protective effect of the CD is lost in hiatus hernia and the hernia sac may serve as an acid reservoir that refluxes whenever the LOS relaxes, of which the evidence has been shown in the above section.

Evidence also suggests that pathological TLOSRS and hypotensive LOS are the primary mechanisms underlying GORD, more so with pathological TLOSRS. It has been shown that the threshold for TLOSRS to occur is lower in GORD in the presence of hiatus hernia than GORD without hiatus hernia. Whether this is due to an increased likelihood for hiatal hernia formation in patients with a low threshold for TLOSRS is not known. It is known however that in TLOSRS, there is often gross proximal movement of the GOJ across the diaphragmatic hiatus (as much as 9 cm) and if so, does this not represent a severe but transient hiatus herniation? It is not difficult to postulate that an excessive stretching of the POL during GOJ migration in TLOSRS may over time predispose to wear and later hiatus hernia.

The postulation that a damaged POL results in formation of hiatus hernia is not new. Early investigators have shown anatomically that the POL was often stretched or damaged in the presence of hiatus hernia. What puzzled the investigators are the underlying mechanisms for damaging the POL. Wear due to aging process and replacement of the elastic tissue abundance in the POL with fat are thought to be the primary mechanisms. However not all hiatus hernia are seen in the elderly with some developing even at an early age.

It is difficult to demonstrate experimentally in humans the physiology and pathophysiology of the POL during TLOSRS and hiatus hernia due to limitations of available techniques to study the structure. The following section will describe on available techniques used to detect hiatus hernia and their limitations. The pathogenesis underlying formation of hiatus hernia is then discussed.

Firstly, a brief historical introduction to hiatus hernia is presented in the next section.

### **1.6.2 What is hiatus hernia? A brief history and overview**

The complexity of anatomy of the GOJ increases its vulnerability to anatomical defects especially in the face of offensive mechanical challenge and with time due to the ageing process. Hiatus hernia is the permanent displacement of the GOJ above the diaphragmatic hiatus. There is a physiological tendency for herniation to occur due to constant positive pressure of the IAP if not for the protection from the lower sphincter and diaphragmatic hiatus. However, this protection is constantly threatened during periods of spontaneous LOS and CD relaxation in swallows, respiration and TLOSRS.

The POL with its elastic properties is thought to allow the return of the GOJ to its original position during those periods of spontaneous GOJ opening. The loss of POL function over time may result in a permanent shortening of the oesophagus and formation of hiatus hernia. The functional loss of the POL

can be either structural and or related to motility factors. Structural factors are associated with age-related degeneration, obesity and trauma. Motility factors refer to the various physiological events including peristalsis, TLOSrs, spontaneous contractions, straining and so on.

The surgeons were the first to recognise hiatus hernia. The pioneers include Ambrose Pare (1510-1590), Jean Louis Petit (1674-1750), Lazarus Riverius (1589 - 1655) and Vincent Alexander Bochdalek (1801 - 1883) (Stylopoulos and Rattner, 2005). In 1853, Bodwitch described the distinct pathology of hiatus hernia when he reviewed 88 postmortem cases, but it was Eppinger in 1904, who was the first to diagnose hiatus hernia in a live patient and confirmed at autopsy (Weber *et al.*, 2011). When radiography was popularised in the early 1900s, it allowed an improved recognition of the condition, and the earliest description using barium X-ray came in 1908. With improvement in surgical techniques and therefore a better characterisation of the anatomy of hiatus hernia, Philip Allison made the distinction between sliding and para-oesophageal type of hernia, which is what we have known today (Figure 1.22) (Weber *et al.*, 2011).

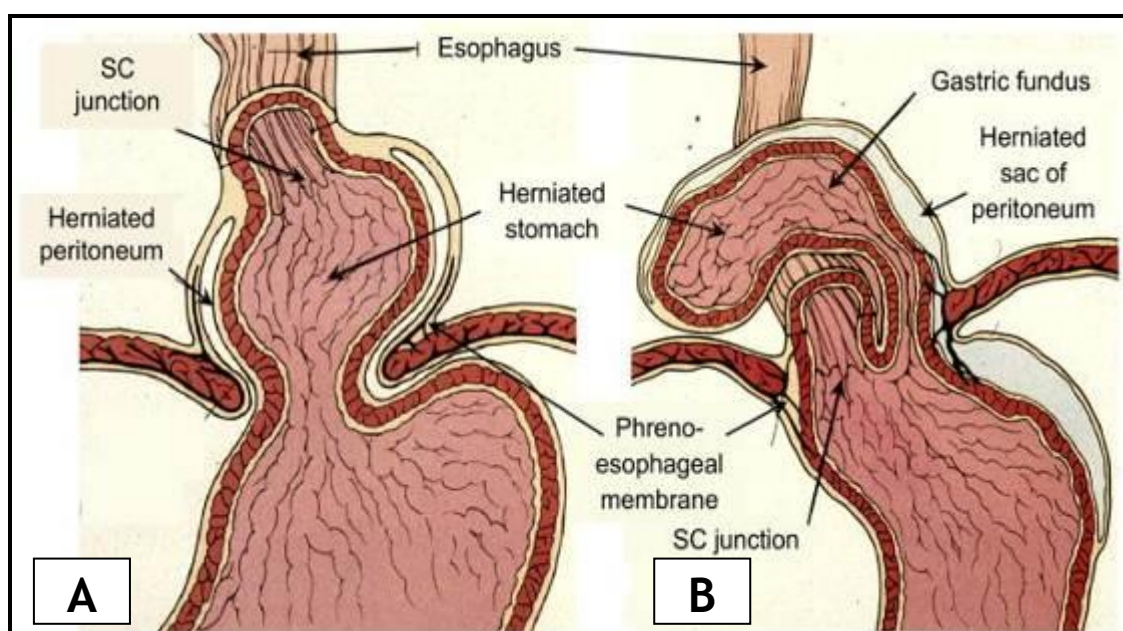


**Figure 1.22:** Types of hiatus hernia, A - sliding type and B - para-oesophageal type (Peter J Kahrilas, Hyon C Kim, *et al.*, 2008).

The sliding type is the more common variety and is the type associated with GORD. A detailed review on the difference between the two types of hernia was given by Kahrilas et al. and is beyond the scope of the current manuscript (Peter J Kahrilas, Hyon C Kim, *et al.*, 2008). The diagnosis of sliding hiatus hernia depends on the anatomical relationship between the distal oesophagus, diaphragmatic hiatus and proximal stomach. However, due to the mobility of the GOJ during respiration, swallows and TLOSRS, the assessment of hiatus hernia can be confounded as a result.

Methods used to evaluate hiatus hernia include radiology, endoscopy and more recently, manometry. Barium swallow is a common mean of radiologic assessment for hiatus hernia, but only hernia with separation of anatomic components beyond 2 cm can be diagnosed reliably, and the anatomical structures are not always well-defined. Ultrasound, CT scan and MRI are newer modalities having better resolution of soft tissues, but experience with them is more limited. Similarly, endoscopy requires a separation of at least 2 cm between the SCJ and diaphragmatic impression before hiatus hernia can be diagnosed reliably (**Figure 1.23**).



**Figure 1.23:** Grading of flap-valve (Peter J Kahrilas, Hyon C Kim, *et al.*, 2008). In grade III, even though there is hiatal opening but the SCJ is not displaced. Hiatus hernia is present in grade IV deformity with the SCJ displaced proximally (red arrow).

It can be further confounded with the presence of Barrett's oesophagus, when the diaphragmatic impression is not well seen due to a patulous hernia or when there is excessive insufflation of the stomach. In such cases, an assessment of flap valve, SCJ and the height of hiatal displacement during retro-flexion can be useful. Hiatus hernia is present in grade IV flap valve deformity where there is a loss of muscular ridge, a permanently opened GOJ and a SCJ displaced into the proximal oesophagus (**Figure 1.23**).

More recently, high resolution manometry can provide a better definition of the GOJ components and therefore facilitates localisation or quantification of CD contraction relative to the LOS. In normal individual, there is no separation between the two components (type I). Progressive separation results in separation of pressure peaks, and hiatus hernia is considered present when the pressure minimum between the two peaks is at or below IGP (Type III) (**Figure 1.24**).

However, the separation between components is not always discernible and pressure of these components can be variable between individuals. In such cases, the ability to localise the SCJ will be advantageous. This has been shown in imaging studies of mucosal placed clips at the SCJ in hiatus hernia (P J Kahrilas *et al.*, 1999). However, such an approach is not practical for routine clinical assessment, but this may change with the availability of a new technique allowing continuous monitoring of location of the SCJ.

### **1.6.3 What causes hiatus hernia?**

Possible proposed mechanisms for causation of hiatus hernia include the following. Firstly, the increased IAP forces the GOJ to migrate proximally into the thorax. Secondly, oesophagus is shortened from fibrosis or excessive vagal nerve stimulation. Thirdly, there is widening of the diaphragmatic hiatus from age-related or congenital changes in the muscle or connective tissue. These theories and their supportive evidence are discussed in more detail in the following sections.

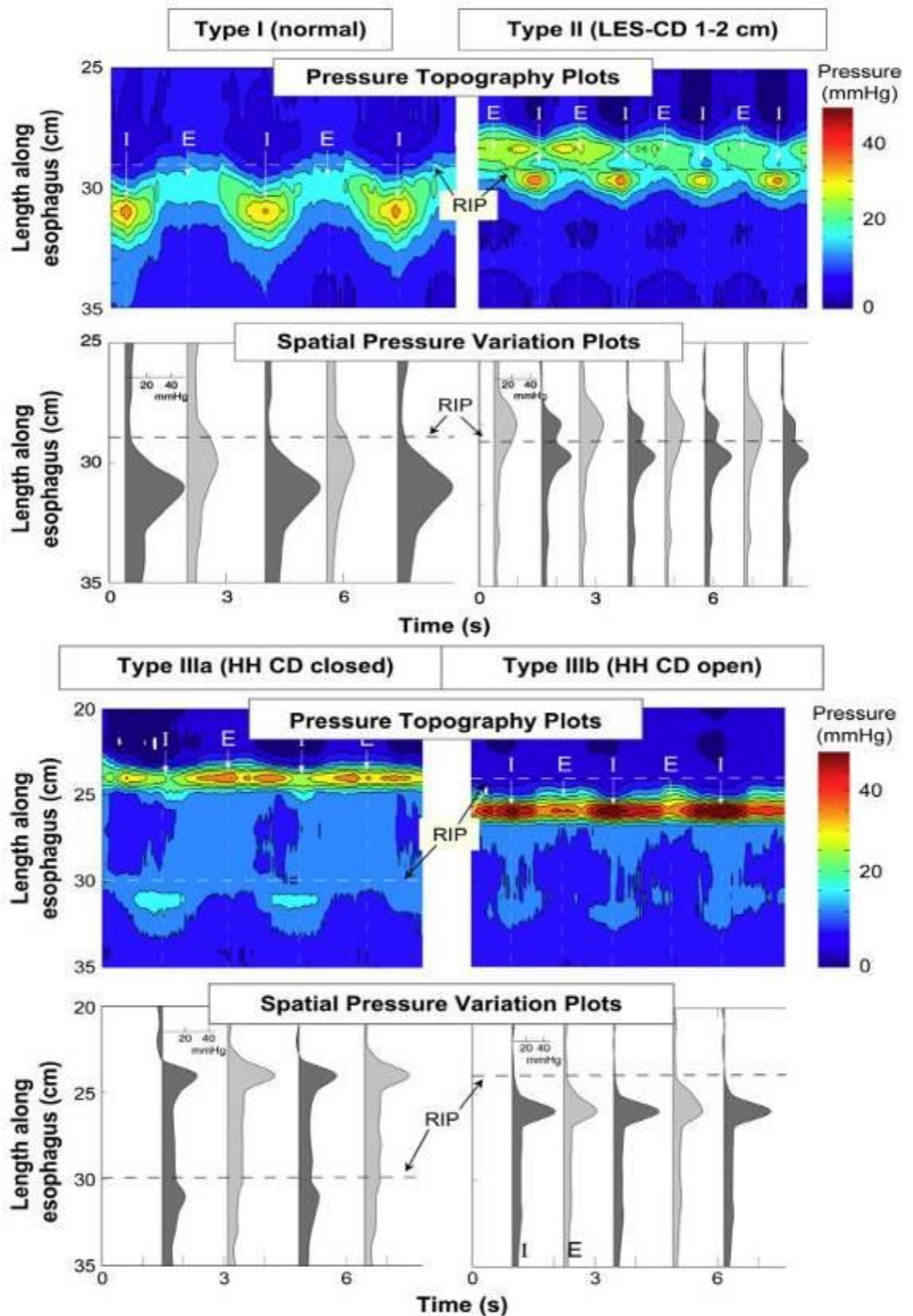


**Figure 1.24:** Manometric grading on the separation of lower sphincter components during hiatus hernia (Kahrilas, Kim & Pandolfino, 2008). Type 1 is normal, Type II is separation of LOS and CD but the pressure minimum between peaks is above IGP and Type III is more separation of LOS and CD (2 cm apart and more) with pressure minimum between peaks is at or below IGP. Type III is subtyped into IIIa (PIP above CD) and IIIb (PIP above LOS).

### 1.6.3.1 Mechanical challenge from raised IAP

The basis of this theory arises from the observation that hiatus hernia is more common among obese subjects and in pregnancy. The rising incidence of obesity worldwide is also seeing a parallel rise in the incidence of GORD. The underlying mechanism for this parallel rise is unknown but an increased risk for hiatus hernia formation among the obese due to mechanical challenge from raised IAP has been suggested. In a recent meta-analysis, of the 4 out of 52 studies involving 3597 patients (51% males), hiatus hernia was associated with increasing BMI with a pooled odds ratio of 1.93 (95% CI: 1.1 - 3.4) (Menon and Nigel Trudgill, 2011) (Table 1.2).

**Table 1.2 Hiatus hernia and BMI**

Author	Country	Study period	Method	Number of patients	OR (95% CI)
Stene-Larsen et al.	Norway	1985-86	Prospective	1224	1.2 (0.9 - 1.6)
Wilson et al.	USA	1974-95	Retrospective	1205	4.2 (2.4 - 7.5)
Van Oijen et al.	Netherlands	2002-04	Prospective	1023	2.1 (1.3 - 3.4)
Yoshimura et al.	Japan	2005-06	Retrospective	280	1.9 (1.1 - 3.4)

In the study by Pandolfino et al. involving 285 patients, high resolution manometer was passed to study the relationship between anthropometric variables and pressure elements of the GOJ (John E Pandolfino, Hashem B El-Serag, *et al.*, 2006). There was significant correlation between BMI and waist circumference (WC) with IGP (both inspiration and expiration) and GOPG (both inspiration and expiration). The IOP was also found to be positively correlated with BMI and WC in particular during expiration. The association with WC was stronger than BMI when both were examined separately. This

can explain the reason why obese men were found to have greater pressure effects than women because the men had a higher WC. In addition, obesity was associated with separation of the GOJ pressure components.

### **1.6.3.2 Acid-induced oesophageal shortening**

The second mechanism is oesophageal shortening from fibrosis as a result of inflammatory damage. The strong link between hiatus hernia and GORD suggests that acid damage is a potential cause for oesophageal shortening. The first evidence that acid can induce shortening comes from a study reported by Shirazi *et al.* (Shirazi *et al.*, 1989). In that study, an oral displacement of the LOS with manometric technique was observed in the opossums after prolonged intra-luminal acid perfusion. The group of Paterson from Ontario, Canada also confirmed the presence of oesophageal shortening with short term acid perfusion in the opossums measured using the strain gauge technique (Paterson, 1997; Paterson & Kolyn, 1994).

The oesophageal shortening was shown to be more permanent when mucosal inflammation was more severe from prolonged acid exposure and when the longitudinal muscles were hyperexcitable as a result of the acid (White *et al.*, 2001). The investigators had ruled out the possibility of intramural nerve injury from acid but the associated inflammation may have caused a fundamental change to the longitudinal muscle physiology. The investigators also proposed that some inflammatory mediators might have resulted in this fundamental change, but the exact mediators are not fully appreciated. One possible pathway is by the mast cell-derived mediators since it was found to be associated with acid-induced mucosal injury in the opossums (Feldman *et al.*, 1996; Paterson, 1998). More recent evidence suggests that luminal acid activates a reflex pathway involving mast degranulation, activation of capsaicin-sensitive afferent neurons and release of substance P (or other related neurokinins) (William G Paterson *et al.*, 2007). This evokes a sustained contraction of the LM and the pathway is suggested as a potential target treatment for oesophageal pain syndromes.

While animal studies provided most of the evidence for acid-induced shortening, this has been replicated in human studies. In twelve volunteers,

the axial length of LOS was determined manometrically at baseline and after normal saline or acid perfusion in a double blind cross-over design one week apart (Dunne and W G Paterson, 2000). It was shown that acid perfusion resulted in a more proximal migration of the LOS by an average of 0.5 cm and a maximum of 1.8 cm. A more recent study using HFIUS also identified acid induced oesophageal contraction in humans (N Pehlivanov *et al.*, 2001). In this study, using an increase in the muscle thickness as a marker for LMC, it was observed that sustained oesophageal contractions were identified in 13/20 heartburn episodes associated with acid reflux but only 2/40 matched control periods. The sustained contractions were reproduced in 75% of acid perfusion (Bernstein)-positive tests but only 14.3% in Bernstein-negative tests.

Above studies suggest that acid can induce shortening of the oesophagus and this has been suggested as a potential cause of hiatus hernia. However, the magnitude of shortening is relatively small even though there may be variation between individuals (some study subjects had shortening of more than 1 cm). Also this only explains why hiatus hernia can occur in association with GORD but it is known that hiatus hernia does not always associate with GORD.

### **1.6.3.3 Changes in connective tissue and crural muscle**

There have been an increasing number of studies reported on changes in muscle and connective tissue (extracellular matrix) being associated with hiatus hernia. Some of these changes are age and gender-related. In a meta-analysis of 30 studies involving 5103 patients, it was found that hiatus hernia was more common in patients above 50 years old with a pooled odds ratio of 2.2 (95% CI: 1.4 - 3.5) (Menon and Nigel Trudgill, 2011). With respect to the effect of gender, 18 out of 56 studies involving 7464 patients, hiatus hernia was more common in males with a pooled odds ratio of 1.4 (95% CI: 1.1 - 1.7) (Menon and Nigel Trudgill, 2011).

Three extra-cellular matrices, viz. elastin, collagen and matrix metalloproteinases were commonly studied. The POL of 13 patients with hiatus hernia, were found to contain 50% less elastin (Curci *et al.*, 2008),

thought to result in a reduction in its recoil property and the ability of the GOJ to return to its normal position. Collagen is important in providing strength to the extracellular matrix. It was observed in a Swedish study that patients with hiatal hernia had abnormal collagen deposition (Asling *et al.*, 2009). Male patients with GORD were associated with overexpression of collagen type III alpha 1 (COL3A1) and this was proposed to be a tissue remodeling mechanism resulting in acid reflux. Matrix metalloproteinases or MMP are important in the degradation and remodeling of the macromolecules in the extracellular matrix. In 6 patients without hiatus hernia undergoing laparoscopic oesophageal myotomy, it was found that increased levels of MMP-2 were detected in the gastrohepatic ligament but not gastrophrenic ligament or POL (Lora Melman *et al.*, 2010). This study suggests that MMP-2 is an important protease in the remodeling of primary ligaments in the GOJ and studying this in patients with hiatus hernia may provide important clue to its etiology.

In addition to changes in the connective tissue, muscle changes in the CD have been reported to be associated with hiatus hernia. In a study involving 93 patients (33 patients with GORD and hiatus hernia) undergoing laparoscopic Nissen fundoplication, intraoperative biopsies were taken from the CD and examined under electron microscopy (Fei *et al.*, 2009). Ultrastructural abnormalities were seen in almost all subjects with hiatus hernia and more than 2/3 abnormalities were severe.

#### **1.6.3.4 Abnormal physiology associated with hiatus hernia**

The most clinically important pathology associated with hiatus hernia is GORD and this has been discussed in section 1.5.4 above.

The formation of phrenic ampulla during swallow has been discussed in section 1.4 above. The emptying process during phrenic ampulla depends on non-peristaltic mechanism involving the LOS, CD and POL. With hiatus hernia, this emptying process is likely to be impaired and has been studied by Kahrilas *et al.* in 1995 (P J Kahrilas *et al.*, 1995). The study involved 7 asymptomatic volunteers and 11 patients with hiatus hernia. Metal clips were endoscopically placed at the SCJ and its location as well as the LOS was

assessed with concurrent manometry and videofluoroscopy with and without abdominal compression. It was found that peristaltic shortening was reduced especially in subjects having larger hiatus hernia (1.1 cm vs. 2.0 cm in upright position). The re-elongation or re-lengthening process (5.4 s vs. 2.9 s in upright position) was longer with a greater degree of hiatus hernia. In the presence of hiatus hernia, the mobility of the SCJ was found to be greatly reduced with or without abdominal compression. The author concludes that oesophageal shortening with hiatus hernia may be a consequence of distal LM partially shortened from the reduced function of the POL or LOS.

## **1.7 EFFECTS OF OBESITY ON THE GOJ AND GORD**

### **1.7.1 Introduction**

In recent decades, obesity has been a growing epidemic affecting the whole world population. The prevalence of obesity has been steadily growing since the end of World War II, initially affecting the Western world and more recently, the Asian countries including China, Japan, Korea and India. The primary cause is consumption of high fat diet and a lack of exercise. Unused calories are then deposited throughout the body but most of its complications arise from deposition of fats in the viscera and blood vessels. Due to its association with coronary heart disease, this is the major cause of mortality worldwide. In a recent report from a multicentre registry involving 13, 874 individuals without known coronary heart disease undergoing coronary CT angiography, after multivariable adjustment, BMI was positively associated with coronary artery disease with odds ratio 1.3 per +5 kg/m<sup>2</sup> (95% CI: 1.2 - 1.3) (Labounty *et al.*, 2012). Besides the US, Scotland is the other country in the world topping the chart with the highest incidence of obesity. From the recent published Scottish Health Survey, more than a quarter of adults in Scotland are obese (Keenan *et al.*, 2011).

Obesity is also a major cause for the 2-fold increase in the incidence of GORD and its complications including erosive oesophagitis, Barrett's oesophagus and oesophageal adenocarcinoma (Hashem B El-Serag, 2005). The exact mechanism of how obesity promotes GORD remains elusive. It has been shown that increases in IGP and GOPG are associated with obesity (Hashem B

El-Serag *et al.*, 2006). This is thought to increase the chance for reflux to occur across the LOS. However, there are conflicting results from early studies on the association between obesity and oesophageal acid exposure. These studies were limited by small sample size. For example, Lundell *et al.* found no association between GORD and massive obesity (BMI 42.5 Kg/m<sup>2</sup>) in 50 patients referred for gastroplasty (Lundell *et al.*, 1995). In a more robust study involving 206 patients undergoing 24 h pH-metry, El-Serag *et al.* reported that a BMI > 30 Kg/m<sup>2</sup> was associated with increase in reflux episodes, longer reflux episodes (> 5 min) and time pH < 4 in all postures (Hashem B El-Serag *et al.*, 2007). When a model adjusted for WC was included, the measures for oesophageal acid exposure were less significant, suggesting that WC is the more important mediator.

In addition to acid exposure, obesity is associated with changes to the GOJ. It has been shown by Pandolfino *et al.* that obesity was associated with increased separation of the lower sphincter components using the high resolution manometry technique (John E Pandolfino, Hashem B El-Serag, *et al.*, 2006). The exact relationship between the different components in the GOJ is not clear and further studies are needed.

The next section discusses IAP and its relationship with obesity. The mechanical link between IAP and obesity to changes in the GOJ is then discussed. The last section deals on obesity and GORD by providing epidemiology evidence and pathophysiological mechanisms besides the rise in IAP.

### **1.7.2 IAP and obesity and their effects on the GOJ**

Detrimental effects of raised IAP are well-recognised from trauma and critical care literature. These effects include decreased cardiac output from reduced venous return, reduced perfusion to abdominal viscera (liver and kidneys) and formation of hernias. Direct measurement of IAP is invasive and therefore other less-invasive techniques have been developed including measurement of the urinary bladder, rectal or anal manometry and measurement of the IGP. Studies have shown that these indirect techniques provide good approximation to direct IAP measurement (Fusco, Martin & Chang, 2001;

Iqbal, Haider, Stadlhuber, *et al.*, 2008). Using bladder measurement in 20 normal subjects, the mean IAP during sitting and standing were 16.7 and 20 mmHg respectively (Cobb *et al.*, 2005). Coughing and jumping generated the highest IAP but lifting 10-pound weights and bending at the knees did not generate excessive levels of pressure. The mean pressure between males and females was not different in the above-mentioned manoeuvres. A significant correlation between higher IAP and increased BMI was also seen in these normal subjects.

In a study involving 322 patients undergoing manometry at an open access centre, measurement of the IGP was correlated with anthropometric measures (Hashem B El-Serag *et al.*, 2006). There was a correlation between IGP with BMI and WC even after adjustment for age, race or gender. In another study involving 355 patients undergoing high resolution manometry, BMI and WC were also shown to correlate positively with IGP and GOPG (John E Pandolfino, Hashem B El-Serag, *et al.*, 2006). Again, the correlation remained significant after adjusting for age, gender and patient type. These studies suggest that the effect of obesity is mediated through a rise in the IAP. Besides a rise in IGP, obesity also produces other pressure effect on the GOJ. Experimental studies to assess the effect of raised IAP on the GOJ can be simulated with application of abdominal belt. It has been shown that the application of abdominal belt can adequately raise the IAP (McGill *et al.*, 1990). The actual effect of raised IAP on the LOS tone remains controversial. Some studies have shown that increases in IAP buttress the intra-abdominal segment of the LOS but without changing the LOS tone (Vanderstappen & Texter, 1964; Nagler & Spiro, 1961). However, others have shown an increase in the LOS tone as an adaptive response to raise IAP (Lind, Warrian & Wankling, 1966; Cohen & Harris, 1970). These differences between studies may have been due to differences in techniques used. In addition, different degrees of LOS shortening and the presence of hiatus hernia may produce a different effect. In a 4-side channel manometric study involving 20 normal volunteers and 35 patients with reflux oesophagitis, proximal LOS movement was seen with abdominal compression (Dodds *et al.*, 1975). The LOS-IGP gradient did not change significantly with abdominal compression in both normal subjects and patients with oesophagitis. In another study using Dent

sleeve in 10 asymptomatic subjects, the increase in IAP with straight leg-raising resulted in the increase of IGP and LOS pressure (DiLorenzo *et al.*, 1989). The increase was considered to be a passive phenomenon since the response of the LOS did not persist with removal of IAP.

A recent study from Glasgow had shown a strong association between BMI and oesophageal acid exposure in both erect and supine position in a group of 103 dyspeptic subjects with normal endoscopy (Derakhshan *et al.*, 2012). A strong positive correlation was also seen between BMI with IGP, inspiratory GOPG and inspiratory LOS pressure (atmospheric) but not LOS pressure relative to IGP on expiration. Using a constricting abdominal belt in 18 healthy subjects, similar manometric changes to those associated with BMI were found other than the reduced LOS pressure to IGP. This has been suggested to be due to the chronic effect of BMI on the LOS and this has not been replicated with the use of belt which produces acute effect.

As a summary, the effect of obesity is mediated through an increase in the IAP and this produces a mechanical challenge to the GOJ. There is also accompanying changes to the lower sphincter physiology but the direction of change can be variable. This may depend on the length of sphincter being exposed to the effect of IAP. A shorter oesophagus as a result of hiatus hernia may remove the buttress effect of abdominal LOS from raised IAP. This altered physiology predisposes obese subjects to acid reflux and the next section will discuss on association between obesity and GORD.

### **1.7.3 Obesity and GORD**

Epidemiological evidence suggests a linear relationship between obesity and GORD. A higher BMI is found to be associated with increase in reflux symptoms including heartburn and/or regurgitation. Similarly, a higher BMI is associated with increase in oesophageal acid exposure when measured using 24-h pH monitoring. The OR for GORD in the obese subjects derived from larger population-based studies (German National Health Survey and Bristol Helicobacter Project) using symptoms as end-point was approximately 2.6 to 2.9. The Glasgow study had found that in 105 patients with upper GI symptoms, normal endoscopy and *H. pylori* negative, PPI therapy was

superior to placebo (Fletcher *et al.*, 2011). BMI is a highly significant predictor of response to PPI and is similar to oesophageal pHmetry or manometry. The strong predictive value of BMI is probably due to its association with reflux disease (PPI responder) and it is a more reproducible measure than symptom characteristics.

Central adiposity is likely more important than BMI in the pathogenesis of GORD. The measure of central adiposity including WC or WHR has been found to be a better predictor for GORD than BMI including reflux symptoms and oesophageal acid exposure. In addition to mechanical challenge, central obesity may affect oesophageal motor activity through humoral mechanisms including cytokines IL-6 and TNF-alpha. Evidence also suggests that obesity is associated with complications of GORD including erosive oesophagitis, Barrett's oesophagus and oesophageal adenocarcinoma.

One of the pathophysiological mechanisms underlying GORD in obesity is mechanical change to the GOJ mediated through an increase in the IAP. Above sections (1.7.2 and 1.6.3.1) have discussed on the LOS abnormalities and increased prevalence of hiatus hernia associated with obesity. The current section discusses other possible mechanisms including TLOSRS, oesophageal body motor abnormalities and gastric motor abnormalities. An introduction to TLOSRS has been given in section 1.4.4. In a study from Hong Kong, 84 subjects (obese 28; overweight 28 and normal weight 28) were studied using multichannel perfusion manometry and 24-h pHmetry. It was found that the rate of TLOSRS was higher during postprandial period in obese and overweight subjects (obese 7.3; overweight 3.8 and normal weight 2.1). The proportion of TLOSRS with acid reflux was also significantly higher in obese and overweight subjects (obese 63.6%; overweight 51.8% and normal weight 17.6%). A smaller study involving 14 subjects (7 obese) reached a similar conclusion (J H Schneider *et al.*, 2009). The reason for the increase in rates of postprandial TLOSRS among the obese is not clear. The authors postulated that the higher IAP associated with obesity leads to more intense stimulation on the mechanoreceptors in the proximal stomach. The higher GOPG is thought to contribute to a higher proportion of TLOSRS with acid reflux among the obese.

In studies of obese patients undergoing bariatric surgery, it was found that oesophageal dysmotility was common with the largest study reporting prevalence of 25.6% in 345 patients (Jaffin, Knoepflmacher & Greenstein, 1999; Suter, Dorta, Giusti, *et al.*, 2004). Most common dysmotility disorders reported include nutcracker oesophagus and non-specific motility disorder. A large majority of these patients were asymptomatic. In a more recent study utilising combined impedance, manometry and pH techniques, it was more common to find defective emptying of the oesophagus in GORD and in morbid obesity (Quiroga *et al.*, 2006). These studies suggest that obese subjects may have more GORD partly as a result of dysmotility and impaired emptying of the oesophagus.

Gastric motor abnormalities are also more common among the obese subjects. In a study, obese patients with acid reflux were found to be more sensitive to distension of the proximal stomach compared to obese patients who did not have reflux (Iovino *et al.*, 2006). Obese subjects have significantly larger stomach capacity compared to non-obese subjects, increasing the risk of reflux (Granström and Backman, 1985). Finally, obesity is associated with delay in gastric emptying (Maddox *et al.*, 1989). These gastric motor abnormalities among the obese can increase the risk for acid reflux.

## 1.8 SUMMARY OF LITERATURE REVIEW

The GOJ is a highly complex anatomical region at the distal oesophagus before it enters the proximal stomach. The primary physiology of oesophagus is bolus transport through the process of peristalsis. The GOJ is involved in the process of bolus emptying through the formation of phrenic ampulla. Another important physiological process involving the GOJ is TLOSRS which allow belching of air after meals. Oesophageal manometry is a technique allowing measurement of pressure dynamics (circular muscle function) during swallows and TLOSRS. Manometry has evolved into a highly sophisticated technique in recent decades with the development of high-resolution and high-definition sensors. One deficiency is measurement of shortening (longitudinal muscle function) of which available techniques (fluoroscopy and intraluminal ultrasound) are limited by radiation and complicated image processing analysis. While LOS movement can be appreciated with the HRM

technique, it is less sensitive during smaller movement. Using available techniques, however it has been shown that oesophageal shortening can be up to 9 cm during TLOSRS. Another deficiency is the lack of a technique to reliably measure the position of the SCJ. Acid exposure especially during postprandial period right across the SCJ but within the sphincter (acid pocket and short segment reflux) is important determinant for metaplastic change in Barrett's oesophagus. Abnormality in the GOJ can accelerate this process especially in the presence of hiatus hernia. So is mechanical challenge to the integrity of the GOJ barrier in the presence of obesity. Based on the above review, it seems prudent to develop a reliable technique allowing precise and continuous monitoring of the GOJ and SCJ in order to gain a better understanding on the complex relationship between hiatus hernia, obesity and acid exposure. As such, the next section deals in the objectives for the research presented in this thesis.

## 1.9 OBJECTIVES OF RESEARCH

It is postulated that an elevated IAP related to increased visceral obesity will affect the dynamics of proximal migration of the GOJ potentially leading to permanent hiatus hernia but that this effect will initially only be apparent during TLOSRS. It is only during TLOSRS that the CD is completely relaxed and the POL thus exposed to the effects of the pressure gradient between the abdominal and thoracic cavity. During these relaxations, the high pressure gradient will cause excessive craniad stretching of the POL and CD eventually leading to hiatus hernia.

Due to limitations of other techniques to measure movement and location of the GOJ, we developed new techniques (2-dimensional or 2-D and 3-D locator probes) allowing monitoring of pressure and pH with respect to position of the GOJ and used these to investigate TLOSRS in both normal and pathological conditions.

In chapter 2, a general description of materials and methods used in all of the clinical experiments performed in this thesis is given. Technical details, test preparation and parameters measured using manometry, pHmetry and

locator probe are described in this chapter. Programs, data processing and statistical analysis used are also mentioned. Finally, ethical approval for all human studies is detailed in the current chapter.

In chapter 3, the development and challenges on the use of the novel GOJ locator probe is described. Firstly, the Hall Effect and magnet, both the driving principles behind the novel probe are introduced. It is then followed with a detailed description on the development and challenges of the 2-D locator probe.

In chapter 4, in-vitro studies performed to evaluate the strengths and weaknesses of the 2-D probe and its interference with other probes are detailed. The chapter is concluded with description of in-vivo validation of the new probe against the current gold standard, fluoroscopy.

In chapter 5, due to limitation of 2-D probe, based upon results of in-vitro and in-vivo studies described in chapter 4, a newer 3-D probe has been developed but the life span is limited due to poor design. Finally, introduction to a new generation 3-D probe based on magnetoresistive sensor is given.

In chapter 6, a detail study on the behaviour of normal migration of the GOJ during TLOSRS and swallows in normal subjects is described. Firstly, the methodology of study is being described. The results are then presented followed by discussion of the findings.

In chapter 7, we explore the effect of raised IAP and obesity on the behaviour of the GOJ, both during period of stable lower sphincter tone and during TLOSRS. The methodology is first presented followed by key results. The discussion is based on findings of partial hiatus herniation and short segment reflux with effect of central obesity and waist belt in asymptomatic healthy subjects.

In chapter 8, the final chapter, it provides the conclusion and limitations to all the works presented in this thesis. Possible future studies with the novel probe are also discussed.

# CHAPTER 2

## MATERIALS AND METHODS

---

- 2.1 Introduction
- 2.2 Upper gastrointestinal endoscopy
- 2.3 Imaging studies
- 2.4 The GOJ locator probe
- 2.5 In-vitro studies on magnet orientation relative to the locator probe
- 2.6 High resolution 36-channel manometry system
- 2.7 High resolution 12-channel pHmetry
- 2.8 Combining different catheters, their time synchronization and techniques for nasal intubation
- 2.9 Test meals
- 2.10 Abdominal belt
- 2.11 Specialised Gastrointestinal Investigation Unit
- 2.12 Software and data processing
- 2.13 A curve fitting approach to movement of the GOJ during TLOSrs
- 2.14 Data and statistical analysis
- 2.15 Ethical committee approval

## **2 MATERIALS AND METHODS**

### **2.1 INTRODUCTION**

The current chapter provides a detailed description of the equipment used to carry out all research presented in this thesis i.e. endoscopy and fluoroscopy, pHmetry, high resolution manometry and the GOJ locator probe were among the most frequently used equipment. The GOJ locator probe is briefly described here with more details on its development, in-vitro and in-vivo studies given in chapters 3, 4 and 5. A description of how the locator probe, manometry and pHmetry are combined during studies in chapter 6 and 7 follow. The test meals and abdominal belt used for studies in chapter 6 and 7 are also presented in the current chapter. The software used to process and analyse the data acquired from the equipment are then described. The curve-fitting approach to model the movement of the GOJ during TLOSRS is also detailed in the current chapter. Statistical approaches to analysis of data are likewise discussed. Lastly, the chapter ends with information on the ethical approval for all research performed in human subjects.

### **2.2 UPPER GASTROINTESTINAL ENDOSCOPY**

#### **2.2.1 Description of equipment**

The gastroscope consisted of a fibre optic bundle tube approximately 100 cm in length, incorporating a light source and camera and irrigation, suction or working channels. When passed orally or trans-nasally into the oesophagus and stomach, images were obtained and recorded on a video imager. A working channel allowed sufficient passage for a clipping device. In these studies, the models employed were either from Pentax UK Ltd. or from Olympus Keymed Ltd.

#### **2.2.2 Preparation for test**

Prior to a study day, each subject had to fast for at least 8 to 12 hours, to allow full emptying of any stomach contents and therefore avoiding any possible risks

of aspiration pneumonia. Most studies in this thesis involved healthy volunteers who were not on any medication. A few study subjects who were on PPI medications were asked to discontinue these for at least seven days prior to endoscopy and remain off them until the study was completed. These subjects were prescribed either Gaviscon® and or Ranitidine for any symptoms but were asked to avoid these on the morning of the endoscopy test. All subjects were required to avoid alcohol 24 hours and smoking 12 hours prior to and after the examination. All of the above information was available on an information leaflet which was given to study subjects prior to the study day. On the day of examination, after informed consent, the subject was administered either a local lignocaine spray or placed under moderate sedation with 2 - 4 mg of IV midazolam. The subject lay in the left lateral decubitus position and the endoscope passed orally.

### 2.2.3 Description of procedure

A quick survey of the stomach was performed and biopsies were taken from the antrum and or body to check for *H. pylori* status (CLO test from Kimberly Clark ltd., Kent, UK and or histology). In all studies involving the GOJ locator probe, a metal-clip was placed at the SCJ during upper endoscopy using a clipping device (Olympus HX-201UR-135; Tokyo, Japan) which was passed through the working channel (Figure 2.1).

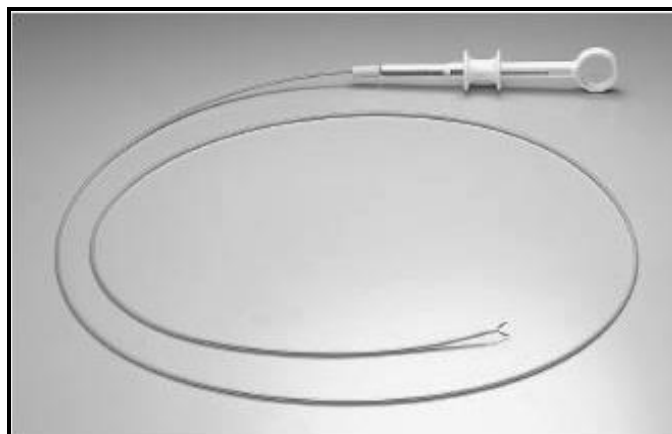


**Figure 2.1:** Clip fixing device with endoclip (model HX-201UR-135, Olympus, UK) that passes through the working channel of a standard 27F endoscope.

The metal-clip was made from stainless steel, a length of 15 mm with two jaws. A small magnet (2 mm diameter and 1mm thick) made from samarium cobalt (grade SmCo30; e-Magnets UK, Sheffield, UK) was attached to one of the jaws of the metal-clip as shown in **Figure 2.2**. Only one magnet was allowed to be placed for each subject. This was to avoid having free magnets in the lumen of the intestines and the consequent risk of them attaching to each other between two loops of bowels. The whole procedure took 5 to 10 min depending on the anatomy, technical difficulties, subject's tolerance and nursing assistance. After completion of the procedure, the subject would be transferred to a nearby observation ward to monitor blood pressure and oxygen saturation if sedation had been administered. Otherwise, the subject was allowed food only after an hour if he had received lignocaine spray. The procedure was uncomplicated and safe in healthy subjects.

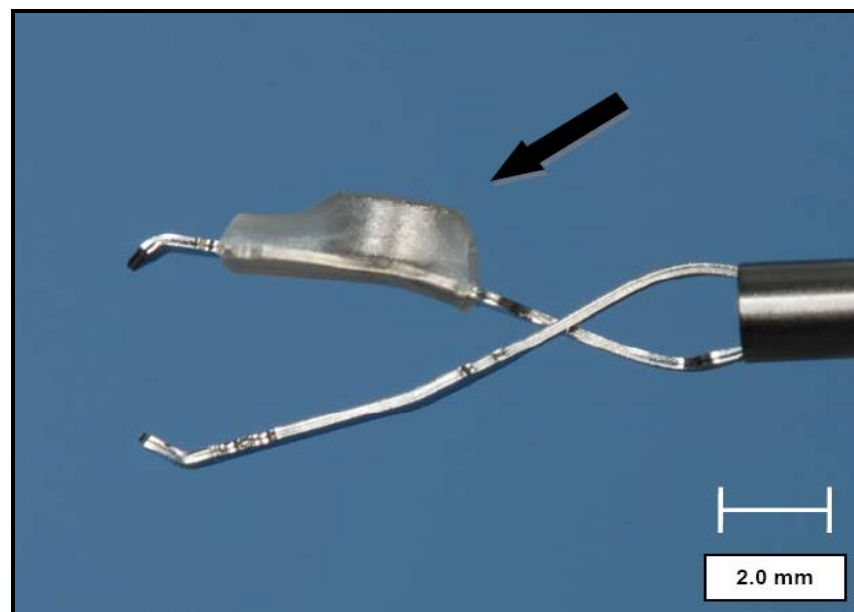


**Figure 2.2:** Photo illustrating a single use endoclip (model HX-201UR-135, Olympus, UK) with a small samarium cobalt magnet attached on the jaw by heat shrinkable and medically safe polyvinylidene fluoride (PMG Plastronic, UK) (shown with black arrow). A scale is drawn on the lower right to depict the size.

## 2.3 IMAGING STUDIES

In order to validate the GOJ locator probe (chapter 4) in-vivo, fluoroscopy, an X-ray imaging technique allowing real-time video images of internal structure, was used concomitantly to record the movement of the metal-clip applied at the SCJ (**Figure 2.3**). For the in-vivo studies (chapter 4), X-ray screening was performed using a portable C-arm fluoroscope (BV Pulsera, Philips Healthcare, Surrey, UK). Total screening time lasted approximately 60 - 80 s in each subject and each screening was fixed at 5 frames per s. To synchronise the two systems, a metal marker was placed at start and end of fluoroscopic screening with simultaneous digital markers placed for the GOJ locator system.

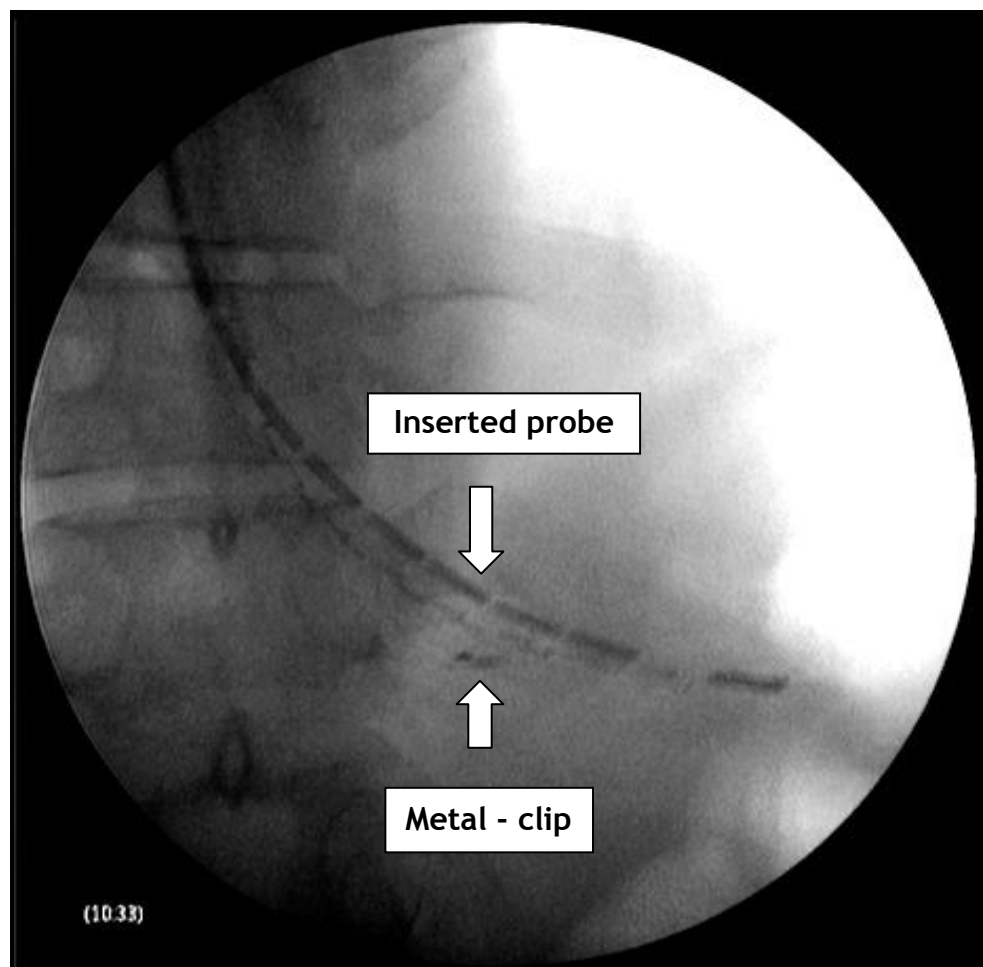


**Figure 2.3:** An example of x-ray screening of the clip position relative to the inserted probe.

All images recorded during fluoroscopy screenings were transferred and stored within the Picture Archiving and Communications System (PACS). The built-in software within the PACS allowed reliable measurement of the distances of the clip from the probe or spine during screening period (**Figure 2.3**). The position data from fluoroscopic screening were then compared with the position data recorded by the GOJ locator system.

Chest radiograph or chest X-ray was the other imaging study which was utilised in the current study. All subjects who had a metal-clip fixed at the SCJ had a chest X-ray within 6 - 8 weeks to document clearance of the clip. A posterior-anterior (PA) view held in respiration was adequate for assessment of the clip. If the subjects required an MRI before 6-8 weeks, then an earlier chest x-ray would be arranged. The radiation doses resulting from these studies were assessed and approved by the Radiation Protection Service, NHS Greater Glasgow and Clyde.

## **2.4 THE GOJ LOCATOR PROBE**

### **2.4.1 Technical details and calibration**

The locator probe was a new technique allowing precise and continuous measurement of position of the SCJ. The technique firstly required a small magnet to be clipped at the SCJ during upper endoscopy examination. A catheter-based probe was then passed nasally to detect the position and movement of the magnet along its length. The probe was developed in-house and is therefore not commercially available. A detailed description of its components and its construction is explained in chapter 3. It was available in two versions. The first and older version was a 2-D Hall Effect probe with an outer diameter of 4.8 mm and a recording length of 120 mm. The second and newer version was a 3-D Hall Effect probe with an outer diameter of 4.5 mm and a recording length of 180 mm. The probe was connected to a microprocessor unit which converted analog data to a digital format. The microprocessor unit was connected to a Polygraf® recorder and its accompanying software, the PolygramNET™ (Synectics Medical Ltd, UK), which allowed the data to be displayed in real time at a frequency of 8 Hz and saved for later analysis. The

raw data could be extracted in ASCII format and transferred to a Microsoft Excel spreadsheet.

## 2.4.2 Calibration and cleaning

Using a plastic basin containing warm water at 37°C and a depth of 1.5 - 2.0 cm, the probe was immersed for 1 min before undergoing calibration. The steps for calibration were the same for both the old 2-D and the new 3-D Hall Effect probes. Calibration was performed by first zeroing the probe at the minimum position value of 0 mm and minimum strength value of 0 mV without any presence of magnet and then calibrating the probe with a small magnet pole placed directly on top of the last sensor which would calibrate the maximum position value of 120 mm (180 mm for the 3-D probe) and the maximum strength of 1200 mV (880 mV for the 3-D probe).

After calibration, the probe was cleaned each time using Tristel sporicidal wipe (Tristel Solutions Ltd, UK) before any nasal intubation. Tristel sporicidal wipe contains patented chlorine dioxide (ClO<sub>2</sub>) allowing high level disinfection of a medical device. The technique for intubating the probe nasally is described in section 2.8.3 of this chapter. After each use, the probe would be cleaned using a detergent solution mixed with water first and then followed by clean water. It would then be kept away in a box and stored in a cool dry place.

## 2.4.3 Parameters measured with the locator technique

The measurement outputs from the locator probe include the position of the SCJ (in cm) and signal strength (in mV). The signal strength is a measure of strength of detected magnetic field, indicating the presence of magnet. The position and migration of the SCJ is the most important measurement in this regard. The migration of the mucosal clip at the SCJ was under the assumption that the mucosa movement closely reflects the oesophageal wall movement. The proximal migration of the mucosal clip at the SCJ is a result of longitudinal muscle shortening but there may be a very slight difference due to shear movement between the two layers, previously described in section 1.4.5.1. The position of the SCJ is analysed using a custom-made software (drcontour6)

described in section 2.9. Movement of the GOJ during TLOSRS was defined by the following parameters (**Figure 2.4**):

Amplitude of GOJ migration: This was the maximum height (cm) of movement occurring during a TLOSRS and a swallow. Amplitude was taken as the difference between the height at the peak and the height at baseline during a TLOSRS.

Duration of GOJ migration: This was the time (s) taken to complete the movement during a TLOSRS and a swallow from the start to the end.

### GOJ migration (cm)

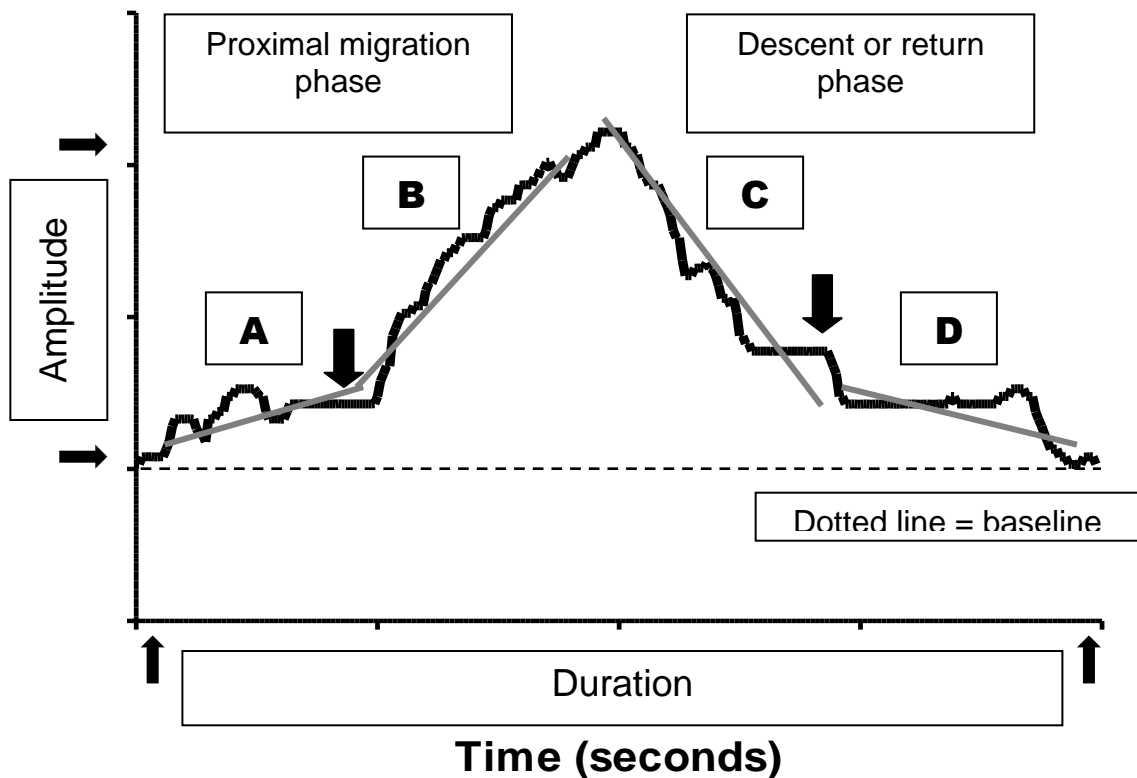


**Figure 2.4:** Illustration of parameters that describe the migration behaviour of the GOJ during TLOSRS.

Phase A velocity: This was the velocity (cm/s) for the initial and often slow phase of GOJ movement during its proximal migration in a TLOSRS.

Phase B velocity: This was the velocity (cm/s) for the later (after phase A) and often more rapid phase of GOJ movement during its proximal movement in a TLOSR.

Phase C velocity: This was the velocity (cm/s) for the initial and often rapid descent phase of GOJ movement during a TLOSR.

Phase D velocity: This was the velocity (cm/s) for the later and often slower phase of GOJ movement during a TLOSR.

## **2.5 A CURVE-FITTING APPROACH TO MOVEMENT OF THE GOJ DURING TLOSRS**

The ability to precisely and continuously measure the position and migration of the GOJ using the locator probe is novel and has not been previously reported in scientific literature. Hence, an approach to analyse the data was needed to describe the observed migration of the GOJ especially during TLOSRS, detailed in chapter 6 and 7. Initial approaches to analysis involved graphical and crude descriptions on the observed migration behaviour. The pattern of GOJ migration during TLOSRS involves two separate phases, initially a proximal migration phase followed by its return to baseline or descent phase (**Figure 2.4**).

During proximal migration, the curve is observed to have two phases - an initial slow phase (phase A) followed by a later fast phase (phase B). During descent, the curve is also observed to have an initial fast phase (phase C) followed by a slower phase (phase D). These different phases represent different physiology that manifests the GOJ movement during TLOSRS. A first approach to describe data of velocities for each of these migration phases was to calculate the average velocities in each of the four quadrants, separated equally based on the total duration of migration (**Figure 2.5**).

However, the first approach did not reveal any significant differences in average velocities between these phases. As a result, a different approach was explored to assess the velocities, since the migration pattern from the plots suggested that the phases were physiologically different. In the absence of a compartmental or physiologically validated model to describe the movement of

the GOJ, a curve-fitting approach was adopted to objectively describe the various phases of GOJ movement.

### GOJ migration (cm)

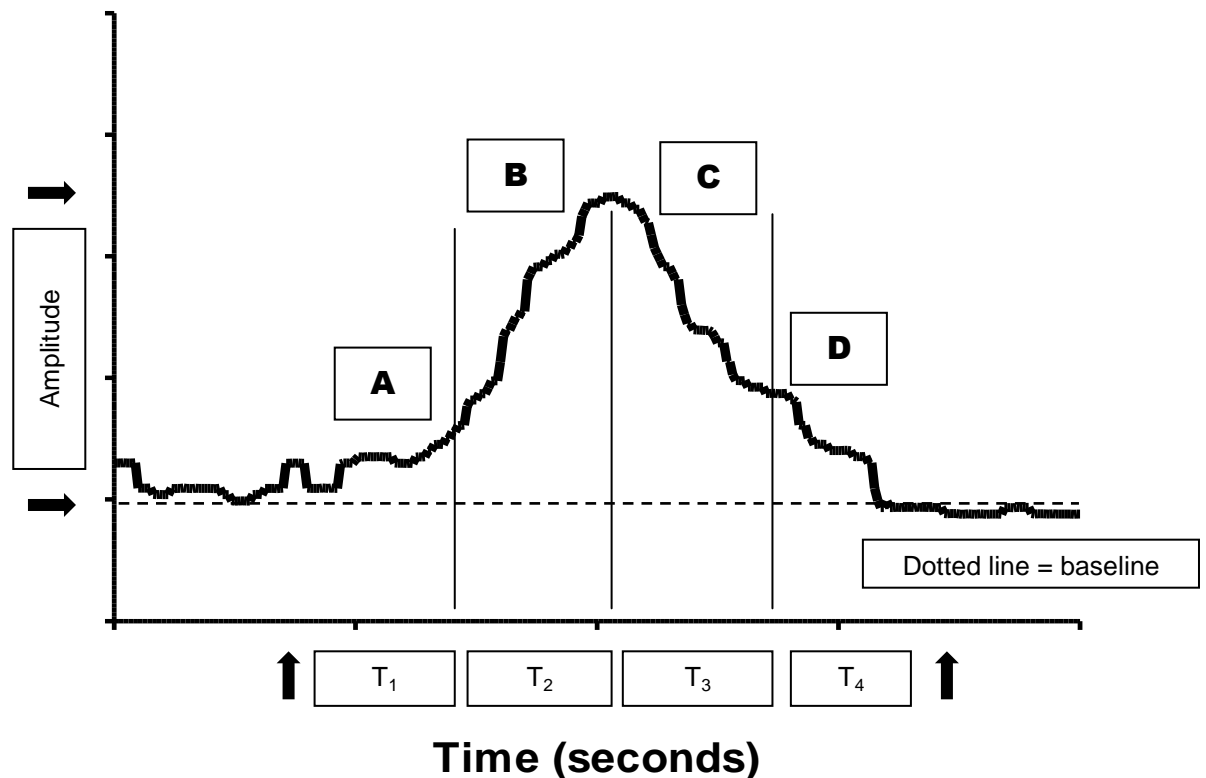


**Figure 2.5:** Average velocities in each quadrant A-D, calculated by distance migrated in that quadrant divided by the duration of quadrant. Each quadrant has similar duration, divided equally by total duration of migration.

Due to a lack of uniformity in the data (**Figure 2.4**), Gaussian and exponential models were deemed not to be suitable curve-fitting approaches. A polynomial curve-fitting approach was adopted on the principle that the multiphase proximal migration could be modelled independent of the multiphase descent using higher order polynomial functions. The proximal migration and the descent phase were described separately using a curve-fitting approach. The goal of curve-fitting, in our case, was to determine the maximum rate (s) or velocities of migration in each phase described above. Initial assessment of curve-fits indicated that high order polynomial could describe these two separate phases of GOJ migration during TLOSrs.

A sixth order polynomial equation was able to fit these phases of migration. The sixth-order equation is described as below (1). Two separate equations were used: one for proximal migration phase (**Figure 2.6**) and another equation for the descent phase.

$$y = ax^6 + bx^5 + cx^4 + dx^3 + ex^2 + fx \quad (1)$$

where  $y$  was amplitude (cm),  $x$  was time (s) and  $a$ ,  $b$ ,  $c$ ,  $d$ ,  $e$  and  $f$  were non-linear regression parameters. The values of the parameters  $a - f$  could be determined by setting up a model in Microsoft Excel 2010 (Microsoft Corp., USA). Using the “LINEST” function (add-in) in Excel, values of parameters  $a - f$  could be determined by non-linear regression and was the solution to the line which best fitted the data. Briefly, LINEST calculates the statistics for a line using the “least squares” criterion to calculate the line that best fits the data, and returns an array of parameters that describe the line. The LINEST function also allows regression statistics including standard error for parameters, F statistic, degrees of freedom (df), regression sum of squares (ssreg) and residual sum of squares (ssresid).

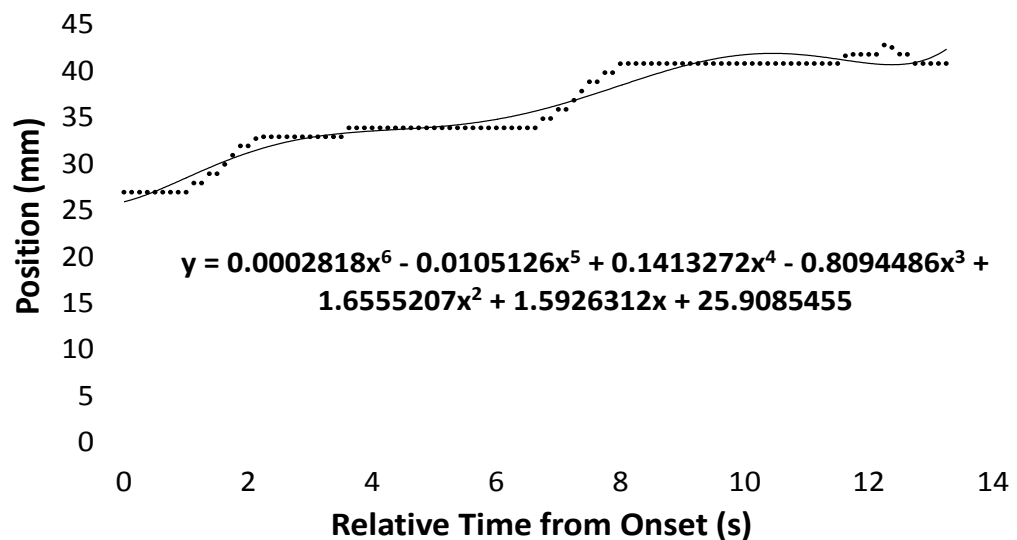


**Figure 2.6:** Curve-fitting using 6<sup>th</sup> order polynomial equation. The figure is an example of curve-fit using the 6<sup>th</sup> order equation during proximal migration phase in one of the TLOSRS.

Physiologically, anything above sixth order polynomial would be likely fitting noise but more importantly, they would be unlikely to alter interpretation since the fit of the data on the slopes could not be much better. To illustrate that sixth order was fitting slopes better than lower orders, Akaike Information Criteria (AIC) was calculated for second, third, fourth, fifth and sixth order polynomials. This is one of the measures in statistics to assess goodness of fit of a model with many different regression parameters. The goodness of fit describes how well a model fits a set of observations.

The formula for AIC is as follows:

$$AIC = N \cdot \ln(\text{weighted ssresid}) + 2 \cdot \text{npar}$$

where N was number of data points assessed, weighted ssresid was the weighted value for residuals sum of squares and npar was number of parameters or orders.

**Table 2.1:** Calculation of AIC for different orders of polynomial equations

	2 <sup>nd</sup> Order	3 <sup>rd</sup> order	4 <sup>th</sup> order	5 <sup>th</sup> order	6 <sup>th</sup> order
AIC	230.1	447.0	167.8	151.7	129.2

---

AIC; Akaike information criteria

For a given set of candidate models for the data, the preferred model is the one with the least AIC value. One advantage of AIC is the inclusion of a penalty that discourages overfitting. Data points for 8 subjects were analysed and AIC calculated (Table 2.1). The sixth order had the least AIC value of 129.2, which indicates that the sixth order is a better fit compared to other tested lower order models but not higher orders.

When fitting the equation, it was noted that there were further two distinct phases (two maximal rates) in each of the proximal migration and descent

phases of the GOJ during TLOSRS (Figure 2.7). The maximal rates or velocities for the two different phases during the proximal migration and descent of GOJ were measured using elementary calculus to determine the value (slope) of a tangent at the points of inflection on the curve,  $y$ .

The first derivative of equation (1) is:

$$dy/dx = 6ax^5 + 5bx^4 + 4cx^3 + 3dx^2 + 2ex + f \quad (2)$$

where  $dy/dx$  was the first differential of  $y$ ,  $x$  was time (s) and  $a$ ,  $b$ ,  $c$ ,  $d$ ,  $e$  and  $f$  were the parameters determined by the regression fit. The tangent to the slope at the point of inflection on the curve,  $y$  was also the value of  $dy/dx$  at the local minimum or maximum near to that point on the curve. This could be solved mathematically by finding the values of  $x$  of the second differential of  $y$ ,  $d^2y/dx^2$  given in equation (3) when  $d^2y/dx^2 = 0$ :

$$d^2y/dx^2 = 30ax^4 + 20bx^3 + 12cx^2 + 6dx + 2e \quad (3)$$

where  $d^2y/dx^2$  was the second derivative of  $y$ ,  $x$  is time (s) and  $a$ ,  $b$ ,  $c$ ,  $d$  and  $e$  were the parameters determined by the regression fit. The value of  $x$  at  $d^2y/dx^2 = 0$  could be determined using the “Goal Seek” function in Microsoft Excel. Briefly, the “Goal Seek” function is another add-in of the Microsoft Excel software, and is part of “what-if” analysis tools. It allows us to determine the input value ( $x$  value in our case) of the formula when the desired output ( $d^2y/dx^2 = 0$ ) is known. The calculated value of  $x$ , using Goal Seek, when entered into  $dy/dx$  gave the rate of change at the point of inflection of the curve,  $y$ .

The maximal rates or velocities for each phase in every TLOSRS were then calculated and analysed. Using this approach, the velocities for each phase A - D were able to be determined and separated out physiologically. All of the above steps could be automated for easier analysis of each TLOSRS event using the Microsoft Excel 2010 program.

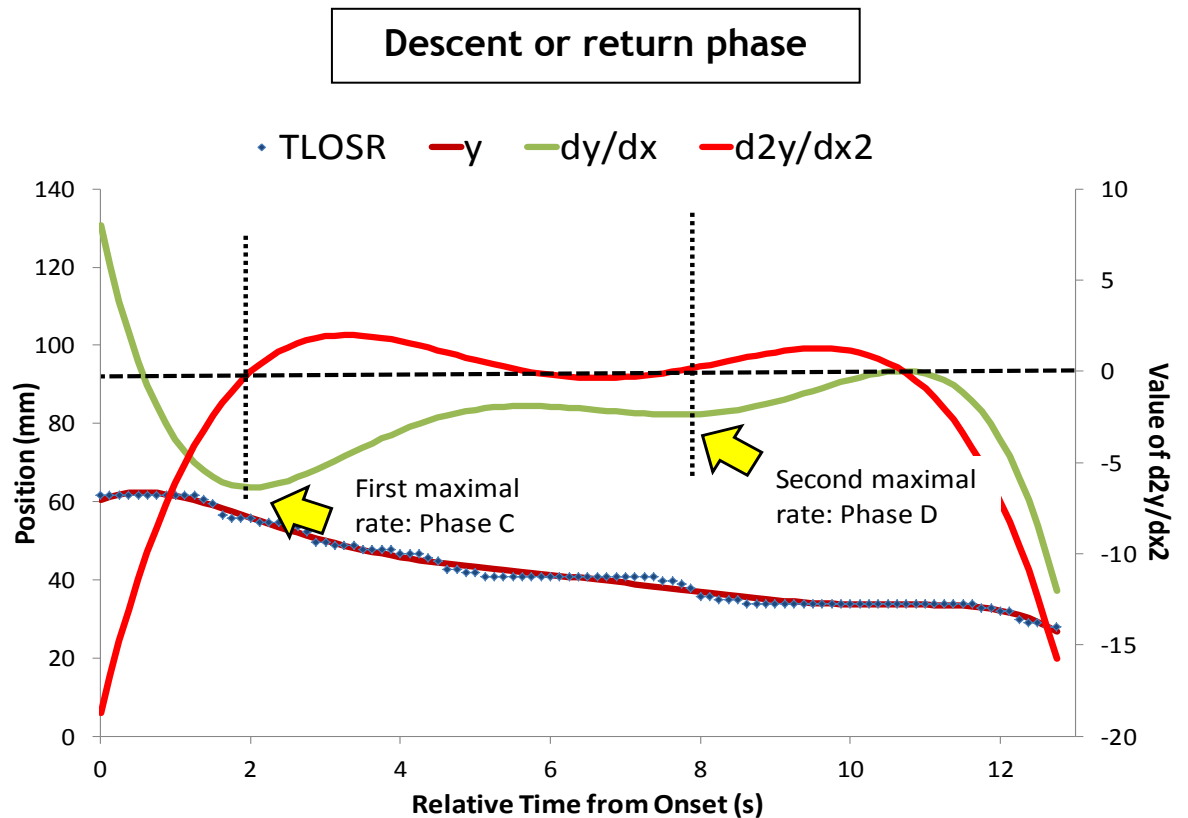
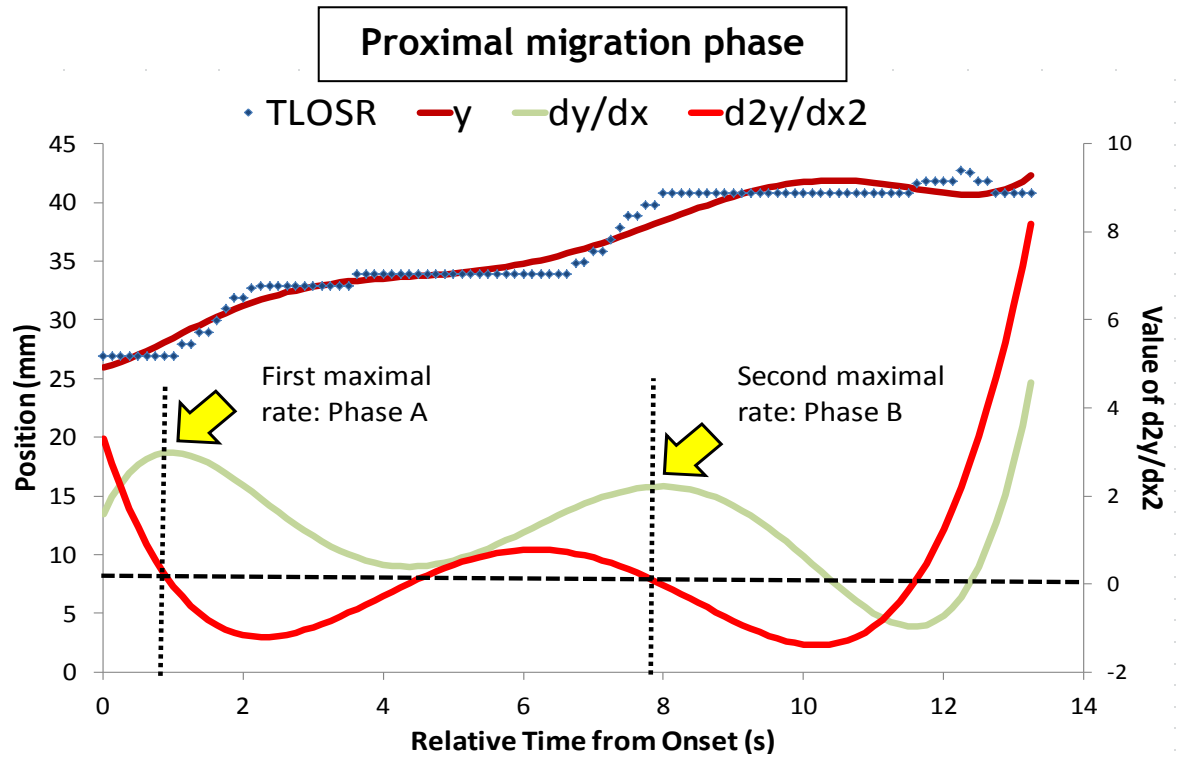


**Figure 2.7:** Determination of maximal rate (s) or velocities in different phases of migration of the GOJ during TLOS R s using elementary calculus.

## 2.6 HIGH RESOLUTION 36-CHANNEL MANOMETRY SYSTEM

### 2.6.1 Technical details

For studies presented in chapter 4, 5 and 6, oesophageal manometry was performed using a solid-state 36-channel HRM assembly (Manoscan®, Sierra Scientific Instruments Inc., USA). The solid state catheter with 4.2 mm outer diameter and comprised 36 pressure-sensing elements can detect pressure over a length of 2.5 mm in each of 12 radially dispersed sectors. Sector pressures are averaged to provide circumferential pressure. Each pressure-sensing element utilises proprietary pressure transduction technology (TactArray) which can record pressure transients in excess of 6000 mmHg/s and is accurate to within 1 mmHg of atmospheric pressure. The manometer catheter was commercially available in 2 sizes - one with a diameter of 4.2 mm and another with a diameter of 2.7 mm (“slimline” version) (**Figure 2.8**). The inter-sensor distance was 5 mm with the larger manometer and 7.5 mm with the slimline version. The larger diameter catheter was used for studies described in chapter 4 and 6, and the smaller diameter catheter was used for studies described in chapter 7.

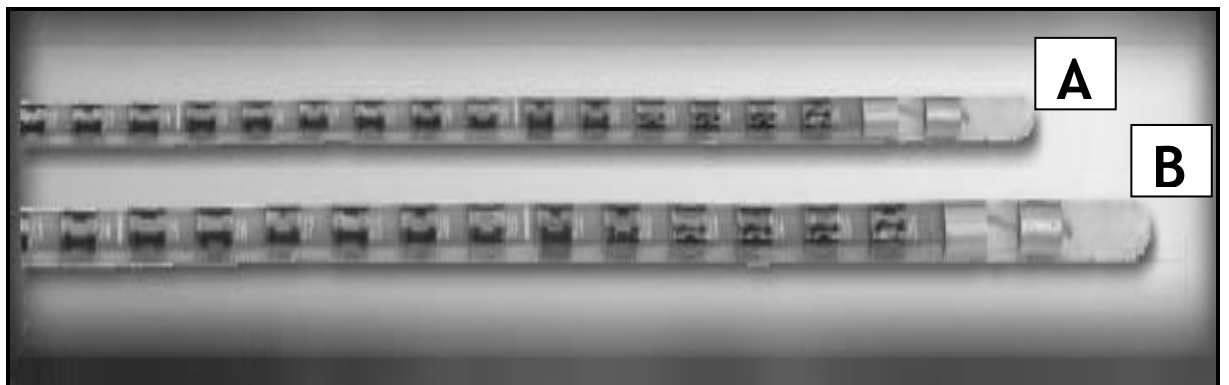


**Figure 2.8:** The smaller 2.7 mm “slimline” manometer (A) and the larger 4.2 mm diameter manometer (B) are shown.

The sensor technology was liable to “thermal drift”, where the pressure recorded using the manometry is affected by temperature. There were two methods to correct for thermal drift which incorporated into the system. One of the correction methods was “in-vivo calibration” and was performed weekly. The catheter was first placed in a shallow water bath (depth 1 - 2 cm) at 37°C. The Manoscan system records the change in pressure as a result of temperature rise for each of the immersed sensors and uses these values to reset the baseline. The second correction was performed immediately after extubation of the probe. The process, termed “thermal compensation” is applied to correct for in-vivo pressure drift after a period of clinical study. This process corrects the differences in measured pressures of all sensors upon extubation from their baseline pressures. A short clinical study (15 - 20 min) could be adequately compensated using the above corrective measures but it was found to be inadequate for more prolonged studies (1 - 2 hours). This was shown in our experiments described in chapter 4. For prolonged studies, a linear correction was also carried out in addition to the above described processes.

Prior to each recording, the catheter would be calibrated at 0 and 300 mmHg using an externally applied pressure. A thin plastic sheath, Manoshield™ (Sierra Scientific Inc., USA), was applied to cover the whole catheter. The sheath avoids any bodily secretions contaminating the probe. The technique for intubating the probe nasally is described in section 2.8.3. The Manoscan® acquisition (Sierra Scientific Inc., USA) program was utilised to store and extract the recorded data from the Manoscan® machine. Version 1.0 of the software was utilised for data acquisition from the 4.2 mm manometer at a preset frequency of 40 Hz. Version 2.0 of the software was utilised for data acquisition from the slimline manometer at a preset frequency of 100 Hz. The Manoshield™ sheath was removed and then disposed after extubation of the catheter.

### **2.6.2 Definitions of pressure-time data**

Manometric studies were analysed using commercially available software (Manoview® analysis, Sierra Scientific Inc., Los Angeles, USA) provided with the Manoscan system. An example of manometric tracing is shown in **Figure 2.9**.

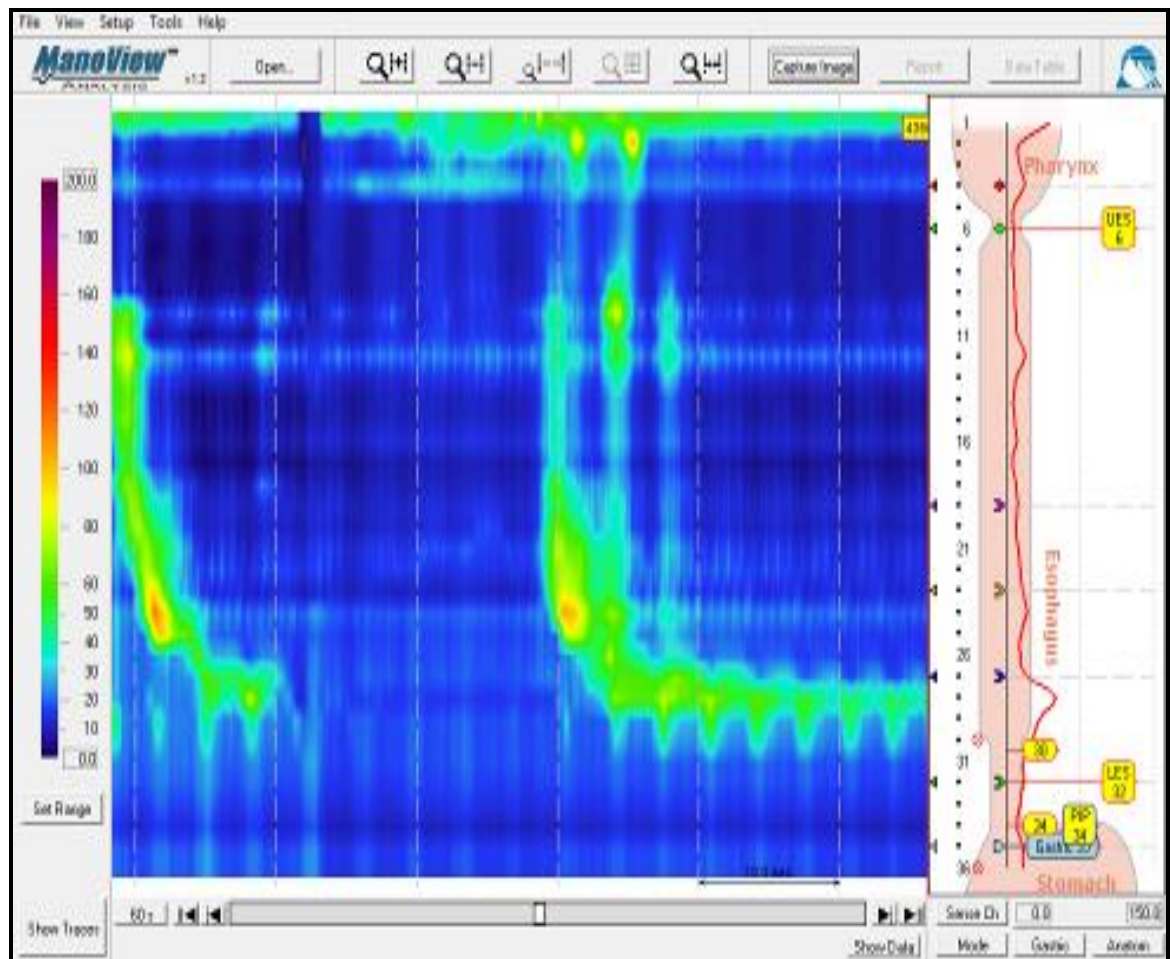


**Figure 2.9:** A colour contour plot extracted from the Manoview® analysis software. A TLOS event was shown in the current example.

In addition, manometric data could be exported in ASCII format and analysed separately using custom-made software described in section 2.9. An important event detected by the manometry was TLOS. The Holloway's criteria define TLOS based upon pressure-time characteristics derived from studies using conventional manometry (R H Holloway *et al.*, 1995) (chapter 1). Even though the criteria were meant for conventional manometry, the criteria could still be applied to HRM, since HRM can also display conventional tracings. Definitions for the pressure-time data derived from the manometry in relation to the Holloway's criteria are given below (section 1.4.4.2) (**Figure 2.10**):

Pressure (mmHg)

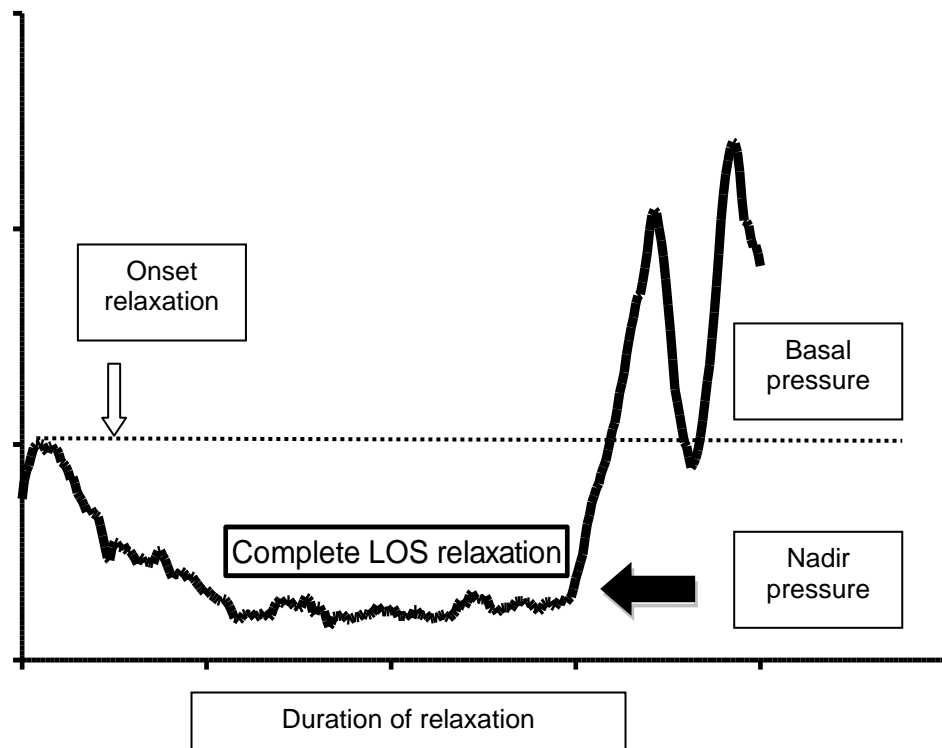


**Figure 2.10:** Illustration of manometry parameters measured with TLOSRS. White arrow indicates the onset of LOS relaxation, black arrow indicates the level of nadir pressure.

- **LOS Pressure:** LOS pressure was measured at end expiration and referenced to atmospheric pressure and IGP. For HRM, LOS pressure was assessed using the e-sleeve sensor function incorporated in the Manoview analysis software.
- **Basal LOS Pressure:** This was the minimum LOS pressure at end-expiration referenced to the IGP in the 5 - 10 s before the onset of a visually identified LOS relaxation. Where the relaxation followed a swallow, the last preceding period of stable sphincter tone would be assessed.
- **Onset of LOS relaxation:** This was defined as the point at which LOS pressure fell below the basal LOS pressure.

- Nadir Pressure: This was the minimum pressure reached during period of complete LOS relaxation.
- Complete LOS relaxation: This was the period of time during LOS relaxation where the pressure was within 1 mmHg of nadir pressure.
- Duration of LOS relaxation: This was the period of time during which LOS pressure was < 20% of basal LOS pressure.

To assist in more reliable identification of TLOSRS with HRM, the following were additional criteria:

- Duration of LOS relaxation was almost always longer than 10 s.
- After-contractile events were very often found following TLOSRS. These events included primary peristalsis, full secondary contraction or partial secondary contraction. Briefly, primary peristalsis was defined as a full propagating wave from UOS to LOS after swallow-related UOS relaxation/pharyngeal contraction, full secondary contraction was defined as full propagating wave from UOS to LOS without UOS relaxation/pharyngeal contraction and partial secondary contraction was defined as secondary contraction commencing below the level of UOS.
- Commonly associated with common cavity. During complete LOSR, the oesophagus and stomach become one cavity (common cavity) allowing movement of gastric contents into the oesophagus. A common cavity occurs when there is simultaneous increase of IOP of at least 5 - 10 mmHg, in at least two channels above the LOS. With normal physiology, the end expiratory IGP is 4 - 6 mmHg higher than the IOP. With TLOSRS, the IOP rises to equalize the IGP and therefore forms the common cavity.
- Commonly associated with reflux events - gas or liquid or mixed. This will require either a pH or impedance probe being used alongside.
- Proximal migration of the LOS appreciable on HRM. This is seen as movement of the pressure band representing the LOS. The amplitude of

movement is the difference between peak heights of migration of either the upper or lower border of the LOS from its baseline.

- Inhibition of CD. This is deemed to have occurred when there is at least 50 % drop in the magnitude of the inspiratory pressure transients on the LOS pressure recordings.

## 2.7 HIGH RESOLUTION 12-CHANNEL PHMETRY

This is a custom made pH probe with a 2.1 mm outer diameter and has 12 antimony electrodes along its length and an external reference electrode for application to the upper arm (Synectics Medical, Enfield, UK) (Figure 2.11).

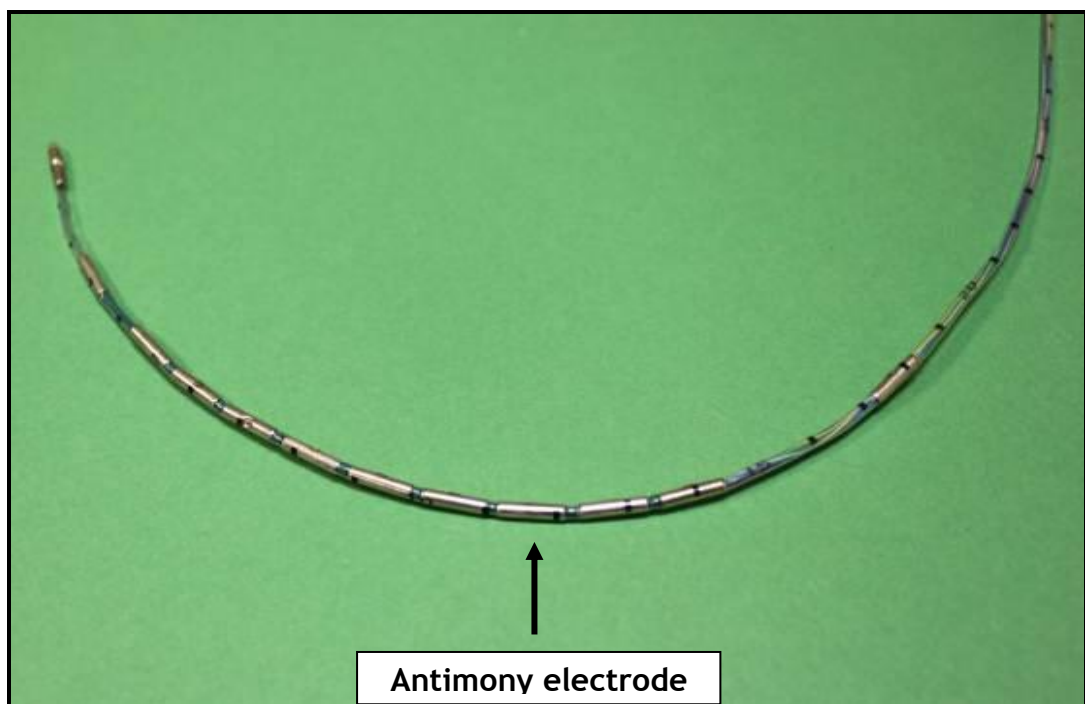


**Figure 2.11:** The assembly of 12 channel high definition pH probe.

The pH catheter was used alongside the locator and HR manometer in studies performed in chapter 6. The distal pH electrode was located at the tip of the catheter and the other 11 electrodes were 35, 65, 80, 95, 110, 125, 140, 155,

170, 185 and 205 mm proximal to it. This probe has a longer recording length than the previous version (length 172 mm) (Clarke *et al.*, 2009) so that it can cover more recordings of acid exposure associated with TLOSRS. Prior to recording, individual electrodes were calibrated in buffer pH 1.07 and pH 7.00, with acquisition of data using the PolygramNET™ software. Calibration at room temperature was automatically corrected by the software for pH measurement at body temperature. Raw data were extracted at the end of recording using the PolygramNET™ software at a frequency of 8 Hz and exported in ASCII text format.

## **2.8 COMBINING DIFFERENT CATHETERS, THEIR TIME SYNCHRONIZATION AND TECHNIQUES FOR NASAL INTUBATION**

### **2.8.1 Combining different catheters into one assembly**

In chapter 5, studies were performed with the 2-D locator probe and 4.2 mm manometer being passed through a nostril as one assembly. The overall maximal outer diameter with both probes combined was almost 9 mm (locator 4.8 mm and manometer 4.2 mm) but this size was not tolerated by all study subjects, resulting in a number of drop-outs. Subsequently, attempts were made to reduce the size of locator probe and to use a slimline version of manometer instead of the larger version. In chapter 7, studies were performed using the new 3-D locator probe (outer diameter 4.5 mm) and 2.7 mm manometer both combined providing an overall maximal diameter of 7.2 mm. This assembly provided a better comfort and fit for all subjects. In studies performed in chapter 7, there was in addition a pH probe (diameter 2.1 mm) alongside locator and manometer but the maximal diameter remained the same since the pH probe was sitting between the two larger probes, forming like a triangle on cross-section. The probes were positioned alongside each other in a manner to ensure the measured events (TLOSRS) were covered by all sensors from the three probes (Figure 2.12).

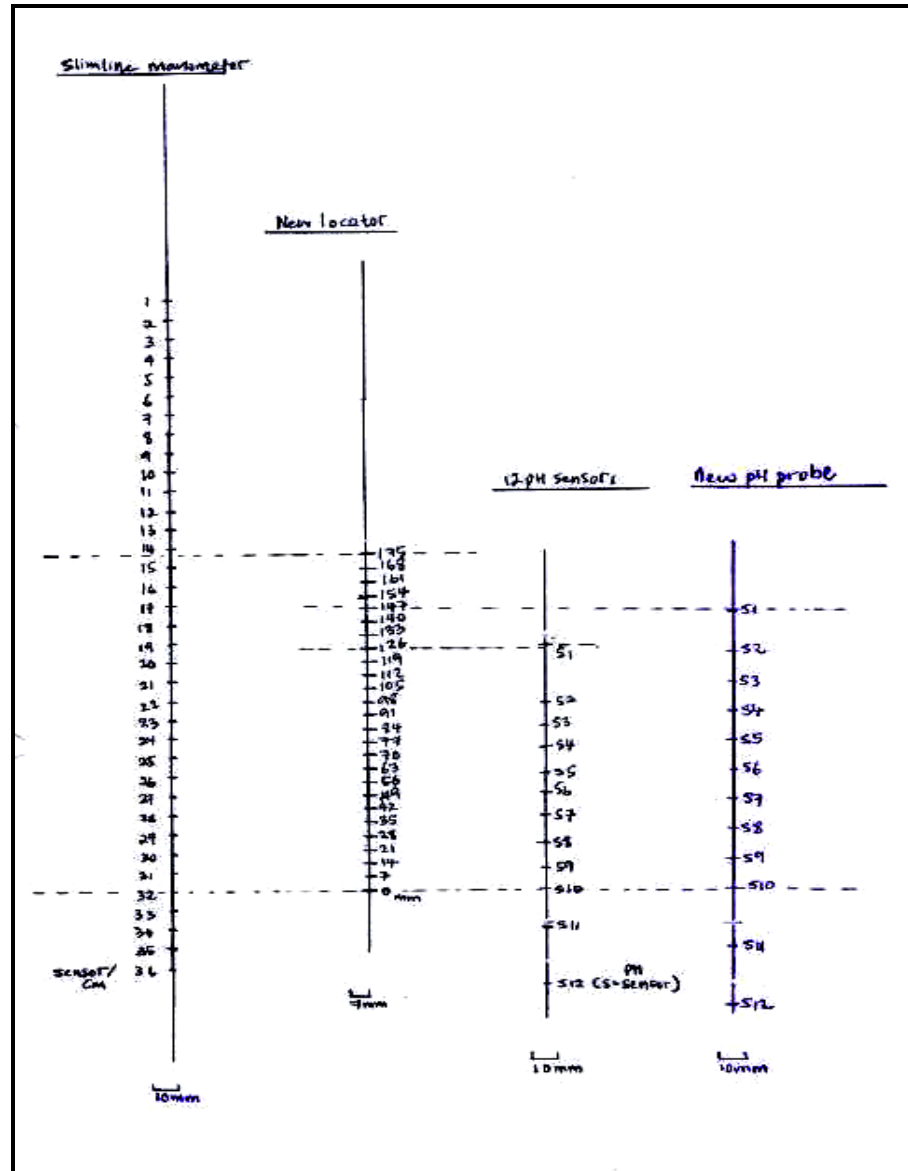


**Figure 2.12:** A schematic diagram on the relative positioning of different probes in the combined assembly for studies in chapter 6. The new pH probe shown in above figure (explained in section 2.7) was compared to a previous version of pH probe.

## 2.8.2 Synchronizing between different systems

Both pH and manometry systems sampled at different nominal frequencies and since recording times for each study could be extended (i.e. on average 2 hrs), it was therefore necessary to provide a check to ensure there was no time discrepancies or asynchrony between the two systems. This can be done by providing synchronisation signals or markers through either external or internal means. Internal signals could be applied using digital markers at the start and

the end of recording, a function available within manufacturer's software provided with recording systems. External markers were external means in producing simultaneous artefacts to both systems. A respiratory sensor (Respsense; Medtronic Inc., USA) containing a soft pad could be used for this purpose (**Figure 2.13**).

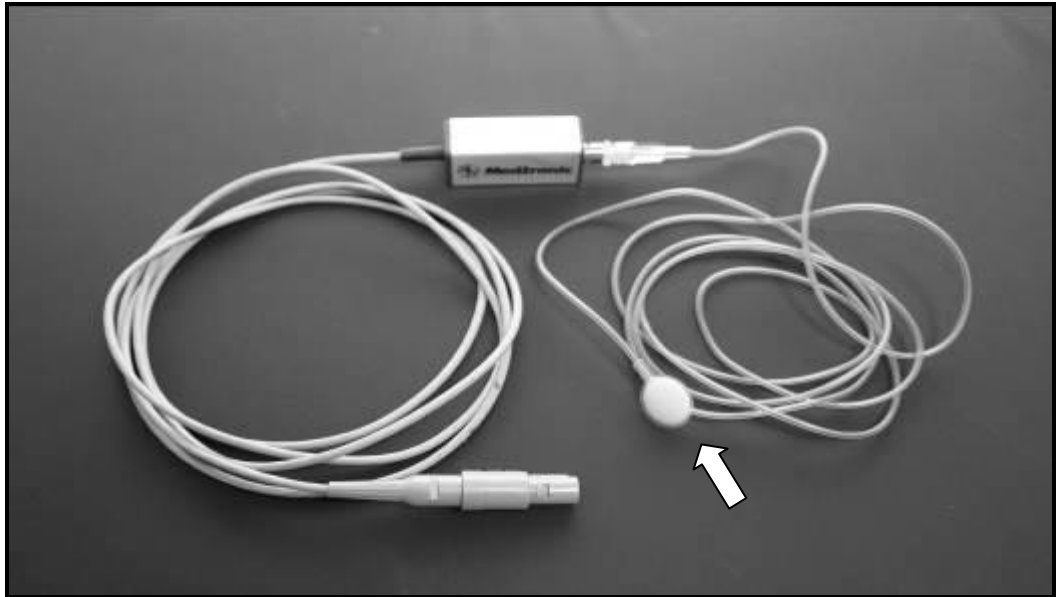


**Figure 2.13:** Respiratory sensor that connects to the Polygraf® machine. The arrow indicates soft pad for introducing external signal as marker.

This device, when connected to the Polygraf® machine, was intended to be placed on the chest wall for detection of chest wall movement during respiration. Introducing a tap on its soft pad (arrow in **Figure 2.13**), when the soft pad was placed on the top of a manometer sensor, created an instantaneous artefact (high pressure line to the Manoscan® and high signal to the Medtronic Polygraf® machine) to both systems. These external signals produced reliable synchronisation signals, and provide a check point to ensure there was no time discrepancy between systems. The reliability for this approach was confirmed by comparing external with the internal markers during pilot studies.

### **2.8.3 Technique for nasal intubation of combined assembly**

All studies involving catheters were performed with assistance from a specialised GI nurse within the GI unit of Gartnavel General Hospital, Glasgow. Before the procedure, the nurse verified that the subject had fasted for a minimum of 6 hours. Study subjects were asked to sit at an angle of 60° on the bed. One nostril would be anaesthetised with local lignocaine spray (similar to the one used for upper endoscopy). The subject was allowed a minute or two to accommodate the numb sensation before intubation. Some KY-jelly was applied at the tip of combined assembly of catheters for better lubrication. The assembly was passed slowly through the anaesthetised nostril until it reached to the back of the throat. It was then slowly introduced into the oesophagus as the subject swallowed. Further swallowing efforts allowed the assembly to pass easily into the stomach. Gagging, tearing and feeling nauseous were common during the intubation but these symptoms were often transient.

Occasionally, it was difficult to pass through one nostril (small nares, swelling, previous surgery etc.) and if so, the other nostril could be tried instead. If both nostrils failed, then the procedure would have to be abandoned. Once the assembly had reached the desired depth, it was anchored by taping the nasal end with adhesive tapes. During recording, it was prudent to check at regular intervals to ensure the adhesive and depth of the assembly remained at their correct position. Following the completion of study, the assembly was withdrawn by first removing the adhesive tapes followed by a rapid withdrawal of the catheters. It was usually uncomplicated during this stage although it could be uncomfortable at the back of the nose. Study subjects were allowed to have water or food as soon as the catheters were withdrawn. Other commonly reported problems included sore throat and nose bleeding but these problems were usually minor.

## **2.9 SOFTWARE AND DATA PROCESSING**

The computer programs used to record, save and extract data from recording machines were commercially available (PolygramNET™, Synectics Medical Ltd, UK, and Manoscan® acquisition, Sierra Scientific Inc., USA) and for analysis, the

data were extracted in ASCII format. These extracted data could then be imported by Microsoft Excel (edition 2007/2010, Microsoft Corp., USA) or Statistical Package for the Social Sciences (SPSS) version 18.0 (SPSS Inc., IL, USA) for further analysis.

The data from pH and manometry systems were extracted into intermediate data files using an in-house program (DrNewData). The user defined the time synchronisation points and the program combined these intermediate files into a single file containing the data from the pH, manometry and locator systems into a single data file with data sampled at 8 Hz.

The data in this combined file was displayed by a further program (DrContour6) which allowed the data at various time points to be displayed, measured and stored (**Figure 2.14**). DrContour6 displays the data in a 90 s time frame, with two panels providing high resolution colour contour plots for both the manometry (lower panel) and pHmetry (upper panel). The movement of the GOJ is superimposed as thick white line on the two panels. The program incorporates buttons allowing user to capture and store data during events for further analysis.

## 2.10 TEST MEALS

It is common for clinical studies to elicit TLOSRS by means of a test meal. For studies reported in chapter 5 and 6, test meals were given during the experiments as part of the study protocol. The test meals were either liquid or solid. The liquid meal (chapter 5) was Fortisip from Nutricia Ltd, UK and is available in bottled form (200 ml/bottle) and in different flavours (including chocolate, strawberry and vanilla etc.). Two bottles of Fortisip provide 600-calorie and 23.2 g of fats. For solid meals (chapter 6), battered fish and French fries (In Scotland, it is known as fish supper) were provided. It was important that the volume or portion of test meals should be the same on each study day. The amount of food was measured before and after meal using a standard weighing scale.

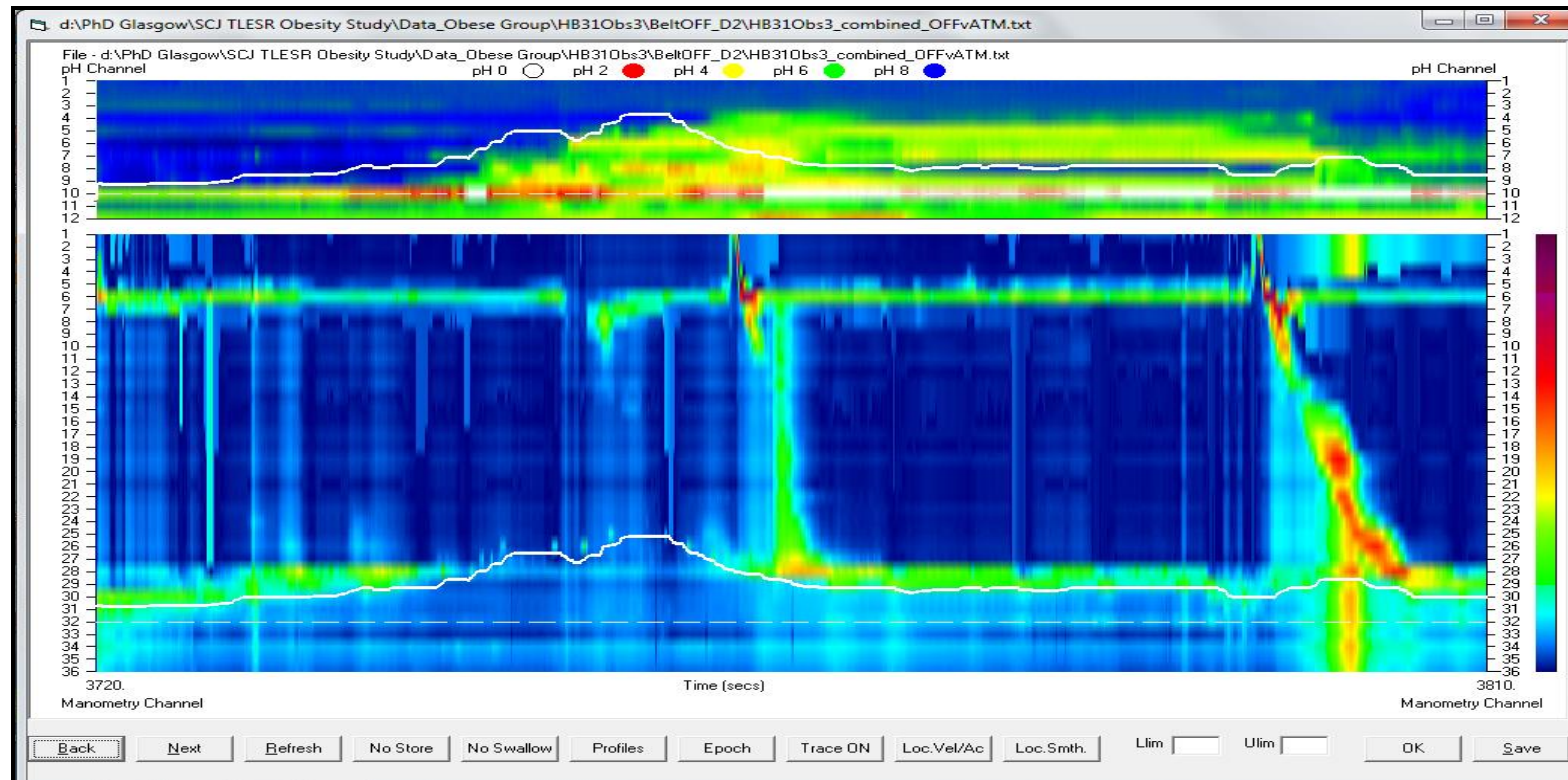


**Figure 2.14:** An example of high resolution colour plot displayed using the DRContour version 6.0 program. One of the TLESR events is shown in this example. The upper panel is pH plot and the lower panel is manometric contour plot. On both, the thick white line is the movement of the GOJ from the locator system.

## 2.11 WAIST BELT

A waist belt was used to increase IAP and mimic the effects of obesity. Weight training belts (Nike Inc., USA) made from synthetic polymers, available in various sizes (small; 61 - 76 cm, medium; 76 - 91.5 cm, large; 91.5 - 106.6 cm and extra-large; 106.6 - 122 cm), were used in studies performed in chapter 6 (**Figure 2.15**). Putting on the weight lift belt alone at the waist, even when it was tightened, would not have achieved the targeted rise in the IGP, based on initial pilot studies. The targeted rise could only be achieved by placing a pressure cuff from a sphygmomanometer beneath the waist belt. A cuff pressure of 50 mmHg produced the needed rise in IGP without causing too much discomfort to the study subjects.



**Figure 2.15:** A photo showing two sizes (medium and large) of abdominal belts and the sphygmomanometer (pressure cuff).

A pilot study involving four subjects, and, using the waist belt and pressure cuff approach as described above, the median rise of IGP was 8.9 mmHg (range 9.8 mmHg) during inspiration and 7.3 mmHg (range 10.0 mmHg) during expiration. The pressure rise was sustained after meals with a median IGP of 8.2 mmHg (range 4.8 mmHg) during inspiration and 7.1 mmHg (range 6.3 mmHg) during expiration. The pilot study showed that the waist belt and

pressure cuff approach was an appropriate experimental technique to raise IGP.

## 2.12 SPECIALISED GASTROINTESTINAL INVESTIGATION UNIT

All clinical studies were performed in a specialised motility unit except for the upper endoscopy test. The specialised GI unit was situated at Gartnavel General Hospital, Glasgow and was within close distance to the endoscopy suite, where the endoscopy examination was performed.

The unit contained work stations for manometry, polygraf® machine and locator equipment (**Figure 2.16**) as well as storage of consumables. There was a bed where the subjects would lie or sit during the test (**Figure 2.16**). It was well equipped with oxygen and suction equipment. The unit was inspected regularly by the infectious control unit and all procedures were performed in strict accordance to regulations.



**Figure 2.16** The working station in the specialised GI unit

## 2.13 DATA AND STATISTICAL ANALYSIS

All data and statistical analyses used in the current thesis were performed using either Microsoft Excel 2007/2010 (Microsoft Corp., USA) or SPSS version 18.0 (SPSS Inc., USA). It is not the intention of the current section to detail the techniques of statistics but it is aimed to provide an overview to some of the techniques used in this thesis. Data were either categorical or continuous. Categorical data were expressed as frequency and percentages, and continuous data were expressed as median (range or inter-quartile range/IQR) or mean (standard deviation/SD or standard error of mean/SEM) depending on its distribution. Data were initially explored utilising descriptive analyses, tables and graphs. Statistical tests were then employed to determine association, differences and correlations between data. Choice of tests used to compare between groups depended on whether the data were normally distributed and also types of data. Normal distribution described sets of data when plotted with histogram would show the greatest frequency in the middle and smaller frequencies at the extreme. Besides histogram, normality was tested using Kolmogorov-Smirnov statistics which was calculated using the SPSS software. With normal distribution, data were expressed as mean and tested using parametric techniques. These parametric techniques included t-test and analysis of variance (ANOVA). If the distribution of data was skewed, then data were expressed as median and non-parametric tests were used. These non-parametric tests included Mann-Whitney U test, Wilcoxon Signed Rank test and Kruskal-Wallis test. Each chapter 4, 5 and 6 has a section of statistical analysis detailing the exact tests performed. The statistical significance of each test performed in this thesis was expressed using *P* values with the null hypothesis rejected if the *P* value was  $< 0.05$ . Reliability of estimates of some data presented in this thesis was also expressed as 95% confidence interval (95% CI).

In chapter 5, the identification of TLOSRS was performed by two clinicians and the simple percentage was calculated to assess for agreement between two sets of observations. On the other hand, correlation analysis was used to describe the strength and direction of linear relationship between two variables. For continuous variables (for example velocities and amplitude of

GOJ migration), Pearson coefficient (known as  $r$ ) was calculated with values between -1 to +1. The size of the absolute value is an indication of strength of the relationship.

In the same chapter 5, it was of interest to know if the migration characteristics of the GOJ were more variable between individuals or within individuals. The test used was the calculation of mean centered coefficient of variation (CV). The definition of CV is ratio of standard deviation ( $\delta$ ) to the mean ( $\mu$ ):

$$CV = \frac{\delta}{\mu} \times 100\%$$

As the expressed value is a percentage, this allows a comparison between variation of different parameters with different units (for example, amplitude in cm and duration in seconds). To derive within-individual CV ( $CV_w$ ), the CV for each of the 12 individuals was first calculated for each parameter and the mean for all 12 CVs was taken as  $CV_w$ . To derive between-individual CV ( $CV_B$ ), using SPSS software v 18.0 (SPSS Inc., Chicago, USA), the computed between-individual variance ( $\delta_B^2$ ) and the grand mean or weighted average of 12 individuals ( $\mu_B$ ) was first derived for each parameter using the random effects one-way ANOVA test. The  $CV_B$  was then calculated as below:

$$CV_B = \frac{\sqrt{\delta_B^2}}{\mu_B} \times 100\%$$

The ratio of  $CV_w/CV_B$  was also calculated to compare the relative effect of variation within and between individual. The one-way ANOVA test was used to test for differences between and within-individuals with significance difference between individuals as  $P < 0.05$ .

Also in chapter 5, it was of interest to compare the sensitivity and specificity between two techniques (new locator technique vs. established

HRM technique) in identification of TLOSRS. Receiver operating characteristic (ROC) curves were useful in this respect. In addition to values of sensitivity and specificity for each of the tested parameters derived from the two techniques, this test could determine the cut-off scores for each parameter. An indication of diagnostic accuracy for each tested parameter was the area under the curve (AUC) where a value closer to 1 was more accurate but a value of 0.5 only meant that the parameter was no better than chance.

## **2.14 ETHICAL COMMITTEE APPROVAL**

The declaration of Helsinki (1964) has placed utmost importance in the safeguarding of interests of human subjects involved in medical research. Within Scotland, the Research Ethics Committees (REC) are responsible for reviewing all proposed human studies in order to protect the dignity, rights, safety and well-being of all actual or potential research subjects.

All studies involving human subjects in the current thesis were approved by the West Glasgow Research Ethics Committee. For studies in chapter 4 and 6, the REC reference was 07/S0709/98 and for studies in chapter 7, the REC reference was 10/S0704/40.

# CHAPTER 3

## DEVELOPING THE GOJ LOCATOR SYSTEM

---

- 3.1 Overview
- 3.2 Hall Effect and magnet
- 3.3 Developing the 2-D GOJ locator probe
- 3.4 Conclusion

## 3.0 DEVELOPING THE GOJ LOCATOR SYSTEM

### 3.1 OVERVIEW

In this chapter, the development of systems to record the position of the pH and manometry sensors with respect to the GOJ is described. These locator systems use linear arrays of sensors, fixed with respect to the pH and manometry sensors, but whose position and movement can be related to a small magnet fixed at the GOJ (**Figure 3.1**). The sensors used in the locator arrays use the Hall Effect in which a signal voltage results from the movement of the array past the magnet, and this voltage is recorded in real-time.

### 3.2 HALL EFFECT AND MAGNET

#### 3.2.1 Introduction

The first prototype 2-D probe is made up of linear Hall Effect sensors mounted on a flexible printed circuit board. With a 2x1 mm sized magnet fixed on a metal-clip, this is then clipped to the SCJ endoscopically and the movement of the magnet can then be detected by the Hall Effect sensors (**Figure 3.1**).

Among the many magnetic field sensing technologies, the Hall Effect is perhaps the most universally used around the world. The Hall Effect transducers can be manufactured cheaply, really small in size and are of high quality. This technology can often be found in our daily appliances including automobile gear-boxes, washing machine, watches, cell phones etc. just to name a few.

The knowledge of Hall Effect is not new. It was first discovered in the late 19<sup>th</sup> century by Edwin Hall. In 1879, the American physicist was trying to determine whether the generation of force from the current carrying wires in a magnetic field was acting upon the wires or the current itself. He found

that the force was acting upon the current and this force displaced the current to one side which also created a small voltage.

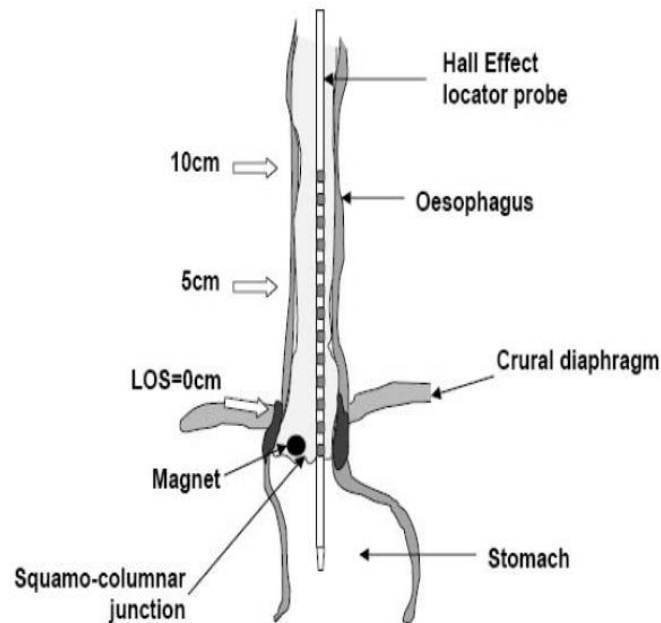


**Figure 3.1:** Diagram depicting the Hall Effect-based locator probe within the oesophagus and straddling the GOJ. LOS=lower oesophageal spincter.

### 3.2.2 What is Hall Effect?

Since its initial discovery, the Hall Effect was not used beyond the laboratory walls until in the late 20<sup>th</sup> century when the semiconductors were easily available from mass-production. The first real application outside the laboratory was the microwave power sensor in 1950s. Since then, the Hall Effect sensors were built on integrated circuits with on-board signal processing capabilities.

Despite technological advancement, the basic principle of Hall Effect remains the same. It is characterised by a generation of a measurable small voltage across a conductive material (contained within a transducer) that occurs when an electrical current is flowing through the conductive material

and is influenced by a magnetic field (**Figure 3.2**). Examples of commonly used conductive materials include silicon or gallium arsenide.

Quantitatively, the force exerted on charged particles within the conductive materials, when exposed to an electromagnetic field is described by the Lorentz force equation:

$$F = qE + qBv \quad (1)$$

where  $F$  is the force,  $E$  is the electrical field,  $v$  is the velocity of the charged particle,  $B$  is the magnetic force and  $q$  is the magnitude of the charge. The magnetic field forces the charge carriers to one side of the conductive material but the generated electrical field eventually maintains the equilibrium by returning charge carriers to its original position. With equilibrium,  $F = 0$  therefore

$$\begin{aligned} qE + qBv &= 0 \\ E &= -Bv \end{aligned} \quad (2)$$



**Figure 3.2:** Principle of Hall Effect. A transducer (black box) with applied current flow (green arrow) is shown here and is exposed to a magnetic flux (red arrows). The resulting Hall voltage (blue arrow) is also shown (Gary Pepka, Allegro Microsystem, Inc.).

The equation suggests that the Hall electric field or Hall voltage is solely a function of velocity of charge carriers and the strength of magnetic field. The velocity of charge carriers in metals e.g. copper is extremely small and therefore the resultant Hall voltage is also very small. Semiconductors e.g. silicon, germanium and gallium-arsenide are better conductive materials which produce higher velocity of its charger carriers when they are exposed to magnetic fields. As a result, these semiconductors are commonly used in Hall Effect sensors.

### 3.2.3 Good and bad of Hall Effect sensors

There are a number of advantages for using the Hall Effect sensors or transducers (**Figure 3.3**). Besides from its small size and cost, the output produced is insensitive to ambient conditions (dust, humidity or vibrations). The sensor is less predisposed to wear and or tear since the sensor lacks mechanical contacts. The sensitivity of a transducer is directly linked to its performance and generally speaking, the greater the sensitivity the better, as this reduces the output processing required. The sensitivity or gain of output from Hall Effect sensors is, however, dependent upon the distance of applied magnetic field.

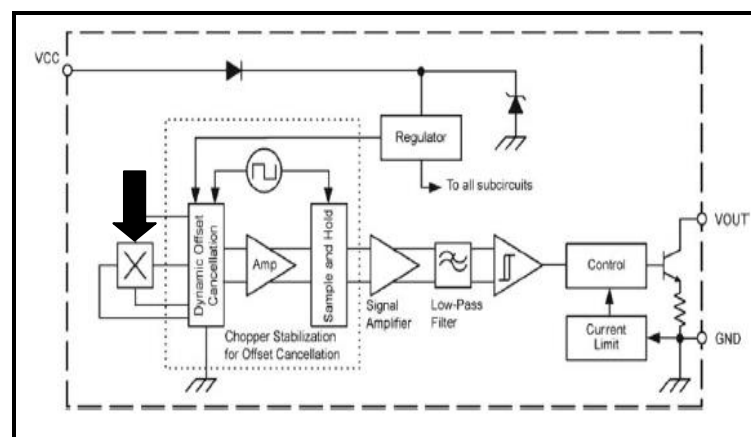


**Figure 3.3:** An example of miniature-sized Hall Effect transducer with integrated circuits (Ramsden, 2006). Black arrow indicates the position of the Hall Effect sensor.

A disadvantage with Hall Effect sensor is that it is affected by temperature. This is largely due to a change in the metal conductive properties at different temperatures (Ramsden, 2006). Briefly, there are four characteristics of the sensor which can be affected by temperature namely changes in the coefficient of sensitivity, ohmic offset, resistance and noise. Coefficient of sensitivity is a phenomenon that varies the transducers' sensitivity with change in temperature and to some extent depends on the type of power supply. A constant-current supply will produce less effect on sensitivity as a result of temperature rise than with a constant-voltage power source. Ohmic offset is a result of imperfection in the sensor during the manufacturing process and a change in temperature may result in an output drift which is often random. Each transducer has an input and an output resistance, measured across the appropriate terminals and this can be affected with a change in temperature. Finally, Johnson noise is an electrical noise as a result of thermally induced motion of electrons, generated by the resistance of the device and the operating temperature.

### **3.2.4 Basic features of Hall Effect sensors**

Linear Hall Effect sensors produce a ratiometric analog voltage output that respond proportionately to magnetic field strength which in turn depends on “effective air gap” or distance between the sensor and magnetic pole. In general these devices require a regulated voltage of 5V supply and the quiescent voltage output is 2.5V when there is no significant presence of magnetic field.

Nowadays Hall Effect sensors are built with standard integrated circuits consisting of application-specific signal processing which can vary with different companies. Some of these applications can include signal amplification, temperature compensation and offset cancellation (**Figure 3.3**).

### 3.2.5 Permanent rare earth magnets

The two common rare earth magnets consisting of Lanthanide elements are Neodymium (Nd) and Samarium (Sm), both are commercially available in alloy forms (Neodymium-Iron-Boron and Samarium cobalt respectively). Commercial magnets are available either in sintered or bonded forms. Sintered forms are plated or coated with material to prevent corrossions and bonded forms use a polymer base to hold the alloys together. The following table (Table 3.1) summarises the differences between the two commonly available rare earth magnets:

**Table 3.1:** Differences between samarium and neodymium rare earth magnet

Samarium Cobalt	Neodymium Iron Boron
1. Highly resistant to oxidation	1. More easily oxidized
2. Magnetic strength and energy product less than neodymium (approximately 9000 Br (G) and 20 BH <sub>max</sub> )	2. Magnetic strength and energy product higher than samarium (approximately 13000 Br (G) and 45 BH <sub>max</sub> )
3. Better temperature resistance than neodymium. Can withstand temperature up to 350 °C	3. Temperature resistance much less than samarium
4. Sintered forms are more brittle	4. Mechanically stronger than samarium when coated
5. Costs are higher	5. More economical

Grade of magnets refers to the maximum energy product of the rare earth material used or in other words the “strength” of the magnet. A higher grade indicates a “stronger” magnet. Modern magnets do not degrade significantly over time without damages from corrossions, high heat or mechanical impact. For example a neodymium magnet only has a loss rate of 1% in 100 years!

Rare earth magnets are commonly used in our daily appliances. Many electronic devices including televisions, computers, automobiles, cell phones and microwave have magnets as components.

### 3.2.6 Basic characteristics of magnet and magnetic fields

Magnetic field results from motion of electrical charges either from electron spin or moving charges. All materials contained charged particles and therefore exhibit some magnetic properties but only ferromagnetic materials exhibit significant magnetic flux density. At atomic levels, these ferromagnetic materials consist of clusters of atoms or “domains” which are aligned in the same direction in magnetised state but aligned in random directions in unmagnetised state. A magnetised material that can resist demagnetisation force is considered to have high coercivity. The B-H curve (B stands for magnetic flux density and H stands for magnetising force) describes the transition between the two states and its pattern is specific for a particular ferromagnetic material.

In **Figure 3.4**, the intrinsic curve represents the flux contributed by the magnetic material and the normal curve represents the actual levels of B in the material subjected to an external magnetising field.  $BH_{\max}$  or maximum energy product is a product of B and H along the normal curve and represents the amount of mechanical work that can be stored as potential magnetic energy.

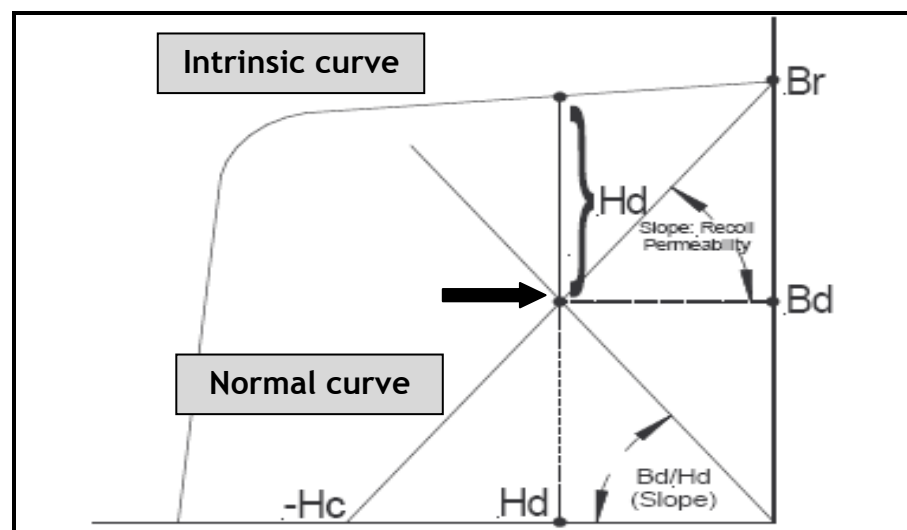


**Figure 3.4:** B-H curves of ferromagnetic material; intrinsic curve is the outer plot and normal curve is the inner plot;  $B_d$  = operating flux density,  $H_d$  = operating field strength,  $H_c$  = coercive force,  $B_r$  = residual flux density; black arrow =  $BH_{\max}$  or maximum energy product (Ramsden, 2006).

## **3.3 DEVELOPING THE 2-D GOJ LOCATOR PROBE**

### **3.3.1 Introduction**

With the fundamentals of Hall Effect and magnet briefly introduced, this section describes on the technical side of the new technique. After a brief history on its conception, detailed descriptions on its components are then discussed. These components include the Hall Effect sensor, the flexible printed circuit boards, microprocessor unit and its software (section 3.3.3). One very important aspect to the success of this new technique is the magnet. Many thoughts and time have been given to the choice of magnet and also to how and where the magnet could be fixed on the metal-clip. The technique and site for placement of the magnet within the GOJ are other important considerations that have contributed to the success of this technique. All of these are described in the section on the magnet (section 3.3.4).

### **3.3.2 A brief history on conception of the novel probe**

The upper GI Investigators from the University of Glasgow have for a long time hoped to have a technique that allows them to monitor the SCJ continuously and to use it alongside the high resolution 12-channel pHmetry. This came as a need when the investigators were interested to know the exact location of the SCJ in their studies on short segment reflux and acid pocket. However it is known that to monitor the SCJ in such a situation can be really difficult because of its constant cranial/caudal movements during respiration and swallows.

For a number of years, these investigators from Glasgow had tried various methods to achieve their aim. More recently, the miniature Hall Effect sensors have been considered as a potential technique. With the help from engineers and physicists within Glasgow, the first design of the prototype locator probe was born. This novel probe consisted of a series of linear Hall Effect sensors mounted on a printed circuit board and spaced 10 mm apart.

While initial bench tests found that the probe could reliably detect the magnet along its length but it was greatly limited by spatial resolution, distance and rotation of the magnet. The weakness was confirmed during an in-vivo trial run in a human subject. The detection of position was poor due to a significant lack of signal strength. The poor signal had been postulated to be due to rotation of the magnet within the oesophagus.

Recognising the research potential of this new technique, further studies were conducted to improve on the observed weaknesses. Further improvement to increase the spatial resolution was achieved by overlapping two circuit boards to reduce the distance between sensors to 5 mm. I started my PhD with the task to investigate on the weaknesses and find my ways to improve on the technique. To achieve this, I need to understand the function of each component that made up the probe. These components are described in the following section.

### **3.3.3 Components of the 2-D locator probe**

The probe consists of 13 Hall Effect sensors mounted on a flexible printed circuit board with two of these boards overlap to provide acceptable spatial resolution. These are encased in a durable silicone tube and the probe is connected to the microprocessor unit to allow data recording. These components are explained in greater details as below.

#### **3.3.3.1 Allegro® A1395 sensors**

The Hall Effect sensor (model A1395, Allegro Microsystems Inc., US) used in the prototype probe, had a dimension 2 x 3 x 0.75 mm, sensitivity of 10 mV/G, recommended supply voltage in the range of 2.5 to 3.5V (our device uses 3.0 V) and an offset voltage which was half of the supply voltage (our device has offset voltage of 1.5 V). The maximum magnetic field strength that the sensor could detect was approximately 250 Gauss (when a samarium cobalt magnet with  $B_r = 10.2$  to 10.5 kG was used).

### 3.3.3.2 Printed circuit boards and microprocessor

Thirteen Hall Effect sensors were soldered onto two flexible printed circuit boards (width 3 mm) at 10 mm spacing (Figure 3.5). One circuit board was superimposed on the other, with corresponding sensors offset, giving a linear separation of 5 mm between sensors.

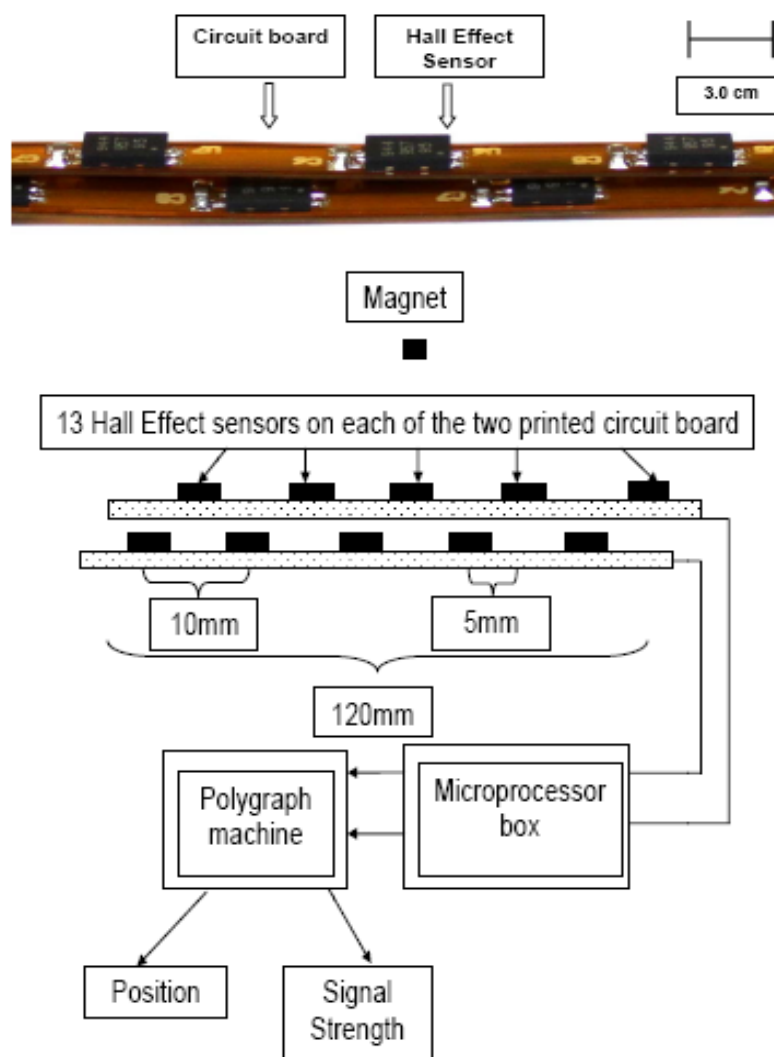


**Figure 3.5:** A schematic diagram of the locator system. A photo of the actual overlapping Hall Effect arrays is shown above it (the scale on the upper right). There are 13 Hall Effect sensors soldered on each of the two overlapped printed circuit boards which are then coated with silicon tubing (Altecweb Ltd, UK). The probe is connected to a microprocessor box which outputs through the polygraph machine (Medtronic®) as position (mm) and signal strength (mV).

An Initial attempt to coat the probe did not work out because the sensors were affected by the chemicals used in the coating. Subsequently, alternatives were sought and tested and the final coating consisted of a medical grade, high tensile strength silicone tubing which was commercially available in various sizes (AlteSil™, Altecweb.com Ltd, UK).

The tubing was translucent in colour and could tolerate temperatures between -55°C to 220°C. Made of specially blended elastomer providing non-toxic and consistent tubing life, the silicone tubing prevented bodily contact with the probe's electrical components. The bore of the selected tubing was 3.2 mm based on the width of the circuit boards and the height of the sensors. This bore was as tight as possible, while not causing wrinkling of circuit boards as this would reduce its overall length. A suitable thickness of tubing wall is important so that it would not compromise patient comfort during nasal intubation. However, too thin a wall might saturate the signal strength and affect the position reading. A wall size of 0.8 mm was selected. The circuit board could be easily threaded through the tubing with the use of fine wires.

The device was compliant to electrical safety guidelines and International Organization for Standardization (ISO) certified (BS: EN 60601-1:2006). Electrical safety measures included the probe interface unit's electronics being powered from a medical grade power adapter; a class II device with a leakage current <10 µA and enhanced with a DC-DC converter between the mains adapter and the electronic circuitry. The circuit boards were connected to a microprocessor unit (**Figure 3.6**) and its digital output connected to a Medtronic Polygraf™ recorder (Synectics Medical Ltd, UK) and displayed using the PolygramNET™ software (version 4.1.1322.28.7; Synectics Medical Ltd, UK). There were two outputs recorded from the locator probe, namely, position (in mm) along the length of the probe with a range of 0 to 120 mm and signal strength (in millivolts or mV) with a range of 0 to 1200 mV (**Figure 3.7**). The probe required calibration for its minimum and maximum working range with the Polygraf™ machine prior to its actual use.



**Figure 3.6:** Microprocessor unit (front panel - left, and rear panel - right showing how the unit connects to the Polygraf® recorder).

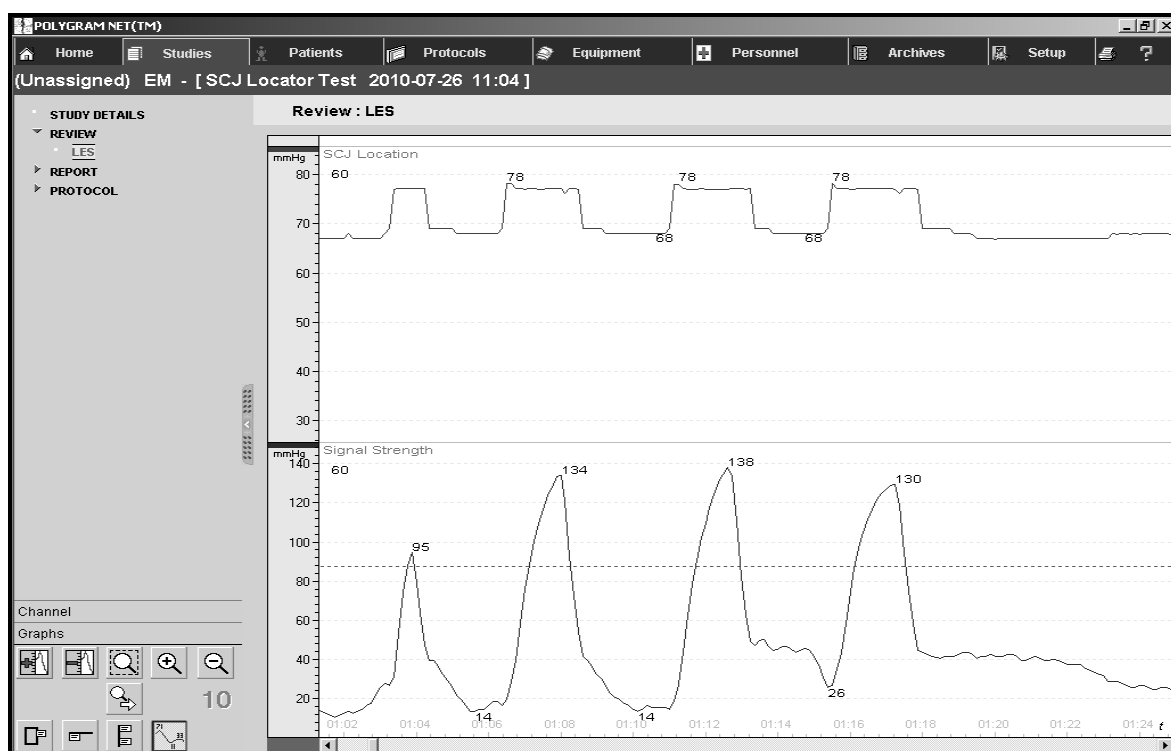


**Figure 3.7:** An example of display for the position and signal strength output from the Hall Effect probe using the PolygramNET™ software.

The unit was calibrated by firstly zeroing the probe at the minimum position value of 0 mm and minimum strength value of 0 mV without any presence of magnet, and then calibrating the probe with the magnet pole placed directly on top of the last sensor i.e. calibrating to the maximum position value of 120 mm and the maximum strength of 1200 mV. With the knowledge of the thermal effects on Hall Effect sensors (chapter 4), the calibration process was performed with the probe immersed in a water-bath heated to body temperature prior to intubation. Raw data could be extracted

from the PolygramNET™ software at a frequency of 8 Hz and exported in ASCII format for future analysis.

### 3.3.4 The importance of magnet

The next step was to optimize the magnet. Preliminary in-vitro and in-vivo studies had shown that signal strengths could be a result of rotation of the magnet placed within the oesophagus. Only through numerous discussion and experimentations, that we finally found a reliable method to overcome this issue. Plenty of considerations have been given to the choice of magnet and its dimension, the position of magnet on the endoclip and finally its placement within the GOJ. This is described in detail within the next three sections (3.3.4.1 to 3.3.4.3).

#### 3.3.4.1 Magnet material and dimension

In general, the magnetic field strength degradation with distance or “effective air gap” is determined by the material of the magnet, the distance between the magnet and the sensor, direction of the magnet polar face and the dimension of the magnet. It can be expressed mathematically as the following:

$$\text{Magnetic field} = B_r / 2 \left[ \frac{L+X}{[R^2 + (L+X)^2]^{-2}} - \frac{X}{[R^2+X^2]^{-2}} \right]$$

Where  $B_r$  = Residual magnet inductance of the magnet (G)

L=Length of the magnet (mm)

X=Distance between surface of the magnet and the device (mm)

R=Radius of the magnet (mm)

We first considered the material of the magnet. A high grade samarium cobalt (SmCo) rare-earth permanent magnet (e-magnets UK Ltd, UK) was initially employed in our studies. The SmCo magnet was selected due to its high magnetic strength and resistance to corrosion by biological fluids including gastric hydrochloric acid. This is important because the GOJ

environment is constantly exposed to acid from the stomach. SmCo rare earth magnet is commonly used in orthodontic application and its biological effects were studied previously in animals and humans where it was shown to have no direct toxic effects (Noar & Evans, 1999; Darendeliler, Darendeliler & Mandurino, 1997).

In addition to the magnetic field strength, the magnet's shape and size had to be considered, specifically whether it could be accommodated by the endoclip. The best compromise was an axially magnetised disc shaped magnet with a diameter of 2 mm and 1 mm in length. Not only did the disc shape allow a larger surface area of magnetic field (**Figure 3.8**), but the placement on the endoclip was easier. This magnet dimension also allowed access through the working channel of a standard endoscope which was essential.

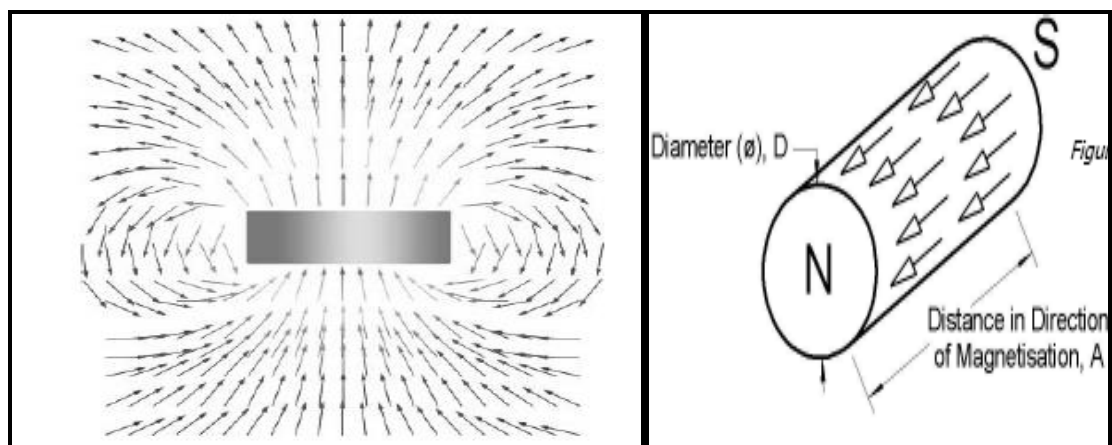


**Figure 3.8:** Disc-shaped magnet. The axially magnetised disc shaped 2x1 mm magnet has a larger surface area of magnetic field at the polar face of the magnet.

#### 3.3.4.2 Placement of magnet on the endoclip

The best orientation of magnet was when either of its poles was facing directly at the Hall Effect sensors. Two factors were probably important in ensuring this orientation with the current system. First was the position of

the fixed magnet on the endoclip. Initial attempts to place the magnet at the clip barrel showed that there were two problems with this position (**Figure 3.9, red arrow**). The magnet would actually rotate more in the lumen of the oesophagus because the barrel was the protruding part of the endoclip. Also the magnet at this position did not allow the passage of the endoclip and its fixing device through the working channel of the endoscope.

The magnet was placed on the top surface on one of the clip jaw (**Figure 3.9, black arrow**) but not the surface between the two jaws (**Figure 3.9, white arrows**).

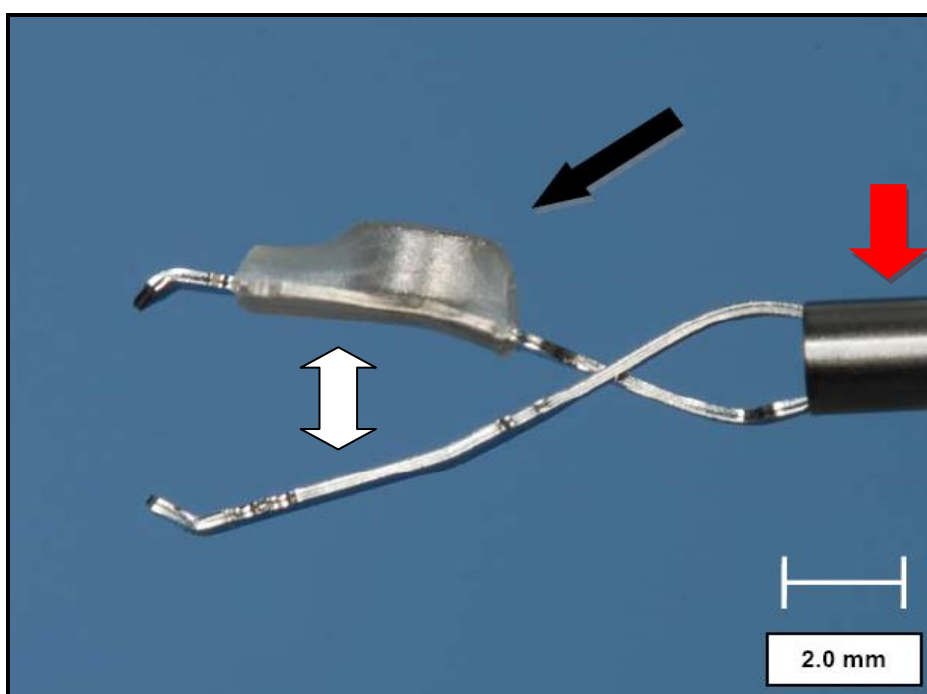


**Figure 3.9:** Metal clip with magnet. Photo illustrating a single use endoclip (model HX-201UR-135, Olympus, UK) with a small samarium cobalt magnet attached by heat shrinkable polyvinylidene fluoride (PMG Plastronic, UK) (shown with black arrow). A scale is drawn on the lower right to depict the size. The red and white arrows indicate unsuitable positions for placement of the magnet.

This was the optimal position because the magnet was less likely to rotate on the mucosa wall and also the magnet weight naturally placed the polar surface towards the lumen. This position allowed the endoclip and its fixing

device to pass through the working channel as the jaws could approximate each other during the passage into the working channel.

The magnet was securely attached using medical grade heat shrink material (PLK175; PMG Plastronic Ltd, UK) onto the single use endoclip (HX-201UR-135; Olympus Keymed Ltd, UK) and reliably ensured that the magnet remained in the same position on the endoclip. The heat shrink material was thin enough that it did not increase the overall thickness of the magnet. Other methods were tried, including glues or resins, but these did not work as well as the heat shrink in securing the position of the magnet on the clip.

#### **3.3.4.3 Placement of magnet within the GOJ**

The endoclip with magnet was deployed onto the SCJ using a clip fixing device via a standard 27 F endoscope (Pentax Ltd, UK). The endoclip is commonly used for securing haemostasis during bleeding ulcer in the stomach but is less commonly used in the oesophagus. Due to anatomical differences between stomach and oesophagus, there are technical challenges needed to overcome when placing the metal-clip within the oesophagus. The stomach has a larger lumen and, therefore, has a greater space to manipulate the clip. However, the oesophagus has a smaller lumen and straight walls which make it more challenging to place a clip.

In addition, the SCJ is constantly moving with respiration and peristalsis. A collapsed SCJ is easier for clip placement and therefore only minimal air insufflation should be allowed during the endoscopy. It was found that placing the magnet between 2 and 6 o'clock position of the oesophagus was not only technically easy, but the signal strength was often good when the probe was passed down. The reason why this was so is unknown but it might relate to the natural angulation of the GOJ into the proximal stomach.

In some subjects the clip fell away within 72 hours. Therefore, ideally all clinical studies had to be performed within the time period when the clip was in place. The tendency for the clip to fall away was partly because some of these clips seem to have caught more of the squamous epithelium which is

relatively more fragile than the columnar epithelium. Another reason might have been that the clip is less robust after manipulation during endoscopy and with the use of heat shrink.

If the clip was not successfully placed at the SCJ and was lost in the stomach lumen (<10% of cases) the procedure had to be abandoned to avoid the potential of having two or more magnets free in the lumen of the intestines, and the consequent risk of them attaching to each other between two loops of bowel. This could potentially cause intestinal torsion or localised ischaemic necrosis of the bowel wall. In 50% of subjects in whom the placement of the magnet was unsuccessful, the magnet was detected in the stomach and easily retrieved using biopsy forceps. A suggestion to increase the chance of recovering a lost endoclip by attaching a string to it was abandoned since the frequency of clip failure was low.

The coordination between the endoscopist and the nurse was of utmost importance in ensuring a successful placement of the clip at the SCJ. The nurse should be ideally trained to handle the clip fixing device and be alert to the instructions given by the endoscopist during clipping.

### **3.4 CONCLUSION**

Developing new device is a challenging task and the process requires plenty of trials and errors as well as thoughts into its design. The GOJ locator probe, utilising the Hall Effect technology and magnet, allows a continuous and reliable measurement of position and movement of the GOJ. To bring this development further, it was necessary to perform in-vitro and in-vivo tests to better understand the effects of magnet orientation on the performance of the new technique. This is discussed in great details in the next chapter.

# CHAPTER 4

## IN-VITRO AND IN-VIVO STUDIES ON THE GOJ LOCATOR PROBE

---

- 4.1 Background
- 4.2 In-vitro studies
- 4.3 In-vivo validation studies
- 4.4 Discussion
- 4.5 Summary and conclusion

## 4 IN-VITRO AND IN-VIVO STUDIES ON THE GOJ LOCATOR PROBE

### 4.1 BACKGROUND

The very first prototype locator probe has been limited in-vivo by poor sensitivity as a result of poor signal strength. This has been postulated to be a result of magnet orientation of the magnetic field relative to sensor in-vivo. In order to confirm this, bench or in-vitro studies are needed to assess the behaviour of magnet in different axes relative to the probe.

There is also a potential effect of body temperature on the Hall Effect sensors. Previous literature indicate that the sensitivity of Hall Effect sensors can be affected by a rise in temperature (Ramsden, 2006). The probe is initially at room temperature (18°C or lower) before it is being intubated and subsequently remains within the GI lumen at body temperature (37°C). The effect of this rapid followed by prolonged change in temperature on the Hall Effect sensors is unknown. The 36-channel solid state manometer which was used alongside the locator probe in clinical studies in this thesis is also affected by temperature but the manufacturer has incorporated thermal compensation mechanism. This effect of temperature on the manometer has been discussed briefly in section 1.4.2. However, while the thermal compensation may work for short studies (20 - 30 min) in routine clinical setting, the adequacy for thermal compensation for prolonged studies (beyond an hour) is unknown.

The manometer and pH catheter contain solid state sensors and these sensors can potentially generate electromagnetic field during their operation. Whether these electromagnetic field can interfere with the working of Hall Effect sensor is unknown. An important part of in-vivo study involves deployment of magnet within the GOJ and this can potentially remain for a significant amount of time. During this period of time, there is a possibility that the patient may need to undergo MRI examination. The MRI can generate a huge magnetic field, enough to tear the magnet away and results in perforation. However, the actual translational effect on the luminal effect is not known.

The current chapter aims to investigate the above issues through bench or in-vitro experiments. The next section of this chapter presents the finding of in-vivo validation of the new technique against the gold standard, fluoroscopy. The validation is important to confirm that the novel locator probe is as good as the fluoroscopy if not better in the detection of position and movement of the SCJ. The final section is dedicated to the discussion of findings from both in-vitro and in-vivo studies. We shall begin with in-vitro experiments first as follow.

## 4.2 IN-VITRO STUDIES

The current section explores the effect of magnet distance and rotation on the position accuracy and signal strength of the locator probe in an in-vitro environment within the laboratory.

### 4.2.1 Effects of orientation on the accuracy

#### 4.2.1.1 Experimental setup and methods

During in-vitro experiments, the locator probe (without silicone casing) was secured on a standard ruler with mm markings. With the ruler, the distance between Hall Effect sensors could be accurately determined. Using a set of metal clamps, the ruler with locator probe was fixed vertically except for the base to allow free rotation of the probe (**Figure 4.1**).

The magnet (2 x 1 mm) was fixed using another set of metal clamps, allowing testing of effects of varying the distances and orientations of magnet from the probe. For accurate determination of degree of magnet orientation, a standard clear plastic protractor (in degrees) was used.

In-vitro experiments were aimed to assess the accuracy of locator system at different orientations between the magnet and probe. Four different orientations (A, B, C and D) of magnet at different distances (5, 10 and 15 mm) from the probe were assessed. These orientations were identified to provide a 3-D (x, y and z axis) assessment of the magnet relative to the probe. Detail descriptions on the above-mentioned orientations are given in chapter 4. All experiments were performed by one investigator using the same standard instruments described in this section.

At each orientation (for example, the magnet at 60 degrees of rotation A and distance of 5 mm from the probe), the magnet would be moved in 1 mm steps along the length of probe (over 210 mm). The locator probe would record the movement of the magnet at a frequency of 1 Hz and its data extracted using the PolygramNet™ software. The following parameters were analysed using the Microsoft Excel 2007 software:

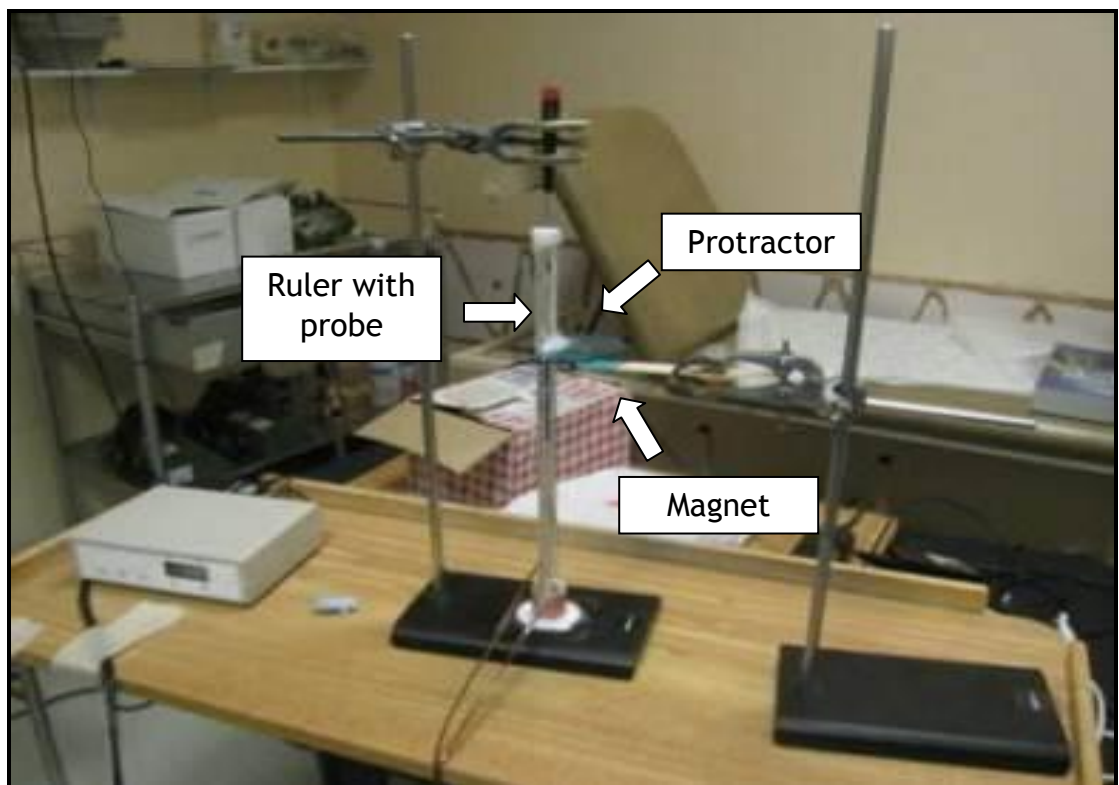


**Figure 4.1:** Setup of in-vitro experiments

Position error and its standard deviation: The position error is the difference between the actual position (determined on ruler) and that displayed by probe. The standard deviation denotes the spread of position error.

Signal strength: The displayed signal strength represents the highest output from any one of the individual Hall Effect sensor. Signal strength lower than approximately 10 mV can be attributed to electromagnetic noise and with such low signal strength, the displayed position may not be valid. When signal

strength is unrecordable as a result of magnet absence then the locator recording will default to a sensor or location with the highest baseline voltage or signal strength value.

The system was assessed by measuring the signal strength with the magnet at different distances from the probe as well as in different positions and magnetic field orientation relative to the probe (**Figure 4.2**).

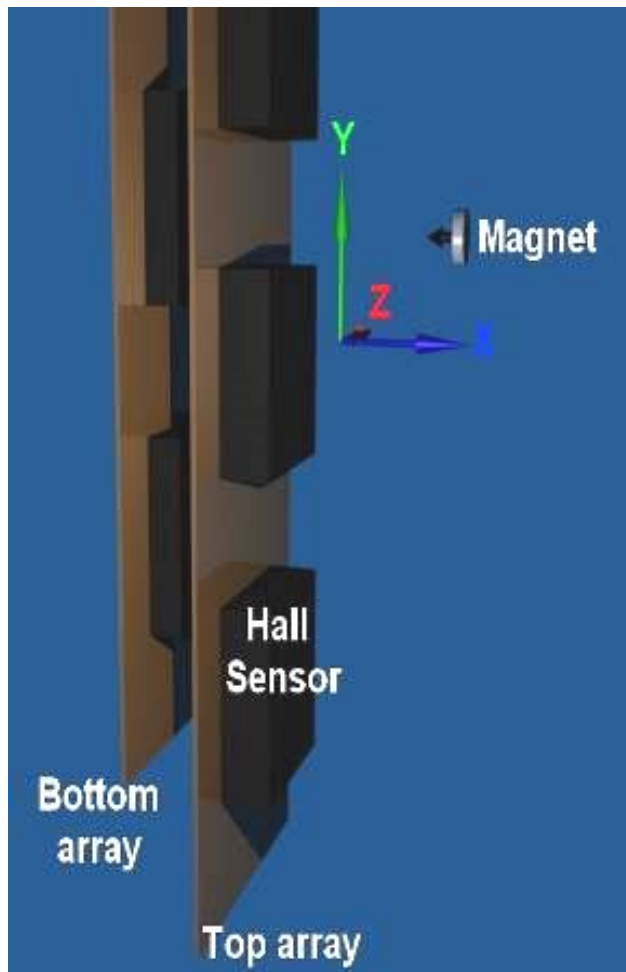


**Figure 4.2:** Assessment of accuracy with the magnet at different distances and orientation relative to the probe.

The ability to accurately measure the location of the magnet along the length of the probe was also assessed with the magnet at different distances, positions and orientations relative to the probe. The parameters measured were position error and signal strength and their definitions have been described above.

### 4.2.1.2 Results: Signal Strength

With the magnet maintained at a constant position along the probe and with its north-south pole always pointing directly toward the probe, the signal strength was monitored as it was rotated around the probe at a distance of 5 mm and 10 mm from the probe. This rotation is termed rotation A and is shown in **Figure 4.3** and **Figure 4.4 (rotation A)**. Maximal signal strength was obtained when the magnet was anterior to the probe, a reduced signal strength posteriorly and least strength when positioned lateral to the probe.

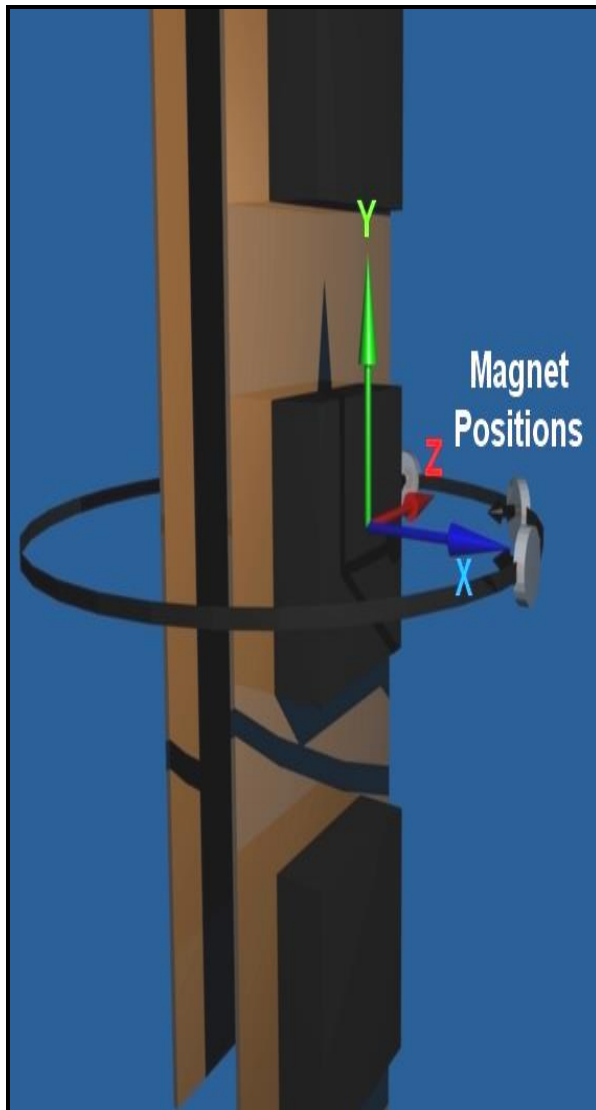


**Figure 4.3:** Rotation A and D. In rotation A, with magnet at constant position along the length of probe, its north-south pole pointing the probe, it was rotated around the probe. In rotation D, also with magnet at constant position along the length of probe, but its non-polar surface pointing the probe, it was rotated around the probe.

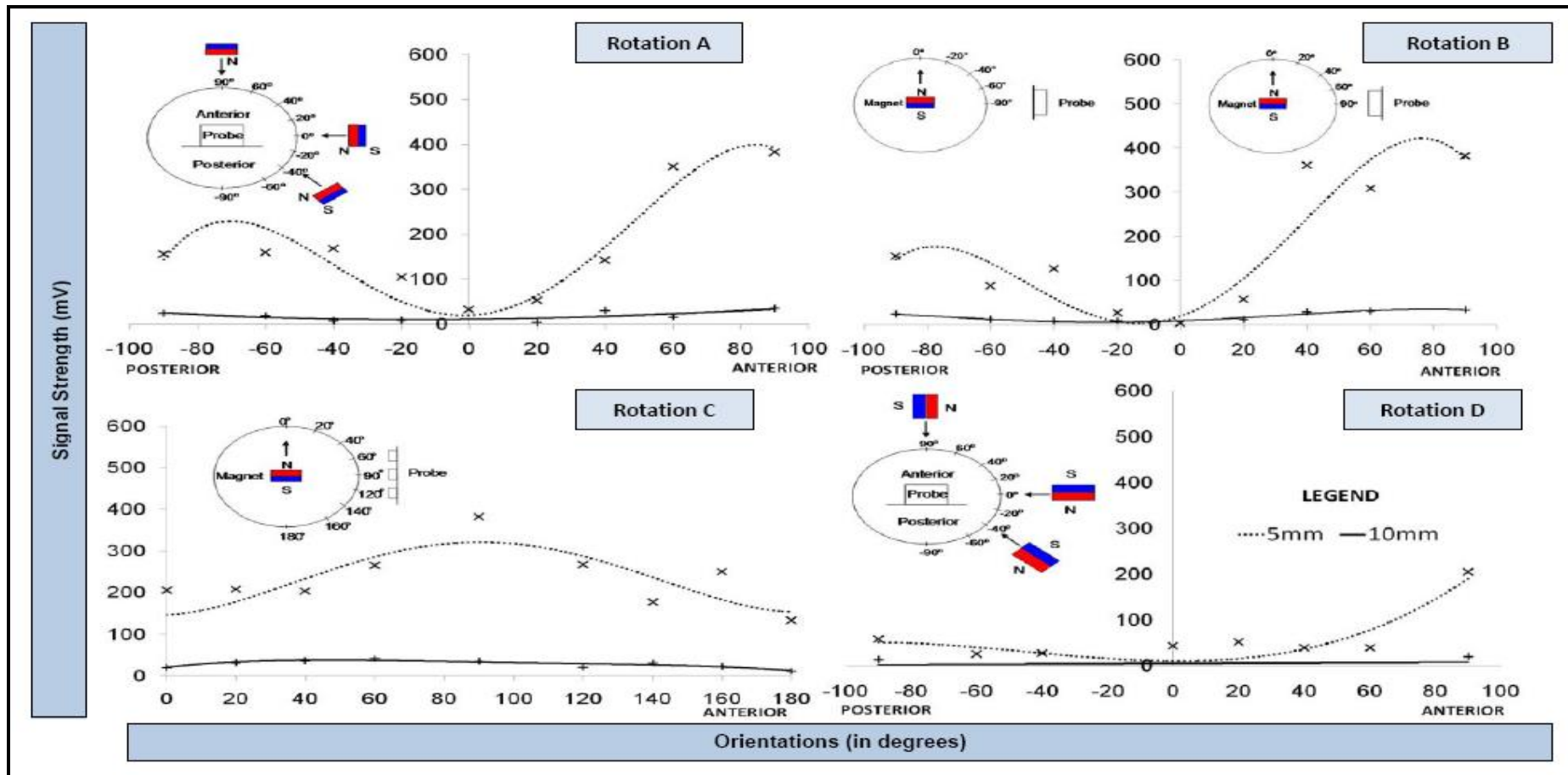
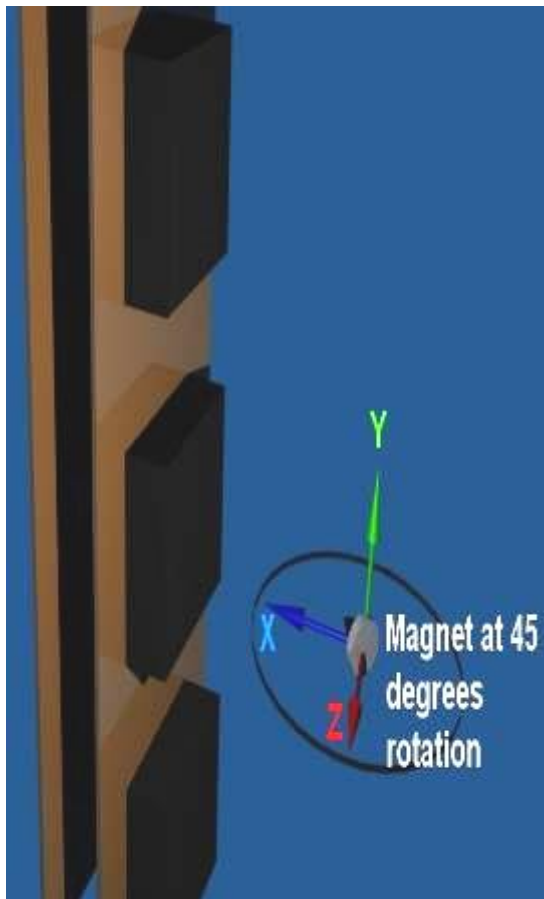


Figure 4.4: Relationship between signal strength (mV) against various orientations in rotation A, B, C and D. In rotation A, B and D the length of the probe is perpendicular to the page. For rotation A, B and D, orientations from  $-20^{\circ}$  to  $-100^{\circ}$  on the graph axis are indicative of magnet placement posterior to the probe.

With the magnet maintained at a constant length along the probe and kept directly anterior to the probe, the magnet was rotated so that its north-south pole was kept in a plane perpendicular to the length of the probe. This rotation is referred to as rotation B and shown in **Figure 4.5** and **Figure 4.4 (rotation B)**. This manoeuvre was performed with the magnet at 5 mm and 10 mm distance from the probe. Signal strength was greatest when the magnetic field pointed directly toward or away from the probe and least when it was midway between those two orientations.



**Figure 4.5:** Rotation B. In rotation B, with magnet maintained at constant length and kept anterior to the probe, the magnet was rotated so that its north-south pole was kept in a plane perpendicular to the length of probe.

With the magnet maintained at a constant length along the probe and kept directly anterior to the probe, the magnet was rotated to a plane parallel to the length of the probe. This is referred to as rotation C and is shown in **Figure 4.6** and **Figure 4.4 (rotation C)**. The manoeuvre was again performed at 5 mm and 10 mm distance from the probe. This rotation produced only very small variation

in magnet strength with strength being least when north-south pole axis was parallel to the length of the probe.

The magnet was initially placed anterior to the probe and with its north-south axis perpendicular to an imaginary line from the centre of the Hall sensor to the centre of the magnet. The magnet was then rotated around the probe while maintaining the same magnetic field orientation relative to the probe (**Figure 4.3 and Figure 4.4, rotation D**). This rotation produced the least signal strength across all degrees of orientation and the strength being least when the magnet was at either side of the probe.

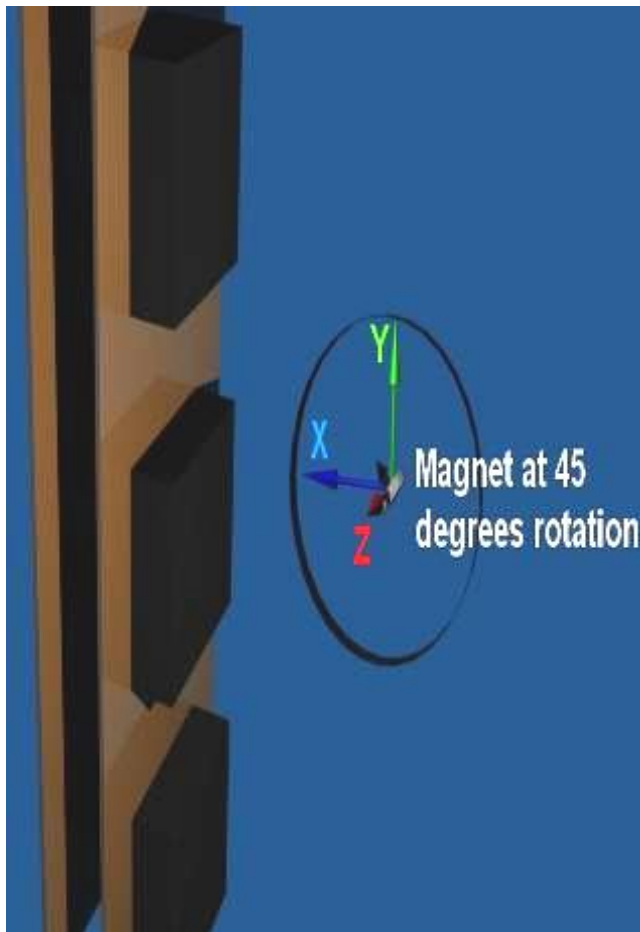


**Figure 4.6:** Rotation C. In rotation C, with magnet maintained at constant length and kept anterior to the probe, the magnet was rotated to a plane parallel to the length of probe.

When the signal strength was analysed with respect to distance from 5 mm to 15 mm in various degrees of orientations for rotations A, B and C (**Figure 4.7**), there was an exponential decay of signal strength with increasing distance.

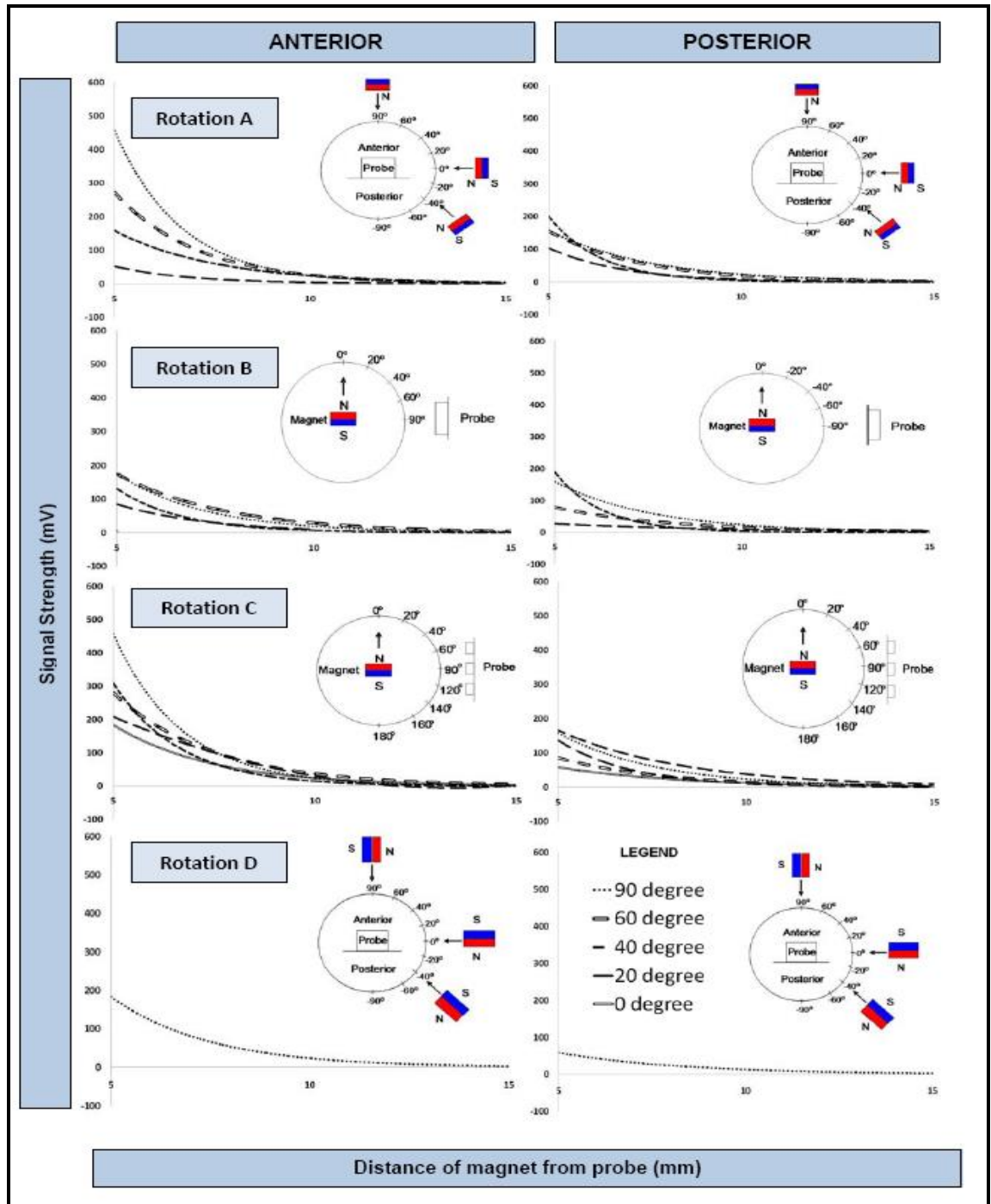


**Figure 4.7:** Relationship between signal strength (mV) against distances at 5, 10 and 15 mm in rotation A, B, C and D. In rotation A, B and D the length of the probe is perpendicular to the page. For each rotation A, B, C and D, figures for magnet placement anterior to the probe are shown on the left and figures for magnet placement posterior to the probe are shown on the right. For rotation A and B, results for 0 degree are not present due to un-recordable signal strength. For rotation D, only result for 90 degree is available since other orientations do not have adequate signal strength after 5 mm distance.

The decay in signal strength was greater with decreasing degrees in rotation A compared to rotation B with absence of data for 0 degree in both. A lesser degree of decay in signal strength for all different degrees of orientations was seen in rotation C. The strength variation across all orientations was the least with rotation D. With posterior placement of magnet to the probe, all rotations A, B, C and D showed a greater degree of decay in strength compared to anterior placement with a lesser degree seen in rotation C.

The in-vitro studies indicated that a poor signal strength of < 10 mV occurred only during 17.8% of all orientations and positions of the magnet within 10 mm distance of the GOJ locator probe.

#### **4.2.1.3 Results: Position accuracy**

With the probe stationary, the magnet was moved along the length of the probe at 1 mm increments and the distance recorded by the probe compared with the actual position along the probe. This was performed at 0 mm, 5 mm, 10 mm and 15 mm distance between the magnet and probe and with the magnet in different positions and orientations with respect to the probe as described on the above section on signal strength (Table 4.1).

The magnet was first of all moved along the length of the probe in the varying angles of rotation described as rotation A above. At distance  $\leq 10$  mm an accuracy of 0 - 3.4 mm was found for all rotations studied except for 0° at 10 mm distance when studied signal strength was inadequate. At 15 mm an accuracy of 1.2 - 6.0 mm was recorded for all rotations except 0°, +20° and -20° when again signal strength was inadequate.

The magnet was then moved along the length of the probe in the varying angles of rotation described as rotation B above. At distance  $\leq 10$  mm, an accuracy of 0.8 - 3.0 mm was found for all rotations except 0° when signal strength was inadequate. At 15 mm the error was 2.1 - 5.8 mm for all rotations except 0°, +20° and -20° when signal strength was inadequate.

**Table 4.1: Effects of rotation and proximity on locator probe position error and standard deviation**

Rotation (Degrees)	Rotation A						Rotation B						Rotation C						Rotation D					
	5mm		10mm		15mm		5mm		10mm		15mm		5mm		10mm		15mm		5mm		10mm		15mm	
	Error	SD	Error	SD	Error	SD	Error	SD	Error	SD	Error	SD	Error	SD	Error	SD	Error	SD	Error	SD	Error	SD	Error	SD
0	2.89	3.27	-	-	-	-	1.41	1.65	-	-	-	-	2.31	2.26	7.15	1.22	7.93	1.59	0.94	1.08	-	-	-	-
20	2.43	2.71	1.47	1.85	-	-	0.61	0.83	1.11	1.42	-	-	4.44	1.58	7.58	1	2.58	0.85	1.30	1.37	-	-	-	-
40	1.39	1.34	1.30	0.86	1.18	1.45	1.01	0.82	1.45	1.08	5.45	5.77	4.88	1.27	6.56	0.84	6.33	7.72	1.03	1.12	-	-	-	-
60	3.40	1.32	1.52	0.76	2.25	1.35	0.9	0.96	1.04	0.62	3.64	2.42	4.15	0.98	5.67	0.66	6.79	1.21	0.84	0.97	-	-	-	-
90	2.26	0.75	2.88	0.62	2.70	2.12	2.26	0.75	2.88	0.62	2.70	2.12	2.26	0.75	2.88	0.62	2.70	2.12	2.31	2.26	7.15	1.22	7.93	1.59
120	-	-	-	-	-	-	-	-	-	-	-	-	2.43	1.04	2.03	1.03	12.45	3.89	-	-	-	-	-	-
140	-	-	-	-	-	-	-	-	-	-	-	-	2.42	1.27	1.30	1.02	10.88	2.71	-	-	-	-	-	-
160	-	-	-	-	-	-	-	-	-	-	-	-	2.89	1.43	1.17	1.29	10.14	5.92	-	-	-	-	-	-
180	-	-	-	-	-	-	-	-	-	-	-	-	2.22	2.70	7.65	1.02	15.86	6.05	-	-	-	-	-	-
-180	-	-	-	-	-	-	-	-	-	-	-	-	3.42	3.78	5.29	5.32	-	-	-	-	-	-	-	-
-160	-	-	-	-	-	-	-	-	-	-	-	-	1.75	1.38	2.48	0.92	-	-	-	-	-	-	-	-
-140	-	-	-	-	-	-	-	-	-	-	-	-	0.95	1.13	0.73	0.8	-	-	-	-	-	-	-	-
-120	-	-	-	-	-	-	-	-	-	-	-	-	2.44	1.19	0.53	0.64	-	-	-	-	-	-	-	-
-90	3.14	1.41	2.04	1.51	3.06	3.72	3.14	1.41	2.04	1.51	3.06	3.72	3.14	1.41	2.04	1.51	3.06	3.72	3.70	2.12	5.28	1.20	-	-
-60	2.62	1.11	2.53	0.79	3.61	4.54	2.11	1.29	3.09	1.74	3.64	2.42	4.23	0.80	4.62	1.12	-	-	3.00	4.01	-	-	-	-
-40	2.67	1.35	2.55	0.81	5.30	5.98	1.32	1.04	2.67	1.26	5.45	5.77	3.61	0.93	4.44	0.91	-	-	2.90	3.58	-	-	-	-
-20	1.75	1.19	1.38	0.84	-	-	1.68	0.78	2.21	1.07	-	-	3.70	1.77	7.68	0.97	-	-	-	-	-	-	-	-
-0	2.89	3.27	-	-	-	-	1.41	1.65	-	-	-	-	3.70	2.12	5.28	1.20	-	-	0.94	1.08	-	-	-	-

Error denotes the mean of difference for 210 experiments between actual position and the probe recorded position in mm, SD; standard deviation denotes the spread of error in mm, “-“denotes the absence of data due to inability of the system to detect any position in that particular rotation as a result of poor magnetic field strength or in the case of rotation A, B and D, the movement from 0 to 90 degrees is symmetrical to 90 to 180 degrees, and so is not included. Degrees between -180 to -0 are indicative of posterior placement of magnet relative to the probe for rotation C but for rotation A, B and D the degrees 0 and -0 are the same.

The magnet was moved along the probe at different rotations described as rotation C. At distance  $\leq 10$  mm the error was 0.6 - 7.7 mm. At 15 mm distance the error was 1.2 - 12.5 mm for 0-160° and -90°. For 180°, -160°, -140°, -120°, -60°, -40°, -20°, -0° the signal strength was inadequate.

Finally, the magnet was moved along the probe at different rotations described as rotation D. At distance  $\leq 10$  mm the error was 0.8 - 7.1 mm. At 15 mm distance the error was 7.9 mm for +90° with the rest of rotations having inadequate signal strength.

Including all the possible orientations of the magnet at or nearer than 10 mm from the probe, the median accuracy of distance along the length of probe was 2.4 mm (inter-quartile range (IQR) 2.1 mm). The proportion of all possible orientations within 10 mm of the probe giving an accuracy of  $\pm 10$  mm was 88.9% (Table 4.2).

**Table 4.2:** Analyses on orientations with poor signal strength  $< 10$  mV and orientations with error  $< 10$ mm for experiments of  $\leq 10$  mm between the magnet and the probe

Orientations	Total Studied Orientations	Orientations with significantly poor signal strength $< 10$ mV	Orientations with error $< 10$ mm
Rotation A	18	4	17
Rotation B	18	4	17
Rotation C	36	0	36
Rotation D	18	8	10
Total	90	16	80
Percentage	100	17.8	88.9

## 4.2.2 Effects of temperature on the locator probe

The sensitivity of Hall Effect sensors can be affected with temperature. In order to appreciate the error induced as a result of change in temperature on the Hall Effect sensors, drift over time at constant temperature must first be investigated.

### 4.2.2.1 Methods

To test for time drift, the probe was placed in the incubator (Stuart Scientific SI 60, UK) for 1 hour at a fixed temperature (at 18° C and 33° C) with the magnet and probe stationary. The experiment was then repeated with the incubator initially at 18°C and then increasing the temperature to 40°C. These temperature and time drift experiments were performed after calibrated the probe at 37° C versus calibrating at room temperature.

### 4.2.2.2 Results

There was no measurable change in signal strength or recorded position over time for up to a period of one hour at 18° C or 33°C (**Figure 4.8**). There was significant change in signal strength (36.0 %) but not position recording when the temperature was increased from 18° C to 40°C and the change appears to be dependent on the initial signal strength, where initially high signal strengths decrease and initially low signal strengths increase (**Figure 4.9**). The probe calibrated at 37° C showed no drift when heated to body temperature. However, the probe calibrated at room temperature showed a significant decrease in signal strength (49.2%) when heated to body temperature.

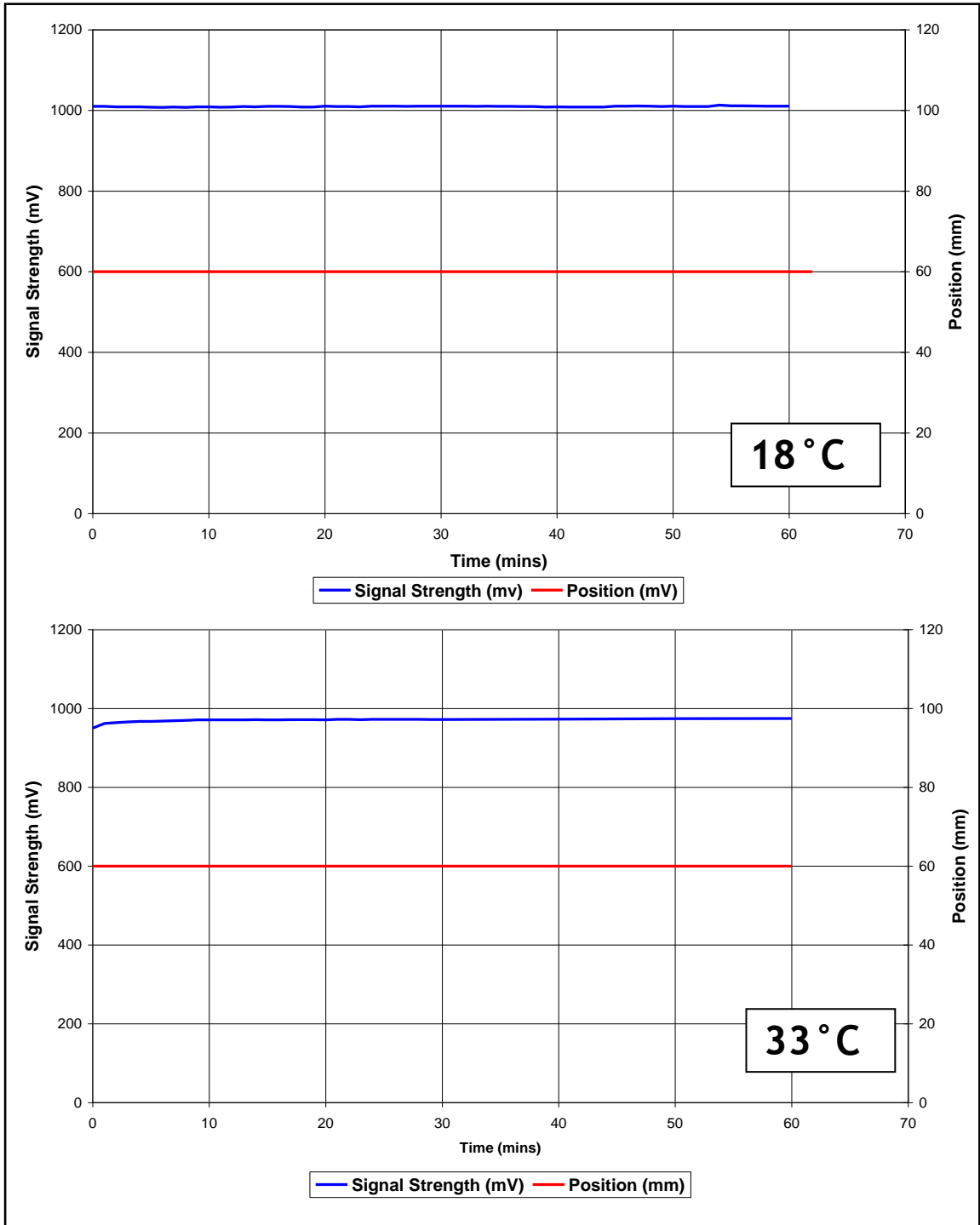
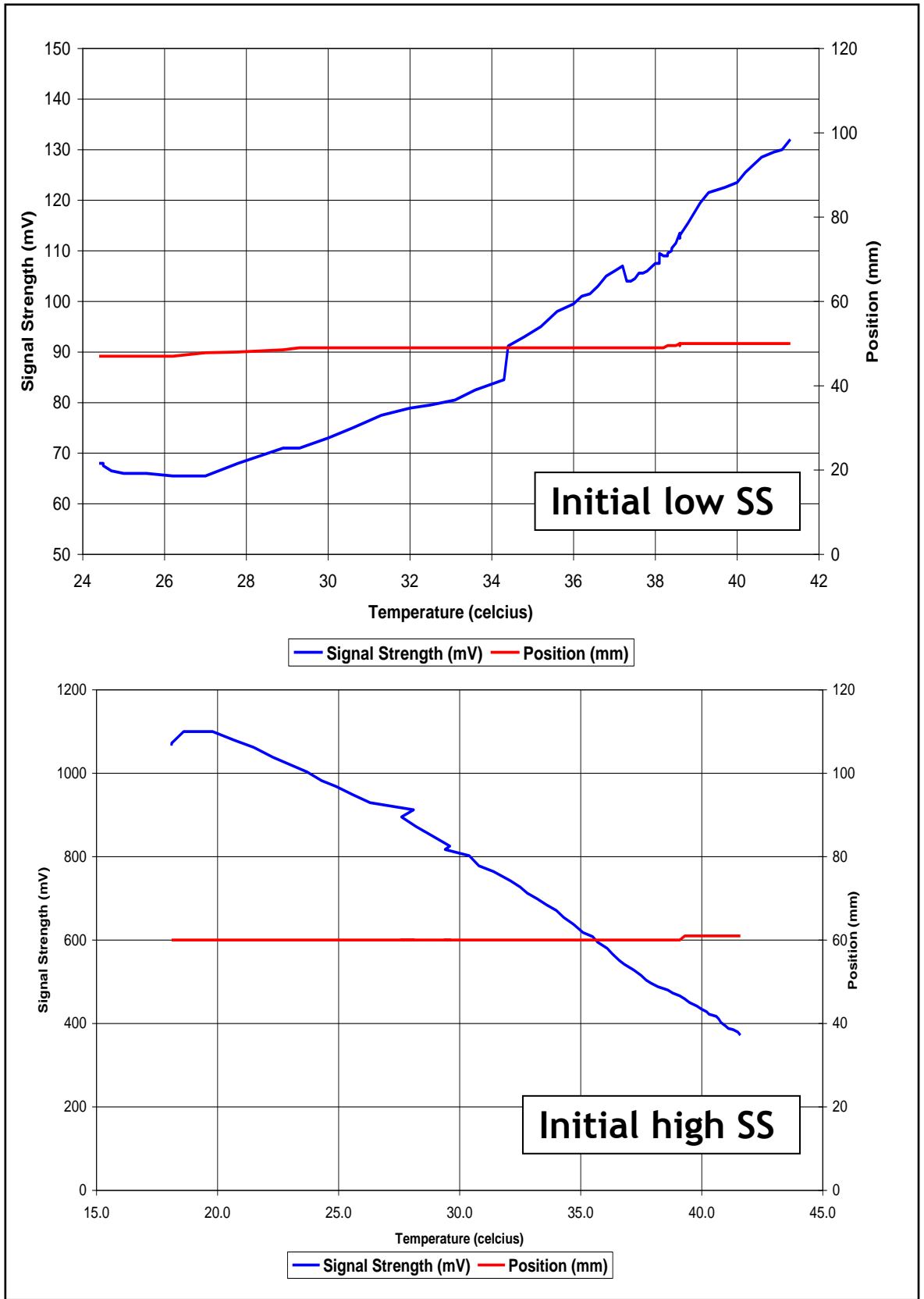


Figure 4.8: Signal strength and position drift at 18°C and 33°C, over 1 hour.



**Figure 4.9:** Signal strength and Position vs. temperature at initial low signal strength (SS) (above) and initial high SS (below).

### 4.2.3 “Thermal drift” of the manometer probe

A recognised limitation of the solid state HRM system (Given Imaging, USA) is “thermal drift” where the pressure recorded using the manometer is affected by temperature. This effect is less striking with short studies (20 - 30 min) but with prolonged studies (2 hours) there were marked increases in pressure at the end (Figure 4.10). The built-in correction in the system did not appear to adequately correct the elevated pressures in prolonged studies.

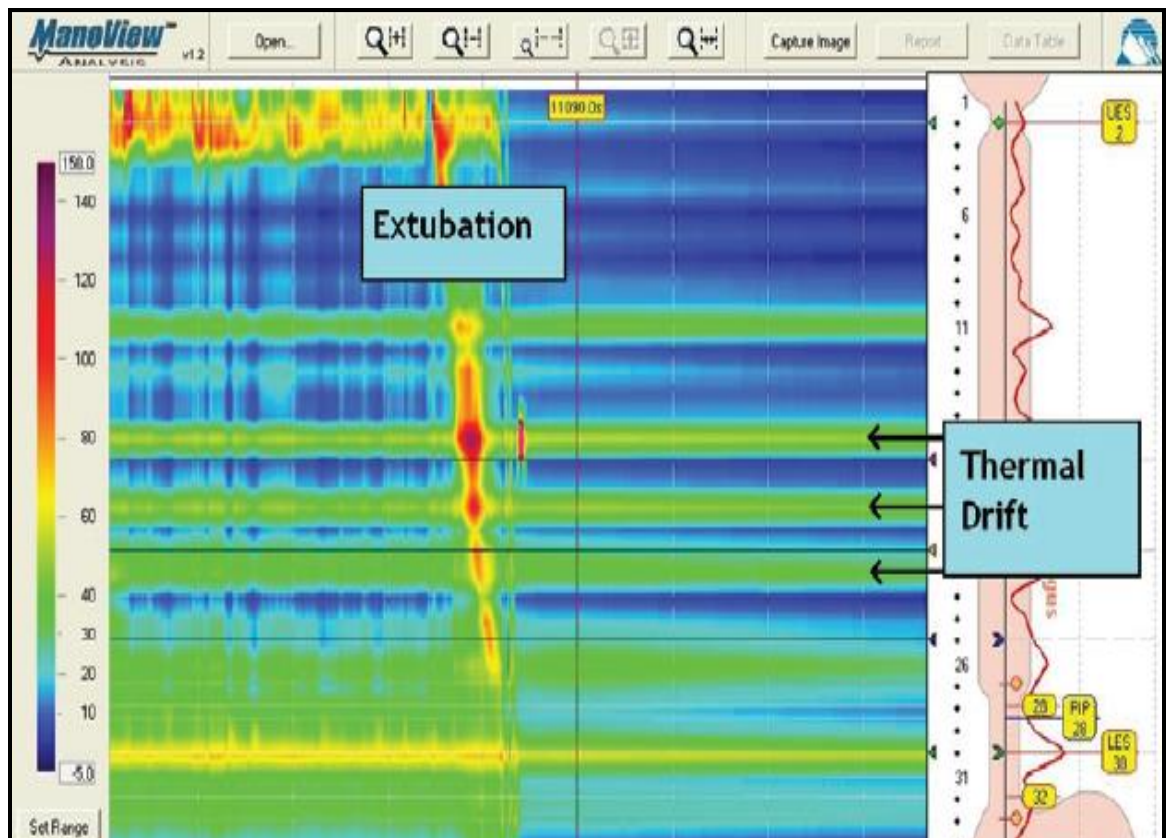


**Figure 4.10:** Thermal drift of the HRM system. With extubation of the manometer, pressures should be equal to atmospheric pressures (blue colour). In some sensors the pressure is in the range of 40-60 mmHg represented by green/yellow colour in the pressure scale. These values represent the magnitude of baseline or thermal drift in a prolonged study.

Given the potential impact of this pressure change on measured physiological values, the following in-vitro experiments were performed to characterise the behaviour of the system with temperature and time (E. V. Robertson *et al.*, 2012).

#### 4.2.3.1 Methods

To characterise “thermal drift”, experimental tests were performed to assess firstly for immediate effect of temperature change on the manometer and secondly the measurement of a constant pressure at a constant temperature of 37°C.

Experiment 1: A water bath was prepared at 37°C and 2 cm depth. Atmospheric pressure was recorded at room temperature by holding the probe in mid-air and this was compared with pressure when the probe was immersed in the prepared water bath. The calculated pressure of 2-cm water (1.5 mmHg) was subtracted from readings taken in the water bath.

Experiment 2: Six experiments were performed with the probe immersed in the water bath at a constant depth of 10 cm and temperature of 37°C. Pressure recordings from the 36 sensors were plotted against time at 5-min intervals for 2 h. Pressure change for each sensor was calculated as the difference between the last recorded pressure and the pressure recorded at 60 s into the study.

#### 4.2.3.2 Results

Results were summarised as median and inter-quartile range. Comparison between sensors was made using the Kruskal-Wallis test.

Experiment 1: The median immediate pressure rise for all 36 sensors was 7.0 mmHg (3.8 mmHg) with significant variability between sensors ( $P < 0.001$ ).

Experiment 2: The median pressure change was 11.1 mmHg (9.9 mmHg) with the magnitude of change varied between sensors (range 3.0 - 33.2 mmHg),  $P <$

0.001. For any given sensor, the change in measured pressure with time was linear ( $R^2 > 0.85$ ) (Figure 4.11).

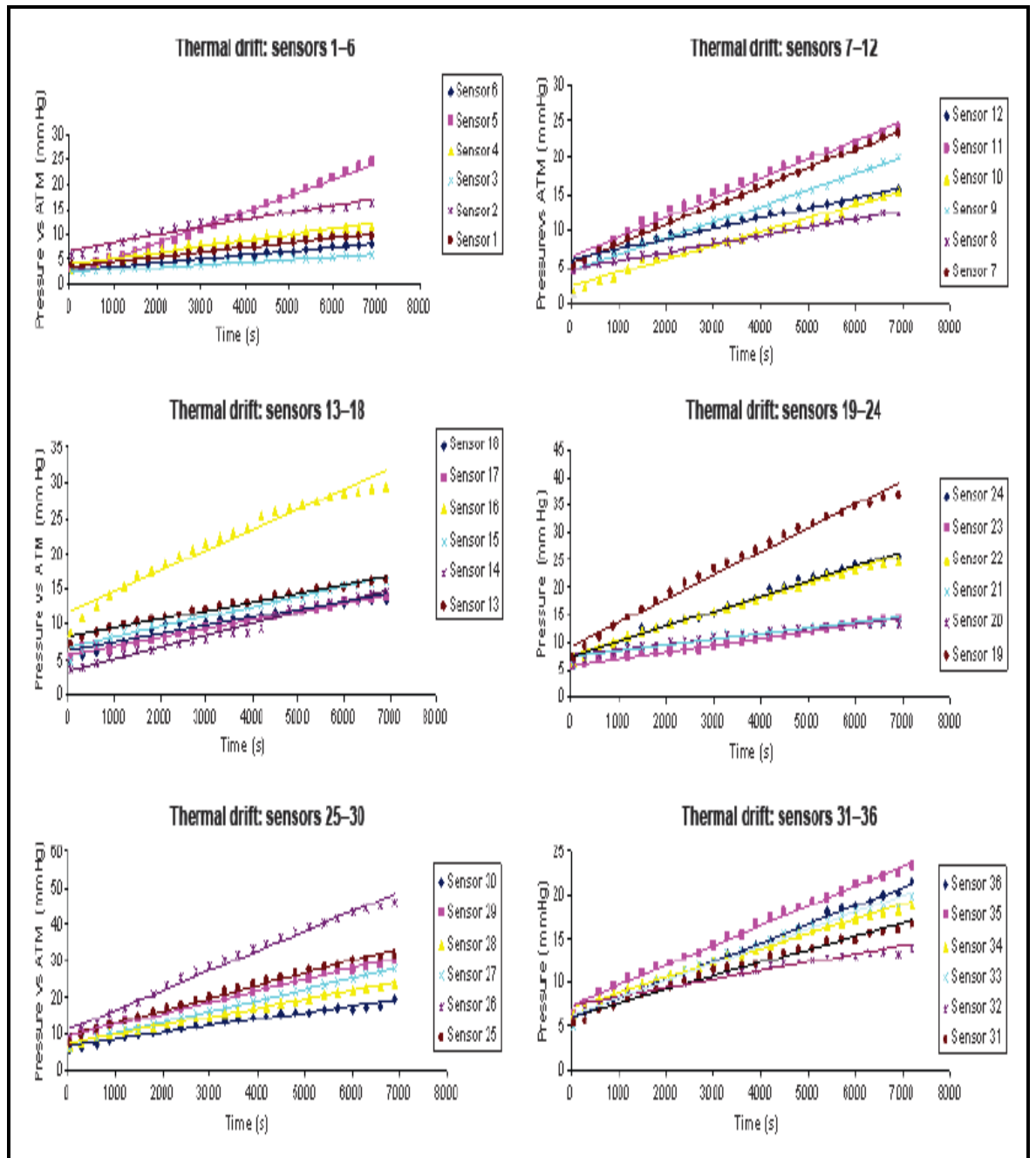


**Figure 4.11:** Pressure-time graphs from a single experiment for all 36 sensors. For any given sensor within a given experiment the pressure drift with time is linear.

For all 36 sensors, the median line gradient was 0.1 mmHg/ min and this was equal to a pressure change of 1.5 mmHg in 15 min, 3 mmHg in 30 min and 6 mmHg in 60 min.

#### **4.2.4 Electromagnetic interference with other probes**

The manometer and pH catheters contained solid state sensors which could generate electromagnetic field and perhaps interfere with the Hall Effect sensors. Interference between the locator probe and the other two solid state arrays was investigated.

##### **4.2.4.1 Methods**

The combined probes were placed in a water bath heated to 37°C and a magnet was placed at a fixed position on the locator probe at low signal strength. Any effects in the locator output would be significant at low signal strength since signal strength is indicative of magnet's presence.

Tests were conducted with manometer and pH probe in a turn "on" and turn "off" mode. Turn "on" mode was with the probe having electricity running and turn "off" mode was with the electricity turned off. In addition, tests were conducted with the manometer exposed to a known hydrostatic pressure (water bath at constant room temperature and depth of 10 cm) and pH probe being exposed to abrupt change in pH (from pH 7 to pH 1 and vice versa) by addition of appropriate molar of alkali or acid.

Finally, tests were conducted on the manometer to determine whether the metallic components within the sensor could interfere with locator's output (**Figure 4.12**). Two different sizes of manometer (4.2 mm and 2.7 mm diameter) were used in the current experiment with the 2.7 mm manometer having smaller sensor and therefore less metallic components.

In experiment A, both 4.2 mm diameter and 2.7 mm diameter manometer (slim-line model, Given Imaging, USA) were initially tested when placed anterior

relative to the locator probe. A magnet was used to move to-and-fro along one sensor containing the manometer's metallic part and this was repeated for the non-metallic portion without any sensor.

In experiment B, experiment A was repeated but with the 4.2 mm diameter and 2.7 mm diameter manometers placed posterior to the locator probe.

Lastly for experiment C, the 4.2 mm diameter manometer probe was compared with the 2.7 mm diameter manometer probe for their difference in accuracy. Both probes were placed anterior to the locator probe during each experiment. A magnet then moved along the probes over a distance of 50 mm. Recordings from the polygraph machine were then analysed for all of the above tests.

#### **4.2.4.2 Results**

The position output of the locator did not change whether the manometer or the pH probe was in a turn "on" or turn "off" mode suggesting that there was no electrical interference between the probes. Similarly, the position output remained the same whether the manometer was exposed to a pressure over time or the pH probe was exposed to an abrupt change in pH.

However, there was a loss of accuracy when the 4.2 mm diameter manometer was placed anterior to the locator probe especially when the magnet was placed overlying the metallic part of the manometer (Experiment A, **Figure 4.12**). The opposite effect on accuracy occurred when the manometer was placed posteriorly (Experiment B, **Figure 4.12**).

Finally the smaller 2.7 mm diameter manometer, having less metal in its sensors produced a better accuracy than the 4.2 mm diameter manometer probe when their tracings were compared (Experiment C, **Figure 4.12**).

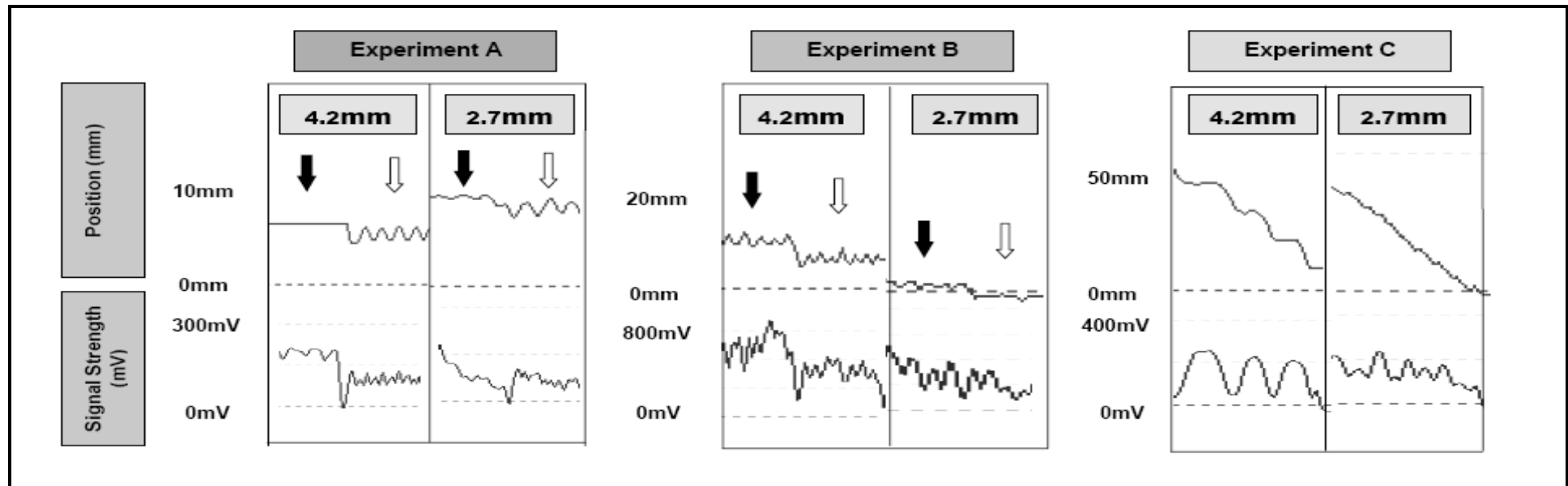


**Figure 4.12:** Experiments on magnetic interference between the metallic sensors of solid-state manometer (Given imaging, USA) and the locator probe as recorded by the Polygraf® machine. In experiment A, the 4.2 mm diameter and 2.7 mm diameter manometers are placed anterior to the locator probe. A magnet is moving to-and-fro along one metallic sensor of the manometer probes as indicated by the black arrow and the test is repeated with the non-metallic portion of the manometer probes as indicated by the white arrow for comparison. In experiment B, the 4.2 mm diameter and 2.7 mm diameter manometers are placed posterior to the locator probe. Similar to experiment A, the magnet is moving to-and-fro along the metallic and non-metallic portion of the manometer probes. As noted in these experiments, there was a loss of accuracy when the 4.2 mm diameter manometer was placed anterior to the locator probe especially when the magnet was moving along the metallic portion of the manometer probe. This loss in accuracy was less with the 2.7 mm diameter manometer. In experiment C, the recordings for 4.2 mm diameter manometer was compared to the smaller 2.7mm diameter manometer. Both the manometer probe was placed anterior to the locator probe. A magnet then moves along the probes during each experiment over a distance of 50 mm. As shown in this experiment, the 2.7 mm diameter manometer has a better accuracy compared to the 4.2 mm diameter manometer and this is presumably due a less metallic content in the smaller sensors for the 2.7 mm diameter manometer. Note the difference in scales for all three figures.

## 4.2.5 Magnet in the MRI environment - a pilot study

### 4.2.5.1 Background

There are concerns about the safety of performing MRI in the presence of ferromagnetic materials within the GI tract. In medicine, ferromagnetic materials are commonly used as implants in patients and they may pose potential injuries to surrounding tissues if exposed to MRI.

There were various reports on the ex-vivo assessments to test for MRI compatibility for a variety of implants used to date. However reports on safety for MRI for metal clips in the GI tract are surprisingly scarce despite the fact that gastroenterologists and surgeons alike are deploying thousands of them worldwide. Part of the reason is the assumption that clips usually fell off in a matter of days. However there were reports that metal clips can remain in the GI tract for many years or possibly indefinitely if left alone (Swellengrebel *et al.*, 2010). The only paper which has assessed for clip compatibility with MRI suggests that metal clips were not safe for MRI examination (Gill *et al.*, 2009).

We are deploying clips with a small disc magnet (2 mm x 1 mm) in the oesophagus for our study to detect the movement of the GOJ. We do not know the effects for having such a clip in-situ if the volunteer is going for a MRI. It is commonly reported that children ingest small magnets contained in toys (Oestreich, 2006). In such cases, doctors are advised not to perform MRI since there are no reports on the safety of MRI in such situation. We have advised our volunteers in the same manner until we have confirmed that the clip has fell off from their GI tract by performing a chest x-ray between 4 - 6 weeks after the clinical study.

In the current pilot study, we hope to get some idea on what could be the effect of having the metal clip with and without the magnet within the MRI environment.

#### 4.2.5.2 Methods - measuring the translational force

Translational force was proportional to the spatial gradient of the static magnetic field and the magnetization component was parallel to the direction of the gradient. The method to measure this force was first described by New et al. in 1983 (New *et al.*, 1983). This method is widely adopted by the American Society for Testing and Material (ASTM) as a standard test.

A magnet (samarium cobalt, 2 x 1mm) was suspended by a fine thread at the edge of the MRI portal where the static magnetic field gradient is the greatest (Figure 4.13 and 4.14).

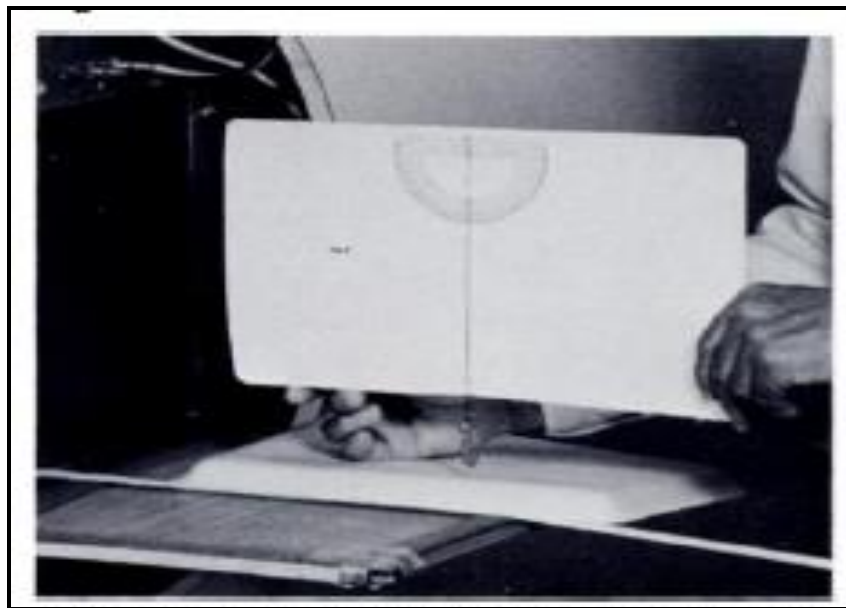


**Figure 4.13:** Photographic depiction on the experiment for measuring translational force of magnet (s) and endoclip (New *et al.*, 1983).

The deflection angle of the clip with and without the magnet was measured using a protractor from the vertical axis. If the angle was above  $65^\circ$  then weights (for example blu-tack or lead) were added to the mass to reduce the angle below  $65^\circ$ . Tests were repeated 3 times and the translational Force,  $F$  (Newton, N) was calculated using the following formula:

$$F = mg \tan \theta$$

Where  $m$  = mass of clip/magnet (g),  $g$  = gravity force equivalent to  $980 \text{ cm/sec}^2$ ,  $\theta$  = deflection angle ( $^\circ$ ). The calculated forces from three experiments were then averaged. Experiment was repeated with five same-sized magnets (equivalent to  $2 \times 5 \text{ mm}$ ) that were stuck together.

It was of interest to know the translational force acting on a stainless steel endoclip alone without any magnet. The above experiment was therefore repeated with a stainless steel endoclip suspended with a fine thread and the deflection angle measured in a similar way. Tests were repeated 3 times and translational force calculated as described above.

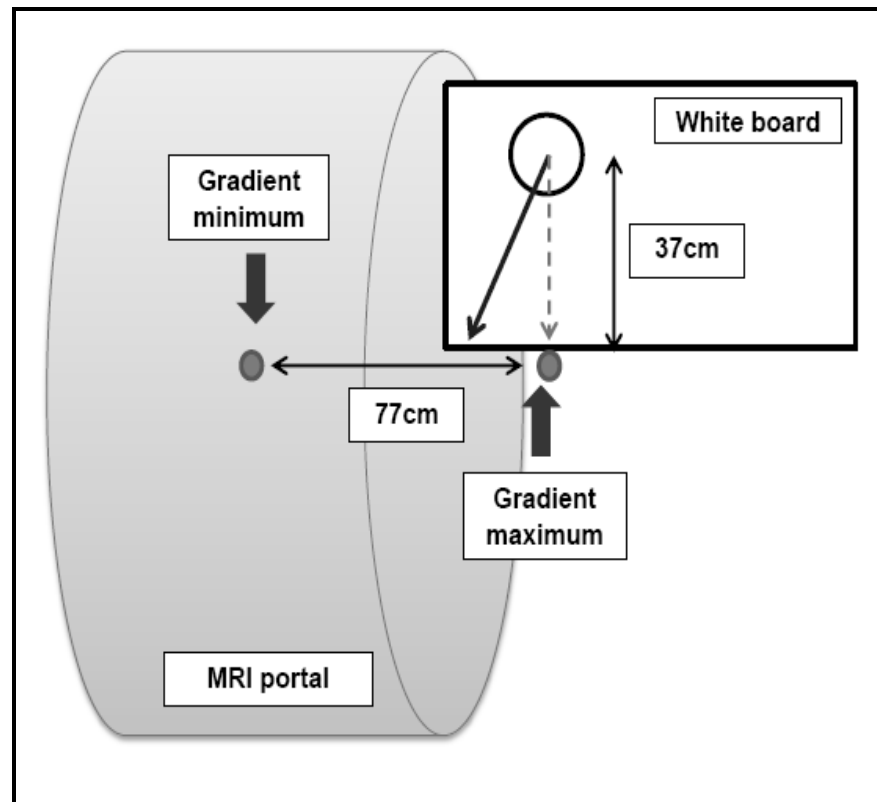


**Figure 4.14:** Measuring translational force in the MRI environment. A cartoon depicting the site of placement of the white board at the edge of MRI portal and the deflection angle of the magnet or endoclip suspended by a fine thread as measured using a protractor.

### 4.2.5.3 Results

The translational force acting on one magnet was 0.0067 N and on five magnets was 0.027 N (Table 4.3). Compared to a weight of an apple (1 N = 100 g), one magnet was exerted a force equivalent to less than 1 g of a free-falling apple and five magnets was exerted a force equivalent to less than 3 g of a free-falling apple. The force acting on five magnets was not five times of the force acting on one magnet. This was most likely a result of manufacturing process on the magnet.

The translational force acting on one stainless steel endoclip was 0.00033 N (Table 4.4) and this was equivalent to a force of less than 0.1 g of a free-falling apple, or 20 times less than a 2 x 1 mm magnet ( $0.0067/0.00033 = 20$ ).

**Table 4.3:** Ex-vivo experiments to assess translational force on samarium cobalt disc magnet in the 1.5T MRI

Magnet Strength	Experiment	Angle $\Theta$ ( $^{\circ}$ )	Tan $\Theta$	Weight (g)	Force (N)	Average Force (N)
One	1	64.00	2.05	0.36	0.0072	0.0067
	2	54.00	1.37	0.48	0.0065	
	3	39.00	0.81	0.82	0.0065	
Five	1	59.00	1.66	1.71	0.028	0.027
	2	65.00	2.14	1.09	0.023	
	3	49.00	1.15	2.62	0.030	

Magnet strength; one refers to a single magnet (size 2 x 1 mm) and five refers to five same-sized (2 x 1 mm) magnets sticking together (equivalent to 2 x 5 mm), Experiment; sequence of experiments performed, Angle  $\Theta$ ; deflection angle of the magnet from the vertical axis of the board, Tan  $\Theta$ ; tangent calculated from the deflection angle measured, Weight; total mass including the added blu tack/lead, Force; translational force in newton (N) calculated from formula  $F=mg \tan \Theta$  where  $m$  = weight (g) and  $g$ =gravity force or  $980\text{cm}/\text{sec}^2$ , Average Force (N); mean of three calculated translational forces.

**Table 4.4:** Ex-vivo experiments to assess translational force on stainless steel Quickclip2® without any magnet (Keymed Olympus, UK) in the 1.5T MRI

Experiment	Angle $\Theta$ (°)	Tan $\Theta$	Weight (g)	Force (N)	Average Force (N)
1	18.00	0.32	0.10	0.00032	0.00033
2	9.00	0.16	0.20	0.00031	
3	14.00	0.25	0.15	0.00037	

Experiment; sequence of experiments performed, Angle  $\Theta$ ; deflection angle of the magnet from the vertical axis of the board, Tan  $\Theta$ ; tangent calculated from the deflection angle measured, Weight; total mass including the added blu tack/lead, Force; translational force in newton (N) calculated from the formula  $F=mg \tan \Theta$  where  $m$  = weight (g) and  $g$ =gravity force or  $980\text{cm}/\text{sec}^2$ , Average Force (N); mean of three calculated translational forces.

## 4.3 IN-VIVO VALIDATION STUDIES

### 4.3.1 Introduction and aims

Fluoroscopy was introduced in chapter 1 (section 1.4.5.1), and this has been the “gold standard” for measuring the position of the GOJ. In the current section, the new locator array is compared to this “gold standard”. This was carried out during various manoeuvres including breathing, swallowing and advancing and withdrawing the probe, this varying in the location of the magnet relative to the probe.

## **4.3.2 Methods**

### **4.3.2.1 Study subjects**

Ten volunteers participated in these in-vivo studies. Of these, eight subjects successfully completed the study, while the remaining two were excluded due to absence of magnet during fluoroscopy. The median age of the eight subjects was 41.5 years (range 26 - 58 years old), five subjects were males and three subjects females. Two males reported symptoms of gastro-oesophageal reflux, and one of them had evidence of reflux oesophagitis on endoscopy. Two females had evidence of hiatus hernia during upper endoscopy but did not report any symptoms of reflux.

### **4.3.2.2 Study protocols**

Subjects attended fasted following overnight fast and had the magnet attached endoscopically to the SCJ. The locator probe was calibrated at room temperature before it being passed down through the nostril. However in three subjects the locator probe was calibrated in warm water bath at body temperature of 37°C. This was performed in three subjects after we noticed the effect of body temperature had on signal strength when the probe was calibrated in room temperature.

The probe was passed per nasally until signals were seen on the computer display confirming detection of the magnet. Screening fluoroscopy was performed at this stage to adjust the locator probe to the desirable depth and position for subsequent screening. The setting for fluoroscopy machine was adjusted for correct dosing and fixed for continuous screening at 5 frames per seconds (PV Pulsera, Philips, UK).

The volunteers then rested for 10 - 15 min. Subsequently, they were asked to perform a series of manoeuvres which were recorded simultaneously with fluoroscopy screening. This lasted between 15 - 20 s per series of manoeuvre. The manoeuvres performed included normal respiration, deep inhalation and full

expiration, water swallowing and lastly advancing the probe as far possible followed by its full withdrawal. Each manoeuvre was performed at least twice. Total fluoroscopy screening lasted approximately 60 - 80 seconds for each volunteer. Markers were placed at the start and the end of each event on both the PolygramNET™ and the fluoroscopy. The markers were checked to ensure time synchronization between the two methods. All images were then transferred and stored using PACS. The images can be analysed using measuring tools built in the PACS software. Recordings from the locator probe were then extracted from the PolygramNET™ software as described above and subsequently exported into Microsoft Excel 2007 and SPSS version 18.0 (SPSS Inc, IL, Chicago) for analysis. Each volunteer had a chest x-ray performed 6-8 weeks after the study to ensure that the clip and or magnet had dislodged.

The research was approved by West Glasgow Research Ethics Committee and all subjects gave informed consent.

#### **4.3.2.3 Data and statistical analysis**

Data analyses were divided according to the four manoeuvres or “events” as described above. The fluoroscopy clip position data (which is regarded as the “standard”) extracted from PACS were correlated and compared with the locator position data. The change in amplitude during each event was determined from both sets of data. Change in amplitude denotes a change from the baseline (selected from an average of 2 s of data prior to the actual event) to the peak of studied event. Wilcoxon matched pair ranks sum test was used to test if there is a difference between the locator and the fluoroscopy amplitude change during the studied event where null hypothesis is the median of differences between the two variables equals zero. Null hypothesis is retained if the *P* value > 0.05.

Linear regression analysis and Pearson correlation co-efficient were used to correlate the events’ position data-points at 1 second interval from both the locator probe and the fluoroscopy. A correlation co-efficient >0.80 and adjusted residual squared ( $R^2$ ) > 80% suggest a good correlation between the two

parameters. Signal strength of locator position recording was expressed as median of average signal strength for each event, maximum value, minimum value and the percentage of signal strength above 10mV during each event.

The median relative movement of the probe against the spine was measured and calculated from the fluoroscopy screenings during each studied events except for insertion and withdrawal of locator probe. This relative movement was measured against a fixed point at the spine and a fixed point at the probe determined at the start of fluoroscopy screening. All statistical analyses were carried out using Microsoft Excel 2007 and SPSS version 18.0 (SPSS Inc., Chicago, IL, USA).

### 4.3.3 Results

There were a total of 31 analysable events of which six from normal respiration, ten from deep respiration, seven from water swallows and six from insertion and withdrawal of locator probe. Representative traces of the locator probe and fluoroscopic positions of each of these events are shown in **Figure 4.15**. Overall a total of 225 data-points at 1 second interval for both locator and fluoroscopy were acquired from these events. The overall correlation co-efficient was 0.96 ( $P < 0.001$ ; 95% confidence interval (CI) 0.89 - 0.96) and adjusted  $R^2$  was 0.91. The median amplitude of fluoroscopic positions for each of the events was similar to median amplitude of locator probe positions (**Table 4.5**).

When the signal strength was analysed for the entire locator recording for all volunteers from the beginning when the probe first detected the magnet upon insertion to the end when the probe last detected the magnet upon withdrawal (median recording time of 1045.44 seconds) there was a median proportion of 96.82% (range 87.05 - 99.29) of data points where signal strength was above 10mV (**Table 4.6**).

So far all volunteers turned up for chest x-ray after 6 to 8 weeks. All but one volunteer were documented cleared from the magnet. None of the volunteers reported any side effects from having the magnet in the gut.

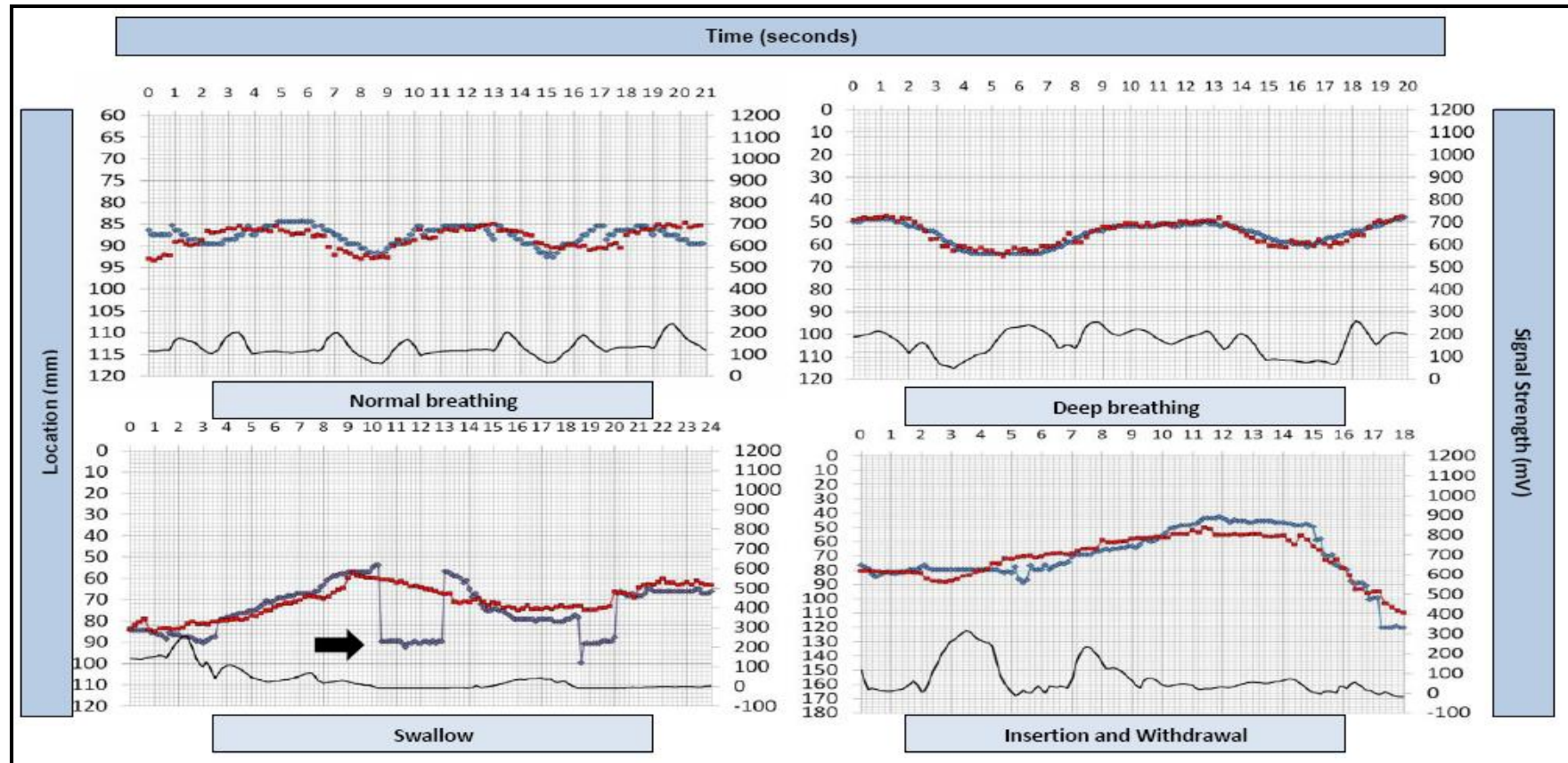


**Figure 4.15:** Graphs showing four studied manoeuvres from four different volunteers. All graphs have two scatter-plots for the position data of locator (blue dots) and the fluoroscopy clip position data (red dots) and a bottom line graph for the signal strength (black). The low signal strength below 10mV will result in a loss of position and therefore the location will default to a sensor with a higher baseline voltage (example as shown as with a black arrow).

**Table 4.5:** Comparison and correlation of data from locator probe and fluoroscopy screenings

Events (N; n)	Median fluoroscopy amplitude change (mm)	Median locator amplitude change (mm)	Wilcoxon matched pair signed rank test (P value)	Correlation co-efficient (95% CI)	Adjusted R <sup>2</sup>	Signal Strength (maximum, minimum) (mV)	Signal strength above 10mV (%)	Relative movement of probe against spine (mm)
Normal breathing (N=6, n=24 )	5.50	5.17	0.92	0.94 (0.93 - 1.28)	0.88	193.84 (79.51,337.33)	100	1.27
Deep breathing (N=10,n=66)	12.25	12.01	0.17	0.95 (0.91 - 1.07)	0.90	129.87 (30.05, 304.23)	100	1.00
Water Swallow (N=7,n=55)	25.00	26.23	0.61	0.92 (0.58 - 0.94)	0.84	166.83 (12.01,436.38)	100	2.74
Insertion and Withdrawal (N=6,n=80)	92.80	85.59	0.92	0.95 (0.82 - 0.96)	0.90	99.84 (0.80,297.03)	89.57	-

N; number of events, n; number of data points per 1 second interval, CI; confidence interval, R<sup>2</sup>; residual squared, mm; millimeters, mV; millivolts, signal strength; median, maximum and minimum range of average signal strength during studied events (mV)

**Table 4.6:** Analysis of signal strength reliability during total recording time for each volunteer

Volunteer	Time (seconds) with signal strength <10mV	Total Recording time (seconds)	% time with signal strength >10mV
1	25.5	353.5	92.79
2	12.75	1180.87	98.92
3	19.75	1229.87	98.39
4	79.25	611.75	87.05
5	63.62	703.12	90.95
6	6.50	910	99.29
7	73.25	1540.5	95.25
8	21.12	1322.75	98.40
Median	23.31	1045.44	96.82

Total recording time = range of recording time of in-vivo study starting from the time when the probe first detected the magnet as it was inserted into the volunteer until the time when the probe last detected the magnet when it was withdrawn from the volunteer.

## 4.4 DISCUSSION

The current studies indicate that it is possible to monitor the position of the SCJ by means of clipping a magnet to it and which is detected by a linear probe consisting of a series of Hall Effect sensors (Lee *et al.*, 2012). This technique allows the detection of location of the SCJ for the first time without fluoroscopy and the associated risk of radiation exposure. Consequently, the technique can be applied over much longer periods of time than has been previously possible.

The system was initially assessed by in-vitro studies. Three main factors influenced the signal strength and the ability to accurately localise the position of the magnet along the length of the probe, namely distance between the magnet and Hall Effect sensor probe, the orientation of the magnetic field relative to the Hall Effect sensors and whether the magnet was positioned anterior, posterior or lateral to the Hall Effect sensors. The human oesophagus normally has a small diameter which is unlikely to be

more than a few millimetres except when it dilates temporarily during swallowing of food boluses. It was found that when the magnet was within 10 mm distance of the probe, then the system could detect its position along the length of the probe with an accuracy of within  $\pm 10$  mm over 88.9% of the full range of possible orientations and positions relative to the probe. Including all possible orientations of the magnet at or nearer than 10 mm from the probe, the median accuracy of position detection along the length of probe was 2.43 mm (IQR 2.11 mm).

The system constantly displayed the signal strength as well as position so that position data obtained during periods of low signal strength were interpreted with caution. When the signal strength arising from detection of the magnet became very low, the system would display the highest output from the Hall Effect sensor with the highest background output. The location reported by the system only changes to another location when the signal strength from another Hall sensor becomes higher than the one currently recording. Similarly, positions obtained during signal strength saturation should be interpreted with caution. Saturation only occurs when the magnet is less than 2 mm from the probe. However, with tubing and coating of the probe along with secretion and folds within the oesophagus, signal saturation does not pose a problem. This was supported by data of in-vivo studies where signal strength saturation never occurred.

Information regarding the location of the SCJ would be highly valuable in interpreting information obtained from pH and pressure sensors positioned in the gastro-oesophageal lumen. We therefore determine whether there was any interference from multiple pH sensors or solid state high resolution manometry probes. We did not test water perfusion manometry as they have no metallic content or electrical activity. There was no noticeable interference between the Hall Effect sensor probe and solid state pH probes. However, there was some interference between the large diameter 4.2 mm diameter HRM and the locator probe. When the magnet was positioned with one of the 1 cm long metal segments of the manometer probe between it and the Hall Effect sensors, the accuracy was reduced. This did not occur when the manometer was on the other side of the Hall Effect sensors from the

magnet and indeed this tended to enhance the signal strength and accuracy. When the slim-line 2.7 mm HRM probe was used, there was much less interference with the accuracy of the locator probe and this can be explained by its presumably much reduced metal content.

The in-vitro studies indicate that the probe is able to detect the position of the SCJ to an accuracy superior to 10 mm for the great majority of the recording period. However, the accuracy is likely to be reduced slightly if used alongside a large diameter solid state high resolution manometry system and we would therefore recommend employing the slim-line manometer. It is also much more comfortable to pass the slim-line manometer along with the pH and locator probe per nasally than to pass the wide manometer along with these two other probes. It is important to pass the equipment nasally in order that the effect of meals can be studied. It is difficult to consume a test meal with three probes per orally.

Change in temperature is a potential modifier that may decrease the accuracy of the Hall Effect array and this was discussed briefly in chapter 3 (section 3.2.3). The effects of temperature on the transducers include a change in coefficient of sensitivity, ohmic offset, increased in resistance and noise. These effects would result in a drift in the signal strength or position reading from the locator probe array. Therefore bench experiments were performed to assess changes or drift in signal strength and position with time at fixed room and body temperatures. Experiments were also performed to assess thermal drift starting at room temperature followed by controlled heating to body temperature. Results showed that there was no drift with time on either signal strength or position but that there was thermal drift on the signal strength depending on its initial strength. While the absence of drift on position is encouraging, the drift on signal strength may eventually affect position reading. To overcome the thermal effect, the locator probe could be calibrated at body temperature using a water bath heated to 37°C. The increase in temperature, possibly accentuated the offset, resistance or noise in the transducers which, when calibrate, could differ further in-vivo, illustrating the importance of calibrating the probe externally at body temperature first.

The issue of thermal drift did not just apply to the locator probe but also to the HRM probe from Sierra Scientific Inc., USA. We have noticed a marked pressure drift at the end of prolonged clinical studies with the manometer which was not adequately compensated using standard thermal compensation method. This prompted us to perform bench experiments in order to characterise and assess the error potential of the thermal drift. There was a median pressure step up of 7 mmHg from room to body temperature but this can be compensated by “in-vivo calibration” of the Manoscan® system. However there was in addition a baseline drift which is not adequately compensated by the “thermal compensation” of the Manoscan® system unless with short studies. Baseline drift is progressive upward step from in-vivo pressure with time. With prolonged studies, a baseline drift of up to 33.2 mmHg can be demonstrated. Instead of using “thermal compensation”, “interpolated linear correction” can adequately reduce the error of baseline drift of approximately 0.3 mmHg.

The main problem with this novel locator technique was the poor performance with respect to orientation and the distance of the magnet from probe. These affected the signal strength and the accuracy of location. In order to improve the sensitivity of this technique is to incorporate more advanced sensors having 3-dimensional capabilities in future design. This has been discussed in chapter 5. Safety is a critical issue with any in-vivo device. The electronics are ISO certified. The magnet needs special consideration. Clipping the magnet to the mucosa was usually straightforward, but it would not be recommended to clip two magnets or to clip a further magnet if one failed to attach. This is to avoid the potential of two magnets being free within the lumen of the intestines and the consequent risk of them attaching to each other between two loops of bowel. This could potentially cause intestinal torsion or localised ischaemic necrosis of the bowel wall.

The other concern with the new technique is the effect of the clipped magnet should the study subjects require a MRI examination before it fell off spontaneously. We therefore performed a pilot study to provide some idea on how much of a force can be exerted by the MRI on the 2 x 1 mm sized magnet and the stainless steel endoclip. The above results in section 4.2.5.3 suggest

that the effects are possibly negligible unless we are using really strong magnets. This provides some assurance that it is probably safe but further more conclusive experiments are needed. It is observed from our volunteers during in-vivo studies that the magnet with clip attached usually spontaneously detaches within 6 weeks. When the clips without a magnet attached are used in routine clinical practice, it is not customary to check whether they have spontaneously detached and passed in the stool. It is uncertain whether this should be done with the clip with magnet attached. The manufacturer advises not to perform MRI procedures on patients who have clips placed within their gastrointestinal tract as this can be harmful without further details. We routinely advise patients that if they subsequently have an MRI scan that they should inform the operator that a clip with magnet attached was fixed to their GOJ.

Other challenges which were observed during the in-vivo studies included that not all subjects could tolerate endoscopy and there were certain risks related to the endoscopy procedure. Further, training and experience were needed to deploy the endoclip with magnet onto the SCJ with an endoscope. The ideal position for deployment onto the SCJ was found to be between 2 to 6 o'clock when looking at the circular SCJ face-on. Furthermore, after deployment, studies with using the Hall Effect locator probe should be performed within 48 - 72 hours since it was noticed that the clip tended to fall away after 72 hours in many subjects. Finally, the size of the probe (outer diameter of 4.2 mm) could be passed through the nostril for most people, although for 2 study subjects, it was attempted to pass the probe through the oral route. However, the oral route was uncomfortable and the position of probe was difficult to maintain.

## **4.5 SUMMARY AND CONCLUSION**

Taking the in-vitro and in-vivo studies together showed that the locator probe could detect the position of the SCJ to an accuracy superior to 10 mm for the great majority of the recording period. The correlation co-efficient was 0.96 (0.001) and the mean amplitude for each of the manoeuvres was similar when

recorded by the probe or fluoroscopy. The proportion of total recording time that the signal strength was more than 10 mV was 96.82% (range 87.05 - 99.29%). A main limitation of this new technique was that in the presence of poor orientation and distance of magnet in relation to the probe, the signal strength and accuracy of location monitoring could be affected. Temperature was another modifier which could affect the accuracy of Hall Effect sensor. Calibrating the probe to body temperature prior to intubation reduced the effect. The 4.2 mm HRM might interfere with accuracy of the probe and the effect was less with the 2.7 mm HRM. Finally, the small magnet in the presence of MRI exerted little translational force but more conclusive studies were needed. In the meantime, subjects having a magnet placed in their GOJ were advised on this potential risk with the MRI examination. Due to limitation in accuracy in the presence of poor orientation, new probes were designed, and this is detailed in the next chapter.

# CHAPTER 5

## THE 3-D GOJ LOCATOR PROBE

---

- 5.1 Introduction
- 5.2 Hall Effect 3-D GOJ locator probe
- 5.3 New generation 3-D GOJ locator probe
- 5.4 Summary and conclusion

## **5 THE 3-D GOJ LOCATOR PROBE**

### **5.1 INTRODUCTION**

The major weakness of the 2-D locator probe is orientation in which 18% of the time, the signal strength was poor for any magnet positions within 10 mm distance from the probe. The Hall Effect sensor (Allegro® A1395) used in the development of the prototype probe was only useful for 2-D position detection with the best magnet orientation being one that faced the sensor directly. However, it is difficult to predict or to control how a magnet clipped at the SCJ would orientate against the sensor during in-vivo studies. There are many factors that can potentially affect the orientation of magnet within the GI luminal tract. Among others, these factors can include the folds of the oesophageal wall, the contraction of lower sphincter, heavy secretions, passage of food during test meals and the presence of other catheters. Recognising this major weakness, a new probe with 3-D magnet-detection properties was developed. The construction of this new probe was a collaborative work with experts from the University of Strathclyde, Glasgow and the Medical Devices Unit, Southern General Hospital.

### **5.2 HALL EFFECT 3-D GOJ LOCATOR PROBE**

#### **5.2.1 Components of the 3-D probe**

The main components of the new probe were similar to the prototype 2-D probe. These components included the Hall Effect sensor, printed circuit boards and its wirings, tubing, microprocessor unit and its software. Details of these components are described in the following sections.

##### **5.2.1.1 Hall Effect sensor - Allegro® A1395**

Initially, advanced Hall Effect sensors having 3-D capabilities were sought, but unfortunately there was none available commercially. Thus, the new design

consisted of two sensors at right angle to each other allowing all orientations to be covered. Furthermore this option used the same Allegro® A1395 sensors as in the earlier 2-D version (section 3.3.3.1).

### 5.2.1.2 Circuitry and microprocessor

The design of the sensor array is illustrated in **Figures 5.1 and 5.2** and consisted of a tab or “ear” arrangement for the sensors, again fixed to a main flexible strip.

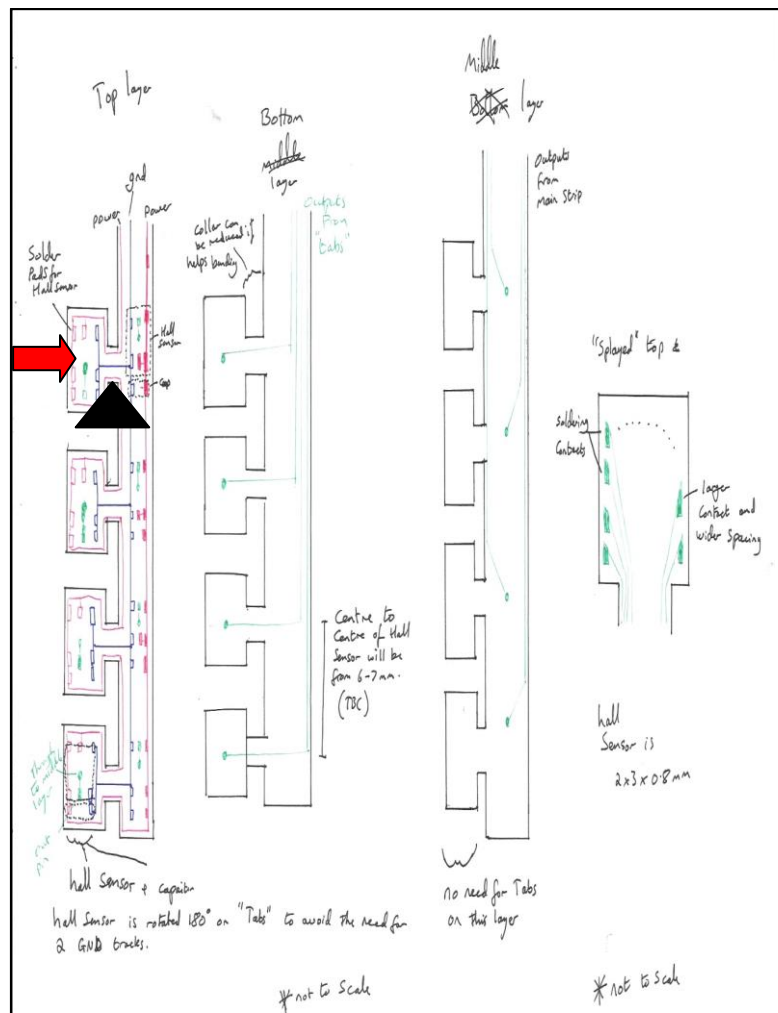


**Figure 5.1:** A sketch on the design of the 3-D GOJ locator probe. The red arrow is showing one of the tabs that connect to the main strip. The black triangle is showing the potential point of weakness due to bending.

The tab could then be bent at right angle and involved less wiring. One weakness was that the bending could potentially stress and break the connecting external copper wires between the tab and the main strip, but this was overcome by using thicker flexible boards.

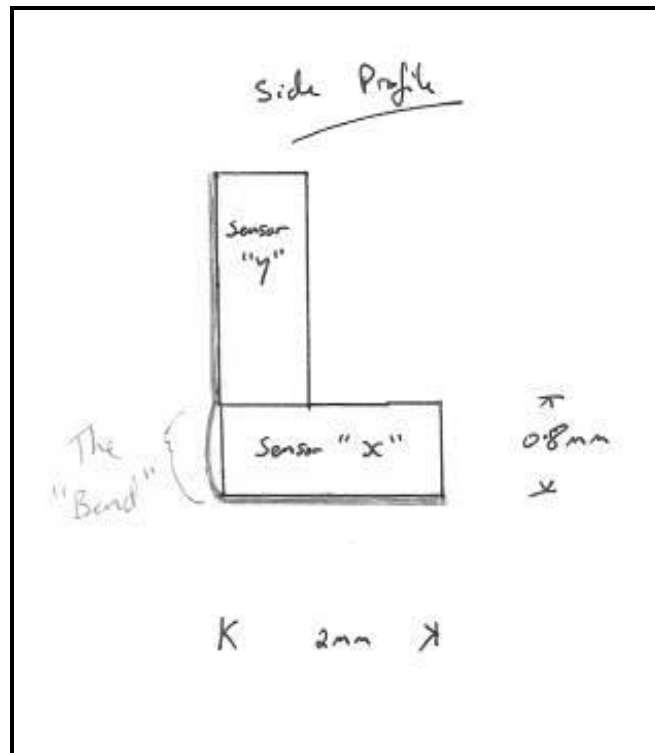


**Figure 5.2:** A sketch showing the side profile of the proposed probe with sensor “y” on the tab at right angle to sensor “x” on the main strip. The “bend” highlighted in green is the site where the tab is bent at right angle and it contains copper wires that connect between the tab and the main strip.

The total number of Hall Effect sensors needed for the new probe was  $26 \times 2$  (main strip and ears) = 52 sensors. The spacing between sensors was reduced to 7 mm from the previous 10 mm resulting in a recording length of 180 mm instead of the previous 120 mm. The new design did not compromise the width of the flexible board which remained at 3 mm ensuring that the diameter of the probe was not larger than the previous probe, thus maintaining patient comfort during intubation.

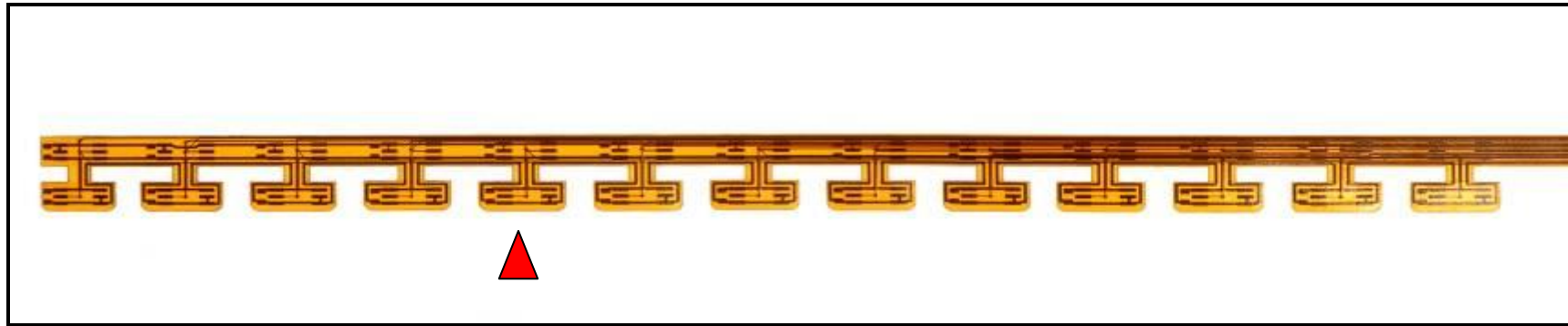


**Figure 5.3:** Manufactured flexible circuit board without any sensors yet populated. One of the tabs is highlighted (red triangle).



**Figure 5.4:** Flexible circuit board populated with sensors. A sheath of silicone tube (AlteSil™, Altecweb.com Ltd, UK) is also shown to demonstrate how the tabs are bent onto the main strip (red triangle). Araldite epoxy adhesive (RS Components Ltd, UK) is used as bonding agent between the sensors.

After finalising the design, the circuit boards were manufactured by a private company (Stevenage Circuits Ltd, UK) (Figure 5.3), and the population of sensors was performed by an electronic assembly company (Newbury Electronics Ltd, UK) (Figure 5.4). The final populated circuit board was then coated with a medical grade high tensile strength silicone tubing similar to the one used for the 2-D prototype probe (AlteSil™, Altecweb.com Ltd, UK). However, the bore of the tube was larger at 3.5 mm. Even though the width of board (3 mm) remained the same, bending of the sensors caused the diameter become larger. However the larger bore was compensated by a thinner outer wall (0.5 mm) to achieve a final outer diameter of 4.5 mm (compared to 4.8 mm for the prototype probe).

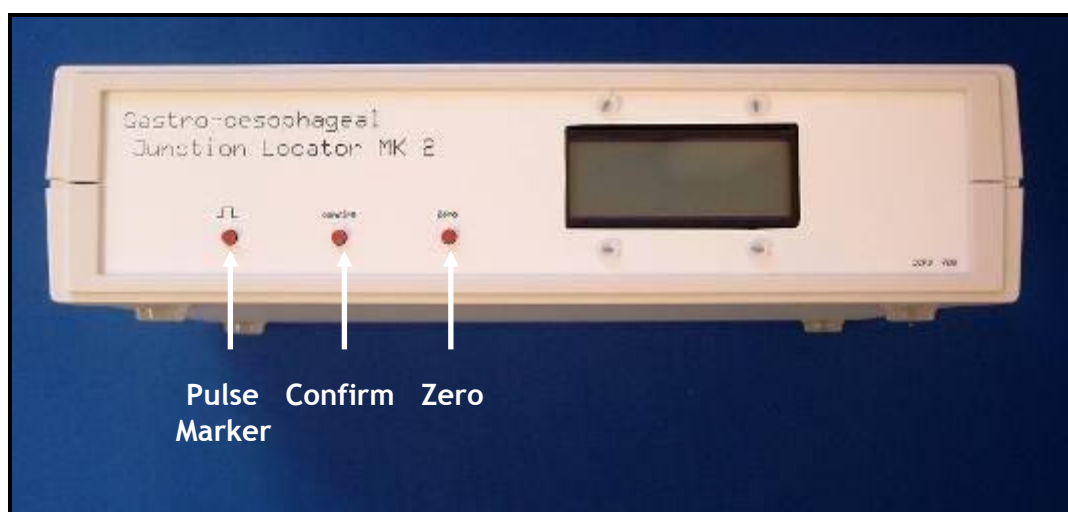


**Figure 5.5:** The front interface of the microprocessor unit. The LCD panel displays the position and signal strength of the magnet. The “zero” button is to zero the device without any magnet nearby. The “pulse marker” button generates a pulse as an output voltage. Both buttons only have an effect if pressed together with “confirm” button to avoid accidental press.

This device was also compliant to electrical safety guidelines and International Organization for Standardization (ISO) certified (BS: EN 60601-1:2006) as previously described for the 2-D version (section 3.2.3.2). The probe was connected through wires to a new microprocessor unit (Figure 5.5 and 5.6). The design of the interface was similar to the original probe except

for changes in the microchip and software which allowed processing of more sensors, and the unit was connected to the Polygraf™ machine with its output displayed and stored using the PolygramNET™ software.

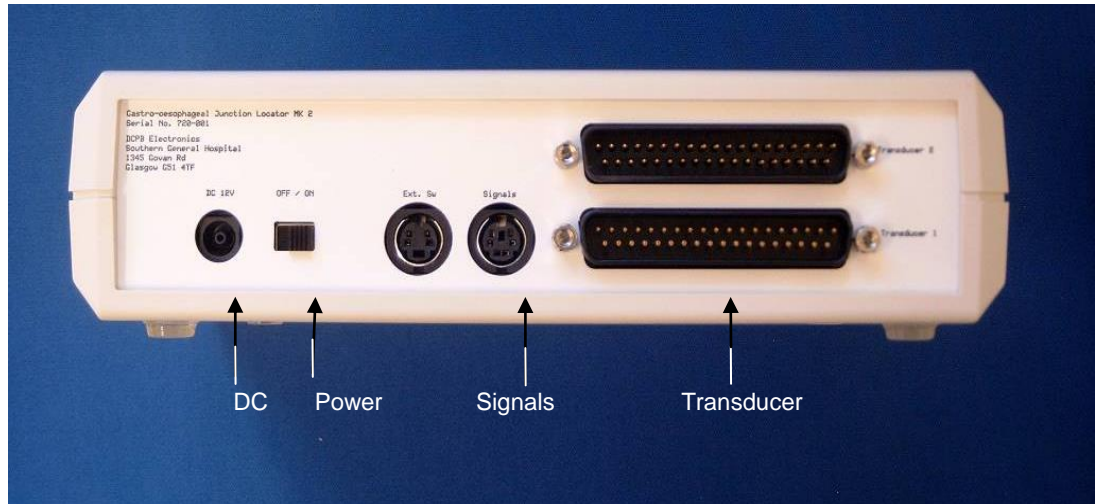


**Figure 5.6:** The back interface of the microprocessor unit. It contains sockets for power supply, devices and the on/off switch.

The two outputs from the system consisted of position (in mm) along the length of the probe with a range of 0 to 180 mm, and signal strength (in millivolts or mV) with a range of 0 to 880 mV. The probe was calibrated for minimum and maximum working range with the Polygraf™ in a similar manner to that described for the 2-D prototype (section 3.3.3.2).

### 5.2.1.3 Magnet choice and placement

The type, size and grade of magnet, placement of the magnet on the endoclip and within the GOJ were the same as previously described (section 3.3.4.2).

### 5.2.2 A probe with better accuracy

The new probe has been designed to overcome the limitation of orientation with the 2-D probe based upon the results of in-vitro and in-vivo tests. The new 3-D probe was pilot-tested in-vivo to assess its accuracy. This testing

involved 3 healthy volunteers, and the new 3-D probe was found to perform better than the old 2-D probe. Firstly, the loss of signal strength due to the loss of magnet orientation was less of an issue with the new probe (**Figure 5.7 vs. Figure 5.8**).

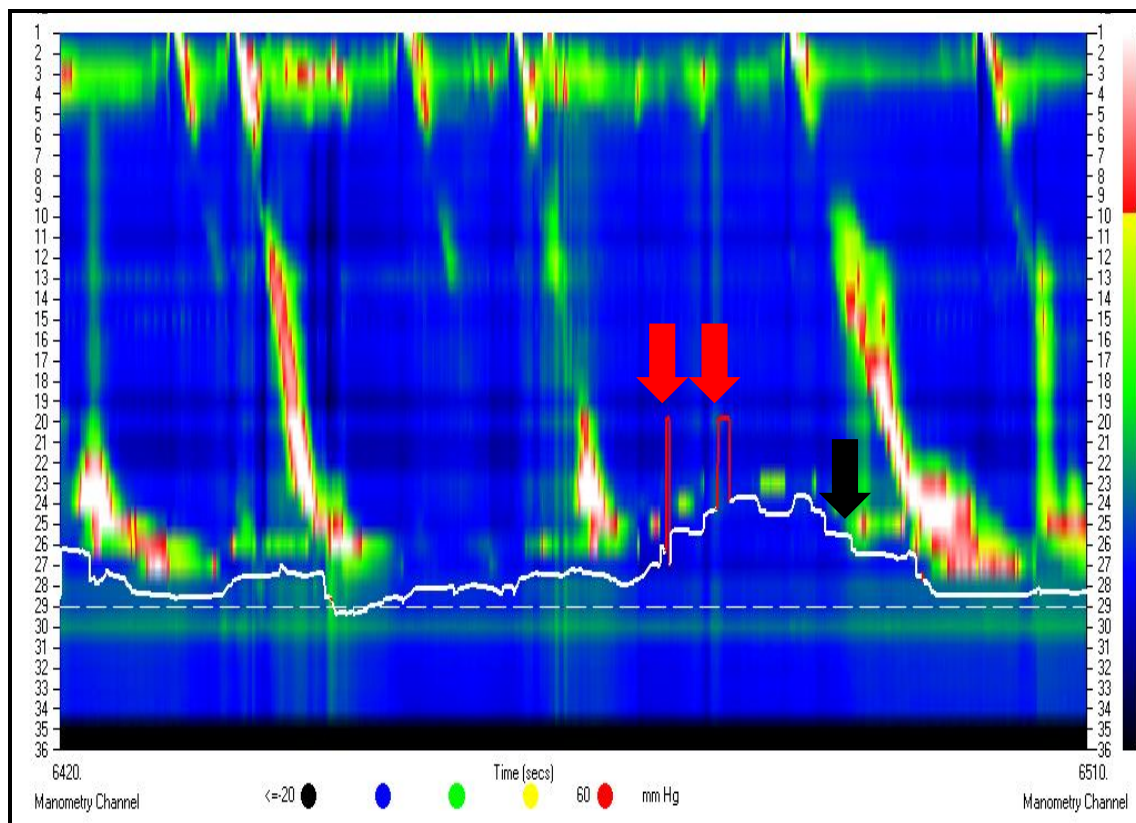


**Figure 5.7:** Colour contour plot with superimposed GOJ movement recorded with the old 2-D Hall Effect probe during a TLOS. The red arrows indicate loss of signal strength and the black arrow indicates an example of a “step”.

Over an hour of continuous recording, the percentage when the signal strength was less than 10 mV was between 2 and 10.7 % with the new probe compared to 3.4 and 91.2% with the old probe. Secondly, the movement of the GOJ was notably smoother and fewer “steps” were seen. One of the problems with the old 2-D probe was the presence of “steps” (**Figure 5.7 - black arrow**), most likely resulting from poor signal strength during movement of the GOJ between sensors. The new 3-D arrangement with sensors at closer interval allowed the new probe to have less noise during movement of magnet between sensors and therefore produced a smoother recording.

Thus, this probe was used for the subsequent clinical studies described in chapter 7.

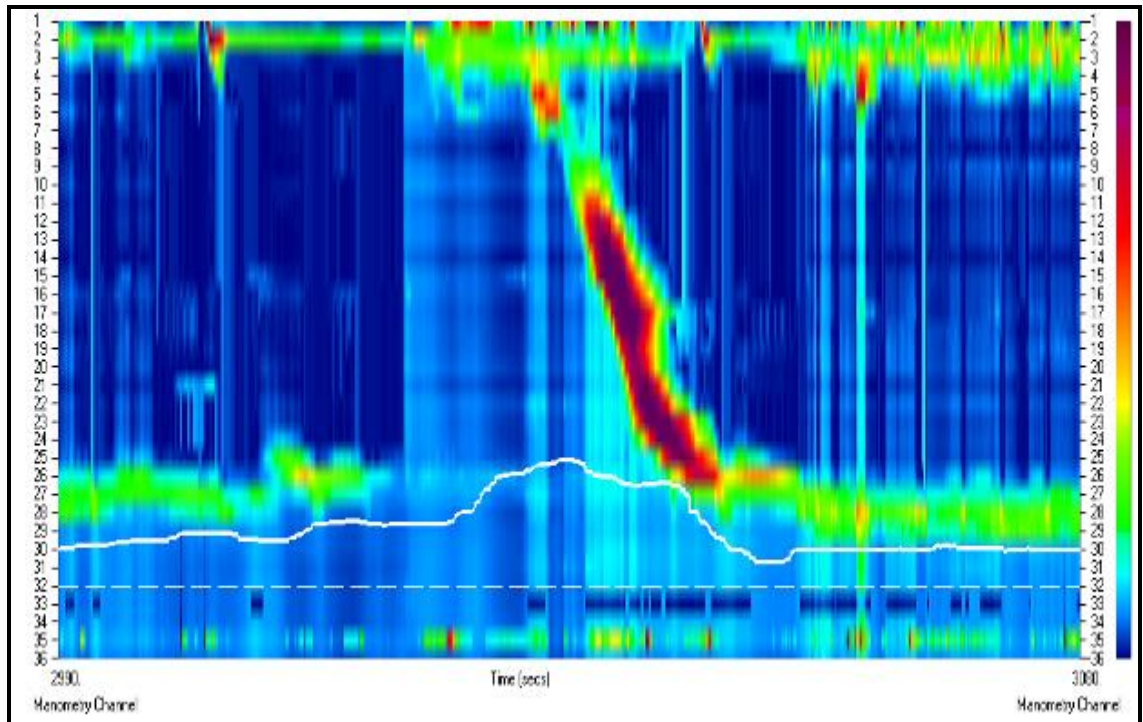


**Figure 5.8:** Colour contour plot with superimposed GOJ movement recorded with the new 3-D Hall Effect probe during a TLOS. Note the smoother recording of the GOJ movement.

### 5.2.3 Problems faced with the new probe

The new 3-D probe utilised a greater number of sensors and therefore the circuitry was more complex. The copper wires connecting the “tabs” to the main circuit strip were found to be stressed during bending despite the thicker circuit board. If any of these wires was broken, there was no possibility to repair the probe. The larger number of sensors resulted in correspondingly, more cables at the soldering end for each circuit. Thus, the bulky end was subjected to stress during handling and could distort or lift the solder from its pad.

The life-span of the 3-D probe was short approximately 10 - 15 uses for one probe, after which some of the sensors stopped functioning. Although, the other sensor could compensate if one sensor broke down, this compromised the orientation detection. Also, during handling of the probe, for example during intubation, it was inevitable that it would result in stress on the bending portion especially at the intubation end of the probe. This coupled with the stress on the bulky connection end resulted in the reduced life span of the probe.

Due to unforeseen damage which was also not repairable, the clinical studies were halted. There were many problems identified to the design of the 3-D probe, including the complex circuitry and it was decided to abandon the manufacture of the same probe again. However, during this time, newer and smaller advanced sensors became commercially available.

## **5.3 NEW GENERATION 3-D GOJ LOCATOR PROBE**

### **5.3.1 Introduction**

A new sensor with true 3-D capabilities was the MEMSIC MMC328xMS (MEMSIC Inc., Andover, USA). This was a 3-axis sensor of the magnetoresistive type. The following section provides an overview of this new sensor including its characteristics and limitations. This is followed by an overview of the circuit design.

### **5.3.2 An overview to the MEMSIC 3-axis sensor**

While the Hall Effect sensors typically sense magnetic field above 10 gauss (High field sensing), magnetoresistive sensors typically sense field between 1 microgauss to 10 gauss (Earth or medium field sensing) (Caruso *et al.*, 1998). There are two types of magnetoresistive sensor namely anisotropic magnetoresistive (AMR) and giant magnetoresistive (GMR). Both types exhibit a change in resistance in response to exposed magnetic field but the GMR resistors exhibit larger (hence the term “giant”) resistance (between 10 -

20%) than AMR (less than 10%). The MEMSIC sensor belongs to the AMR type. AMR resistors are made of permalloy thin film deposited on a silicon wafer. During the manufacturing process, a strong magnetic field is applied to the film to establish a magnetisation vector. An externally applied magnet will cause this vector to rotate and therefore vary its resistance. As the resistor is placed in a Wheatstone bridge, the change in resistance is detected as a change in differential voltage (Figure 5.9).

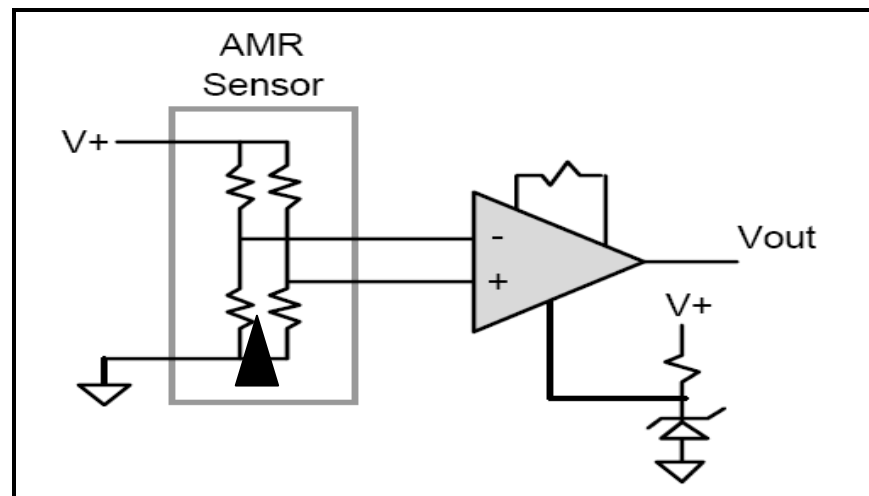


**Figure 5.9:** A graphical diagram of AMR sensor (Caruso *et al.*, 1998). The resistors are placed within a Wheatstone bridge (black triangle) and the changes in resistance with magnetic field are detected as differential voltage ( $V_{out}$ ).

A problem with the MEMSIC AMR sensor is if when a strong magnetic field is being placed near to it, then the magnetisation vector will upset (or “flip”) the polarity and change the sensor characteristics. The sensor can restore the original vector by providing another electrically-generated strong magnetic field. However, this can only occur after removal of the initial strong field. This characteristic has important implication on the design of the new generation probe. Despite this limitation, the sensor itself reacts very quickly to a magnetic field change and is small in size.

The MEMSIC MMC328xMS consists of 3-axis sensor with on-chip signal processing and integrated I<sup>2</sup>C bus, allowing a high speed 400 KHz direct

connection of the device to microprocessor. The sensor, having a size of 3.0 x 3.0 x 1.0 mm can measure a field of  $\pm 8$  gauss. Initial evaluation of the sensor on the bench suggested that the MEMSIC sensor was twice as sensitive as the Hall Effect sensor which we were currently using. While the sensor was sensitive even at distances greater than 15 mm, the output became non-linear (or saturated) at distances closer to 5 mm. This limitation is due to inherent characteristic of the AMR sensor described above (the “flip” phenomenon).

Once saturated, the system cannot be reset unless the magnet was removed. While this was possible on the bench, it will not be possible once the probe is in-vivo. There are two possible ways to overcome this. Firstly, a lower grade magnet may reduce the saturating possibility and secondly, to use a thicker silicone tubing so that the distance between the magnet and sensor is always above 5 mm. In addition, our observation from previous in-vivo studies performed using the Hall Effect probe, showed that saturation of signal strength never happened. There are additional barriers between the magnet and probe including oesophageal secretion and folds which increase the distance between them. Initial testing using the first option, i.e. lower grade magnet, was found to cause borderline saturation when placed next to 0.8 mm thickness tube. Along with thicker tube (without compromising the overall diameter) and the natural barrier in-vivo, the effect of saturation on the new MEMSIC sensor will likely be negligible.

### **5.3.3 An overview to the circuit board design**

The circuit board had been redesigned to accommodate the new MEMSIC sensor. With a width of 3.2 mm and length of 64.9 cm, the single strip flexible circuit board was designed to accommodate 32 sensors separated at 7 mm (recording length of 22 cm) (**Figure 5.10**). The board was manufactured by Stevenage Circuits Ltd, UK, and the sensors populated by Newbury Electronics Ltd, UK.

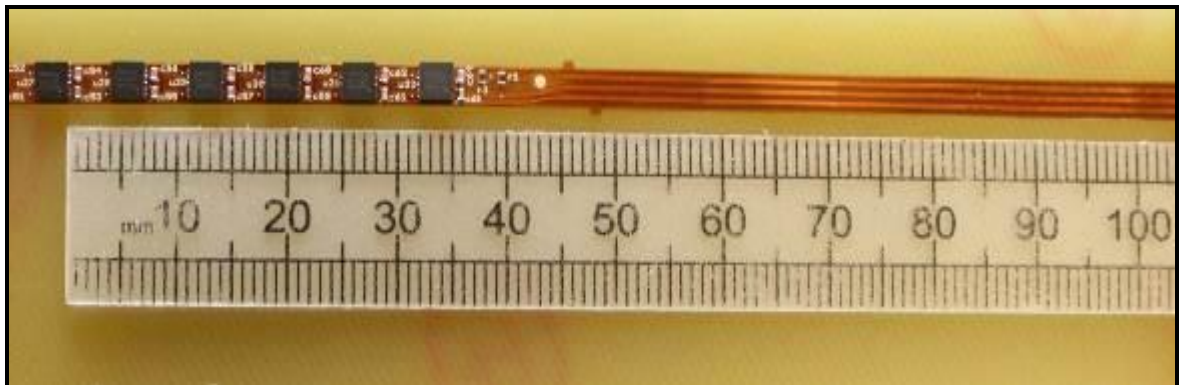


**Figure 5.10:** The new circuit board populated with the MEMSIC sensor

### 5.3.4 Concluding remark

The new MEMSIC sensor provides a true 3-D detection of the magnet. The limitation of saturation due to inherent characteristic of AMR sensor has been overcome. The new generation probe is now in its final stage of development at the time of writing of this thesis.

## 5.4 SUMMARY AND CONCLUSION

There have been impressive advances in the development of high resolution tools allowing detailed measurement of physiology of the GI luminal tract especially the oesophagus. Most involve insertion of catheters straddling the GOJ allowing recording of luminal pH, the movement of fluids and pressure of the LOS. One deficiency is the lack of ability to monitor the location and movement of the GOJ. The current chapter described new techniques to circumvent this deficiency. A small magnet was clipped to the SCJ allowing the position of the latter to be monitored using a series of Hall Effect sensors mounted along the probe. The first prototype was limited by poor sensitivity in certain orientations, but a new 3-D probe overcame this limitation. However, the new 3-D probe had a short life span and a new generation of 3-D probe is currently in its final stage of development. This probe utilises the advanced 3-axis magnetoresistive sensor. The future is promising for this new

technique and will certainly set a new mark in an expanding field of oesophagology.

# CHAPTER 6

## KINETICS OF TRANSIENT HIATUS HERNIA OCCURRING DURING TLOSRS AND SWALLOWING IN NORMAL SUBJECTS

---

6.1 Introduction

6.2 Methodology

6.3 Results: Behaviour of the GOJ during TLOSRS

6.4 Results: Comparing behaviour of the GOJ  
between TLOSRS and swallows

6.5 Discussion: Transient or potential hiatus  
hernia or both?

6.6 Summary and conclusion

## 6 KINETICS OF TRANSIENT HIATUS HERNIA OCCURRING DURING TLOSRS AND SWALLOWING IN NORMAL SUBJECTS

### 6.1 INTRODUCTION

Hiatus hernia is characterised by proximal displacement of the GOJ relative to the diaphragmatic hiatus. The GOJ is normally secured at the diaphragmatic hiatus by the POL which attaches it to the CD. The POL is comprised of an abundance of elastic and collagen fibres which are gradually replaced with adipose tissue in older subjects (Kwok *et al.*, 1999). Hiatus hernia is thought to be due to stretching and damage of the POL and/or weakness of the CD. However, the mechanisms leading to dysfunction of these structures responsible for maintaining the position of the GOJ within the diaphragmatic hiatus are unclear.

Hiatus hernia plays a key role in the pathogenesis of gastro-oesophageal reflux (McColl *et al.*, 2010). The proximal displacement of the GOJ means that the intrinsic LOS and extrinsic compression by the CD are not superimposed and this reduces the competence of the GO barrier. Hiatus hernia also results in impaired oesophageal clearance (P J Kahrilas *et al.*, 1988). It had been thought that hiatus hernia was a permanent abnormality. However, recent studies indicate that hiatus hernia may appear and disappear due to proximal migration of the GOJ (Bredenoord, Weusten, Timmer, *et al.*, 2006; Bredenoord, Weusten, Carmagnola, *et al.*, 2004).

During swallowing, there is a minor degree of proximal migration of the GOJ amounting to 1.5 to 2 cm. However, a recent study with combined fluoroscopy and HRM indicated that more marked migration occurs during TLOSRS of up to 9 cm (median 3 cm) (Pandolfino, Zhang, *et al.*, 2006). In this study, only a limited number of volunteers could be involved and studies cannot be performed over a long period of time due to risk of radiation exposure with fluoroscopy. Studying movement during TLOSRS is difficult as the loss of sphincter tone means that manometric techniques alone are of limited value. The GOJ locator probe is a novel technique developed to allow

reliable and continuous measurement of the GOJ without the risk of radiation associated with fluoroscopy (chapter 3). In this way we have been able for the first time to fully and directly document the movement of the GOJ during TLOSRS over a prolonged period of time.

In the current study of the behaviour of the GOJ during TLOSRS and swallows using the combined techniques of locator probe and HRM is described. Results are then presented and it is divided into 2 separate sections. The first section deals with the behaviour of the GOJ during TLOSRS and the second section compares the behaviour of the GOJ between swallows and TLOSRS. There is a discussion about the novel findings from the study and, finally, the chapter concludes with a summary and the conclusions resulting from this study.

## **6.2 METHODOLOGY**

### **6.2.1 Study subjects**

Twelve healthy subjects (nine men; aged 20 - 77) with no prior history of medical consultation for upper GI symptoms and a normal upper GI endoscopy were included in the study. None of the subjects had previous GI surgery or were taking any medications which could affect acid secretion or GI motor function.

### **6.2.2 Magnet placement**

During upper GI endoscopy, a stainless steel endoclip, attached with a small magnet was placed at the GOJ using a clipping device through the working channel of the standard endoscope. Details on the equipment of endoscopy and techniques employed to place the magnet have been given in chapter 2. All subjects who had a magnet placed in their oesophagus were booked to have a chest x-ray at 6 - 8 weeks later to document the clearance of magnet.

### 6.2.3 Study protocol

After the upper endoscopy, the volunteer will attend for another study day fasted for at least 6 hours. An assembly of probes comprising the locator probe (prototype version) and high resolution manometer (diameter 4.2 mm) was passed down through one of the nostril (**Figure 6.1**).

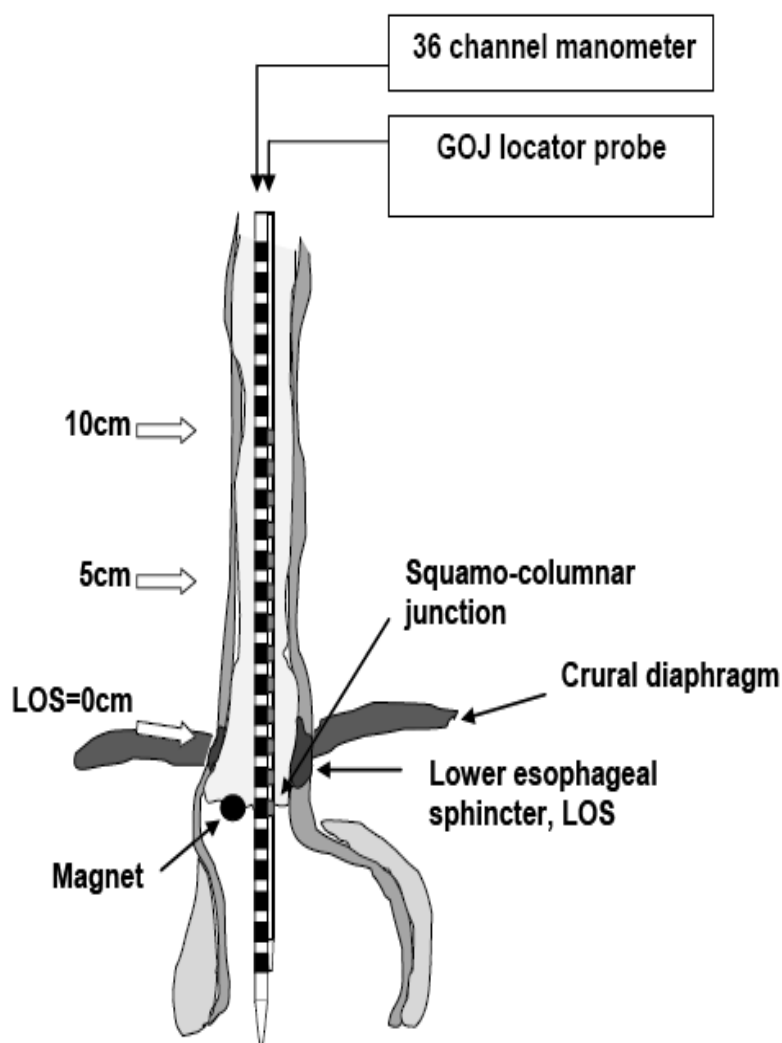


**Figure 6.1:** A schematic diagram of the combined assembly of 36 channel HRM and the GOJ locator probe and its positioning within the oesophagus. The magnet clipped to the SCJ is also shown.

Details on the technique of intubation have been given in section 2.8.3. The GOJ locator probe used in the current study was the first and older version 2-D probe that comprised of two flexible circuit boards populated with 13 Hall Effect sensors on each and spaced at 10 mm apart (recording length 120 mm). Technical details on the 2-D locator probe (including calibration and data extraction) have been described in chapter 2 and 3. A solid-state HRM probe with 36 circumferential sensors spaced at 1-cm intervals (outer diameter, 4.2 mm) was employed alongside the locator probe (Sierra Scientific Instruments Inc., USA). Again detailed technical description of this HRM system has been given in chapter 2. An additional linear correction was applied to the collected data to compensate for baseline drift, a result of thermal effects on the sensors.

Most importantly, the combined assembly was positioned to ensure the locator probe would detect the position of the GOJ at its distal end during quiet respiration and, therefore, allowed detection of the large GOJ migration. In addition, the manometer was positioned to record from the hypopharynx to the stomach. For subjects to adjust to the presence of probes, 10 minutes of accommodation in a sitting position was allowed. There were 3 - 5 attempts of 20 ml water swallows and 3 - 5 attempts of standard bolus swallows (mini croissant). This was followed by a standard 400 ml liquid meal which provided 600-calorie (Fortisip, Nutricia, UK). The recording continued over 90 min postprandially of which at the end, the 3 - 5 attempts of 20 ml water swallows and bolus swallows were repeated. A respiratory pad (Respsense, Medtronic, USA) which connected to the Polygraf® machine (Medtronic, USA) was applied to the abdomen below the xiphisternum. To check for synchronization between the three systems, a tap was sent to both respiratory pad and manometer at the beginning and the end of study to create a matching signal.

All subjects who had a magnet placed in their oesophagus were booked to have a chest x-ray at 6 - 8 weeks later to document the clearance of magnet.

## 6.2.4 Defining parameters for TLOSRS and swallows

### 6.2.4.1 Manometric parameters for TLOSRS and swallows

The TLOSRS were first identified from colour contour plots of high resolution manometry using the software, Manoview® Analysis Version 1.0 (**Figure 6.2**). Supportive characteristics (duration of LOS relaxation, after-contractile events, common cavity and LOS migration) might be used during initial identification of TLOSRS using HRM. These have been previously described in chapters 1 and 2. All identified TLOSRS from HRM were assessed using Holloway's criteria (Holloway *et al.*, 1995). To ensure reliability and consistency in diagnosis, two independent clinicians, who were experienced in TLOSRS, were asked to identify TLOSRS from HRM tracings and Holloway's criteria of all recruited healthy volunteers. Calculated agreement was expressed in %. Only agreed TLOSRS were included for analysis.

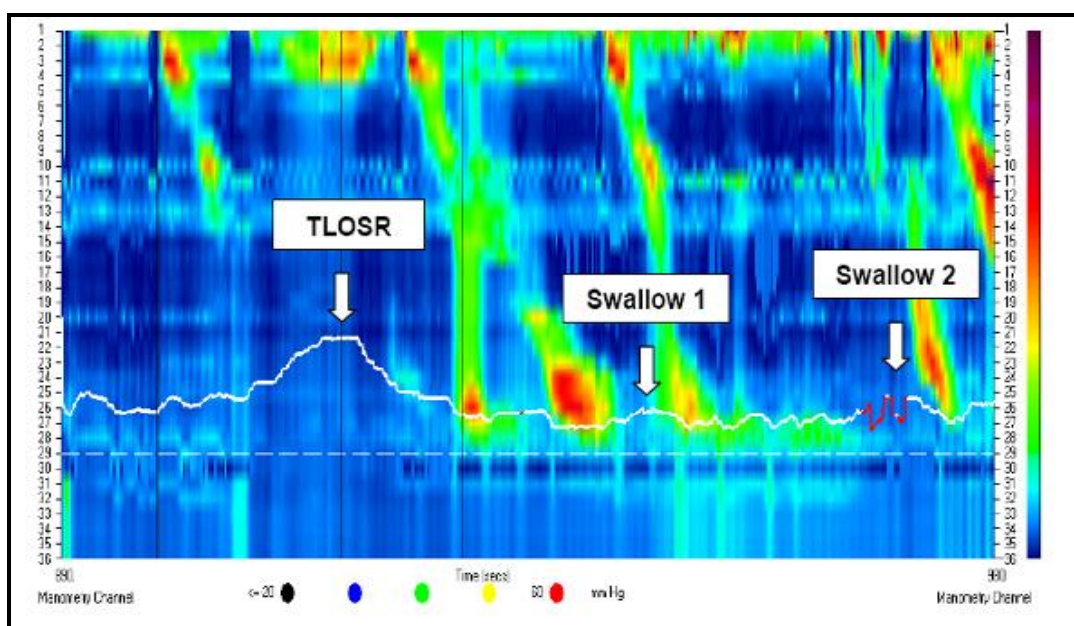


**Figure 6.2:** High resolution colour contour display of combined data from the locator probe and manometer in a 90s frame. The thick white line is the movement of the GOJ recorded with the locator probe. An example of TLOSRS and two examples of swallows are shown. In swallow 2, the red-coloured line indicates a loss of position as a result of poor magnetic field strength.

Similar to TLOSRS, normal swallows were initially identified visually from the colour contour plot of HRM and then assessed in greater detail (**Figure 6.2**). Due to the high frequency of normal swallows per hour, only one swallow was randomly assessed for each 90 s frame of manometric recording. Each swallow had its onset measured at the start of UOS contraction or the start of upstroke if viewed using the conventional manometric tracing. The other characteristics of a swallow included a fall in LOS pressure with an early rapid phase followed by a slower decrease with a relaxation rate  $\geq 1$  mmHg/s, a nadir pressure  $\geq 2$  mmHg, duration from onset to complete LOS relaxation of less than 7 s, total duration of complete LOS relaxation  $< 10$  s and did not occur in proximity to a TLOSRS. All identified swallows were matched with their GOJ movement from the Hall Effect probe. Swallows having poor tracings were excluded from analysis.

#### **6.2.4.2 GOJ migration parameters for TLOSRS and swallows**

Data were recorded, combined, displayed and points of interest selected as described earlier (Chapter 2). All identified TLOSRS were then matched to their GOJ movement as recorded by the locator probe. The events prior to TLOSRS (whether isolated or preceded by swallows) and after-contraction events were also identified.

GOJ migration during TLOSRS was characterised by initial proximal or orad-directed movement from its baseline into a peak. This was followed by an aborad-directed or descent movement to baseline (**Figure 6.2 and 6.3**). The parameters that characterised the movement of the GOJ during TLOSRS were amplitude, duration and velocities for phases A to D (**Figure 6.3**). The definitions for these parameters were given in chapter 2. Velocities from each different phases of migration were derived using the mathematical modelling technique, also described in chapter 2.

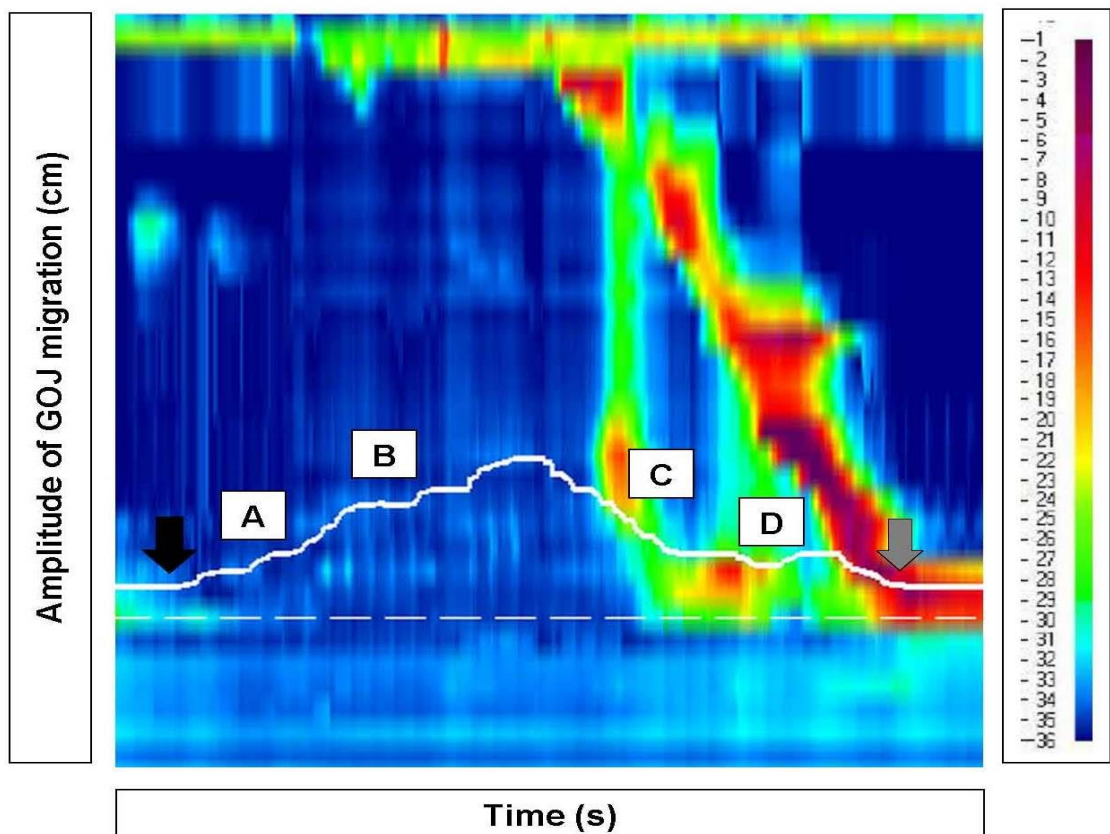


**Figure 6.3:** High resolution contour display of combined data from GOJ locator probe and HRM. The thick white line represents the movement of the GOJ recorded with the GOJ locator probe. The black and grey arrows indicate the start and end of the GOJ movement respectively. Alphabets' A, B, C and D indicate phases A, B, C and D respectively.

The behaviour of GOJ migration for a normal swallow was similarly characterised by an upward movement from baseline to a peak followed by a downward movement to baseline (**Figure 6.2 and 6.4**). The definitions for amplitude and duration of GOJ migration during a normal swallow were similar to a TLOS. In contrast to TLOS, there were no different phases observed during proximal migration of the GOJ and its descent in a normal swallow.

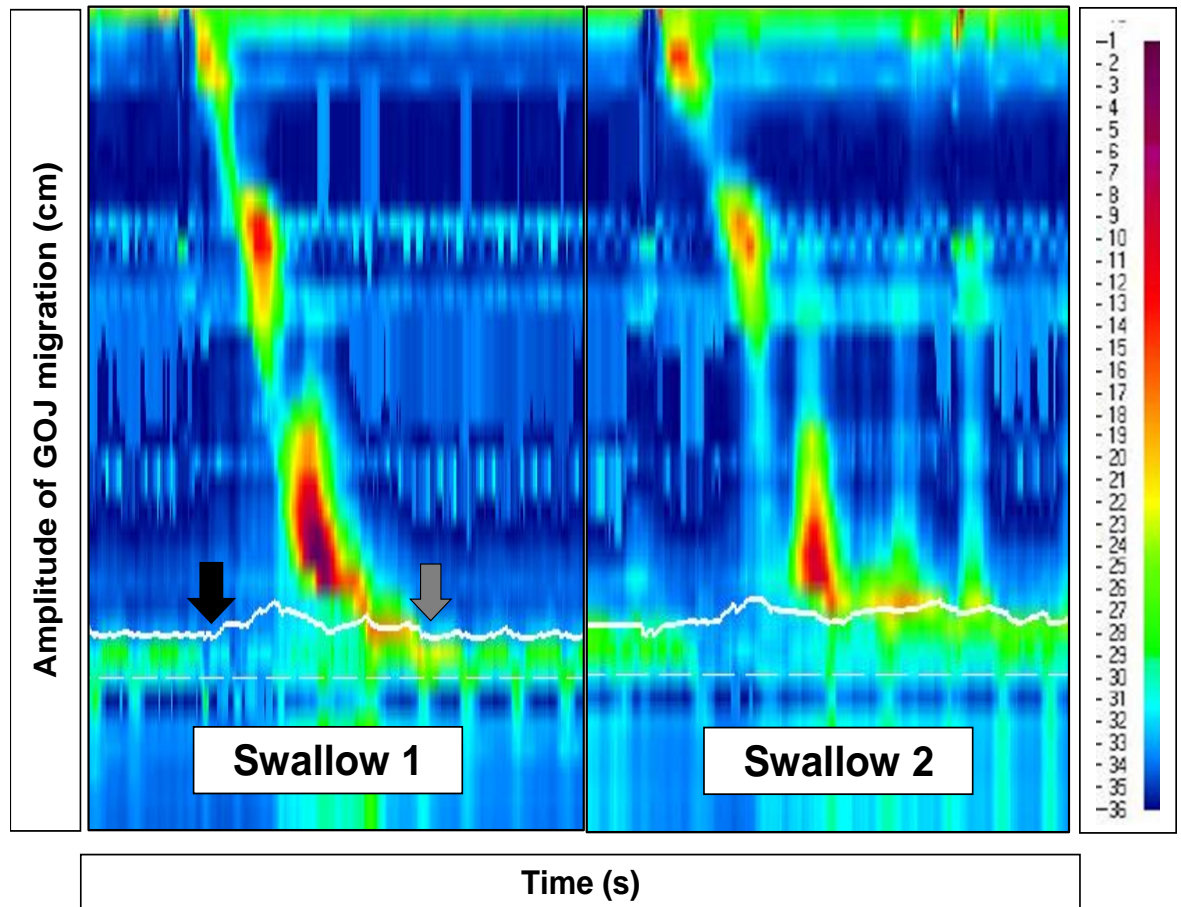


**Figure 6.4:** Two examples of GOJ movement during swallows are shown. The black and grey arrows in swallow 1 indicate the start and end of the GOJ movement respectively. No different phases are observed in normal swallows, unlike in TLOSRS.

### 6.2.5 Statistical analysis

The median with its inter-quartile range (IQR) for each of the studied characteristics were determined for all analysable events. The Wilcoxon rank sum non-parametric test was used to test for differences in the GOJ migration characteristics between TLOSRS and swallows. Correlation between median velocities of different phases and median peak amplitude of GOJ migration during TLOSRS in 12 individuals was performed using the Pearson correlation test (coefficient,  $r$ ). To determine variability between individuals in the characteristics of GOJ migration, the mean centered coefficient of variation (CV) was calculated. This has been described in section 2.13. Receiver operating characteristic (ROC) curve analysis was performed to

compare the reliability of GOJ migration parameters against the manometric parameters in characterising TLOSRS from swallows. The detail on this test is described in section 2.13. Significance for all statistical tests was set at  $P$  value  $< 0.05$ .

## 6.3 RESULTS: BEHAVIOUR OF THE GOJ DURING TLOSRS

The inter-observer agreement for identification of TLOSRS was 88%. There was a total of 71 TLOSRS identified from manometry, but only 64 of these were analysable for GOJ migration. The events which were not analysable resulted from poor tracings due to poor signal strength of magnet position.

### 6.3.1 LOS relaxation during TLOSRS

The medians for nadir pressure (referenced to gastric pressure) and duration of complete LOS relaxation during TLOSRS were 0.9 mmHg (IQR 1.1 mmHg) and 16.8 s (IQR 7.4 s) respectively (Table 6.1). 68.8% (44/64 events) of TLOSRS were preceded by swallows and the rest were isolated.

**Table 6.1:** Characteristics of LOS relaxation during TLOSRS and swallows

Parameters Median (IQR)	TLOSRS	Swallows
Duration of LOS relaxation (seconds)	16.8 (7.4)	4.0 (1.8)
Nadir pressure (mmHg)	0.9 (1.1)	1.6 (4.6)

Median values (IQR) are shown; the nadir LOS pressure is referenced to gastric pressure

### 6.3.2 Behaviour of GOJ migration during TLOSRS

The median amplitude of GOJ migration was 4.3 cm (IQR 2.0 cm) and the median duration of GOJ migration was 23.6 s (IQR 8.8 s) (Table 6.2). GOJ migration started significantly later than LOS relaxation with a median time interval of 1.1 s (IQR 1.7 s),  $P = 0.01$ . Return of the GOJ to its original position was completed a median of 3.8 s (IQR 1.0 s) later than the start of return of LOS tone during TLOSRS,  $P < 0.001$ .

**Table 6.2:** Characteristics of GOJ migration during TLOSRS and swallows

Parameters Median (IQR)	TLOSRS	Swallows
Duration of event (seconds)	23.6 (8.8) <sup>#</sup>	7.9 (3.9)
Amplitude of proximal GOJ migration (cm)	4.3 (2.0) <sup>#</sup>	1.2 (0.8)
Velocity of proximal GOJ migration (cm/seconds)	Phase A: 0.3 (0.4) Phase B: 0.7 (0.4) <sup>#</sup>	0.3 (0.2)
Velocity of GOJ descent to its baseline (cm/seconds)	Phase C: 0.9 (0.3) <sup>#</sup> Phase D: 0.4 (0.4)	0.3 (0.2)

Median values (IQR) are shown; Results for velocities of phases A to D are derived using mathematical modelling

<sup>#</sup>significant difference between TLOSRS and swallows

Mathematical modelling of the GOJ migration indicated the presence of 2 different rates or phases of movement for both the proximal migration and the descent of the GOJ during TLOSRS. The modelling had been described in detail in chapter 2. The proximal migration of the GOJ started off with a slow phase (Phase A) followed by a more rapid phase (Phase B) (Figure 6.3). The median velocity of phase B was 0.7 cm/s (IQR 0.4 cm/s) which was significantly faster than phase A with a median velocity of 0.3 cm/s (IQR 0.4 cm/s),  $P < 0.001$ . There was a significant correlation between the median

velocities of both phase A ( $r = 0.7$ ,  $P = 0.01$ ,  $n = 12$ ) and phase B ( $r = 0.7$ ,  $P = 0.01$ ,  $n = 12$ ) with the median peak amplitude of GOJ migration. The median peak amplitude of proximal migration was however not correlated with the median duration of proximal migration ( $r = 0.2$ ,  $P = 0.6$ ,  $n = 12$ ).

The return (descent) of the GOJ during TLOSRS started off with a rapid phase (Phase C) followed by a slower phase (Phase D) (Figure 6.3). The median velocity of phase C (initial descent) was 0.9 cm/s (IQR 0.3 cm/s) and this was significantly faster than phase D with a median velocity of 0.4 cm/s (IQR 0.4 cm/s),  $P < 0.001$ . Phase C velocity was also faster than phases A and B of the upward movement,  $P < 0.001$ . The median velocity of phase C was strongly correlated with the median peak amplitude of GOJ migration ( $r = 0.8$ ,  $P < 0.001$ ) but this was not seen with phase D (Figure 6.5).

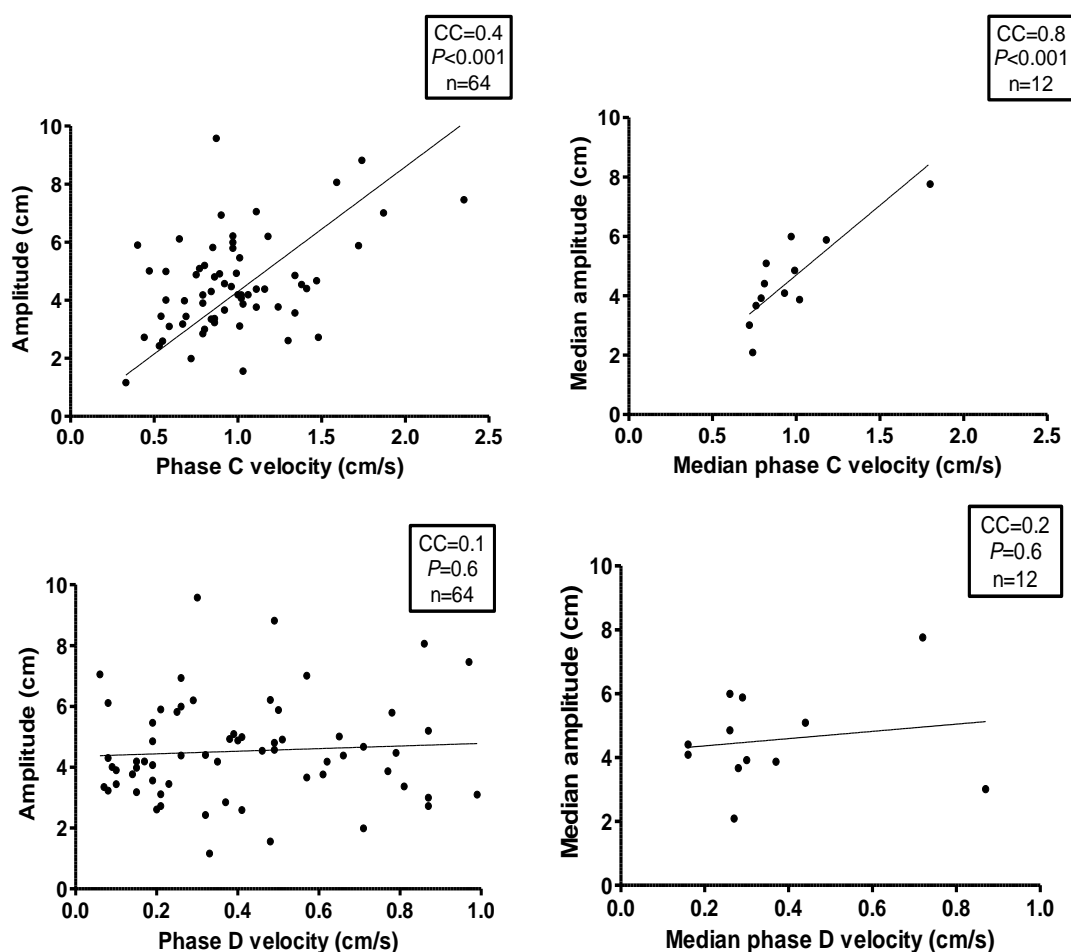


**Figure 6.5:** Correlations between velocities of phases during descent of the GOJ (phases C and D) and amplitude of proximal migration of the GOJ during TLOSRS. CC; Pearson correlation coefficient

### 6.3.3 Subsequent oesophageal contractile events

All TLOSRS were followed by an oesophageal contractile event most of which were secondary peristalsis (44 events or 68.8%) while the rest were primary peristalsis. The commencement of the oesophageal contractile event occurred a median of 3.5 s (IQR 5.4 s) after the GOJ had reached its peak amplitude of proximal migration, and thus between phases C and D (**Figure 6.2 and 6.3**).

The median time of commencement of primary peristalsis after peak GOJ amplitude was 2.3 s (IQR 4.0 s) and this was significantly earlier than secondary peristalsis with a median time of 3.4 s (IQR 3.4 s),  $P = 0.04$ . The peristaltic wave terminated at the GOJ a median of 13.9 s (IQR 8.3 s) after the GOJ had returned to its normal position following the TLOSRS. There was marked variation between the time of return of the GOJ to its original position and the time of the post-TLOSRS peristaltic event reaching the distal oesophagus. The most distal extent of the oesophageal peristaltic contraction was always proximal (range 3 - 24 cm) to the position of the GOJ throughout the GOJ movement during TLOSRS.

An association was observed between the type of contractile event at the end of a TLOSRS and the amplitude of migration of the GOJ during the TLOSRS. The median amplitude of GOJ migration was 4.8 cm (IQR 1.8 cm) when the contractile event was a secondary peristalsis and this was significantly greater than that during primary peristalsis with a median amplitude of 3.8 cm (IQR 1.5 cm),  $P = 0.02$ .

### 6.3.4 Variability between individuals

There was a significantly greater variability between individuals (CV = 24.8%) in the amplitude of GOJ migration than within individuals (CV = 14.7%),  $P < 0.001$  (**Table 6.3**). In contrast, a greater variability within individuals (CV = 29.9%) was seen in the duration of GOJ migration than between individuals (CV = 14.8%),  $P = 0.06$ .

**Table 6.3:** Coefficient of variations (CV) between and within individuals in different characteristics of GOJ migration during TLOSRS

Parameters	Between Individuals, CV <sub>B</sub> (%)	Within Individuals, CV <sub>W</sub> (%)	Ratio CV <sub>W</sub> /CV <sub>B</sub>	<i>P</i> value
Amplitude of GOJ migration	24.8	14.7	0.60	<0.001
Duration of GOJ migration	14.8	29.9	2.02	0.06

The amplitude of GOJ migration shows a greater variability between individual than within individual in contrast to duration which shows a greater variability within individual than between individual.

## 6.4 RESULTS: COMPARING BEHAVIOUR OF THE GOJ BETWEEN TLOSRS AND SWALLOWS

There was a total of 153 swallows identified from manometry but only 127 of these swallows were analysable for GOJ migration. The events which were not analysable were a result of poor tracings from poor signal strength of magnet position.

### 6.4.1 LOS relaxation during swallows

The duration of complete LOS relaxation was shorter in swallows than in TLOSRS with a median of 4.0 s (IQR 1.8 s) (Table 6.1). Nadir pressure during LOS relaxation in swallows was relatively higher when compared to TLOSRS with a median of 1.6 mmHg (IQR 4.6 mmHg) (Table 6.1).

### 6.4.2 Behaviour of GOJ migration during swallows

During a swallow, the GOJ also moved proximally followed by its return to baseline (Figure 6.4). The median amplitude of GOJ migration during

swallows was 1.2 cm (IQR 0.8 cm). The onset of peristalsis was a median 3.7 s (IQR 1.9 s) earlier than the onset of GOJ migration and the peristalsis terminated 2.9 s (IQR 1.9 s) later than the return of the GOJ to baseline during swallows. The onset of GOJ migration was temporally similar to the onset of LOS relaxation but the median duration of GOJ migration at 6.9 s (IQR 3.2 s) was longer than the duration of LOS relaxation of 4.0 s (IQR 1.9 s),  $P < 0.001$ . As explained in chapter 1, CDP is a manometric landmark which correlates temporally with the onset of phrenic ampulla emptying during a swallow. This occurred at a median of 2.9 s (IQR 1.5 s) after the onset of GOJ migration and terminated temporally with the return of the GOJ to its baseline. There was a prominent after-contraction of the LOS after ampullary emptying.

### 6.4.3 Comparing GOJ migration between TLOSRS and swallows

The median amplitude of GOJ migration during swallows at 1.2 cm (IQR 0.8 cm) was significantly less than with TLOSRS at 4.3 cm (IQR 2.0 cm),  $P = 0.002$  (**Figure 6.6**).

The median duration of GOJ migration during swallows at 6.9 s (IQR 3.2 s) was significantly shorter than during TLOSRS at 23.6 s (8.8 s),  $P = 0.003$  (**Figure 6.6**). With both swallows and TLOSRS the proximal movement and return of the GOJ showed precisely the same temporal relationship to relaxation of the LOS. For both the proximal movement of the GOJ started 1 - 1.1 s after relaxation of the LOS and the return of the GOJ to its normal position occurred 3.8 - 4 s after return of LOS tone. Unlike TLOSRS, the proximal and return movement of GOJ in swallows did not have two distinct phases. Average velocities for swallows were calculated for proximal migration and descent of GOJ separately by dividing the amplitude with the time taken for that phase of movement (**Table 6.2**).

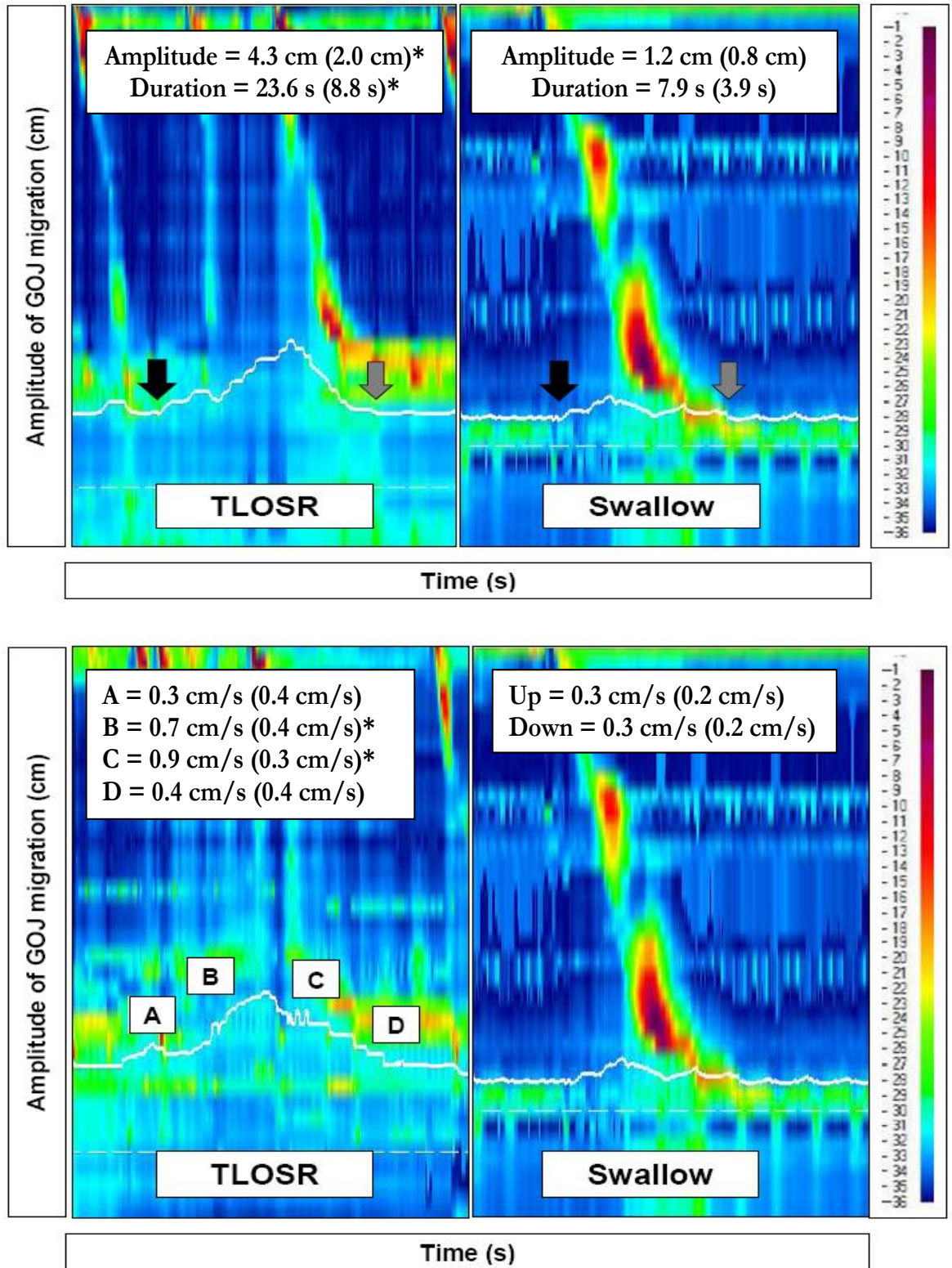


**Figure 6.6:** The movement of the GOJ (thick white line) superimposed on colour contour manometry plot. Examples of characteristics of GOJ movement during TLOSRS (upper) and swallows (lower) are shown. The black and grey arrows indicate the start and end of the GOJ movement respectively. Boxes with alphabets' A, B, C and D indicate phases A, B, C and D that occur during TLOSRS.

\*indicates significant  $P$  value  $< 0.05$ .

The median velocity for proximal migration of the GOJ during swallows at 0.3 cm/s (IQR 0.2 cm/s) was not significantly different from phase A velocity ( $P=0.6$ ) of TLOSRS but it was significantly slower than phase B velocity ( $P=0.002$ ) (Figure 6.6). The median velocity for return movement of the GOJ during swallows at 0.3 cm/s (IQR 0.2 cm/s) was not significantly different from phase D velocity ( $P = 0.2$ ) of TLOSRS but it was significantly slower than phase C velocity ( $P = 0.002$ ) (Figure 6.6).

#### 6.4.4 Comparing locator probe and HRM

Whether the GOJ locator probe could reliably differentiate between TLOSRS and swallows in fashion similar to manometry was not known. This was tested by comparing area under the curve (AUC) for each studied parameter for GOJ migration and LOS relaxation characteristics using ROC analysis (Figure 6.7).

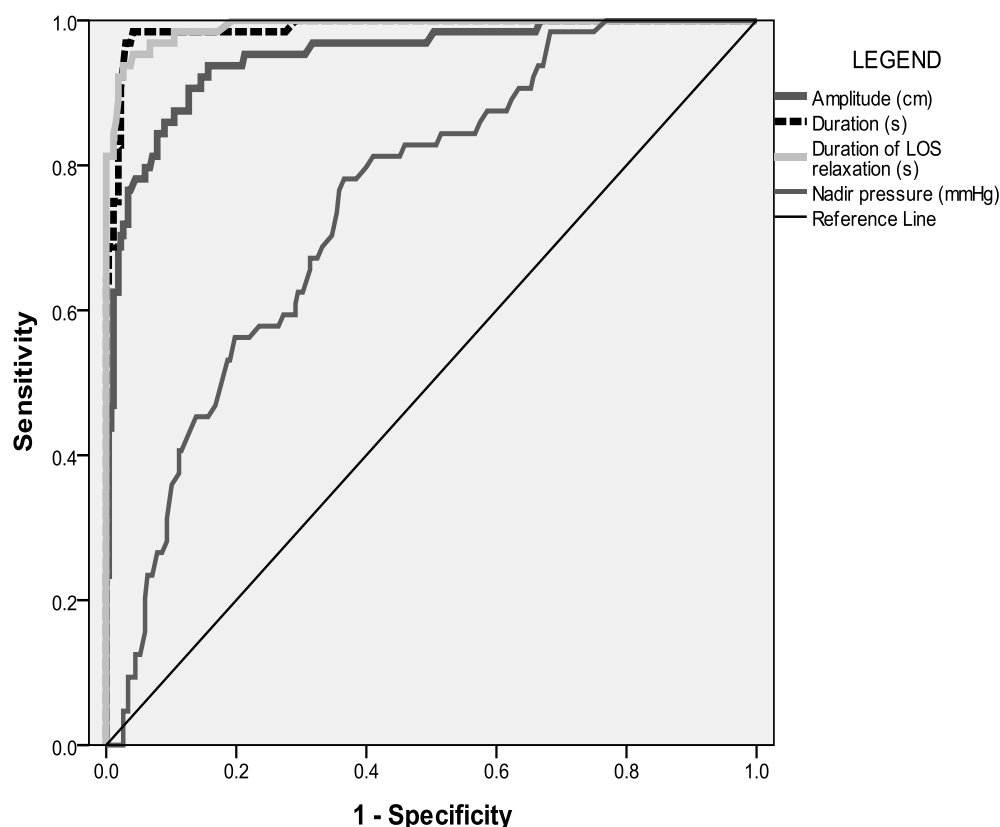


Figure 6.7: ROC curve showing AUCs for GOJ migration and LOS relaxation parameters.

The AUC with 95% confidence interval, cut-off point, sensitivity and specificity for GOJ migration and LOS relaxation parameters to differentiate between TLOSRS and swallows are shown in **Table 6.4**. The GOJ migration parameters of duration and amplitude with AUCs of 0.99 and 0.95 respectively were similar to duration of manometric LOS relaxation with AUC of 0.99 (**Figure 6.7**).

**Table 6.4:** ROC curve analysis of GOJ migration and LOS relaxation characteristics in TLOSRS vs. swallows

Parameters	Area under the curve	95% confidence interval	Cut-off point	Sensitivity (%)	Specificity (%)	<i>P</i> value*
<u>GEJ migration characteristics</u>						
Duration (s)	0.99	0.98 - 1.00	16.8	96.9	97.0	<0.001
Amplitude (cm)	0.95	0.92 – 0.98	2.7	90.6	87.3	<0.001
<u>LOS relaxation characteristics</u>						
Duration of LOS relaxation (s)	0.99	0.98 – 1.00	8.6	95.3	95.1	<0.001
Nadir pressure (mmHg)	0.75	0.69 – 0.81	1.0	87.5	58.6	<0.001

\*significant *P* value <0.05

In TLOSRS where the LOS is not fully relaxed (incomplete TLOSRS), there is appreciable migration of the LOS manifested as movement of the pressure band with HRM. The accuracy for using this observation is not known. The extent of shortening measured using the locator probe was tested against the LOS shortening measured using the HRM during incomplete TLOSRS (**Figure 6.8**).

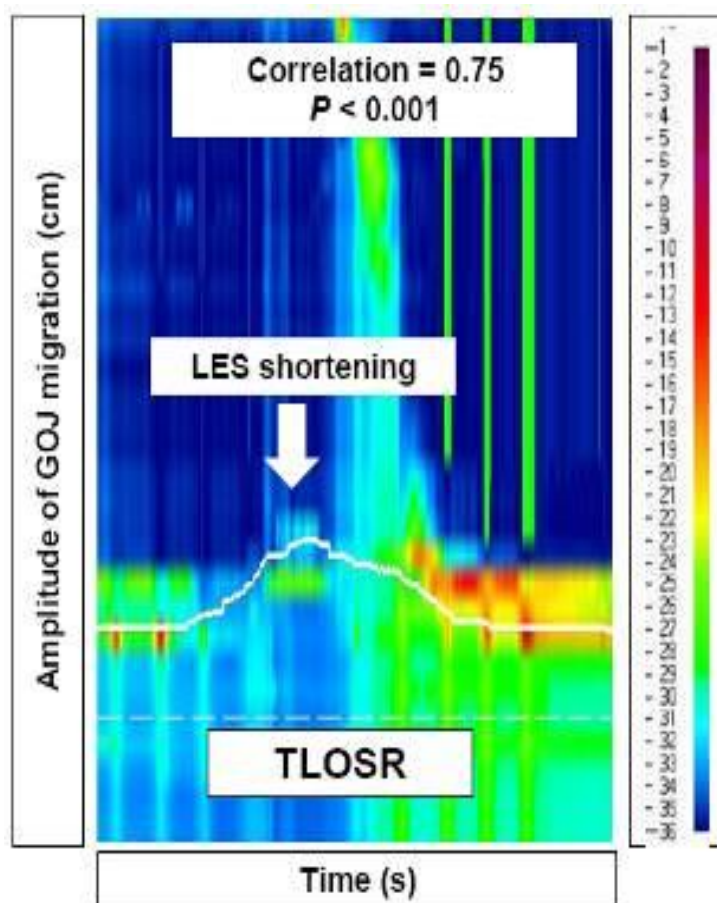


**Figure 6.8:** Comparing GOJ migration and LOS shortening.

Out of 64 TLOSRs, there were 31 TLOSRs with appreciable LOS shortening and GOJ migration. The median LOS shortening was 3.0 cm (IQR 1.0 cm) and the median for GOJ migration was 2.8 cm (IQR 1.4 cm). The Spearman's rho correlation coefficient was 0.75 ( $P < 0.001$ ) suggesting that both measurements were very similar to each other (Figure 6.8).

#### 6.4.5 Clearance of magnet from study subjects

Out of the 12 subjects who had the chest x-ray after 6 - 8 weeks, all except one male showed clearance of the magnet. The latter subject cleared the magnet spontaneously within 24 weeks.

## 6.5 DISCUSSION: TRANSIENT OR POTENTIAL HIATUS HERNIA OR BOTH?

This study confirmed marked proximal migration of the GOJ during TLOSRS (Y. Y. Lee *et al.*, 2012). The median (range) amplitude of proximal migration was 4.3 cm (range 1.6 - 8.8 cm) and this is similar to that reported by Pandolfino *et al.* using fluoroscopy (Pandolfino *et al.*, 2006). GOJ movement was characterised from start to finish and could be correlated to high resolution manometric recordings.

The median duration of GOJ migration during TLOSRS was longer than the duration of complete loss of LOS tone (23.6 s vs. 16.8 s). The onset of GOJ migration occurred slightly later (1.1 s) than LOS relaxation but this could be artefactual due to the 5 mm spacing of the Hall Effect sensors delaying detection of the initial movement (velocity = 0.3 cm/s) by approximately 1 s.

Babaei *et al.* used high frequency intraluminal ultrasound and reported that the thickening of the longitudinal muscle started 1.7 s earlier than the onset of LOS relaxation during TLOSRS (Babaei *et al.*, 2008). They suggested that the upward pulling of the GOJ might trigger the LOS relaxation during TLOSRS and swallows (Dogan *et al.*, 2007; Jiang, Bhargava & Mittal, 2009). Findings from the current study that the commencement of proximal movement and LOS relaxation occurred at a similar time concur with the finding of Pandolfino *et al.* (Pandolfino *et al.*, 2006). The return of the GOJ to its original position occurred 4 s later than the return of LOS tone.

The physiological processes producing the marked proximal movement of the GOJ and then its return to its normal position within the diaphragmatic hiatus need to be considered (**Figure 6.9**). The position of the GOJ is normally maintained within the diaphragmatic hiatus by the POL which attaches it to the CD. During TLOSRS, there is relaxation of the CD as shown by Mittal *et al.* and this will permit the proximal movement of the GOJ (R K Mittal and Fisher, 1990). The active proximal movement will be produced by the pulling effect of the contraction of the longitudinal muscle of the oesophagus (Babaei *et al.*, 2008; Dogan *et al.*, 2007). The explanation for the

initial slow and then later fast phase of upward movement is unclear but the existence of those two phases was also noted by Pandolfino et al. and Babaei et al. (Pandolfino *et al.*, 2006; Babaei *et al.*, 2008). It is possible that the initial slow phase is due to passive shortening followed by relaxation of the CD, and that the more rapid phase is related to contraction of oesophageal longitudinal muscle.

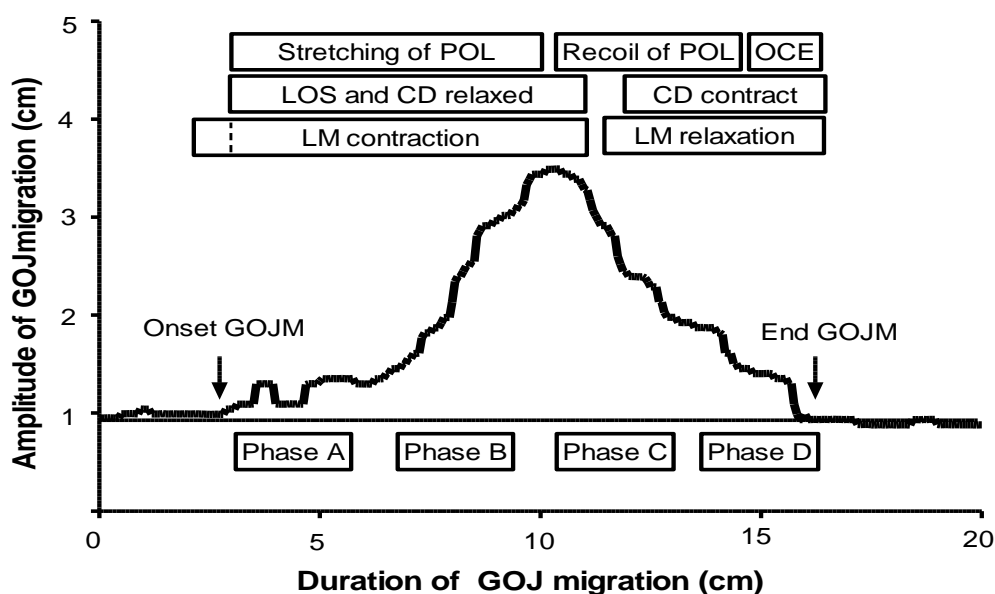


**Figure 6.9:** A summary of physiological processes occurring during the proximal movement and return of the GOJ associated with a TLOS. According to Babaei et al., the LM contraction may have its onset before the start of GOJ migration and LOS relaxation (indicated by shaded line). Similar physiological processes can also be explained for a swallow. Phases A to D indicate the different phases of GOJ movement during a TLOS.

GOJM; GOJ migration, CD; crural diaphragm, LOS; lower esophageal sphincter, POL; phreno-esophageal ligament, LM; longitudinal muscle of esophagus, OCE; oesophageal contractile event

There was a strong correlation between the velocities of upward movement of both phases A and B and the amplitude, but no correlation between amplitude and time to reach peak of proximal movement. This suggests that there are factors controlling the proximal velocity, such as strength of longitudinal muscle contraction, that determine the amplitude rather than the time allocated to that movement.

The return downward movement of the GOJ is particularly important as failure of this process will produce a persisting hiatus hernia (**Figure 6.9**). The downward movement of the GOJ during TLOSRS also consisted of two phases with the velocity of the first being greater than that of the second. The initial descent must be permitted by relaxation of the oesophageal LM after it has completed maximal proximal pulling of the GOJ (Sugarbaker, Rattan & Goyal, 1984; Yamamoto *et al.*, 1998). However there must also be some force or forces pulling the GOJ back down. The initial rapid descent cannot be explained by pulling down by the CD as at this time it is still relaxed as shown by the absence of LOS tone and by previous electromyographic (EMG) studies in both animals and humans (Altschuler *et al.*, 1985; Martin *et al.*, 1992; Liu, Pehlivanov & Mittal, 2002; Mittal, Rochester & McCallum, 1989). The initial rapid descent may be due to elastic recoil of the POL and two of our observations support this. The first is its rapid velocity and the second is the strong correlation between the velocity of this initial descent and the amplitude of proximal movement during TLOSRS. A characteristic of the mechanics of elastic recoil is that the speed of recoil is directly proportional to degree of stretching (Roberts and Azizi, 2011).

Several activities may influence the second and later phase of descent of the GOJ back into the diaphragmatic hiatus (**Figure 6.9**). Elastic recoil of the POL may contribute but to a lesser extent than for phase C due to reduced stretching. Contraction of the CD is likely to be important. We found that LOS tone returned between phases C and D of descent of the GOJ and this is consistent with contraction of the CD which forms the extrinsic LOS.

The return of LOS pressure occurred 4 s before the GOJ completed its descent to its original position within the diaphragmatic hiatus. This may be due to the contraction of the CD restoring LOS tone but then requiring a few seconds to pull the GOJ back to baseline. Alternatively, the earlier return of LOS tone may be due to return of tone in the intrinsic sphincter while the CD (extrinsic sphincter) is mainly exerting an axial downward rather than radial pressure. Whatever the mechanism the earlier return of LOS tone will reduce

the chance of reflux occurring during the downward movement of the GOJ and associated increase in gastro-oesophageal pressure gradient.

It was observed that the amplitude of proximal GOJ movement during TLOSRS was greater when the event was followed by a secondary peristaltic contraction. This is similarly observed in the study by Pandolfino *et al.* where secondary peristaltic contractions were associated with a greater opening of GOJ and reflux (Pandolfino *et al.*, 2006). It is unclear why some TLOSRS are associated with primary and others with secondary peristaltic contraction and to which extent reflux associated with the TLOSRS may contribute to the oesophageal contractile event.

The peak amplitude of GOJ migration achieved during TLOSRS was noted to be more variable between individuals than within individuals (CV 24.8% vs. 14.7%). The magnitude of GOJ migration achieved during TLOSRS is a unique characteristic for an individual. The magnitude of GOJ migration may depend on the elasticity of the POL, height and age of the individual. In contrast, duration of GOJ migration during TLOSRS was noted to vary more within individuals than between individuals (CV 29.9% vs. 14.8%). This suggests that each TLOSRS within an individual may have different duration of GOJ migration. The migration of GOJ is tightly coupled with LOS relaxation via a common neural control mechanism. Therefore duration of GOJ migration can be affected with changes in duration of LOS relaxation or GOJ opening, which in turn can be affected by factors including a change in GOPG and types of contractile event/peristalsis following TLOSRS. There have been no studies on the reproducibility of LOS relaxation parameters between and within individuals.

During swallows, there is also proximal movement of the GOJ and then return to its normal position but the amplitude of this movement is significantly less than that occurring during TLOSRS being 1.2 cm vs. 4.3 cm (**Figure 6.10**). The duration of proximal movement is also less during swallows than TLOSRS at 7.9 s vs. 23.6 s. We compared the average velocities of the movements related to swallows and found them to be similar to those occurring over the same range of movement with TLOSRS (*i.e.* phase A and

D). This is consistent with the movement of the GOJ being controlled by the same process as that occurring during TLOSRS (Pouderoux *et al.*, 1997).

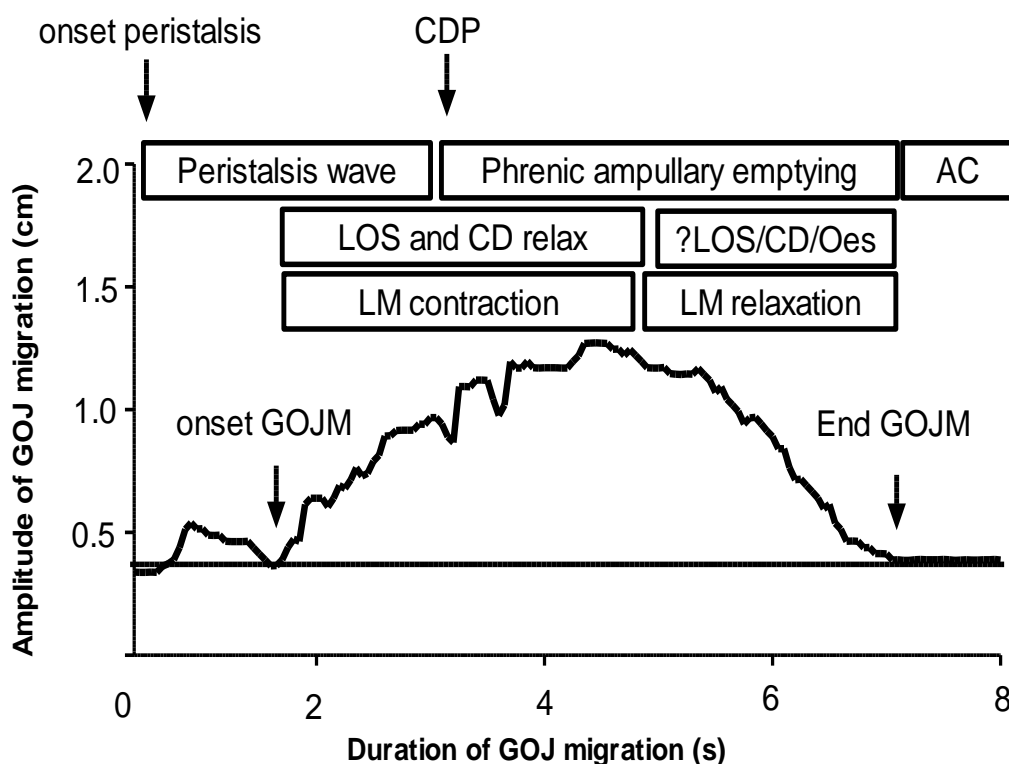


**Figure 6.10:** A summary of physiological processes occurring during the proximal movement of GOJ associated with a swallow. It is not exactly known what contributes to the contracting segment of phrenic ampulla but it may have been the circular muscle of LOS or CD or adjacent oesophageal wall. GOJM; GOJ migration, AC; LOS after-contraction, Oes; oesophageal wall adjacent to phrenic ampulla

It was also observed that the temporal relationship between the movement of the GOJ and relaxation of the LOS was the same with swallows and TLOSRS. For both, the proximal movement of the GOJ started within 1 s of relaxation of the LOS and the return of the GOJ to its normal position occurred 3.8 - 4 s later than return of LOS tone. This suggests that these two processes are intimately linked in both swallows and TLOSRS. This is further evidence of common control of GOJ function in TLOSRS and swallows.

A recent study by Kwiatek demonstrated that there was proximal SCJ migration of approximately 1.5 cm above the hiatal centre at the onset of

phrenic ampulla emptying. The peak amplitude of SCJ migration of 1.6 cm was reached at approximately 25% of ampullary emptying. This is similar to what has been observed in the current studies (**Figure 6.10**). With CDP as the manometric guide for onset of ampullary emptying, this had been shown to occur 2.9 s after the onset of GOJ migration. The termination of ampullary emptying was temporally similar with return of the GOJ to baseline. The emptying process during phrenic ampulla is thought to be aided by POL, CD, LOS and or adjacent oesophageal wall. Dysfunction of this emptying process may potentially contribute to hiatus hernia formation.

The return of the GOJ following its proximal movement during TLOSRS appears to be due to a similar mechanism to that associated with swallowing and again not by peristalsis. The primary or secondary peristalsis wave following a TLOSRS may provide clearance of any reflux occurring during the TLOSRS but there is no association between the timing of these events and return of the GOJ to its original position (Kuribayashi *et al.*, 2009).

What is the physiological purpose of this marked proximal movement? TLOSRS are thought to be mechanisms by which excess gastric air can be vented. It has been shown that simple relaxation of the LOS tone is inadequate to allow opening of the GO barrier due to the flap valve formation. The proximal movement may therefore be a means by which the flap valve is overcome and the GOJ lumen opens in order to allow air to escape. Studies have shown that most episodes of belching occurred during TLOSRS, and many were associated with common cavity (Wyman *et al.*, 1990). Impedance studies showed that gas reflux was found in half of acid reflux episodes during TLOSRS, but that liquid reflux tended to precede the gas reflux in such cases (Sifrim *et al.*, 1999).

The traditional method of recording TLOSRS has been manometry and using the criteria described by Holloway *et al.* (Holloway *et al.*, 1995). The ability to detect TLOSRS by movement of the GOJ versus traditional manometry was compared and found to be similar. The ability to record movement without manometric intubation could allow one, for the first time, to document TLOSRS under more physiological conditions. It was noted a

number of years ago that pharyngeal stimulation may increase the frequency of TLOSRS (Mittal *et al.*, 1992). Current knowledge of TLOSRS is entirely based on intubation studies and therefore the prospect to artefacts produced by this technique.

HRM is less useful for measuring LM shortening in particular during TLOSRS due to a loss of sphincter tone. However, in some TLOSRS without total loss of tone (incomplete TLOSRS) there is an appreciable axial movement of the LOS pressure bands. The amplitude can be measured by determining the difference in height of either border of LOS from its baseline. This axial movement or “LOS lift” is thought to be a result of pulling of the longitudinal muscle. However, its reliability has yet to be fully determined, it is less accurate for small movement < 5mm and furthermore, not all TLOSRS or swallows manifest the movement (Mittal *et al.*, 2012). In the current study, in TLOSRS manifesting LOS shortening, the amplitude of GOJ migration was significantly correlated with LOS shortening. Despite being a less useful measurement in TLOSRS without evident LOS pressure bands, if present, it is an accurate measure of GOJ shortening.

The marked proximal movement of the GOJ during TLOSRS temporarily produces an anatomical situation resembling hiatus hernia. It may also be involved in the pathogenesis of established hiatus hernia. Hiatus Hernia is thought to be due to weakness of the POL and CD. As discussed above these structures must be markedly stretched during the proximal movement of the GOJ during TLOSRS and, over time, they may be damaged, resulting in their failure to return the GOJ to its correct position relative to the diaphragmatic hiatus (Curci *et al.*, 2008). TLOSRS are recognised to be the main mechanism by which acid reflux occurs. They may further contribute to reflux disease by contributing to the development of hiatus hernia. The new technique makes it possible to study this process in a similar fashion to pHmetry and manometry, and it may be a useful tool in furthering the understanding of the pathogenesis of hiatus hernia and reflux disease.

## 6.6 SUMMARY AND CONCLUSION

Proximal displacement of the GOJ is present in hiatus hernia, but it also occurs transiently during TLOSRS and swallows. A detailed examination of the GOJ movement during TLOSRS and swallows in twelve healthy subjects has been presented. The marked proximal GOJ migration during TLOSRS of up to 9 cm represents very severe herniation of the GOJ. The rapid initial return of the GOJ following TLOSRS when the CD is relaxed and its correlation with amplitude suggest it is due to elastic recoil of the POL. The marked stretching of the POL during TLOSRS may contribute to its weakening and the development of established hiatus hernia.

# CHAPTER 7

## CENTRAL OBESITY AND WAIST BELT CAUSE PARTIAL HIATUS HERNIA AND INTRASPHERICTERIC ACID REFLUX IN ASYMPTOMATIC HEALTHY VOLUNTEERS

---

- 7.1 Introduction and aims
- 7.2 Methodology
- 7.3 Results
- 7.4 Discussion
- 7.5 Summary and conclusion

# 7 CENTRAL OBESITY AND WAIST BELT CAUSE PARTIAL HIATUS HERNIA AND INTRASPHERINCTERIC ACID REFLUX IN ASYMPTOMATIC HEALTHY VOLUNTEERS

## 7.1 INTRODUCTION AND AIMS

In the western world, there is a high incidence of adenocarcinoma of the GOJ and cardia region of the stomach compared to that of the rest of the oesophagus and stomach (Tytgat *et al.*, 2004; Gajperia *et al.*, 2009). Adenocarcinoma of the stomach is predominantly the result of *H. pylori* infection (Uemura *et al.*, 2001) and that of the oesophagus, the result of reflux-induced columnar metaplasia and dysplasia (Steven R Demeester, 2009). However, the etiology of the high incidence of adenocarcinoma focused at the GOJ remains unclear.

In Japan and other similar countries, where there is a very low incidence of reflux associated adenocarcinoma, but high incidence of *H. pylori*-associated gastric adenocarcinoma, the incidence of adenocarcinoma at the cardia is only 10% of that of the rest of the stomach (Blaser and Saito, 2002). In contrast, in the U.S. and Western Europe, where oesophageal adenocarcinoma is more common, the incidence of adenocarcinoma at the cardia is greater than that of the rest of the stomach (Brown, Devesa & Chow, 2008; Botterweck *et al.*, 2000). This suggests that in the Western world, the vast majority of these cancers of the cardia are not due to *H. pylori* gastritis and probably related to GOR.

Though there is a strong association between a history of reflux disease and adenocarcinoma of the oesophagus in the Western world, this association is much weaker for adenocarcinoma of the cardia despite epidemiological evidence suggesting that they are likely to be due to reflux. This raises the question as to whether the most distal oesophagus may be subject to damage by gastric acid in the absence of reflux symptoms or traditional reflux disease.

It has been recently reported that in healthy volunteers without reflux symptoms, the length of columnar mucosa lying at the cardia between

oesophageal squamous mucosa and gastric oxyntic mucosa is positively correlated with age and WC (Robertson *et al.*, 2012). It has also been observed that in these asymptomatic subjects, increased WC and associated increased IAP causes gastric acid to penetrate further up into the mucosa within the LOS but without traversing it and producing traditional GOR. This ingress of acid may be inducing columnar metaplasia of the most distal oesophagus and thus predispose to progression to adenocarcinoma at this site.

Adenocarcinoma at the cardia and GOJ is associated with increased BMI and WC (Corley *et al.*, 2008). It is also more common in males (Freedman *et al.*, 2010). Males deposit fat within and around the upper abdomen from an early age, whereas females only deposit fat at this site following the menopause. The earlier expansion of WC in males and its effects on the GOJ might explain the earlier rise in the incidence of these cancers in the former (Derakhshan *et al.*, 2009).

Another lifestyle factor which might be important in the aetiology of junctional cancers is the use of waist belt. Similar to abdominal fat, this also increases IAP. Previous reports dated from 1960s through 1980s had utilised abdominal belt as a form of stress test to assess the function of the lower sphincter (Lind, Warrian, & Wankling, 1966; Dodds *et al.*, 1975; Wernly *et al.*, 1980). Challenges from increased IAP can induce acid reflux especially if the LOS is weak and the abdominal oesophagus is shortened. The response of the LOS to IAP from the application of a belt is somewhat controversial. Some studies have claimed that increases in IAP can buttress the intra-abdominal segment of the LOS without changing the intrinsic LOS tone (Vanderstappen and Texter, 1964). Others have presented evidence which indicated that the increase in intrinsic LOS tone was a physiological adaptive response to the increase in IAP (Cohen and Harris, 1970). Studies performed by Dodds and colleagues have instead found the LOS responses to raised IAP are due to mechanical factors rather than physiologic adaptive response (Dodds *et al.*, 1975). The passive mechanical response of the LOS to IAP has also been shown in a more recent work (DiLorenzo *et al.*, 1989).

The primary aim of studies described in the current chapter was to assess the effect of central obesity and waist belt among a group of asymptomatic healthy subjects on the behaviour of the GOJ during periods of stable sphincter tone or quiet respiration. The other aim was to study the effect of obesity and belt on the behaviour of the GOJ migration during TLOSRS. The current chapter starts with a detailed description of the methodology followed by results. These are divided into several sub-sections based upon the effect of obesity and belt on the structure of the GOJ and its acid exposure. Finally, there is a detailed discussion of results and the chapter ends with summary and conclusion drawn from the results.

## **7.2 METHODOLOGY**

### **7.2.1 Study subjects**

The study subjects were healthy volunteers with no prior history of medical consultation for upper GI symptoms, and all gave informed written consent. None of the subjects had previous GI surgery or were taking any medication which could affect acid secretion or GI motor function. Subjects were included regardless of their *H. pylori* infection status, but those with hiatus hernia (confirmed during upper endoscopy) were excluded. Subjects were recruited with reference to age, gender and WC to achieve two groups defined by normal or increased WC and matched with age and gender. Increased WC (obese group) was defined on entry as > 102 cm in males and > 88 cm in females. Normal WC (non-obese group) was defined as < 94 cm in males and < 80 cm in females.

### **7.2.2 Study design or protocol**

All study subjects attended all five study days described below and the protocol is summarised in the flow chart below (**Figure 7.1**).

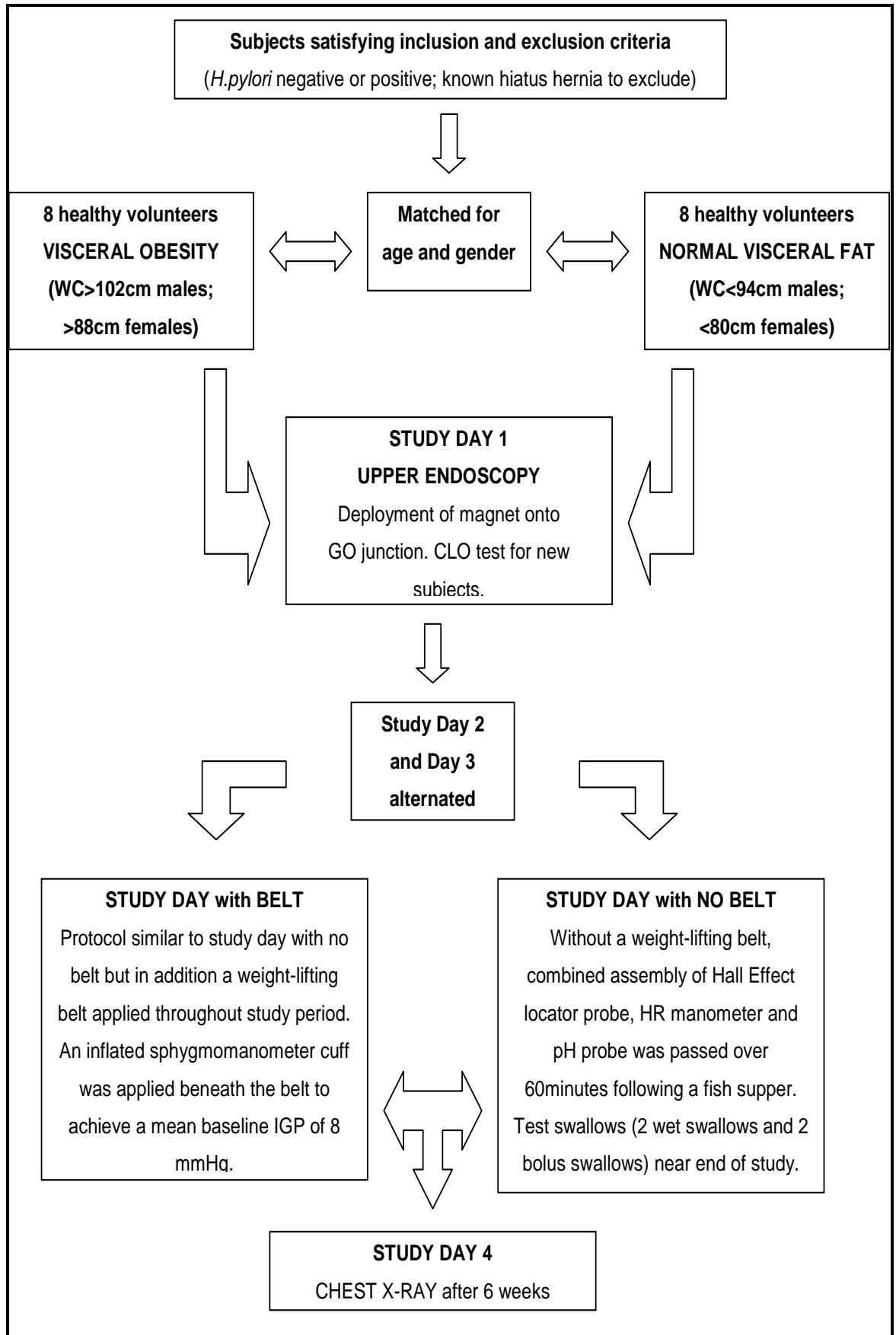


**Figure 7.1:** Flow chart showing the study design

### 7.2.2.1 Study day zero

During initial assessment of study subjects, the following details were recorded using a customised form: age, sex, height, weight, BMI, WC, current medication, history of upper GI symptoms, details of smoking and alcohol consumption. Subjects would be informed in detail regarding the tests conducted throughout the study including upper GI endoscopy examination, magnet placement, passing of probes, use of belt and test meal given over the next 2 - 3 days. Consent would be taken once study subjects understood and decided to participate in the study.

### 7.2.2.2 Study day one

All subjects attended for upper GI endoscopy with either Xylocaine throat spray or 2 - 4 mg IV Midazolam. Detailed descriptions on the preparation and technique for the upper endoscopy test have been previously described in chapter 2. During this examination, any abnormalities were recorded as well as the location of the SCJ and GOJ relative to both the incisor teeth and the diaphragmatic pinch. Biopsies were taken from the antrum and or body region of the stomach to determine for *H. pylori* status. During the endoscopy a metal-clip (Olympus, HX-201UR-135) with a small samarium cobalt magnet (2 x 1mm) attached would be clipped to the SCJ.

### 7.2.2.3 Study day two and three

The subjects reported fasted for two further study days within 2 - 7 days following endoscopy. The combined assembly, consisting of high resolution 36-channel slimline manometer (diameter 2.7 mm), high resolution pH catheter and the GOJ locator probe (3D version), was passed nasally to lie in the oesophagus and stomach (**Figure 7.2**). A respiratory sensor was attached to the chest wall (Respsense, Medtronic) to record the respiratory cycle. The respiratory sensor was also used to provide time synchronisation between the other data channels as previously described (chapter 2).

One of the study days was performed without the application of abdominal belt. Recordings from the inserted assembly were taken fasted for 20 - 30 min and the subjects seated upright on the bed at 60° angle. The preparation and technique for nasal intubation of probes have been described in detail in chapter 2. Subjects would then consume a standardised test meal (fish and chips) over 20 minutes and were asked to eat until full. The fish and chips would be weighted to determine volume using a calibrated weighing scale prior and after completion of meals. Subjects were advised to eat the same amount for each meal to ensure consistency of meal volume. This would be important since the belt constriction effect might reduce the appetite and amount of food taken for some subjects. The postprandial recordings would then be continued for a further 60 minutes.

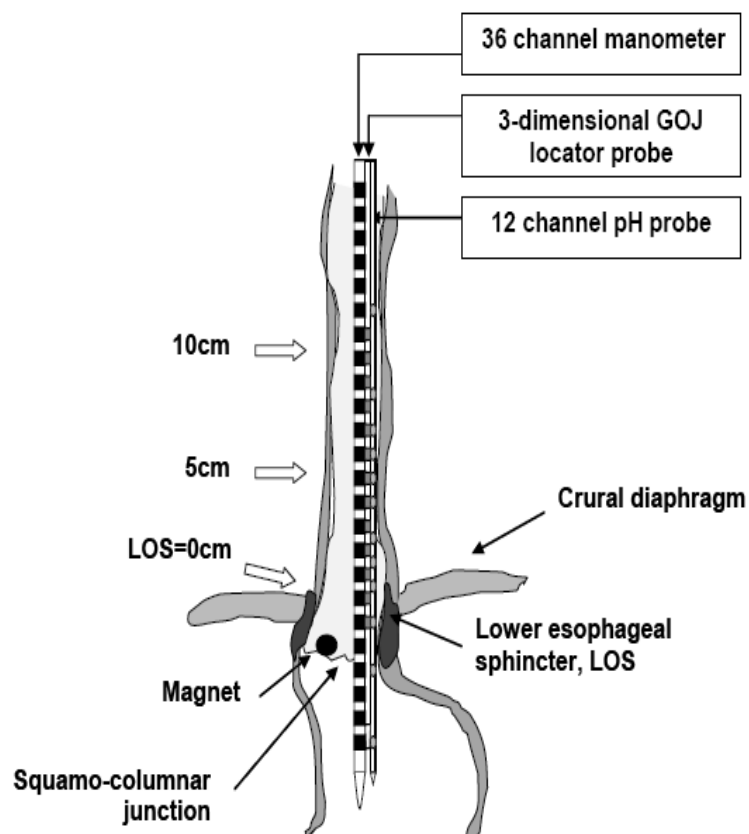


**Figure 7.2:** A schematic diagram of the combined assembly of 36 channel slimline high resolution manometer, 3-dimensional GOJ locator probe and 12-channel pH catheter. The positioning of the assembly within the esophagus and the clipped magnet at the SCJ are also shown.

On the other study day, the above procedure would be repeated except that their IAP would be elevated (by approximately 6 - 8 mmHg) throughout the study period by applying a weight-lifter belt and inflating a blood pressure cuff beneath it (at a constant cuff pressure throughout; approximately 50 mmHg). Pilot studies performed in four subjects had confirmed the efficacy of this method for increasing the IAP. The order between the two study days (with vs. without belt) would be alternated and the order equally distributed between the two groups (obese vs. non-obese). Any upper GI symptoms experienced during the tests would be recorded with respect to time, location, duration and character.

#### **7.2.2.4 Study day four**

Four to six weeks following completion of clinical studies, all subjects would be asked to have a chest x-ray performed. This was to confirm that the magnet placed during the endoscopy had been dislodged.

### **7.2.3 Recording Equipment**

Details of the equipment have been described in chapter 2 (materials and methods) and only brief descriptions for each equipment utilised in the current study is given in the following sections.

#### **7.2.3.1 Three-dimensional GOJ locator probe**

The 3-D locator probe is an improved version utilising Hall Effect technology and allows a more precise monitoring of location of the SCJ and its proximal migration during TLOSRS. Descriptions on its development and technical details have been detailed in chapter 2 and 5. Briefly, this probe consists of one linear circuit board with 26 tabs, each tab having a Hall Effect sensor being placed at right angle to the main board. The linear board with 26 Hall Effect sensors was separated at 7 mm intervals and therefore having a recording length of 180 mm. The probe was sealed with a silicone tube having a bore of 3.5 mm and 0.5 mm wall thickness (Altecweb Ltd, UK). The probe was connected to a microprocessor

unit which was then connected to a Medtronic Polygraf® recorder (Synectics Medical Ltd, UK) (**Figure 7.3**). The position (in mm) of the magnet was recorded in real time with a frequency of 8 Hz and the data was extracted in the ASCII text format using the PolygramNET™ software.

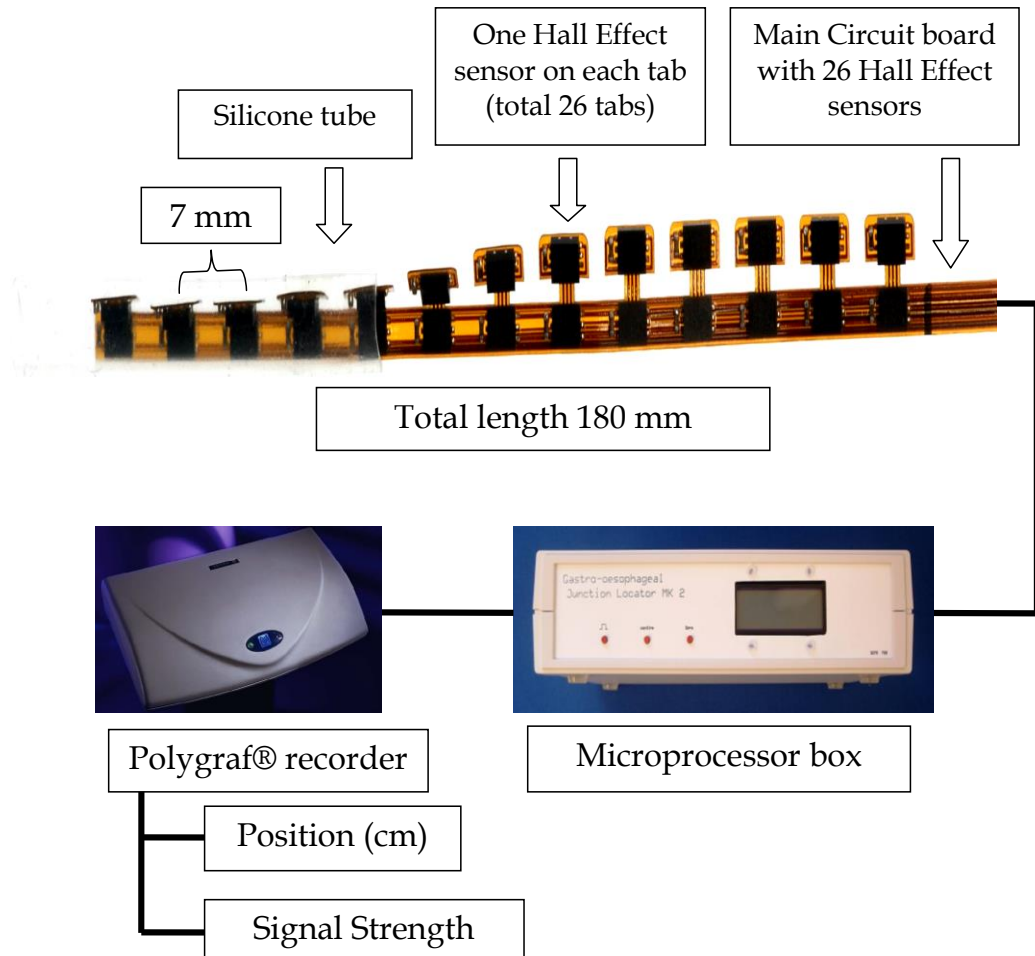


**Figure 7.3:** A schematic diagram of the novel 3-dimensional locator probe

### 7.2.3.2 High resolution slim-line 36-channel manometer

A smaller diameter (outer diameter, 2.7 mm or 7.5 French) solid-state high resolution manometric assembly allowing better patient tolerance was employed (Sierra Scientific Instruments Inc., USA). Recorded data of 100Hz was extracted in text format using the Manoscan Acquisition Version 2.0 software.

### 7.2.3.3 High definition 12-channel pH catheter

This consisted of a custom-made 2.1 mm outer diameter probe with 12 antimony electrodes along its distal end for oesophageal insertion, and an external reference electrode for application to the upper arm (Synectics Medical, Enfield, UK). Raw data were extracted at the end of recording using the PolygramNET™ software at a frequency of 8 Hz and exported in the ASCII text format.

### 7.2.4 Definitions and data analysis

All extracted raw ASCII text data from the three different recording systems was combined into one data file using a custom-made computer program (DrNewData 6, AW Kelman). The data can be displayed as colour contour plot and then analysed using another custom-made program (DrContour6, AW Kelman) (**Figure 7.4**).

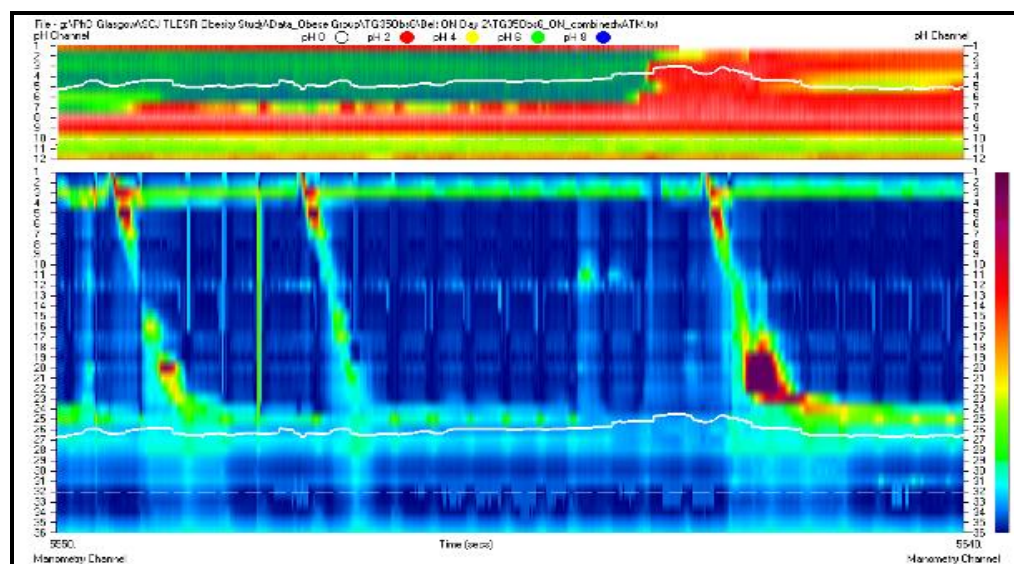


**Figure 7.4:** An example of colour contour plot displayed using a custom-made program. The thick white line represents the position of the SCJ during stable LOS tone and also its migration during swallows and TLOSRs. The upper panel is the colour pH plot and the lower panel is the pressure topography plot.

#### **7.2.4.1 Analysis on manometric characteristics of the GOJ**

Manometric pressures of the GOJ were measured from identified 10-min blocks, one block 10-min before meal and another 10 - 20 min after completion of meal, in each subject. Six inspiratory and six end-expiratory points were randomly selected from a period of stable LOS tone in each 10-min block. Median of these six points was then calculated for each sensor. Intra-gastric pressure or IGP (mmHg) was defined as the median pressure of the first three sensors immediately distal to the lower border of the LOS. Intra-oesophageal pressure or IOP (mmHg) was defined as the median of the lowest three readings between the lower border of UOS and upper border of LOS. Gastro-oesophageal pressure gradient (GOPG) was derived from the difference between IGP and IOP. The peak LOS pressure (mmHg) was measured as the maximum pressure within the high pressure zone of the LOS. This was expressed relative to the atmospheric pressure and IGP.

#### **7.2.4.2 Analysis on relative locations of anatomical structures within the GOJ**

Relative locations of anatomical structures within the GOJ were similarly taken from the 10-min blocks described above. In order to determine the characteristic of location dynamics over time, data were acquired from fasting (Time 0) and five consecutive 10-min blocks (time 1 to 5) during the 60-min postprandial period. All measurements (in cm) of locations were determined from the nares.

The location of upper border LOS was defined as the most proximal position where the pressure fall to within 2 mmHg of IOP. The location of lower border of the LOS was defined as the most distal position where the pressure rose to > 2 mmHg above gastric baseline. LOS length (cm) was calculated on expiration as the distance between positions of upper and lower borders of the LOS. Location of the SCJ was determined from the position of magnet placed on the SCJ during endoscopy. The location of peak LOS was position of the maximum pressure within the high pressure zone of the LOS. PIP was defined as the transition point from abdominal pressure compartment (positive wave deflection) into the

thoracic pressure compartment (negative wave deflection). Both locations of peak LOS pressure and the PIP are physiological markers of position of the diaphragmatic hiatus as previously reported in literatures (Harris and Pope, 1966). Previous studies indicate a greater acidification of the cardia beginning at 30 to 45 minutes after meal (Clarke *et al.*, 2009). This acidification is a potential source of acidic reflux.

#### **7.2.4.3 Analysis on migration of the GOJ during TLOSRS**

TLOSRS were identified using a combination of high resolution colour contour plot, Holloway's criteria and a typical pattern of proximal migration of the SCJ. Definitions for amplitude, duration and velocities for different phases of migration (phase A to D) have been described in chapter 2.

#### **7.2.4.4 Analysis on acid exposure within the GOJ**

The mean pH was calculated for each of the 12 pH sensors during fasting (15 min before meal) and postprandial period (between 30 and 60 minutes after meal). These mean values were examined for minimal change in acid exposure defined as a drop in mean pH of at least 1 unit from proximal to distal. The index sensor recording the first mean pH drop was the pH transition point and acid exposure at this location was examined in detail to identify the mean % of time pH < 4. In addition, acid exposure within the GOJ was determined at the following regions: 1) at the traditional site 5 cm above upper border of the LOS 2) all sensors located between pH transition point and traditional site 3) at pH transition point and 4) sensors below the pH transition point. Short segment acid reflux was considered present if sensors above the index sensor and below traditional site were recording a mean percentage of time pH < 4 between 4 and 30%.

#### **7.2.4.5 Analysis on mechanism of short segment acid reflux**

The percentage of TLOSRS with evidence of acid reflux, defined as acid exposure  $\leq$  pH of 4, that remained above the SCJ during its proximal migration was

calculated. Acid clearance time was the duration (in seconds) taken to clear acid reflux associated with TLOSRS, with clearance defined as pH > 4 immediately above the location of the SCJ. The number of swallows needed to clear the acid reflux was also recorded.

### **7.2.5 Statistical analysis**

All data were presented as mean (SEM) unless otherwise specified. The effect of “central obesity” was assessed by comparing obese (n = 8) vs. non-obese (n = 8) groups, both without application of belt. The effect of “waist belt” was assessed by comparing entire group (n = 16) with and without belt. The effect of “waist belt” was also assessed in obese subjects only, with and without belt (n = 8). Comparison between groups defined above was tested using related-sample and independent-sample t-test. Significance for all statistical tests was set at *P* value < 0.05.

## **7.3 RESULTS**

Sixteen healthy volunteers with a mean age of 37.8 years (12.1 years) were included. Eight of them were “obese” with a mean WC of 106.9 cm (7.6 cm) and the other eight subjects were “non-obese” with a mean WC of 78.0 cm (5.3 cm). The two groups were of similar age (39.5 years in the obese group vs. 36 years in the non-obese, *P* = 0.3) and gender (5 males in the obese group and 4 males in the non-obese group, *P* = 0.6).

### **7.3.1 Upper GI symptoms reported during study**

None of the study subjects reported any upper GI symptoms with or without application of the waist belt throughout the entire recording period.

## 7.3.2 Manometric characteristics of the GOJ

### 7.3.2.1 Expiratory GOJ pressure

#### Effect of central obesity

I<sub>GP</sub> was higher in obese vs. non-obese subjects during fasting ( $15.7 \pm 1.2$  mmHg vs.  $10.3 \pm 1.4$  mmHg respectively,  $P = 0.01$ ) and after meal ( $17.7 \pm 1.1$  mmHg vs.  $12.2 \pm 1.3$  mmHg respectively,  $P = 0.01$ ). I<sub>OP</sub> was higher in obese vs. non-obese subjects only after meal ( $0.8 \pm 0.1$  mmHg vs.  $-1.6 \pm 0.4$  mmHg respectively,  $P < 0.001$ ). The G<sub>OPG</sub> was higher in obese vs. non-obese subjects during fasting ( $17.2 \pm 1.0$  mmHg vs.  $12.9 \pm 1.6$  mmHg respectively,  $P = 0.04$ ) and a higher trend towards significance after meal ( $16.9 \pm 1.0$  mmHg vs.  $13.8 \pm 1.1$  mmHg respectively,  $P = 0.07$ ). No significant difference in peak LOS pressure (vs. atmospheric or vs. I<sub>GP</sub>) was observed in obese vs. non-obese subjects, fasted or after meal (Table 7.1).

#### Effect of waist belt

The I<sub>GP</sub> was greater in subjects with belt-on than in subjects without belt during fasting ( $16.7 \pm 1.4$  mmHg vs.  $13.0 \pm 1.1$  mmHg respectively,  $P = 0.005$ ) and after meal ( $18.6 \pm 1.1$  mmHg vs.  $15.0 \pm 1.1$  mmHg respectively,  $P = 0.03$ ). An increase in I<sub>OP</sub> was seen with belt-on vs. off during fasting ( $4.0 \pm 1.1$  mmHg vs.  $-2.1 \pm 0.4$  mmHg respectively,  $P < 0.001$ ) and after meal ( $5.6 \pm 0.8$  mmHg vs.  $-0.4 \pm 0.3$  mmHg respectively,  $P < 0.001$ ). There was no difference in expiratory G<sub>OPG</sub> between belt-on vs. off during fasting and postprandial period (Table 7.2), a result of equivalence in absolute pressure rise of I<sub>GP</sub> and I<sub>OP</sub>. With belt, after meal, the peak LOS pressure (vs. atmospheric) was greater than without belt ( $38.6 \pm 1.9$  mmHg vs.  $30.5 \pm 1.4$  mmHg respectively,  $P < 0.001$ ) but not during fasting. Similarly, with belt, after meal, the peak LOS pressure (vs. I<sub>GP</sub>) was greater than without belt ( $20.0 \pm 2.3$  mmHg vs.  $15.5 \pm 1.8$  mmHg respectively,  $P = 0.05$ ) but not during fasting.

Table 7.1: Effect of obesity and waist belt on expiratory GOJ pressure

Parameters Mean (SEM)	Effect of central obesity			Effect of waist belt		
	Obese	Non-obese	<i>P</i> value	On	Off	<i>P</i> value
<b>FASTING</b>						
IGP (mmHg)	15.7 (1.2)	10.3 (1.4)	0.01	16.7 (1.4)	13.0 (1.1)	0.005
IOP (mmHg)	-1.6 (0.4)	-2.7 (0.6)	0.1	4.0 (1.1)	-2.1 (0.4)	< 0.001
GOPG (mmHg)	17.2 (1.0)	12.9 (1.6)	0.04	12.7 (1.7)	15.1 (1.1)	0.2
Peak LOS (mmHg vs. atm)	31.8 (3.0)	31.9 (3.7)	1.0	35.1 (2.1)	31.8 (2.3)	0.3
Peak LOS (mmHg vs. IGP)	16.1 (2.6)	21.6 (4.4)	0.3	18.4 (2.1)	18.9 (2.6)	0.9
<b>AFTER MEAL</b>						
IGP (mmHg)	17.7 (1.1)	12.2 (1.3)	0.01	18.6 (1.1)	15.0 (1.1)	0.03
IOP (mmHg)	0.8 (0.1)	-1.6 (0.4)	< 0.001	5.6 (0.8)	-0.4 (0.3)	< 0.001
GOPG (mmHg)	16.9 (1.0)	13.8 (1.1)	0.07	13.1 (1.3)	15.4 (0.9)	0.2
Peak LOS (mmHg vs. atm)	30.3 (1.6)	30.7 (2.4)	0.9	38.6 (1.9)	30.5 (1.4)	< 0.001
Peak LOS (mmHg vs. IGP)	12.6 (1.6)	18.4 (3.0)	0.1	20.0 (2.3)	15.5 (1.8)	0.05

GOJ; gastro-esophageal pressure junction, SEM; standard error of mean, IGP; intra-gastric pressure, IOP; intra-esophageal pressure, GOPG; gastro-esophageal pressure gradient, LOS; lower esophageal sphincter, atm; atmospheric

#### Effect of waist belt in obese subjects

Without belt, the fasting IGP was  $15.7 \pm 1.2$  mmHg and with belt, the IGP increased to  $19.9 \pm 1.6$  mmHg ( $P = 0.02$ ) but after meal, there was no significant difference between belt-on vs. off. Without belt, the fasting IOP was  $-1.6 \pm 0.3$  mmHg and it was increased to  $6.1 \pm 2.0$  mmHg with belt ( $P = 0.01$ ). After meal, the IOP was  $0.8 \pm 0.1$  mmHg without belt and this increased to  $5.2 \pm 1.3$  mmHg with belt ( $P = 0.01$ ). The GOPG did not change with or without belt during both fasting and after meal.

After meal, the peak LOS pressure (vs. atmospheric) was  $30.3 \pm 1.6$  mmHg without belt and it was increased to  $36.2 \pm 1.4$  mmHg with belt ( $P = 0.02$ ) but no significant difference was seen during fasting. The peak LOS pressure (vs. IGP) was not significantly different in belt on vs. off during both fasting and postprandial period.

### 7.3.2.2 Inspiratory GOJ pressure

#### Effect of central obesity

IGP was higher in obese vs. non-obese subjects during fasting ( $15.5 \pm 1.2$  mmHg vs.  $10.3 \pm 1.3$  mmHg respectively,  $P = 0.01$ ) and after meal ( $20.4 \pm 1.0$  mmHg vs.  $13.0 \pm 1.3$  mmHg respectively,  $P = 0.02$ ). IOP was higher in obese vs. non-obese subjects only after meal ( $0.7 \pm 0.1$  mmHg vs.  $-2.5 \pm 0.7$  mmHg respectively,  $P < 0.001$ ). Likewise, the GOPG was significantly higher in obese vs. non-obese subjects only after meal ( $19.7 \pm 1.0$  mmHg vs.  $15.4 \pm 1.5$  mmHg respectively,  $P = 0.05$ ) but a higher trend towards significance was seen during fasting ( $17.1 \pm 1.2$  mmHg vs.  $13.2 \pm 1.6$  mmHg respectively,  $P = 0.07$ ). No significant difference was seen in peak LOS pressure (vs. atmospheric and vs. IGP) in obese vs. non-obese subjects during fasting and after meal (Table 7.2).

#### Effect of waist belt

The IGP was higher than in subjects without belt during fasting ( $18.0 \pm 1.1$  mmHg vs.  $12.9 \pm 1.1$  mmHg respectively,  $P < 0.001$ ) and postprandial period ( $20.0 \pm 0.9$  mmHg vs.  $15.2 \pm 1.0$  mmHg respectively,  $P < 0.001$ ). An increase in IOP was seen with belt-on vs. off during fasting ( $3.0 \pm 0.8$  mmHg vs.  $-2.3 \pm 0.4$  mmHg respectively,  $P < 0.001$ ) and postprandial period ( $5.4 \pm 0.8$  mmHg vs.  $-0.9 \pm 0.5$  mmHg respectively,  $P < 0.001$ ). There was no difference in GOPG between belt-on vs. off during fasting and postprandial period (Table 7.2), also a result of equivalence in absolute pressure rise of IGP and IOP. With belt, after meal, the maximum LOS pressure (vs. atmospheric) was greater than without belt ( $39.4 \pm 2.3$  mmHg vs.  $30.9 \pm 1.5$  mmHg respectively,  $P < 0.001$ ) but not during fasting. Similarly, with belt, after meal, the maximum LOS pressure (vs. IGP) was greater than without belt ( $19.4 \pm 2.1$  mmHg vs.  $15.7 \pm 1.8$  mmHg respectively,  $P = 0.05$ ) but not during fasting.

#### Effect of waist belt in obese subjects

Without belt, the IGP was higher in belt-on vs. off during fasting ( $20.0 \pm 1.5$  mmHg vs.  $15.5 \pm 1.3$  mmHg respectively,  $P = 0.02$ ) and after meal ( $21.1 \pm 1.2$  mmHg vs.  $17.4 \pm 1.0$  mmHg respectively,  $P = 0.05$ ). Without belt, the fasted IOP

was  $-1.5 \pm 0.3$  mmHg and it was increased to  $3.8 \pm 1.5$  mmHg with belt ( $P = 0.01$ ). After meal, the IOP was  $0.7 \pm 0.1$  mmHg without belt and this increased to  $4.7 \pm 1.0$  mmHg with belt ( $P = 0.007$ ). The GOPG did not differ significantly with or without belt during both fasting and after meal. Fasting peak LOS pressure (vs. atmospheric) did not differ significantly in belt-on vs. off but after meal, it was higher with belt ( $36.9 \pm 1.5$  mmHg vs.  $30.0 \pm 1.7$  mmHg respectively,  $P = 0.02$ ). No difference in peak LOS pressure (vs. IGP) was seen in belt-on vs. off during both fasting and after meal.

**Table 7.2: Effect of obesity and waist belt on inspiratory GOJ pressure**

Parameters Mean (SEM)	Effect of central obesity			Effect of waist belt		
	Obese	Non-obese	<i>P</i> value	On	Off	<i>P</i> value
<b>FASTING</b>						
IGP (mmHg)	15.5 (1.2)	10.3 (1.3)	0.01	18.0 (1.1)	12.9 (1.1)	< 0.001
IOP (mmHg)	-1.5 (0.3)	-3.0 (0.7)	0.1	3.0 (0.8)	-2.3 (0.4)	< 0.001
GOPG (mmHg)	17.1 (1.2)	13.2 (1.6)	0.07	13.0 (1.6)	15.1 (1.1)	0.3
Peak LOS (mmHg vs. atm)	31.8 (3.2)	32.7 (2.8)	0.8	36.6 (1.5)	32.2 (2.1)	0.1
Peak LOS (mmHg vs. IGP)	16.2 (2.7)	22.3 (3.7)	0.2	18.6 (1.9)	19.3 (2.4)	0.7
<b>AFTER MEAL</b>						
IGP (mmHg)	20.4 (1.0)	13.0 (1.3)	0.02	20.0 (0.9)	15.2 (1.0)	< 0.001
IOP (mmHg)	0.7 (0.1)	-2.5 (0.7)	< 0.001	5.4 (0.8)	-0.9 (0.5)	< 0.001
GOPG (mmHg)	19.7 (1.0)	15.4 (1.5)	0.05	14.6 (1.1)	16.0 (0.9)	0.3
Peak LOS (mmHg vs. atm)	30.0 (1.7)	31.8 (2.6)	0.6	39.4 (2.3)	30.9 (1.5)	< 0.001
Peak LOS (mmHg vs. IGP)	12.6 (1.7)	18.9 (2.8)	0.1	19.4 (2.1)	15.7 (1.8)	0.05

GOJ; gastro-esophageal pressure junction, SEM; standard error of mean, IGP; intra-gastric pressure, IOP; intra-esophageal pressure, GOPG; gastro-esophageal pressure gradient, LOS; lower esophageal sphincter, atm; atmospheric

### 7.3.3 Location of components within the GOJ

#### 7.3.3.1 Upper and lower border of the LOS and diaphragm

##### Effect of central obesity

The lower border of the LOS was more proximal relative to nares in obese vs. non-obese subjects only after meal ( $43.9 \pm 0.9$  cm vs.  $46.7 \pm 1.4$  cm,  $P = 0.05$ )

(Figure 7.5). However, upper border of the LOS and total length of the LOS did not change significantly in obese vs. non-obese subjects, fasted or after meal (Table 7.3). The location of diaphragm was not displaced as reflected by the unchanged distances of PIP and peak LOS from nares, fasted or after meal (Table 7.3).

**Table 7.3: Effect of central obesity and waist belt on relative locations of anatomical structures of the GOJ**

Parameters Mean (SEM)	Effect of central obesity			Effect of waist belt		
	Obese	Non-obese	P value	On	Off	P value
<b>FASTING</b>						
<u>LOS and diaphragm</u>						
UB LOS (cm from nares)	40.2 (1.1)	41.2 (1.5)	0.6	40.3 (1.1)	40.7 (0.9)	0.6
LB LOS (cm from nares)	45.2 (1.0)	46.6 (1.6)	0.5	44.6 (1.4)	45.8 (0.9)	0.2
LOS length (cm)	5.0 (1.0)	5.3 (1.5)	0.8	4.3 (1.1)	5.2 (0.8)	0.5
PIP (cm from nares)	43.4 (0.8)	45.7 (0.9)	0.1	43.5 (0.6)	44.6 (0.6)	< 0.001
Peak LOS (cm from nares)	43.9 (0.8)	45.3 (1.0)	0.3	43.9 (0.8)	45.1 (0.7)	0.004
PIP above peak LOS (cm)	1.4 (0.5)	0.4 (0.4)	0.2	0.4 (0.4)	0.5 (0.4)	0.5
<u>SCJ and diaphragm</u>						
SCJ (cm from nares)	42.9 (0.6)	47.1 (0.8)	0.001	43.1 (0.7)	45.0 (0.7)	< 0.001
SCJ above PIP (cm)	0.5 (0.8)	-1.4 (0.4)	0.05	0.4 (0.6)	-0.4 (0.5)	0.05
SCJ above peak LOS (cm)	1.9 (0.9)	-1.7 (0.3)	0.02	0.8 (0.7)	0.1 (0.6)	0.4
<b>AFTER MEAL</b>						
<u>LOS and diaphragm</u>						
UB LOS (cm from nares)	39.9 (0.9)	41.8 (1.3)	0.3	39.5 (0.9)	40.8 (0.8)	0.01
LB LOS (cm from nares)	43.9 (0.9)	46.7 (1.4)	0.05	43.2 (1.3)	45.2 (0.8)	0.03
LOS length (cm)	3.9 (0.4)	4.8 (1.1)	0.4	3.6 (1.0)	4.3 (0.6)	0.5
PIP (cm from nares)	42.6 (0.9)	44.4 (0.9)	0.2	42.3 (0.7)	43.5 (0.6)	0.01
Peak LOS (cm from nares)	44.7 (1.0)	45.4 (1.0)	0.6	43.3 (0.8)	44.6 (0.6)	0.003
PIP above peak LOS (cm)	1.2 (0.2)	0.8 (0.3)	0.3	1.0 (0.3)	1.1 (0.2)	0.8
<u>SCJ and diaphragm</u>						
SCJ (cm from nares)	41.8 (0.9)	46.1 (1.0)	0.006	41.3 (1.0)	43.9 (0.9)	< 0.001
SCJ above PIP (cm)	0.9 (1.1)	-1.8 (0.6)	0.05	1.0 (0.7)	-0.5 (0.7)	0.04
SCJ above peak LOS (cm)	2.1 (1.0)	0.9 (0.7)	0.03	1.9 (0.8)	0.6 (0.7)	0.04

GOJ; gastro-esophageal pressure junction, SEM; standard error of mean, LOS; lower oesophageal sphincter, UB; upper border, LB; lower border, peak LOS; position of maximum LOS pressure, PIP; pressure inversion point, SCJ; squamo-columnar junction, The “-” indicates the position of former parameter is below the latter parameter

### Effect of waist belt

The distances from nares to upper and lower border of the LOS were not significantly different in belt on vs. off during fasting (**Table 7.2**). However, after meal, the upper border of the LOS was more proximal to nares with belt on vs. off ( $39.5 \pm 0.9$  cm vs.  $40.8 \pm 0.8$  cm,  $P = 0.01$ ). The lower border of the LOS was also more proximal to nares after meal in belt on vs. off ( $43.2 \pm 1.3$  cm vs.  $45.2 \pm 0.8$  cm,  $P = 0.03$ ). The LOS length did not differ significantly in belt on vs. off, fasted or after meal (**Table 7.3**).

With belt on vs. off, the diaphragm, as reflected by the PIP ( $43.5 \pm 0.6$  vs.  $44.6 \pm 0.6$  cm,  $P < 0.001$ ) and peak LOS ( $43.9 \pm 0.8$  vs.  $45.1 \pm 0.7$  cm,  $P = 0.004$ ), was displaced proximally relative to nares during fasting. Likewise, with belt on vs. off, the PIP ( $42.3 \pm 0.7$  vs.  $43.5 \pm 0.6$  cm,  $P = 0.01$ ) and peak LOS ( $43.3 \pm 0.8$  vs.  $44.6 \pm 0.6$ ,  $P = 0.003$ ) were displaced more proximally after meal.

### Effect of waist belt in obese subjects

The upper and lower borders of the LOS from nares were similar in belt-on vs. off among obese subjects during fasting and after meal (**Figure 7.5**). The LOS length was also similar in belt on vs. off among obese subjects during both fasting and after meal.

The PIP migrated more proximally relative to the nares in belt on vs. off during both fasting ( $42.4 \pm 0.8$  cm vs.  $43.4 \pm 0.8$  cm respectively,  $P = 0.01$ ) and after meal ( $41.6 \pm 0.9$  cm vs.  $42.6 \pm 0.9$  cm respectively,  $P = 0.01$ ). Similarly, the peak LOS was more proximal relative to nares in belt on vs. off during both fasting ( $43.2 \pm 1.1$  cm vs.  $44.7 \pm 1.0$  cm respectively,  $P = 0.03$ ) and after meal ( $42.7 \pm 1.1$  cm vs.  $43.9 \pm 0.8$  cm respectively,  $P = 0.04$ ). However, the relative distance between the PIP and peak LOS did not differ during both fasting and postprandial period.

### 7.3.3.2 Squamo-columnar junction

#### Effect of central obesity

The SCJ was located more proximally in obese vs. non-obese, during fasting ( $42.9 \pm 0.6$  cm vs.  $47.1 \pm 0.8$  cm,  $P = 0.001$ ) and after meal ( $41.8 \pm 0.9$  cm vs.  $46.1 \pm 1.0$  cm,  $P = 0.006$ ) (**Figure 7.5**).

The SCJ was also located more proximally with respect to the peak LOS in obese vs. non obese subjects during fasting, being  $1.7 \pm 0.4$  cm below the peak LOS in former but  $1.9 \pm 0.9$  cm above the peak LOS in latter ( $P = 0.02$ ). Likewise, after meal, the SCJ was  $0.9 \pm 0.7$  cm above peak LOS in non-obese subjects vs.  $2.1 \pm 1.0$  cm in obese subjects ( $P = 0.03$ ). The more proximal location of the SCJ above peak LOS in obese subjects was significant during time 1 ( $P = 0.03$ ) and time 4 ( $P = 0.05$ ) of postprandial period.

In non-obese subjects, the SCJ was located  $1.4 \pm 0.4$  cm below PIP and in obese subjects, it was located  $0.5 \pm 0.8$  cm above PIP during fasting ( $P = 0.02$ ). After meal, in non-obese subjects, the SCJ was located  $1.8 \pm 0.6$  cm below PIP and in obese subjects, it was located  $0.9 \pm 1.1$  cm above PIP ( $P = 0.03$ ). The more proximal location of the SCJ above PIP in obese subjects was significant during time 1 ( $P = 0.05$ ), time 2 ( $P = 0.03$ ), time 3 ( $P = 0.03$ ) and time 5 ( $P = 0.03$ ) of postprandial period.

#### Effect of waist belt

The SCJ was located closer to the nares with belt on vs. off ( $43.1 \pm 0.7$  cm vs.  $45.0 \pm 0.7$  cm,  $P < 0.001$ ) during fasting and also after meal ( $41.3 \pm 1.0$  cm vs.  $43.9 \pm 0.9$  cm,  $P < 0.001$ ) (**Figure 7.5**).

The SCJ was located more proximally with respect to peak LOS with belt on vs. off following meal ( $1.9 \pm 0.8$  cm vs.  $0.6 \pm 0.7$  cm,  $P = 0.04$ ). The SCJ was at similar level to peak LOS during fasting without belt and was unaffected by belt-on (**Table 7.3**).

The more proximal location of the SCJ above peak LOS with belt was significant during time 1 ( $P = 0.04$ ), time 2 ( $P = 0.03$ ), time 3 ( $P = 0.04$ ), time 4 ( $P = 0.003$ ) and time 5 ( $P = 0.03$ ) of postprandial period.

Without belt, during fasting, the SCJ was located  $0.4 \pm 0.5$  cm below PIP and with belt, it was  $0.4 \pm 0.6$  cm above PIP ( $P = 0.05$ ). After meal, without belt, the SCJ was located  $0.5 \pm 0.7$  cm below PIP and with belt, it was  $1.0 \pm 0.7$  cm above PIP ( $P = 0.04$ ). The more proximal location of the SCJ above PIP with application of belt was persistent during time 1 ( $P = 0.04$ ), time 3 ( $P = 0.03$ ), time 4 ( $P = 0.001$ ) and time 5 ( $P = 0.05$ ) of postprandial period.

#### Effect of waist belt in obese subjects

The fasted SCJ from nares was  $41.2 \pm 0.7$  cm with belt and was more distal at  $42.9 \pm 0.6$  cm without belt ( $P = 0.01$ ). After meal, the SCJ from nares was  $39.9 \pm 0.9$  cm with belt and was more distal at  $41.7 \pm 0.9$  cm without belt ( $P = 0.001$ ).

The fasted SCJ was  $1.9 \pm 0.9$  cm above peak LOS pressure without belt and it was similar at  $2.0 \pm 0.9$  cm with belt ( $P = 0.9$ ). After meal, the SCJ was  $2.1 \pm 1.0$  cm above peak LOS without belt and it was  $2.8 \pm 1.1$  cm above peak LOS pressure with belt ( $P = 0.01$ ).

The fasted SCJ was located  $0.5 \pm 0.8$  cm above PIP without belt and it was only relatively more proximal from the PIP at  $1.1 \pm 0.9$  cm ( $P = 0.02$ ). After meal, the SCJ was  $0.8 \pm 1.1$  cm above PIP without belt and was  $1.7 \pm 1.1$  cm above PIP with belt ( $P = 0.04$ ).

#### Effect of obesity and belt on proximal migration of the SCJ during TLOSRS

The magnitude of the migration of the SCJ during TLOSRS was less in obese vs. non-obese subjects ( $4.2 \pm 1.8$  cm vs.  $6.8 \pm 0.6$  cm,  $P = 0.04$ ) and also less with vs. without belt ( $3.9 \pm 0.3$  cm vs.  $5.5 \pm 0.4$  cm,  $P = 0.005$ ). There was no difference in duration of migration of the SCJ during TLOSRS with effect of obesity or with belt (Table 7.4).

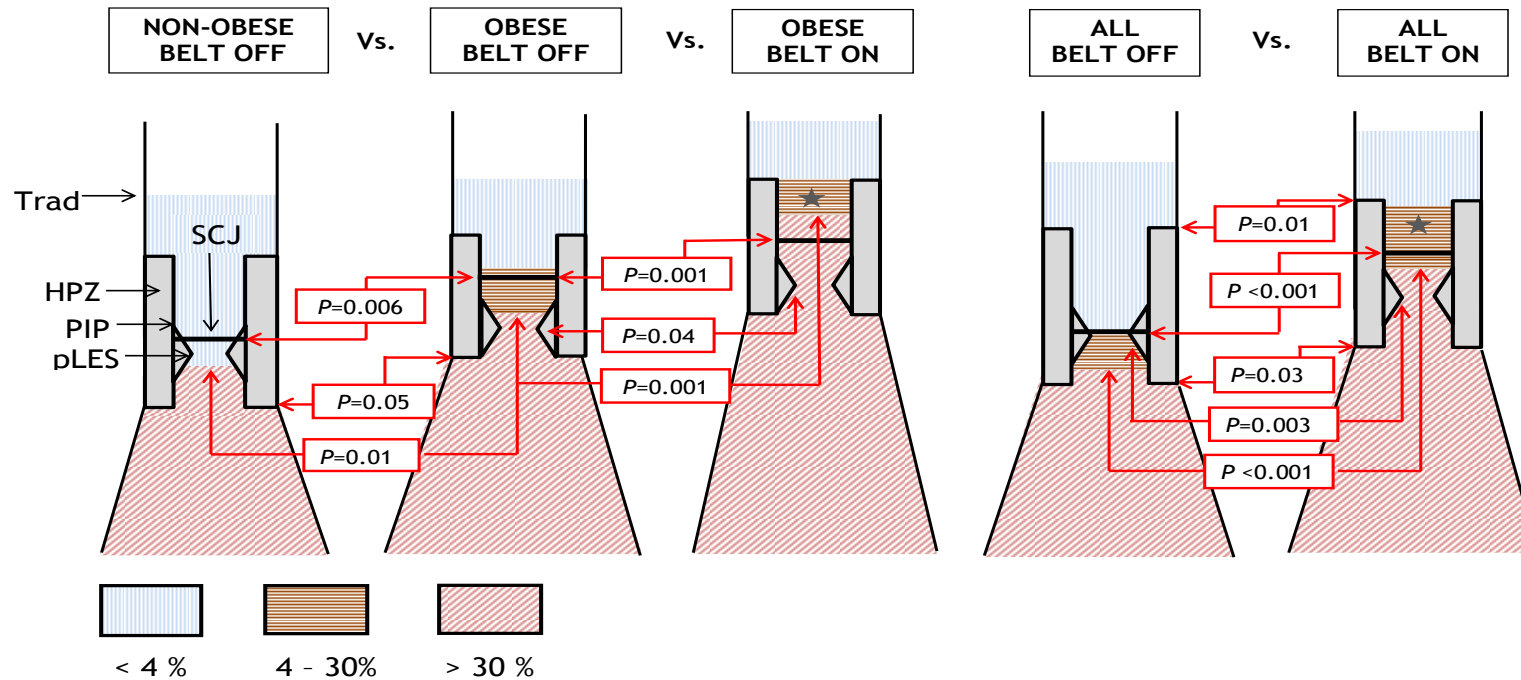


**Figure 7.5:** Partial hiatus herniation and short segment acid reflux after meal. The peak point of triangle within the GOJ is location of maximum LOS pressure. The coloured area indicates acid exposure (mean % time  $pH < 4$ ) within the GOJ and stomach. All values in mean. Comparison between groups (non-obese vs. obese, obese belt on vs. off, belt on vs. off) in location of GOJ structures is indicated by red arrows with  $P$  value significant  $< 0.05$ . Star in yellow-coloured region (short segment reflux) indicates significant changes between comparison groups. Trad; traditional site of reflux, HPZ; high pressure zone, PIP; pressure inversion point, pLES; peak LOS pressure, SCJ; squamo-columnar junction

The velocity of early descent phase (phase C) was however slower with vs. without belt ( $0.5 \pm 0.2$  cm/s vs.  $0.7 \pm 0.1$  cm/s,  $P = 0.02$ ) but this was not observed in obese vs. non-obese subjects.

The amplitude and duration of proximal migration of the SCJ did not differ between belt-on vs. off among obese subjects. The later proximal migration phase of the SCJ during TLOSRS (phase B) was relatively faster with belt-on vs. off in obese subjects ( $0.4 \pm 0.1$  cm/s vs.  $0.2 \pm 0.03$  cm/s respectively,  $P = 0.04$ ). However, the early descent phase of the SCJ during TLOSRS (phase C) was relatively slower with belt-on vs. off ( $0.4 \pm 0.1$  cm/s vs.  $0.7 \pm 0.1$  cm/s respectively,  $P = 0.03$ ).

**Table 7.4: Effect of central obesity and waist belt on proximal migration of the SCJ during TLOSRS**

Parameters Mean (SEM)	Effect of central obesity			Effect of waist belt		
	Obese	Non-obese	<i>P</i> value	On	Off	<i>P</i> value
Amplitude (cm)	4.2 (1.8)	6.8 (0.6)	0.04	3.9 (0.3)	5.5 (0.4)	0.01
Duration (s)	29.7 (7.9)	27.9 (7.0)	0.5	26.7 (5.3)	28.2 (6.8)	0.1
Phase A velocity (cm/s)	0.1 (0.1)	0.2 (0.2)	0.5	0.2 (0.1)	0.2 (0.1)	0.6
Phase B velocity (cm/s)	0.2 (0.1)	0.5 (0.2)	0.2	0.3 (0.1)	0.3 (0.2)	0.9
Phase C velocity (cm/s)	0.7 (0.1)	0.7 (0.2)	0.4	0.5 (0.2)	0.7 (0.1)	0.02
Phase D velocity (cm/s)	0.3 (0.2)	0.4 (0.3)	0.6	0.3 (0.1)	0.3 (0.1)	0.5

SCJ; squamo-columnar junction, TLOSRS; transient lower oesophageal sphincter relaxations

#### Key differences between obesity vs. belt effect on location of the SCJ

The extent of proximal displacement of the SCJ to nares was greater with effect of obesity than with belt during fasting ( $4.3 \pm 1.3$  vs.  $1.5 \pm 0.3$  cm,  $P = 0.04$ ) and after meal ( $4.9 \pm 1.2$  vs.  $1.9 \pm 0.4$  cm,  $P = 0.05$ ). The reduced proximal movement of the SCJ during TLOSRS is consistent with its resting position being already proximally displaced above the diaphragm, and the effect was likewise greater with effect of obesity than with belt ( $2.6 \pm 0.4$  vs.  $0.9 \pm 0.4$  cm,  $P = 0.05$ ).

## 7.3.4 pH transition point

### 7.3.4.1 Acid exposure at pH transition point

As shown in **Table 7.5**, the pH transition point indicated the change from oesophageal to gastric pH. The mean % of time pH < 4 at pH transition point was always above 30%, without any significant difference, in obese vs. non-obese subjects, during fasting (range 38.0 - 100% vs. 35.7 - 100%,  $P = 0.3$ ) or after meal (range 31.8 - 99.1% vs. 37.9 - 100%,  $P = 0.8$ ). Likewise, the mean % of time pH < 4 at pH transition point was always above 30%, without any significant difference, in belt on vs. off, during fasting (range 42.9 - 100% vs. 35.7 - 100%,  $P = 0.2$ ) or after meal (range 31.8 - 100% vs. 37.9 - 100%,  $P = 0.3$ )

### 7.3.4.2 The location of pH transition point

#### Effect of central obesity

The pH transition point relative to nares was more proximal in obese vs. non-obese subjects, during fasting ( $45.0 \pm 0.7$  cm vs.  $48.7 \pm 0.9$  cm,  $P = 0.01$ ) and after meal ( $44.0 \pm 1.0$  vs.  $47.1 \pm 1.4$  cm,  $P = 0.01$ ). The pH transition point was at similar distance distal to SCJ in obese vs. non-obese subjects, during fasting or after meal (**Figure 7.5**).

The fasted pH transition point was  $3.3 \pm 0.6$  cm distal to peak LOS in non-obese subjects and was  $0.2 \pm 0.9$  cm below peak LOS in obese subjects ( $P = 0.02$ ). Likewise, after meal, the pH transition point was  $1.9 \pm 1.2$  cm below peak LOS in non-obese subjects and was  $0.8 \pm 1.1$  cm below peak LOS in obese subjects ( $P = 0.05$ ).

#### Effect of waist belt

The pH transition point was located more proximal to nares with belt on vs. off both during fasting ( $44.4 \pm 0.7$  cm vs.  $46.8 \pm 0.7$  cm,  $P < 0.001$ ) and after meal ( $42.5 \pm 0.9$  cm vs.  $45.5 \pm 0.9$  cm,  $P < 0.001$ ) (**Figure 7.5**). The pH transition point during fasting was  $1.8 \pm 0.4$  cm distal to the SCJ without belt but with belt, was

significantly closer at  $1.0 \pm 0.4$  cm ( $P = 0.02$ ). After meal, the pH transition point was  $1.4 \pm 0.8$  cm distal to the SCJ without belt but with belt only,  $0.1 \pm 0.9$  cm distal to it ( $P = 0.005$ ).

The fasting pH transition point was  $1.7 \pm 0.7$  cm below peak LOS without belt but was only  $0.5 \pm 0.7$  cm below peak LOS with belt ( $P = 0.03$ ). After meal, the pH transition point was  $1.3 \pm 0.9$  cm below peak LOS but was  $1.3 \pm 0.8$  cm above peak LOS with belt ( $P = 0.001$ ). In obese subjects, with belt on, the postprandial pH transition point was  $0.8 \pm 1.3$  cm above the SCJ compared to  $1.1 \pm 0.9$  cm below the SCJ without belt ( $P = 0.05$ ) (**Figure 7.5**). The postprandial pH transition point was located  $2.2 \pm 0.8$  cm above peak LOS with belt in obese subjects compared to  $0.7 \pm 1.3$  cm below peak LOS without belt ( $P = 0.04$ ) (**Figure 7.5**).

#### Effect of waist belt in obese subjects

Location of fasting pH transition point from nares was  $44.9 \pm 0.7$  cm without belt and it was more proximal at  $42.6 \pm 0.7$  cm with belt ( $P < 0.001$ ). After meal, the pH transition point was  $42.9 \pm 1.1$  cm without belt and it was  $39.1 \pm 0.9$  cm with belt ( $P < 0.001$ ). The SCJ was  $1.1 \pm 0.9$  cm above pH transition point without belt but the SCJ was  $0.8 \pm 1.3$  cm below pH transition point with belt only after meal ( $P = 0.05$ ). Likewise, the pH transition point was located  $2.2 \pm 0.8$  cm above peak LOS with belt but was located  $0.7 \pm 1.3$  cm below peak LOS without belt only after meal ( $P = 0.04$ ).

#### **7.3.4.3 Acid exposure below pH transition point**

The mean % of time pH < 4 at 1.5 cm, 3.0 cm and 4.5 cm below pH transition point was always above 30% without any significant difference between obese vs. non-obese during fasting or after meal (**Table 7.5**). The mean % of time pH < 4 at 1.5 cm and 3.0 cm below pH transition point was also above 30% without any significant difference in belt on vs. off during fasting or after meal (**Table 7.5**).

Table 7.5: Regional differences in acid exposure at the GOJ during fasting and after meal

Mean % time pH < 4 (SEM)	Above pH transition point					pH transition point	Below pH transition point		
	Traditional	6.0 cm	4.5 cm	3.0 cm	1.5 cm	0 cm	-1.5 cm	-3.0 cm	-4.5 cm
<u>Non-obese - belt Off</u>									
Fasting	0 (0)	0 (0)	0 (0)	0.8 (0.5)	4.1 (2.8)	73.7 (11.1)	57.6 (13.7)	68.7 (15.7)	72.6 (21.1)
After meal 0-30min	0 (0)	0 (0)	0.2 (0.1)	0.8 (0.4)	2.9 (1.7)	42.0 (5.2)	40.0 (6.0)	45.5 (12.3)	79.3 (8.1)
After meal 30-60min	0.4 (0.4)	0 (0)	0.1 (0.1)	0.3 (0.2)	0.7 (0.3)	51.6 (15.1)	56.9 (16.2)	62.7 (10.7)	83.7 (14.0)
<u>Obese - belt Off</u>									
Fasting	0 (0)	0.2 (0.1)	0.7 (0.5)	1.9 (1.7)	8.3 (2.4)	71.6 (8.5)	77.5 (16.0)	87.4 (11.1)	94.8 (5.0)
After meal 0-30min	0 (0)	0.9 (0.6)	1.1 (0.7)	3.4 (1.0)	7.1 (1.3)	36.0 (12.2)	46.0 (15.3)	50.3 (17.2)	43.5 (16.1)
After meal 30-60min	0.4 (0.3)	0.5 (0.3)	1.3 (1.2)	3.0 (1.8)	9.8 (5.5)	62.4 (9.2)	69.4 (16.1)	67.2 (15.7)	64.6 (16.4)
<u>Obese - belt On</u>									
Fasting	0 (0)	0 (0)	0 (0)	0 (0)	0.3 (0.1)	38.4 (9.0)	47.5 (13.2)	73.1 (8.0)	89.2 (8.1)
After meal 0-30min	0.1 (0.1)	0.1 (0.1)	0.7 (0.2)	2.4 (0.7)	7.6 (2.4)	50.1 (10.7)	58.8 (11.8)	21.2 (11.2)	21.6 (16.0)
After meal 30-60min	1.5 (1.1)	3.0 (2.1)	3.7 (1.5)	9.7 (2.9)#	16.1 (4.7)#	81.5 (6.5)	82.4 (13.9)	54.7 (16.0)	19.3 (16.3)#
<u>All - Belt Off</u>									
Fasting	0 (0)	0 (0)	0 (0)	0.2 (0.2)	1.2 (0.6)	72.8 (7.1)	66.2 (10.4)	77.3 (9.9)	83.7 (7.3)
After meal 0-30min	0 (0)	0.4 (0.3)	0.6 (0.3)	2.0 (0.6)	5.0 (1.2)	47.4 (8.9)	40.9 (8.9)	56.2 (11.0)	39.0 (10.6)
After meal 30-60min	0.4 (0.2)	0.1 (0.1)	0.7 (0.6)	1.6 (0.9)	5.3 (2.9)	57.6 (19.0)	62.7 (11.2)	62.6 (6.9)	75.5 (18.8)
<u>All - Belt On</u>									
Fasting	0 (0)	0.1 (0.1)	0.3 (0.3)	1.3 (0.9)	6.2 (1.9)	53.0 (8.6)	42.9 (8.7)	63.9 (8.6)	46.6 (8.4)
After meal 0-30min	0 (0)	0.1 (0.1)	0.4 (0.1)	1.6 (0.5)	5.6 (1.4)	54.7 (9.1)	48.1 (8.7)	23.9 (7.5)	25.5 (11.0)
After meal 30-60min	0.9 (0.6)	1.3 (0.9)	2.1 (0.9)	6.1 (1.8)#	12.8 (3.1)#	77.4 (6.1)	65.6 (10.4)	50.8 (10.4)	23.8 (11.6)#

#comparison between groups with *P* value significant < 0.05

Only at 4.5 cm below pH transition point that the mean % of time pH < 4 was lower with belt on ( $23.8 \pm 11.6\%$ ) than without belt ( $75.5 \pm 18.8\%$ ) 30 - 60 min after meal ( $P = 0.02$ ). Likewise, at 4.5 cm below pH transition point, the mean % of time pH < 4 was lower in obese subjects with belt on ( $19.3 \pm 16.3\%$ ) than belt off ( $64.6 \pm 16.4\%$ ) 30 - 60 min after meal ( $P = 0.04$ ).

### 7.3.5 Acid exposure above pH transition point

#### 7.3.5.1 Traditional acid reflux

At 5 cm above upper border LOS (traditional site), the mean % of time pH < 4 was minimal (< 4%) in all studied groups, before or after meal (**Table 7.5**). Between traditional site and upper border LOS (4.5 cm and 6.0 cm above pH transition point), the mean % of time pH < 4 was also below 4% in all studied groups, before or after meal (**Table 7.5**).

#### 7.3.5.2 Short segment reflux

##### Effect of central obesity

The mean % of time pH < 4 at 1.5 cm and 3.0 cm above pH transition point was not significantly different in obese vs. non-obese subjects, before or after meal (**Table 7.5**).

##### Effect of waist belt

The mean % of time pH < 4 at 1.5 cm and 3.0 cm above pH transition point was not significantly different in belt on vs. off during fasting (**Table 7.5**). After meal, at 1.5 cm above the pH transition point, the mean % of time pH < 4 was significantly increased in belt-on vs. off ( $12.8 \pm 3.1\%$  vs.  $5.3 \pm 2.9\%$ ,  $P = 0.01$ ) and in obese subjects with belt-on vs. off ( $16.1 \pm 4.7\%$  vs.  $9.8 \pm 5.5\%$ ,  $P = 0.05$ ). After meal, at 3.0 cm above the pH transition point, the mean % of time pH < 4 was significantly increased in belt-on vs. off ( $6.1 \pm 1.8\%$  vs.  $1.6 \pm 0.9\%$ ,  $P = 0.02$ ) and in obese subjects with belt-on vs. off ( $9.7 \pm 2.9\%$  vs.  $3.0 \pm 1.8\%$ ,  $P = 0.04$ ).

### Mechanism of short segment reflux

All short segment acid reflux events documented in all studied groups were associated with TLOSRs (Figure 7.6). TLOSRs were more frequent with belt-on vs. off ( $6.0 \pm 2.7$  vs.  $5.0 \pm 2.0$ ,  $P = 0.005$ ) but not in the obese vs. non-obese ( $5.0 \pm 2.5$  vs.  $5.0 \pm 3.5$ ,  $P = 0.5$ ) (Table 7.6). The % of TLOSRs with acid reflux was  $32.8 \pm 12.9\%$  in obese subjects compared to  $4.2 \pm 2.7\%$  in non-obese subjects ( $P = 0.05$ ). The % of TLOSRs with acid reflux was greater with belt on vs. off ( $46.4 \pm 6.6\%$  vs.  $18.5 \pm 7.4\%$ ,  $P = 0.001$ ). In obese subjects with belt-on vs. off, TLOSRs were more frequent ( $6.5 \pm 3.2$  vs.  $5.0 \pm 2.5$ ,  $P = 0.02$ ) and so was % TLOSRs with acid reflux ( $56.4 \pm 8.5$  vs.  $32.8 \pm 12.9\%$ ,  $P = 0.05$ ).

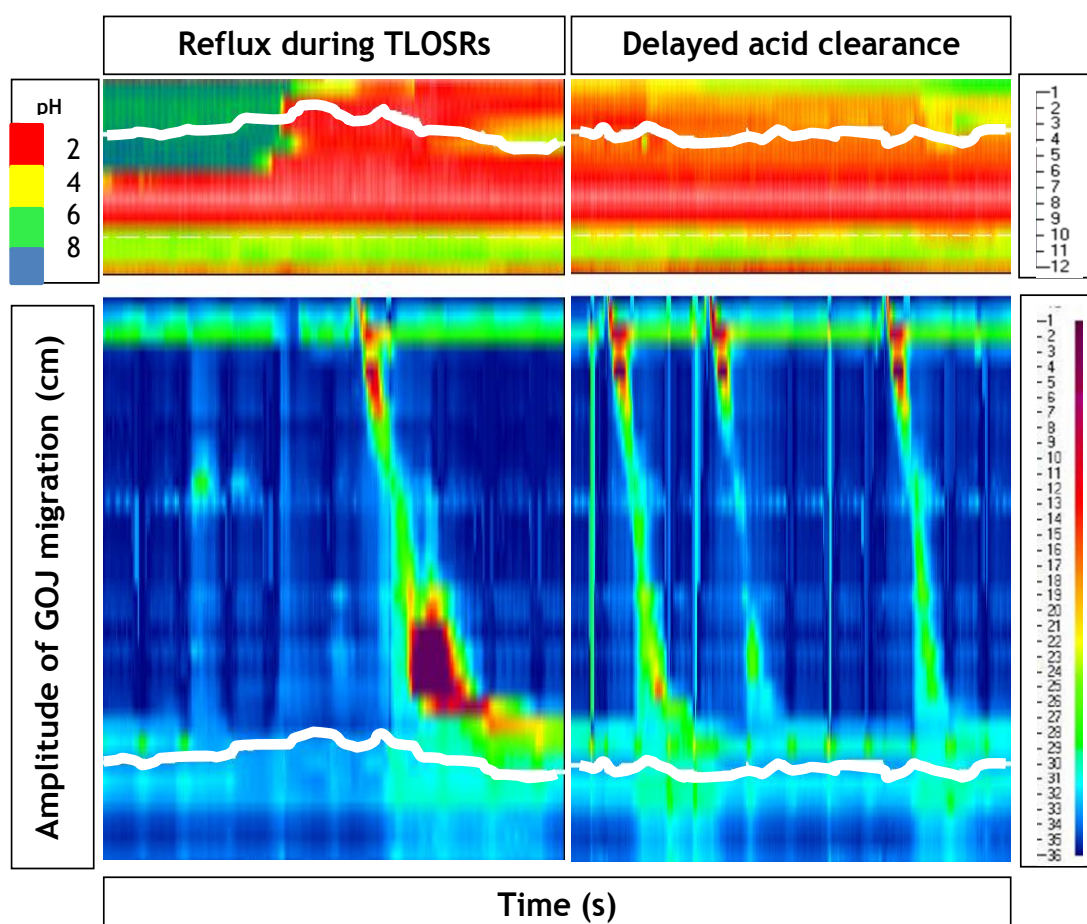


**Figure 7.6:** Mechanism of short segment reflux.

The acid clearance time following episodes of short segment reflux was significantly longer in obese vs. non-obese subjects ( $23.4 \pm 8.3$  s vs.  $4.6 \pm 3.0$  s,  $P = 0.05$ ) and also with belt-on vs. off ( $49.5 \pm 10.1$  s vs.  $14.0 \pm 4.9$  s,  $P = 0.001$ ). The number of swallows needed to clear the acid was greater with belt-on vs. off ( $2.2 \pm 0.4$  vs.  $0.7 \pm 0.2$ ,  $P < 0.001$ ) but it was not significantly different with effect of obesity.

**Table 7.6: Mechanism of short segment acid reflux**

Parameters Mean (SEM)	Effect of central obesity			Effect of waist belt		
	Obese	Non-obese	<i>P</i> value	On	Off	<i>P</i> value
Frequency of TLOSRS (n)	5.0 (2.5)	5.0 (3.5)	0.5	6.0 (2.7)	5.0 (2.0)	0.005
TLOSRS with reflux (%)	32.8 (12.9)	4.2 (2.7)	0.05	46.4 (6.6)	18.5 (7.4)	0.001
Acid clearance time (s)	23.4 (8.3)	4.6 (3.0)	0.05	49.5 (10.1)	14.0 (4.9)	0.001
Swallows to clear acid (n)	1.1 (0.4)	0.4 (0.3)	0.1	2.2 (0.4)	0.7 (0.2)	<0.001

SEM; standard error of mean, TLOSRS; transient lower esophageal sphincter relaxations

### 7.3.6 Chest x-ray at 6-8 weeks after study

All 16 subjects who had chest x-ray after 6 - 8 weeks were cleared from the magnet initially clipped to the SCJ.

## 7.4 DISCUSSION

In our population of asymptomatic volunteers, neither increased waist circumference nor waist belt was associated with traditional GOR assessed as increased acid exposure 5 cm above the upper border of the LOS. However, both were associated with abnormalities of the GOJ and with increased acid exposure of the segment of the distal oesophagus residing within the LOS. These abnormalities were most marked with the combination of increased WC plus waist belt. This increased acid exposure of the most distal oesophagus is

likely to be relevant to the high incidence of inflammation and metaplasia occurring at the GOJ in subjects without a history of reflux of symptoms.

Increased WC was associated with several abnormalities of the LOS. The location of the LOS was relatively unaffected by increased waist circumference with the position of its upper border, peak LOS pressure and PIP relative to nares being unaltered and its lower border was displaced proximally only after a meal. However, marked changes were observed within the sphincter with the SCJ being located much more proximally with respect to both the nares and the point of peak LOS pressure in those of larger WC. Whereas the SCJ was an average 1.7 cm below the peak LOS pressure in those with smaller WC, it was 1.9 cm above it in those with larger WC. Consistent with the more proximal position of the SCJ in the diaphragmatic hiatus, the amplitude of the proximal migration of the SCJ during TLOSRS was substantially less than in those with large circumference at 4.2 cm compared to those with small WC at 6.8 cm.

Gastric acid penetration within the LOS was also different in those with large waist circumference. The pH transition point representing the position where pH changes from oesophageal to gastric extended 3 cm more proximally within the LOS in those with large waist circumference and the magnitude of this proximal displacement was similar to that of the SCJ.

What is the cause of the proximal displacement of the SCJ and more proximal extension of gastric acidity within the LOS? The GOJ is normally held within the diaphragmatic hiatus by the POL which are attached to the diaphragmatic crura which form the extrinsic component of the upper LOS. During TLOSRS, the crura relaxes and contraction of the longitudinal muscle of the oesophagus pulls the GOJ 4 - 8 cm into the chest as previously reported and observed in our current study. A lesser degree of proximal migration occurs during swallowing. The restitution of the GOJ to its original position within the diaphragmatic hiatus comes about by relaxation of the longitudinal muscle, contraction of the diaphragmatic crura and the elastic recoil of the POL. The increased GOPG associated with increased waist

circumference may restrict the descent of the GOJ following TLOS, causing it to reside in an abnormal proximal position.

How does this more proximal location of the GOJ within the diaphragmatic hiatus relate to hiatus hernia? Unlike hiatus hernia, we did not detect proximal displacement of the upper border of the high pressure zone. The HPZ is normally composed of the super-imposed pressures exerted by the intrinsic LOS and the extrinsic LOS i.e. diaphragmatic crura. In our subjects, the GOJ and its intrinsic sphincter may have been displaced proximally within the HPZ of the crura but not sufficiently for it to extend proximally to the proximal margin of the crura and thus proximally displace the upper border of the LOS. We did observe proximal displacement of the lower border of the LOS after a meal in those with increased WC which would be consistent with the intrinsic LOS normally lying slightly distal to the crura and then being displaced proximally to lie more within the crura HPZ.

A full hiatus hernia occurs when the GOJ is permanently displaced sufficiently proximally relative to the diaphragmatic crura to cause clear separation of the two pressure peaks with an area of lower pressure between the peaks representing the hernia sac. This is thought to be due to weakening of the crura and also weakening or rupture of the POL. Bredenoord et al. also described the phenomenon of intermittent hiatus hernia where high resolution manometry demonstrated intermittent double peaks (A J Bredenoord *et al.*, 2004). In patients being investigated for reflux symptoms, increased WC has been associated with higher incidence of intermittent double peaks. Our current study involves subjects with no endoscopic evidence of hiatus hernia and no HRM evidence of double peaks. The more proximal positioning of the GOJ in the hiatus in our asymptomatic subjects without evidence of double peaks suggests that this may be early or partial hiatus hernia and may represent the early stages of its development.

An alternative or additional mechanism might explain the more proximal location of the SCJ and more proximal extension of gastric acidity within the LOS. The increased IAP, partial hiatus hernia and shortening of the distal

segment of the LOS may allow gastric acid to impinge upon the most distal oesophageal squamous mucosa causing it to undergo columnar metaplasia and thus proximal migration of the SCJ. We have previously reported proximal extension of the gastric cardia mucosa associated with increased WC in asymptomatic volunteers.

We found that abdominal constriction by the waist belt produced similar, but not identical, changes to the GOJ to those observed with increased WC. The belt increased IAP by a similar amount to that observed with increased WC. However, unlike increased WC, the belt did not increase the GOPG. With increased WC there was a rise in both IGP and IOP but the increase in the former was greater than the latter, producing a resultant increase in GOPG. In contrast with the belt, the increase in IOP was similar to the increase in IGP resulting in no overall increase in the GOPG. Increased IOP has been previously observed with increased waist circumference and abdominal constriction but the mechanism is not entirely clear. It may be largely related to the effects that increased IAP has on the movement of the diaphragm. Increased IAP will reduce the rate of diaphragmatic descent during inspiration and thus reduce the degree of fall in intrathoracic and IOP associated with inspiration. Likewise, the IAP will increase the rate of ascent of the diaphragm during expiration, again resulting in an increase in intrathoracic oesophageal pressure. The less marked changes in IOP with obesity versus increased WC might be due to the long-standing nature of obesity causing adaptation and strengthening the diaphragm in chronic elevation of IAP.

Unlike increased WC, the waist belt caused a rise in the peak LOS pressure relative to atmospheric pressure and a less marked rise relative to IGP reflecting IAP. Any increase in IAP will cause a rise in pressure of the intra-abdominal segment of the lower oesophageal sphincter due to the abdominal pressure acting on it. The rise in LOS pressure relative to IGP, as well as atmospheric pressure, may be explained by reflex contraction of the crural diaphragm which has been previously observed with increased intra-abdominal pressure caused by abdominal constriction by belt or leg-raising.

Again, unlike increased WC, the waist belt caused proximal displacement of the LOS high pressure zone, though this was only apparent after the meal. The lower and upper borders of the LOS plus peak LOS were all displaced proximally about 1 - 2 cm consistent with displacement of the diaphragmatic hiatus. The lack of this diaphragmatic displacement with increased WC might again be due to its more chronic onset, allowing the diaphragmatic crura to strengthen and maintain its normal position.

Similar to increased WC, the belt caused proximal displacement of the SCJ relative to the nares. The SCJ with the belt following a meal was also displaced proximally with respect to the peak LOS pressure. This indicates that the belt was displacing the GOJ proximally within the displaced hiatus similar to increased WC but, in addition, waist belt was also displacing the whole hiatus proximally. Consistent with the more proximal location of the GOJ, the proximal migration of the SCJ during TLOSRS was also reduced by the belt.

Unlike increased WC, the belt resulted in a slowing of the rate of the initial phase of descent of the GOJ during TLOSRS. This phase of movement is thought to represent the elastic recoil of the POL as we have previously shown. The rate of elastic recoil is directly proportional to its amplitude of stretch. The effect of the belt elevating the diaphragmatic crura to which the POL is attached, will mean that it is less stretched during its proximal displacement and thus explain its reduced rate of initial descent.

Similar to the effects of increased WC, the belt caused the gastric pH transition point to move more proximally within the LOS with respect to both the SCJ and peak LOS pressure. The proximal movement of the pH transition point was more marked with the belt bringing it to the level of the SCJ after the meal. In addition, with the belt after the meal, the pH transition point was 1.3 cm above the peak LOS pressure point compared to 1.3 cm below this point without the belt. This indicates that the belt was proximally displacing the GOJ within the diaphragmatic hiatus to an extent that meant that the

proximal acid secreting gastric mucosa was lying proximal to the peak LOS pressure. Further evidence of the proximal acid-secreting mucosa lying above the peak LOS pressure is the observation that the SCJ after the meal with the belt was also 1.9 cm above the peak pressure point and in *H. pylori* negative subjects the acid secreting mucosa starts only 1 - 3 mm distal to the SCJ.

The presence of gastric acid secreting mucosa proximal to the point of peak LOS pressure has major pathophysiological implications. Even with a closed LOS, any acid present above the peak pressure point will migrate upwards towards the oesophagus rather than downwards towards the stomach with the peak pressure point functioning as a water-shed. This will expose the most distal oesophageal squamous mucosa, even when lying within closed sphincter to a gastric-type luminal environment which will damage it and promote its metaplasia to a columnar type mucosa suited to an acidic environment.

The belt also differed from increased WC by inducing increased short segment acid reflux at 1.5 cm and 3.0 cm above the pH transition point or 1.6 cm and 2.3 cm above the SCJ. This short segment reflux was related to TLOSRS and was due to increase acid reflux during TLOSRS and subsequent delay clearance of that acid.

What is the mechanism of the short segment reflux associated with the belt? The fact that our apparatus allowed constant monitoring of both the location of the SCJ and GO pH, it cannot be attributed to artefacts related to proximal migration of the pH sensor. It is known that the disruption of the juxta positioning of the intrinsic plus extrinsic sphincter in full hiatus hernia causes increased acid reflux and impaired clearance. It seems likely that the proximal displacement of the GOJ within the hiatus associated with the belt may be having a similar effect. In addition, the presence of acid secreting gastric mucosa above the peak LOS pressure point may contribute to short segment reflux during TLOSRS. The reduced volume of acid due to it being

contained within the contracted sphincter may allow it to reflux only a short distance above the SCJ.

Most marked disturbances in the GOJ were observed with the combination of increased WC and abdominal belt. In such subjects, the gastric pH transition point and the SCJ were both displaced above the peak LOS pressure point. Furthermore, the pH transition point was also proximal to the SCJ. This is likely to be due to the acid secreted by the gastric mucosa lying proximal to the peak sphincter pressure point flowing up on to the squamous mucosa. The combination of increased WC and waist belt was also associated with a marked degree of short segment acid reflux.

## 7.5 SUMMARY AND CONCLUSION

Epidemiological evidence suggests an association between obesity and hiatus hernia but mechanism is unclear. A detailed study was performed to assess on the structure and function of the GOJ in asymptomatic healthy subjects with and without obesity and the effects of elevating IAP with abdominal belt. Sixteen subjects were recruited to achieve two groups defined by normal (eight non-obese) or increased (eight obese) waist circumference and matched for age and gender. Combined assembly of 3D-GOJ locator probe, high definition 12-channel pH catheter and 36-channel slimline HRM was used to measure the function and anatomical locations within the GOJ.

Our studies demonstrate that increased WC and waist belt caused marked changes in the functioning of the GOJ and LOS which leads to increased gastric acid penetration within the high pressure zone. This appears to occur by retrograde flow within the closed sphincter and by increased short segment reflux during TLOSRS and subsequent impaired clearance. This increased intra-sphincteric acid exposure is occurring in asymptomatic volunteers and may explain the high incidence of inflammation and columnar metaplasia observed at the gastro-oesophageal junction in asymptomatic subjects. Our observations may also be relevant to the aetiology of adenocarcinoma of the cardia which shares epidemiological risk factors of the

oesophageal adenocarcinoma but has a much weaker association with reflux symptoms.

# CHAPTER 8

## CONCLUSIONS AND FUTURE STUDIES

---

- 8.1 Summary and conclusions
- 8.2 Limitations and challenges
- 8.3 What the future beholds?

## 8 CONCLUSIONS AND FUTURE STUDIES

### 8.1 SUMMARY AND CONCLUSIONS

Both in-vitro and in-vivo studies indicate that it is possible to monitor the position of the SCJ by means of clipping a magnet to it and which is detected by a linear probe consisting of a series of Hall Effect sensors. The accuracy for position detection of the SCJ was superior to 10 mm and the proportion of recording time having signal strength above 10 mV was 96.8%. The new technique compared favourably to fluoroscopy in the detection of position with correlation co-efficient of 0.96. The locator probe could be applied over much longer periods because of the radiation risk associated with fluoroscopy.

Three factors were identified from in-vitro studies which could limit accuracy of the initial 2-D Hall-Effect probe. These factors included poor magnet orientation and distance, the effect of temperature, and the presence of other ferromagnetic materials. In a further development, a new Hall Effect-based probe was developed and this allowed an almost 3-D detection of the magnet. This was later replaced by a tri-axial magneto-resistive based probe allowing true 3-D detection of position, and this is currently under development. The temperature effect on the 2-D and 3-D probes could be reduced by calibrating the probes in a water bath heated to body temperature prior to intubation. The use of 2.7 mm HRM sensors reduced the ferromagnetic effects on the locator probe array.

The use of the 2-D locator probe and the 4.2 mm 36-channel HRM probe, allowed detailed examination of the migration of the SCJ during TLOSRS and swallows in 12 healthy subjects. Proximal displacement of the SCJ was present transiently during TLOSRS and swallows, but the displacement of up to 9 cm during TLOSRS represented very severe herniation of the GOJ. In addition, there was a rapid initial return of the SCJ following transient LOSR when the CD was relaxed, and its correlation with amplitude suggested it was due to elastic recoil of the POL. This marked stretching of the POL during

TLOSRS may contribute to its weakening and development of established hiatus hernia.

Using the 3-D locator, 2.7 mm 35-channel HRM probe and 12-channel pH probe, a detailed examination on the structure, function and acid exposure within the GOJ in asymptomatic healthy subjects with (8 subjects) and without (8 subjects) obesity and the effect of elevating the IAP with belt was performed. Obesity was associated with an elevated GOPG, but, due to an equivalent pressure rise in both IGP and IOP, the GOPG was not affected by the use of a waist belt. Both obesity and the waist belt were shown to displace proximally both the SCJ and markers of diaphragmatic position, but with a greater proximal displacement of the SCJ. This separation suggested a partial hiatus herniation occurring in asymptomatic individuals with central obesity, and this is accentuated with the belt constriction. There was a proximal shift of gastric mucosa into the lower sphincter as evidenced by a proximal shift of pH transition point. Short segment reflux, instead of trans-sphincteric acid reflux, occurred with the application of the belt and it resulted from increased reflux episodes during TLOSRS and a delay in clearing the refluxed acid.

As a conclusion, a new technology has been developed allowing an accurate and prolonged detection of the position of the SCJ without any radiation risk. The new technology was used alongside 36-channel HRM and high definition 12-channel pH catheter to study the function of the GOJ in healthy volunteers. Our finding showed that in TLOSRS in healthy volunteers, there was transient but severe herniation of the GOJ. Also in a group of asymptomatic healthy volunteers, lifestyle factors i.e. central obesity and waist belt could cause partial hiatus herniation, and that a waist belt also caused short segment reflux.

## **8.2 LIMITATIONS AND CHALLENGES**

The new technology involved the deployment of a small magnet at the SCJ during upper endoscopy. Not all subjects could tolerate upper endoscopy,

and the deployment of magnet could be technically challenging due to the anatomy of the GOJ. The magnet could affect the function of LOS but due to its small size (unlike the Bravo Capsule), the effect was negligible. It is advisable to only deploy one magnet at a time or to avoid clipping a further magnet if one fails to attach unless it can be retrieved. This is to avoid the potential of having two magnets free within the lumen of the intestines and the consequent risk of them attaching to each other between two loops of bowel. However, the great majority of study subjects cleared their magnet spontaneously within 6 - 8 weeks. The presence of a magnet may pose a risk if study subjects were planned to have a MRI examination before the magnet is spontaneously cleared. Currently, no studies have addressed this issue.

The limitations of Hall Effect-based probe were discussed in section 8.1 above. Development of probes having 3-D capabilities has been challenging. Suitable 3-D sensors have only recently become available. However, the 3-D Hall Effect-based probe used in the current study did not last long before it malfunctioned. As a result, clinical studies were interrupted. In addition, the locator probe only measured the position and movement of the GOJ. For detailed study on physiology and pathophysiology of diseases related to the GOJ, the locator needs to be used alongside other probes including manometry, pH or impedance. Prolonged studies, beyond 2 hours, were not been possible as the locator and manometry probes were not available in an ambulatory version yet. Combining these probes would increase the overall diameter and could cause difficulty and discomfort during nasal intubation. Thus, some study subjects withdrew from the studies due to failure of intubation. Due to limitations of the resolution of Hall Effect sensors, some data collected from the studies described in chapter 5 had to be abandoned from subsequent analysis. In addition, due to different systems for each type of catheter, there was a need to synchronise the systems and a custom program was required to capture and store the data for future analysis.

The movement of the clip could have been due to shear distortion of mucosa, and not to true shortening of the longitudinal muscle of the oesophagus. However, subsequent studies showed that this was not the case.

It was also possible that relative movements between catheters introduce errors. Relative movement between catheters was prevented using adhesives to combine the probes into a single unit.

Studies described in chapter 6 and 7 excluded patients having hiatus hernia as controls and this constituted a limitation. In chapter 6, it was proposed that TLOSRS represented transient but severe herniation of the GOJ above the diaphragmatic hiatus based on the migration patterns of the SCJ we have observed among a group of healthy subjects. TLOSRS are physiological events occurring frequently at all times whereas hiatus hernia only occurs in 30% of the population, and, therefore it may difficult to link the two. It is known that many factors contribute to the pathogenesis of hiatus hernia including weakness of the POL as part of the aging process. The excessive amount of shortening of the GOJ observed during TLOSRS might, over time, lead to weakness of the POL. Having a group of subjects with hiatal hernia as control group may demonstrate the reduced shortening of the GOJ associated with TLOSRS. This finding may have been similar to a previous report which showed an attenuation of shortening in peristalsis among subjects with hiatus hernia (P J Kahrilas *et al.*, 1995). In chapter 7, it was shown that, in a group of asymptomatic healthy volunteers, lifestyle factors i.e. central obesity and a waist belt, could cause partial hiatus herniation, and that the waist belt also caused short segment reflux. It was intended to include more subjects with hiatus hernia and GORD for this study, but unfortunately, data collection was prematurely terminated due to problems with the 3D locator probe.

Another unanswered controversy is the sequence of events involved in the opening of the GOJ during TLOSRS. Animal studies have indicated that shortening of the GOJ precedes GOR, but using concurrent video-endoscopy and manometry, it has been observed that shortening of the GOJ occurs after opening of the GOJ during TLOSRS. Using concurrent fluoroscopy and the HRM technique, the proximal movement of the GOJ is observed to occur following relaxation of the LOS. However, using intra-luminal ultrasound, the longitudinal muscle contraction is seen to precede the relaxation of the LOS.

Data from the current studies agree with the former observation but further studies are needed. These might involve the use of a high resolution multi-channel impedance probe alongside the GOJ locator probe and HRM. The impedance probe allows detection of flow indicating the start of the opening of the GOJ while the locator probe provides reliable information on initiation of the GOJ movement.

### 8.3 WHAT THE FUTURE BEHOLDS?

One of the possibilities using the new 3-D locator probe is to have an ambulatory system allowing the locator to be used alongside the pH-impedance catheter (**Figure 8.1**). Having knowledge of the location and movement of the SCJ in relation to pH and impedance changes may allow the assessment of short segment reflux on symptoms of GORD. Spontaneous oesophageal longitudinal muscle contraction has been found to be associated with chest symptoms. With an ambulatory locator system, the contraction episodes could be documented over 24 - 48 hours.

A further possibility is to have a system allowing continuous monitoring of the GOJ location and movement without the need to pass a catheter. It was noted a number of years ago that pharyngeal stimulation may increase the frequency of TLOSRS (Mittal *et al.*, 1992). Our current knowledge of TLOSRS is entirely based on intubation studies and therefore the prospect to artefacts produced by catheter technique. The ability to record movement without manometric intubation could allow, for the first time, the documentation of TLOSRS under more physiological conditions. This may also resolve the issue on rate inconsistencies of TLOSRS seen in many studies on GORD (D Sifrim and R Holloway, 2001).

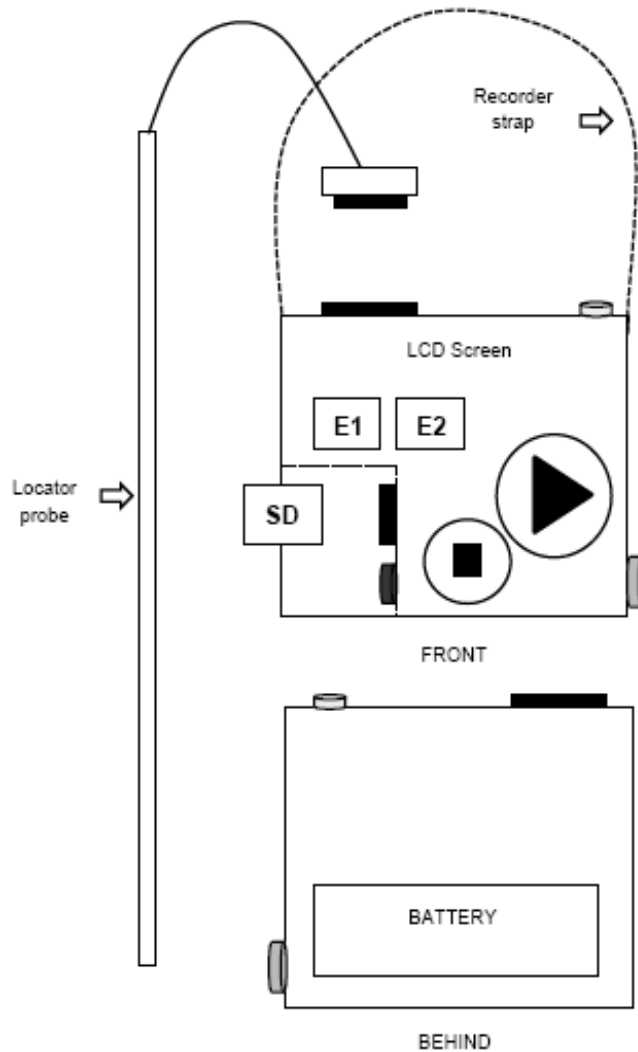


**Figure 8.1:** A schematic of the envisaged ambulatory locator system. Legends: E1 and E2; events button, SD; slot for memory card.

Such a technique may soon become available since a non-luminal based device is currently in development allowing measurement of location of the GOJ outside of study subjects (Whiting *et al.*, 2012) (**Figure 8.2**). This is a project in collaboration with the Biomedical Engineering Department at the University of Strathclyde, Glasgow, UK. A highly sensitive Hall Effect sensor (AHS P15 GaAs, AHS, UK), coupled with alternating current (AC) driving system, can be utilised to improve system's magnetic detection rate.

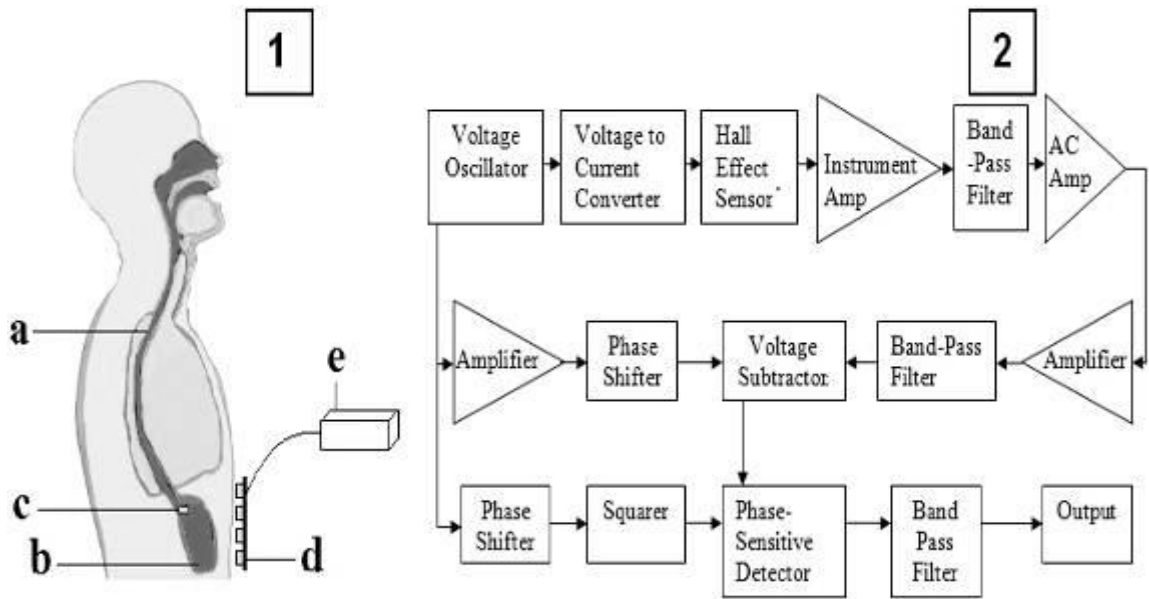


**Figure 8.2:** Non-luminal external locator technique. Left (1) an illustration depicting the anatomy and technology for the external Hall Effect locator probe. Legend: (a) the esophagus, (b) the stomach, (c) magnet, (d) highly sensitive Hall Effect sensors and (e) AC circuitry. Right (2); a schematic of the AC circuit is shown.

The output is amplified and band-pass filtered at the driving frequency then subtracted from a phase matched driving AC signal, producing a sine wave with amplitude proportional to the magnetic field. Besides reducing output noise to improve sensitivity, flux concentrators can be used to passively amplify the magnetic field. Simulations and bench-top testing have shown that the detection range of the new probe is up to 10.2 cm and this translates to a signal improvement of 580% compared to commercially available sensors. The development has so far been encouraging and a prototype may soon be available for in-vivo studies.

To conclude, the new locator technique will be very powerful in both research and clinical applications. Further studies should allow a greater understanding of the detailed behaviour of GOJ migration during TLOSRS in various conditions associated with GORD including reflux oesophagitis, hiatus hernia and Barrett's oesophagus. It is appealing for this technique to be made ambulatory and incorporated with pH or impedance sensors, thereby allowing

continuous measurement of the GOJ and reflux over 24 - 48 hours. Sustained oesophageal contractions were found to be associated with heartburn and acid reflux, and this can be studied in more detailed with the new technique. With the advent of pharmacologic therapy against TLOSRS, this technique can be an alternative to or an addition to manometry in the assessment of therapeutic response.

## LIST OF REFERENCES

- Altschuler, S.M., Boyle, J.T., Nixon, T.E., Pack, A.I., Cohen, S. (1985) Simultaneous reflex inhibition of lower esophageal sphincter and crural diaphragm in cats. *The American journal of physiology*. **249**(5 Pt 1), G586-91.
- Asling, B., Jirholt, J., Hammond, P., Knutsson, M., Walentinsson, A., Davidson, G., Agreus, L., Lehmann, A., Lagerström-Fermer, M. (2009) Collagen type III alpha I is a gastro-oesophageal reflux disease susceptibility gene and a male risk factor for hiatus hernia. *Gut*. **58**(8), 1063-9.
- Ayazi, S., Crookes, P.F. (2010) High-resolution esophageal manometry: using technical advances for clinical advantages. *Journal of gastrointestinal surgery: official journal of the Society for Surgery of the Alimentary Tract*. **14 Suppl 1**, S24-32.
- Babaei, Arash, Bhargava, Valmik, Korsapati, H., Zheng, W.H., Mittal, Ravinder K (2008) A unique longitudinal muscle contraction pattern associated with transient lower esophageal sphincter relaxation. *Gastroenterology*. **134**(5), 1322-31.
- Beaumont, H., Bennink, R.J., De Jong, J., Boeckstaens, G.E. (2010) The position of the acid pocket as a major risk factor for acidic reflux in healthy subjects and patients with GORD. *Gut*. **59**(4), 441-51.
- Blaser, M.J., Saito, D. (2002) Trends in reported adenocarcinomas of the oesophagus and gastric cardia in Japan. *European journal of gastroenterology & hepatology*. **14**(2), 107-13.
- Botterweck, A.A., Schouten, L.J., Volovics, A., Dorant, E., Van Den Brandt, P.A. (2000) Trends in incidence of adenocarcinoma of the oesophagus and gastric cardia in ten European countries. *International journal of epidemiology*. **29**(4), 645-54.
- Bredenoord, a J., Weusten, B L a M, Timmer, R, Smout, a J.P.M. (2005) Sleeve sensor versus high-resolution manometry for the detection of transient lower esophageal sphincter relaxations. *American journal of physiology. Gastrointestinal and liver physiology*. **288**(6), G1190-4.
- Bredenoord, A J, Weusten, B.L.A.M., Carmagnola, S., Smout, A J P M (2004) Double-peaked high-pressure zone at the esophagogastric junction in controls and in patients with a hiatal hernia: a study using high-resolution manometry. *Digestive diseases and sciences*. **49**(7-8), 1128-35.
- Bredenoord, Albert J, Weusten, Bas L a M, Timmer, Robin, Smout, André J P M (2006) Intermittent spatial separation of diaphragm and lower esophageal sphincter favors acidic and weakly acidic reflux. *Gastroenterology*. **130**(2), 334-40.
- Brown, L.M., Devesa, S.S., Chow, W.-H. (2008) Incidence of adenocarcinoma of the esophagus among white Americans by sex, stage, and age. *Journal of the National Cancer Institute*. **100**(16), 1184-7.

- Caruso, M.J., Bratland, T., Smith, C.H., Schneider, R. (1998) A New Perspective on Magnetic Field Sensing. *Sensors*. **15**, 34-47.
- Cheung, T.K., Wong, B.C.Y., Lam, S.K. (2008) Gastro-oesophageal reflux disease in Asia : birth of a “new” disease? *Drugs*. **68**(4), 399-406.
- Clark, M.D., Rinaldo, J.A., Eyler, W.R. (1970) Correlation of manometric and radiologic data from the esophagogastric area. *Radiology*. **94**(2), 261-70.
- Clarke, A T., Wirz, a a, Seenan, J P, Manning, J.J., Gillen, D., McColl, K E L (2009) Paradox of gastric cardia: it becomes more acidic following meals while the rest of stomach becomes less acidic. *Gut*. **58**(7), 904-9.
- Clarke, A.T., Wirz, A A, Manning, J.J., Ballantyne, S.A., Alcorn, D.J., McColl, K E L (2008) Severe reflux disease is associated with an enlarged unbuffered proximal gastric acid pocket. *Gut*. **57**(3), 292-7.
- Clouse, R.E., Staiano, A. (1991) Topography of the esophageal peristaltic pressure wave. *The American journal of physiology*. **261**(4 Pt 1), G677-84.
- Cobb, W.S., Burns, J.M., Kercher, K.W., Matthews, B.D., James Norton, H., Todd Heniford, B. (2005) Normal intraabdominal pressure in healthy adults. *The Journal of surgical research*. **129**(2), 231-5.
- Code, C.F., Fyke, F.E., Schlegel, J.F. (1956) The gastroesophageal sphincter in healthy human beings. *Gastroenterologia*. **86**(3), 135-50.
- Cohen, S., Harris, L.D. (1970) Lower esophageal sphincter pressure as an index of lower esophageal sphincter strength. *Gastroenterology*. **58**(2), 157-62.
- Collen, M.J., Johnson, D A, Sheridan, M.J. (1994) Basal acid output and gastric acid hypersecretion in gastroesophageal reflux disease. Correlation with ranitidine therapy. *Digestive diseases and sciences*. **39**(2), 410-7.
- Cook, I.J. (1991) Normal and disordered swallowing: new insights. *Baillière’s clinical gastroenterology*. **5**(2), 245-67.
- Corley, D.A., Kubo, A., Zhao, W. (2008) Abdominal obesity and the risk of esophageal and gastric cardia carcinomas. *Cancer epidemiology, biomarkers & prevention: a publication of the American Association for Cancer Research, cosponsored by the American Society of Preventive Oncology*. **17**(2), 352-8.
- Curci, J.A., Melman, L.M., Thompson, R.W., Soper, N.J., Matthews, B.D. (2008) Elastic fiber depletion in the supporting ligaments of the gastroesophageal junction: a structural basis for the development of hiatal hernia. *Journal of the American College of Surgeons*. **207**(2), 191-6.
- Darendeliler, M.A., Darendeliler, A., Mandurino, M. (1997) Clinical application of magnets in orthodontics and biological implications: a review. *European journal of orthodontics*. **19**(4), 431-42.

- Demeester, S.R. (2009) Epidemiology and biology of esophageal cancer. *Gastrointestinal cancer research : GCR*. 3(2 Suppl), S2-5.
- Dent, J. (1976) A new technique for continuous sphincter pressure measurement. *Gastroenterology*. 71, 263-271.
- Dent, J., Dodds, W.J., Friedman, R.H., Sekiguchi, T., Hogan, W.J., Arndorfer, R.C., Petrie, D.J. (1980) Mechanism of gastroesophageal reflux in recumbent asymptomatic human subjects. *The Journal of clinical investigation*. 65(2), 256-67.
- Derakhshan, M H, Liptrot, S., Paul, J., Brown, I.L., Morrison, D., McColl, K E L (2009) Oesophageal and gastric intestinal-type adenocarcinomas show the same male predominance due to a 17 year delayed development in females. *Gut*. 58(1), 16-23.
- Derakhshan, Mohammad H, Robertson, Elaine V, Fletcher, Jonathan, Jones, G.-R., Lee, Yeong Yeh, Wirz, Angela A, McColl, Kenneth E L (2012) Mechanism of association between BMI and dysfunction of the gastro-oesophageal barrier in patients with normal endoscopy. *Gut*. 61(3), 337-43.
- Diamant, N.E. (1989) Physiology of esophageal motor function. *Gastroenterology clinics of North America*. 18(2), 179-94.
- DiLorenzo, C., Dooley, C.P., Valenzuela, J.E. (1989) Response of lower esophageal sphincter to alterations of intraabdominal pressure. *Digestive diseases and sciences*. 34(10), 1606-10.
- Dodds, W.J., Hogan, W.J., Miller, W.N., Stef, J.J., Arndorfer, R.C., Lydon, S.B. (1975) Effect of increased intraabdominal pressure on lower esophageal sphincter pressure. *The American journal of digestive diseases*. 20(4), 298-308.
- Dodds, W.J., Stewart, E.T., Hodges, D., Zboralske, F.F. (1973) Movement of the feline esophagus associated with respiration and peristalsis. An evaluation using tantalum markers. *The Journal of clinical investigation*. 52(1), 1-13.
- Dogan, I., Bhargava, Valmik, Liu, Jianmin, Mittal, Ravinder K (2007) Axial stretch: A novel mechanism of the lower esophageal sphincter relaxation. *American journal of physiology. Gastrointestinal and liver physiology*. 292(1), G329-34.
- Dunne, D.P., Paterson, W G (2000) Acid-induced esophageal shortening in humans: a cause of hiatus hernia? *Canadian journal of gastroenterology = Journal canadien de gastroenterologie*. 14(10), 847-50.
- Edmundowicz, S.A., Clouse, R.E. (1991) Shortening of the esophagus in response to swallowing. *The American journal of physiology*. 260(3 Pt 1), G512-6.
- El-Serag, H., Hill, C., Jones, R. (2009) Systematic review: the epidemiology of gastro-oesophageal reflux disease in primary care, using the UK General

Practice Research Database. *Alimentary pharmacology & therapeutics*. **29**(5), 470-80.

El-Serag, H.B. (2005) Obesity and disease of the esophagus and colon. *Gastroenterology clinics of North America*. **34**(1), 63-82.

El-Serag, H.B., Ergun, G. a, Pandolfino, J., Fitzgerald, S., Tran, T., Kramer, J.R. (2007) Obesity increases oesophageal acid exposure. *Gut*. **56**(6), 749-55.

El-Serag, H.B., Tran, T., Richardson, P., Ergun, G. (2006) Anthropometric correlates of intragastric pressure. *Scandinavian journal of gastroenterology*. **41**(8), 887-91.

Eriksen, C.A., Cullen, P.T., Sutton, D., Kennedy, N., Cuschieri, A. (1991) Abnormal esophageal transit in patients with typical reflux symptoms but normal endoscopic and pH profiles. *American journal of surgery*. **161**(6), 657-61.

Fei, L., Del Genio, G., Rossetti, G., Sampaolo, S., Moccia, F., Trapani, V., Cimmino, M., Del Genio, A. (2009) Hiatal hernia recurrence: surgical complication or disease? Electron microscope findings of the diaphragmatic pillars. *Journal of gastrointestinal surgery : official journal of the Society for Surgery of the Alimentary Tract*. **13**(3), 459-64.

Feldman, M.J., Morris, G.P., Dinda, P.K., Paterson, W G (1996) Mast cells mediate acid-induced augmentation of opossum esophageal blood flow via histamine and nitric oxide. *Gastroenterology*. **110**(1), 121-8.

Fletcher, J, Wirz, A, Henry, E., McColl, K E L (2004) Studies of acid exposure immediately above the gastro-oesophageal squamocolumnar junction: evidence of short segment reflux. *Gut*. **53**(2), 168-73.

Fletcher, Jonathan, Derakhshan, Mohammad H, Jones, G.-R., Wirz, Angela A, McColl, Kenneth E L (2011) BMI is superior to symptoms in predicting response to proton pump inhibitor: randomised trial in patients with upper gastrointestinal symptoms and normal endoscopy. *Gut*. **60**(4), 442-8.

Fletcher, Jonathan, Wirz, Angela, Young, J., Vallance, R., McColl, Kenneth E.L. (2001) Unbuffered Highly Acidic Gastric Juice Exists at the Gastroesophageal Junction After a Meal. *Gastroenterology*. **121**(4), 775-783.

Freedman, N.D., Derakhshan, M H, Abnet, C.C., Schatzkin, A., Hollenbeck, A.R., McColl, K E L (2010) Male predominance of upper gastrointestinal adenocarcinoma cannot be explained by differences in tobacco smoking in men versus women. *European journal of cancer (Oxford, England : 1990)*. **46**(13), 2473-8.

Friedland, G.W. (1978) Progress in radiology: historical review of the changing concepts of lower esophageal anatomy: 430 B.C.--1977. *AJR. American journal of roentgenology*. **131**(3), 373-8.

Fusco, M.A., Martin, R.S., Chang, M.C. (2001) Estimation of intra-abdominal pressure by bladder pressure measurement: validity and methodology. *The Journal of trauma*. **50**(2), 297-302.

Gajperia, C., Barbieri, J.M., Greenberg, D., Wright, K., Lyratzopoulos, G. (2009) Recent incidence trends and sociodemographic features of oesophageal and gastric cancer types in an English region. *Alimentary pharmacology & therapeutics*. **30**(8), 873-80.

Gawron, A.J., Hirano, I. (2010) Advances in diagnostic testing for gastroesophageal reflux disease. *World journal of gastroenterology: WJG*. **16**(30), 3750-6.

Gill, K.R.S., Pooley, R.A., Wallace, M.B. (2009) Magnetic resonance imaging compatibility of endoclips. *Gastrointestinal endoscopy*. **70**(3), 532-6.

Granström, L., Backman, L. (1985) Stomach distension in extremely obese and in normal subjects. *Acta chirurgica Scandinavica*. **151**(4), 367-70.

Harris, L.D., Pope, C.E. (1966) The pressure inversion point: its genesis and reliability. *Gastroenterology*. **51**(5), 641-8.

Hill, L.D., Kozarek, R.A. (1999) The gastroesophageal flap valve. *Journal of clinical gastroenterology*. **28**(3), 194-7.

Holloway, R.H. (2000) The anti-reflux barrier and mechanisms of gastro-oesophageal reflux. *Baillière's best practice & research. Clinical gastroenterology*. **14**(5), 681-99.

Holloway, R.H., Boeckxstaens, G.E.E., Penagini, R., Sifrim, D.A., Smout, A J P M (2012) Objective definition and detection of transient lower esophageal sphincter relaxation revisited: is there room for improvement? *Neurogastroenterology & Motility*. **24**, 54-60.

Holloway, R.H., Penagini, R., Ireland, a C. (1995) Criteria for objective definition of transient lower esophageal sphincter relaxation. *The American journal of physiology*. **268**(1 Pt 1), G128-33.

Iovino, P., Angrisani, L., Galloro, G., Consalvo, D., Tremolaterra, F., Pascariello, A., Ciacci, C. (2006) Proximal stomach function in obesity with normal or abnormal oesophageal acid exposure. *Neurogastroenterology and motility: the official journal of the European Gastrointestinal Motility Society*. **18**(6), 425-32.

Iqbal, A., Haider, M., Stadlhuber, R.J., Karu, A., Corkill, S., Filipi, C.J. (2008) A study of intragastric and intravesicular pressure changes during rest, coughing, weight lifting, retching, and vomiting. *Surgical endoscopy*. **22**(12), 2571-5.

Jaffin, B.W., Knoepflmacher, P., Greenstein, R. (1999) High prevalence of asymptomatic esophageal motility disorders among morbidly obese patients. *Obesity surgery*. **9**(4), 390-5.

Jamieson, J.R., Stein, H.J., DeMeester, T.R., Bonavina, L., Schwizer, W., Hinder, R.A., Albertucci, M. (1992) Ambulatory 24-h esophageal pH monitoring: normal values, optimal thresholds, specificity, sensitivity, and reproducibility. *The American journal of gastroenterology*. **87**(9), 1102-11.

Jiang, Y., Bhargava, Valmik, Mittal, Ravinder K (2009) Mechanism of stretch-activated excitatory and inhibitory responses in the lower esophageal sphincter. *American journal of physiology. Gastrointestinal and liver physiology*. **297**(2), G397-405.

Johnson, L.F., Demeester, T.R. (1974) Twenty-four-hour pH monitoring of the distal esophagus. A quantitative measure of gastroesophageal reflux. *The American journal of gastroenterology*. **62**(4), 325-32.

Johnston, B.T., McFarland, R.J., Collins, J.S., Love, A.H. (1992) Symptom index as a marker of gastro-oesophageal reflux disease. *The British journal of surgery*. **79**(10), 1054-5.

Jones, M.P., Sloan, S.S., Rabine, J.C., Ebert, C.C., Huang, C.F., Kahrilas, P J (2001) Hiatal hernia size is the dominant determinant of esophagitis presence and severity in gastroesophageal reflux disease. *The American journal of gastroenterology*. **96**(6), 1711-7.

Jung, H.-K. (2011) Epidemiology of gastroesophageal reflux disease in Asia: a systematic review. *Journal of neurogastroenterology and motility*. **17**(1), 14-27.

Kahrilas, P J, Dodds, W.J., Hogan, W.J. (1988) Effect of peristaltic dysfunction on esophageal volume clearance. *Gastroenterology*. **94**(1), 73-80.

Kahrilas, P J, Lin, S., Chen, J., Manka, M. (1999) The effect of hiatus hernia on gastro-oesophageal junction pressure. *Gut*. **44**(4), 476-482.

Kahrilas, P J, Wu, S., Lin, S., Poudroux, P. (1995) Attenuation of esophageal shortening during peristalsis with hiatus hernia. *Gastroenterology*. **109**(6), 1818-25.

Kahrilas, Peter J (2003) GERD pathogenesis, pathophysiology, and clinical manifestations. *Cleveland Clinic journal of medicine*. **70** Suppl 5, S4-19.

Kahrilas, Peter J, Ghosh, S.K., Pandolfino, John E (2008) Challenging the limits of esophageal manometry. *Gastroenterology*. **134**(1), 16-8.

Kahrilas, Peter J, Kim, H.C., Pandolfino, John E (2008) Approaches to the diagnosis and grading of hiatal hernia. *Best practice & research. Clinical gastroenterology*. **22**(4), 601-16.

Kahrilas, Peter J, Sifrim, Daniel (2008) High-resolution manometry and impedance-pH/manometry: valuable tools in clinical and investigational esophagology. *Gastroenterology*. **135**(3), 756-69.

Keenan, K., Grant, I., Ramsay, J. (2011) *The Scottish Health Survey - Obesity*.

Kim, K.-M., Cho, Y.K., Bae, S.J., Kim, D.-S., Shim, K.-N., Kim, J.-H., Jung, S.W., Kim, N. (2012) Prevalence of gastroesophageal reflux disease in Korea and associated health-care utilization: a national population-based study. *Journal of gastroenterology and hepatology*. **27**(4), 741-5.

Kuiken, S., Van Den Elzen, B., Tytgat, G., Bennink, R., Boeckxstaens, G. (2002) Evidence for pooling of gastric secretions in the proximal stomach in humans using single photon computed tomography. *Gastroenterology*. **123**(6), 2157-8; author reply 2158.

Kuribayashi, S., Massey, B.T., Hafeezullah, M., Perera, L., Hussaini, S.Q., Tatro, L., Darling, R.J., Franco, R., Shaker, R. (2009) Terminating motor events for TLESR are influenced by the presence and distribution of refluxate. *American journal of physiology. Gastrointestinal and liver physiology*. **297**(1), G71-5.

Kwiatek, M A, Pandolfino, J E, Kahrilas, P J (2011) 3D-high resolution manometry of the esophagogastric junction. *Neurogastroenterology and motility: the official journal of the European Gastrointestinal Motility Society*. **23**(11), e461-9.

Kwiatek, Monika A, Nicodème, F., Pandolfino, John E, Kahrilas, Peter J (2012) Pressure morphology of the relaxed lower esophageal sphincter: the formation and collapse of the phrenic ampulla. *American journal of physiology. Gastrointestinal and liver physiology*. **302**(3), G389-96.

Kwok, H., Marriz, Y., Al-Ali, S., Windsor, J.A. (1999) Phrenoesophageal ligament re-visited. *Clinical anatomy (New York, N.Y.)*. **12**(3), 164-70.

Labounty, T.M., Gomez, M.J., Achenbach, S., Al-Mallah, M., Berman, D.S., Budoff, M.J., Cademartiri, F., Callister, T.Q., Chang, H.-J., Cheng, V., Chinnaiyan, K.M., Chow, B., Cury, R., Delago, A., Dunning, A., Feuchtner, G., Hadamitzky, M., Hausleiter, J., Kaufmann, P., Kim, Y.-J., Leipsic, J., Lin, F.Y., Maffei, E., Raff, G., Shaw, L.J., Villines, T.C., Min, J.K. (2012) Body mass index and the prevalence, severity, and risk of coronary artery disease: an international multicentre study of 13 874 patients. *European heart journal cardiovascular Imaging*.

Lam, H.G., Breumelhof, R., Roelofs, J.M., Van Berge Henegouwen, G.P., Smout, A.J. (1994) What is the optimal time window in symptom analysis of 24-hour esophageal pressure and pH data? *Digestive diseases and sciences*. **39**(2), 402-9.

Lee, Y. Y., Whiting, J. G. H., Robertson, E. V., Derakhshan, M. H., Wirz, A. A., Smith, D., Morrison, D., Kelman, A., Connolly, P., McColl, K. E. L. (2012) Kinetics of transient hiatus hernia during transient lower esophageal sphincter relaxations and swallows in healthy subjects. *Neurogastroenterology and motility: the official journal of the European Gastrointestinal Motility Society*. **24**(11), 990-e539.

Lee, Yeong Yeh, Seenan, John P, Whiting, James G H, Robertson, Elaine V, Derakhshan, Mohammad H, Wirz, Angela A, Smith, Donald, Hardy, C., Kelman, Andrew, Connolly, Patricia, McColl, Kenneth E L (2012) Development

and validation of a probe allowing accurate and continuous monitoring of location of squamo-columnar junction. *Medical engineering & physics*. **34**(3), 279-89.

Lin, S., Brasseur, J G, Pouderoux, P., Kahrilas, P J (1995) The phrenic ampulla: distal esophagus or potential hiatal hernia? *The American journal of physiology*. **268**(2 Pt 1), G320-7.

Lind, J.F., Warrian, W.G., Wankling, W.J. (1966) Responses of the gastroesophageal junctional zone to increases in abdominal pressure. *Canadian journal of surgery. Journal canadien de chirurgie*. **9**(1), 32-8.

Liu, Jianmin, Pehlivanov, Nonko, Mittal, Ravinder K (2002) Baclofen blocks LES relaxation and crural diaphragm inhibition by esophageal and gastric distension in cats. *American journal of physiology. Gastrointestinal and liver physiology*. **283**(6), G1276-81.

Locke, G.R., Talley, N.J., Fett, S.L., Zinsmeister, A.R., Melton, L.J. (1997) Prevalence and clinical spectrum of gastroesophageal reflux: a population-based study in Olmsted County, Minnesota. *Gastroenterology*. **112**(5), 1448-56.

Lundell, L., Ruth, M., Sandberg, N., Bove-Nielsen, M. (1995) Does massive obesity promote abnormal gastroesophageal reflux? *Digestive diseases and sciences*. **40**(8), 1632-5.

Maddox, A., Horowitz, M., Wishart, J., Collins, P. (1989) Gastric and oesophageal emptying in obesity. *Scandinavian journal of gastroenterology*. **24**(5), 593-8.

Martin, C.J., Dodds, W.J., Liem, H.H., Dantas, R.O., Layman, R.D., Dent, J. (1992) Diaphragmatic contribution to gastroesophageal competence and reflux in dogs. *The American journal of physiology*. **263**(4 Pt 1), G551-7.

McColl, Kenneth E L, Clarke, A., Seenan, J. (2010) Acid pocket, hiatus hernia and acid reflux. *Gut*. **59**(4), 430-1.

McGill, S.M., Norman, R.W., Sharratt, M.T. (1990) The effect of an abdominal belt on trunk muscle activity and intra-abdominal pressure during squat lifts. *Ergonomics*. **33**(2), 147-160.

McNally, E.F., Kelly, J.E., Ingelfinger, F.J. (1964) Mechanism of belching: effects of gastric distension with air. *Gastroenterology*. **46**, 254-9.

Melman, L., Chisholm, P.R., Curci, J.A., Arif, B., Pierce, R., Jenkins, E.D., Brunt, L.M., Eagon, C., Frisella, M., Miller, K., Matthews, B.D. (2010) Differential regulation of MMP-2 in the gastrohepatic ligament of the gastroesophageal junction. *Surgical endoscopy*. **24**(7), 1562-5.

Menon, S., Trudgill, N. (2011) Risk factors in the aetiology of hiatus hernia: a meta-analysis. *European journal of gastroenterology & hepatology*. **23**(2), 133-8.

Meyer, G.W., Gerhardt, D.C., Castell, D.O. (1981) Human esophageal response to rapid swallowing: muscle refractory period or neural inhibition? *The American journal of physiology.* **241**(2), G129-36.

Mittal, R K, Fisher, M.J. (1990) Electrical and mechanical inhibition of the crural diaphragm during transient relaxation of the lower esophageal sphincter. *Gastroenterology.* **99**(5), 1265-8.

Mittal, R K, Holloway, R.H., Penagini, R., Blackshaw, L. a, Dent, J. (1995) Transient lower esophageal sphincter relaxation. *Gastroenterology.* **109**(2), 601-10.

Mittal, R K, Karstens, A., Leslie, E., Babaei, A, Bhargava, V (2012) Ambulatory high-resolution manometry, lower esophageal sphincter lift and transient lower esophageal sphincter relaxation. *Neurogastroenterology and motility: the official journal of the European Gastrointestinal Motility Society.* **24**(1), 40-e2.

Mittal, R K, Rochester, D.F., McCallum, R.W. (1989) Sphincteric action of the diaphragm during a relaxed lower esophageal sphincter in humans. *The American journal of physiology.* **256**(1 Pt 1), G139-44.

Mittal, R K, Stewart, W.R., Schirmer, B.D. (1992) Effect of a catheter in the pharynx on the frequency of transient lower esophageal sphincter relaxations. *Gastroenterology.* **103**(4), 1236-40.

Mittal, Ravinder K, Liu, Jianmin, Puckett, J.L., Bhalla, V., Bhargava, Valmik, Tipnis, N., Kassab, G. (2005) Sensory and motor function of the esophagus: lessons from ultrasound imaging. *Gastroenterology.* **128**(2), 487-97.

Nagler, R., Spiro, H.M. (1961) Segmental response of the inferior esophageal sphincter to elevated intragastric pressure. *Gastroenterology.* **40**, 405-7.

New, P.F., Rosen, B.R., Brady, T.J., Buonanno, F.S., Kistler, J.P., Burt, C.T., Hinshaw, W.S., Newhouse, J.H., Pohost, G.M., Taveras, J.M. (1983) Potential hazards and artifacts of ferromagnetic and nonferromagnetic surgical and dental materials and devices in nuclear magnetic resonance imaging. *Radiology.* **147**(1), 139-48.

Nicosia, M A, Brasseur, J G, Liu, J.B., Miller, L S (2011) Local longitudinal muscle shortening of the human esophagus from high-frequency ultrasonography. *American journal of physiology Gastrointestinal and liver physiology.* **281**(4), G1022-G1033.

Noar, J.H., Evans, R.D. (1999) Rare earth magnets in orthodontics: an overview. *British journal of orthodontics.* **26**(1), 29-37.

Oberg, S., Peters, J.H., DeMeester, T.R., Chandrasoma, P., Hagen, J.A., Ireland, A.P., Ritter, M.P., Mason, R.J., Crookes, P., Bremner, C.G. (1997) Inflammation and specialized intestinal metaplasia of cardiac mucosa is a manifestation of gastroesophageal reflux disease. *Annals of surgery.* **226**(4), 522-30; discussion 530-2.

- Oestreich, A.E. (2006) Danger of multiple magnets beyond the stomach in children. *Journal of the National Medical Association*. **98**(2), 277-9.
- Palmer, E. (1953) An attempt to localize the normal esophagogastric junction. *Radiology*. **60**, 825-31.
- Pandolfino, J E, Fox, M.R., Bredenoord, a J., Kahrilas, P J (2009) High-resolution manometry in clinical practice: utilizing pressure topography to classify oesophageal motility abnormalities. *Neurogastroenterology and motility: the official journal of the European Gastrointestinal Motility Society*. **21**(8), 796-806.
- Pandolfino, J E, Leslie, E., Luger, D., Mitchell, B., Kwiatek, M A, Kahrilas, P J (2010) The contractile deceleration point: an important physiologic landmark on oesophageal pressure topography. *Neurogastroenterology and motility: the official journal of the European Gastrointestinal Motility Society*. **22**(4), 395-400, e90.
- Pandolfino, John E, El-Serag, H.B., Zhang, Q., Shah, N., Ghosh, S.K., Kahrilas, Peter J (2006) Obesity: a challenge to esophagogastric junction integrity. *Gastroenterology*. **130**(3), 639-49.
- Pandolfino, John E, Ghosh, S.K., Zhang, Q., Jarosz, A., Shah, N., Kahrilas, Peter J (2006) Quantifying EGJ morphology and relaxation with high-resolution manometry: a study of 75 asymptomatic volunteers. *American journal of physiology. Gastrointestinal and liver physiology*. **290**(5), G1033-40.
- Pandolfino, John E, Schreiner, M.A., Lee, T.J., Zhang, Q., Kahrilas, Peter J (2005) Bravo capsule placement in the gastric cardia: a novel method for analysis of proximal stomach acid environment. *The American journal of gastroenterology*. **100**(8), 1721-7.
- Pandolfino, John E, Zhang, Q., Ghosh, S.K., Post, J., Kwiatek, M., Kahrilas, Peter J (2007) Acidity surrounding the squamocolumnar junction in GERD patients: "acid pocket" versus "acid film". *The American journal of gastroenterology*. **102**(12), 2633-41.
- Pandolfino, John E, Zhang, Q.G., Ghosh, S.K., Han, A., Boniquit, C., Kahrilas, Peter J (2006) Transient lower esophageal sphincter relaxations and reflux: mechanistic analysis using concurrent fluoroscopy and high-resolution manometry. *Gastroenterology*. **131**(6), 1725-33.
- Paterson, W G (1998) Role of mast cell-derived mediators in acid-induced shortening of the esophagus. *The American journal of physiology*. **274**(2 Pt 1), G385-8.
- Paterson, W G (1997) Studies on opossum esophageal longitudinal muscle function. *Canadian journal of physiology and pharmacology*. **75**(1), 65-73.
- Paterson, W G, Kolyn, D.M. (1994) Esophageal shortening induced by short-term intraluminal acid perfusion in opossum: a cause for hiatus hernia? *Gastroenterology*. **107**(6), 1736-40.

Paterson, William G, Miller, D. V, Dilworth, N., Assini, J.B., Lourenssen, S., Blennerhassett, M.G. (2007) Intraluminal acid induces oesophageal shortening via capsaicin-sensitive neurokinin neurons. *Gut*. **56**(10), 1347-52.

Pehlivanov, N, Liu, J, Mittal, R K (2001) Sustained esophageal contraction: a motor correlate of heartburn symptom. *American journal of physiology. Gastrointestinal and liver physiology*. **281**(3), G743-51.

Piper, D.W., Fenton, B.H. (1965) pH stability and activity curves of pepsin with special reference to their clinical importance. *Gut*. **6**(5), 506-8.

Pouderoux, P., Lin, S., Kahrilas, P J (1997) Timing, propagation, coordination, and effect of esophageal shortening during peristalsis. *Gastroenterology*. **112**(4), 1147-1154.

Quiroga, E., Cuenca-Abente, F., Flum, D., Dellinger, E.P., Oelschlager, B.K. (2006) Impaired esophageal function in morbidly obese patients with gastroesophageal reflux disease: evaluation with multichannel intraluminal impedance. *Surgical endoscopy*. **20**(5), 739-43.

Ramsden, E. (2006) *Hall-Effect Sensors: Theory and Application*. Second edi. Burlington: Newness, Elsevier.

Ravi, K., Francis, D.L. (2007) New technologies to evaluate esophageal function. *Expert review of medical devices*. **4**(6), 829-37.

Roberts, T.J., Azizi, E. (2011) Flexible mechanisms: the diverse roles of biological springs in vertebrate movement. *The Journal of experimental biology*. **214**(Pt 3), 353-61.

Robertson, E. V., Lee, Y. Y., Derakhshan, M. H., Wirz, A. A., Whiting, J.R.H., Seenan, J. P., Connolly, P., McColl, K. E. L. (2012) High-resolution esophageal manometry: addressing thermal drift of the manoscan system. *Neurogastroenterology & Motility*. **24**(1), 61-e11.

Robertson, Elaine V., Derakhshan, M., Wirz, AA, Lee, Y., Going, J., S, H., S, B., KEL, M. (2012) Central obesity and agre predict cardia mucosal length in healthy volunteers: evidence for an acquired entity. *Gastroenterology*. **5**(Suppl 1), S757.

Rohof, W., Boeckxstaens, G.E., Hirsch, D. (2011) High-resolution esophageal pressure topography is superior to conventional sleeve manometry for the detection of transient lower esophageal sphincter relaxations associated with a reflux event. *Neurogastroenterology & Motility*. **23**, 427-e173.

Roman, S., Zerbib, F., Belhocine, K., Des Varannes, S.B., Mion, F. (2011) High resolution manometry to detect transient lower oesophageal sphincter relaxations: diagnostic accuracy compared with perfused-sleeve manometry, and the definition of new detection criteria. *Alimentary pharmacology & therapeutics*. **34**(3), 384-93.

Roy, S., Fox, M.R., Curcic, J., Schwizer, W., Pal, A. (2012) The gastro-esophageal reflux barrier: biophysical analysis on 3D models of anatomy from

- magnetic resonance imaging. *Neurogastroenterology and motility: the official journal of the European Gastrointestinal Motility Society*.
- Sadowski, D.C., Broenink, L. (2008) High-resolution esophageal manometry: a time motion study. *Canadian journal of gastroenterology = Journal canadien de gastroenterologie*. **22**(4), 365-8.
- Schneider, J.H., Küper, M., Königsrainer, a, Brücher, B. (2009) Transient lower esophageal sphincter relaxation in morbid obesity. *Obesity surgery*. **19**(5), 595-600.
- Schoeman, M.N., Holloway, R.H. (1995) Integrity and characteristics of secondary oesophageal peristalsis in patients with gastro-oesophageal reflux disease. *Gut*. **36**(4), 499-504.
- Shi, G, Pandolfino, J E, Joehl, R J, Brasseur, J G, Kahrilas, P J (2002) Distinct patterns of oesophageal shortening during primary peristalsis, secondary peristalsis and transient lower oesophageal sphincter relaxation. *Neurogastroenterology and motility: the official journal of the European Gastrointestinal Motility Society*. **14**(5), 505-12.
- Shi, Guoxiang, Pandolfino, John E, Zhang, Q., Hirano, I., Joehl, Raymond J, Kahrilas, Peter J (2003) Deglutitive inhibition affects both esophageal peristaltic amplitude and shortening. *American journal of physiology. Gastrointestinal and liver physiology*. **284**(4), G575-82.
- Shirazi, S., Schulze-Delrieu, K., Custer-Hagen, T., Brown, C.K., Ren, J. (1989) Motility changes in opossum esophagus from experimental esophagitis. *Digestive diseases and sciences*. **34**(11), 1668-76.
- Sifrim, D, Holloway, R. (2001) Transient lower esophageal sphincter relaxations: how many or how harmful? *The American journal of gastroenterology*. **96**(9), 2529-32.
- Sifrim, D, Silny, J., Holloway, R.H., Janssens, J.J. (1999) Patterns of gas and liquid reflux during transient lower oesophageal sphincter relaxation: a study using intraluminal electrical impedance. *Gut*. **44**(1), 47-54.
- Sifrim, Daniel, Blondeau, K. (2006) New techniques to evaluate esophageal function. *Digestive diseases (Basel, Switzerland)*. **24**(3-4), 243-51.
- Sifrim, Daniel, Jafari, J. (2012) Deglutitive inhibition, latency between swallow and esophageal contractions and primary esophageal motor disorders. *Journal of neurogastroenterology and motility*. **18**(1), 6-12.
- Silny, J. (1991) Intraluminal Multiple Electric Impedance Procedure for Measurement of Gastrointestinal Motility. *J Gastrointest Motil*. **3**(3), 151-62.
- Spencer, J. (1969) Prolonged pH recording in the study of gastro-oesophageal reflux. *The British journal of surgery*. **56**(12), 912-4.
- Stylopoulos, N., Rattner, D.W. (2005) The history of hiatal hernia surgery: from Bowditch to laparoscopy. *Annals of surgery*. **241**(1), 185-93.

Sugarbaker, D.J., Rattan, S., Goyal, R.K. (1984a) Mechanical and electrical activity of esophageal smooth muscle during peristalsis. *The American journal of physiology*. **246**(2 Pt 1), G145-50.

Sugarbaker, D.J., Rattan, S., Goyal, R.K. (1984b) Swallowing induces sequential activation of esophageal longitudinal smooth muscle. *The American journal of physiology*. **247**(5 Pt 1), G515-9.

Suter, M., Dorta, G., Giusti, V., Calmes, J.M. (2004) Gastro-esophageal reflux and esophageal motility disorders in morbidly obese patients. *Obesity surgery*. **14**(7), 959-66.

Swellengrebel, H.A.M., Marijnen, C.A.M., Vincent, A., Cats, A. (2010) Evaluating long-term attachment of two different endoclips in the human gastrointestinal tract. *World journal of gastrointestinal endoscopy*. **2**(10), 344-8.

Thor, K.B., Hill, L.D., Mercer, D.D., Kozarek, R.D. (1987) Reappraisal of the flap valve mechanism in the gastroesophageal junction. A study of a new valvuloplasty procedure in cadavers. *Acta chirurgica Scandinavica*. **153**(1), 25-8.

Toghanian, S., Wahlqvist, P., Johnson, David A, Bolge, S.C., Liljas, B. (2010) The burden of disrupting gastro-oesophageal reflux disease: a database study in US and European cohorts. *Clinical drug investigation*. **30**(3), 167-78.

Trudgill, N.J., Riley, S. a (2001) Transient lower esophageal sphincter relaxations are no more frequent in patients with gastroesophageal reflux disease than in asymptomatic volunteers. *The American journal of gastroenterology*. **96**(9), 2569-74.

Tuttle, S.G., Rufin, F., Bettarello, A. (1961) The physiology of heartburn. *Annals of internal medicine*. **55**, 292-300.

Tytgat, G.N.J., Bartelink, H., Bernards, R., Giaccone, G., Van Lanschot, J.J.B., Offerhaus, G.J.A., Peters, G.J. (2004) Cancer of the esophagus and gastric cardia: recent advances. *Diseases of the esophagus: official journal of the International Society for Diseases of the Esophagus / I.S.D.E.* **17**(1), 10-26.

Uemura, N., Okamoto, S., Yamamoto, S., Matsumura, N., Yamaguchi, S., Yamakido, M., Taniyama, K., Sasaki, N., Schlemper, R.J. (2001) Helicobacter pylori infection and the development of gastric cancer. *The New England journal of medicine*. **345**(11), 784-9.

Vanderstappen, G., Texter, E.C. (1964) Response of the physiologic gastroesophageal sphincter to increased intra-abdominal pressure. *The Journal of clinical investigation*. **43**, 1856-68.

Wallner, B. (2009) Endoscopically defined gastroesophageal junction coincides with the anatomical gastroesophageal junction. *Surgical endoscopy*. **23**(9), 2155-8.

- Weber, C., Davis, C.S., Shankaran, V., Fisichella, P.M. (2011) Hiatal hernias: a review of the pathophysiologic theories and implication for research. *Surgical endoscopy*. **25**(10), 3149-53.
- Wernly, J. a, DeMeester, T.R., Bryant, G.H., Wang, C.I., Smith, R.B., Skinner, D.B. (1980) Intra-abdominal pressure and manometric data of the distal esophageal sphincter. Their relationship to gastroesophageal reflux. *Archives of surgery (Chicago, Ill. : 1960)*. **115**(4), 534-9.
- Weusten, B.L., Roelofs, J.M., Akkermans, L.M., Van Berge-Henegouwen, G.P., Smout, A.J. (1994) The symptom-association probability: an improved method for symptom analysis of 24-hour esophageal pH data. *Gastroenterology*. **107**(6), 1741-5.
- White, R.J., Zhang, Y., Morris, G.P., Paterson, W G (2001) Esophagitis-related esophageal shortening in opossum is associated with longitudinal muscle hyperresponsiveness. *American journal of physiology. Gastrointestinal and liver physiology*. **280**(3), G463-9.
- Whiting, James G H, Djennati, N., Lee, Yeong Yeh, Robertson, Elaine V., Derakhshan, Mohammad H., Connolly, Patricia, McColl, Kenneth E L (2012) Towards minimally invasive monitoring for gastroenterology -An external Squamocolumnar Junction Locator. *Conference proceedings: ... Annual International Conference of the IEEE Engineering in Medicine and Biology Society. IEEE Engineering in Medicine and Biology Society. Conference*. **2012**(d), 1574-7.
- Wu, J.C.-Y., Mui, L.-M., Cheung, C.M.-Y., Chan, Y., Sung, J.J.-Y. (2007) Obesity is associated with increased transient lower esophageal sphincter relaxation. *Gastroenterology*. **132**(3), 883-9.
- Wyman, J.B., Dent, J., Heddle, R., Dodds, W.J., Toouli, J., Downton, J. (1990) Control of belching by the lower oesophageal sphincter. *Gut*. **31**(6), 639-646.
- Xirouchakis, E., Kamberoglou, D., Kalos, D., Zambeli, E., Doulgeroglou, V., Tzias, V. (2009) The effect of gastroesophageal flap valve appearance on the management of patients with symptoms of gastroesophageal reflux disease. *Digestive diseases and sciences*. **54**(2), 328-32.
- Yamamoto, Y., Liu, J, Smith, T.K., Mittal, R K (1998) Distension-related responses in circular and longitudinal muscle of the human esophagus: an ultrasonographic study. *The American journal of physiology*. **275**(4 Pt 1), G805-11.